

**Reprogramming of tumor-associated macrophages by targeting  
 $\beta$ -catenin-FOSL2-ARID5A signaling  
– novel treatment of lung cancer**

Inauguraldissertation  
zur Erlangung des Grades eines Doktors der Medizin (Humanbiologie)  
des Fachbereichs Medizin  
der Justus-Liebig-Universität Gießen

vorgelegt von Sarode, Poonam Ashwin Kumar, Tambe  
aus Managaon, Raigad, Maharashtra, India

Gießen (2020)

Aus dem Fachbereich Medizin der Justus-Liebig-Universität Gießen

Gutachter: Prof. Dr. Savai

Gutachter: Prof. Dr. Kracht

Tag der Disputation: 28.04.2021

# TABLE OF CONTENTS

<b>1. INTRODUCTION</b> .....	<b>1</b>
1.1 General Introduction .....	1
1.2 Risk factors for lung cancer .....	1
1.2.1 Behavioral risk factors .....	2
1.2.1.1 Tobacco Smoking .....	2
1.2.1.2 Cannabis sativa .....	2
1.2.1.3 Electronic nicotine delivery systems (ENDS) .....	2
1.2.2 Environmental risk factors .....	2
1.2.2.1 Radon .....	3
1.2.2.2 Asbestos .....	3
1.2.2.3 Pollution and air quality .....	3
1.2.2.4 Infection .....	3
1.2.3 Genetic risk factors .....	3
1.3 Pathogenesis of lung cancer .....	4
1.4 Classification of lung cancer .....	4
1.4.1 Small cell lung cancer (SCLC) .....	5
1.4.2 Non small cell lung cancer (NSCLC) .....	5
1.4.2.1 Adenocarcinoma (ADC) .....	5
1.4.2.2 Squamous cell carcinoma (SCC) .....	6
1.4.2.3 Large cell carcinoma (LCC) .....	6
1.4.3 Neuroendocrine Tumors (NETs) .....	6
1.5 Lung cancer treatment .....	7
1.5.1 Surgery .....	7
1.5.2 Radiotherapy .....	8
1.5.3 Chemotherapy .....	8
1.5.4 Molecular targeted therapies .....	9
1.5.5 Immunotherapy .....	9
1.6. Lung tumor microenvironment .....	9
1.6.1 Cellular composition of tumor microenvironment .....	11
1.6.1.1 Cancer-Associated Fibroblasts (CAFs) .....	11

1.6.1.2 Tumor-Associated Neutrophils (TANs).....	11
1.6.1.3 Tumor-Associated Mast Cells (TAMCs) .....	12
1.6.1.4 Tumor-Infiltrating Dendritic cells (TIDCs) .....	12
1.6.1.5 Tumor-Infiltrating Lymphocytes (TILs).....	12
1.6.1.6 Natural killer cells (NK) .....	13
1.6.1.7 Interleukins and chemokines .....	13
1.6.1.8 Extracellular Matrix (ECM).....	13
1.6.2 Tumor-Associated Macrophages (TAMs) .....	14
1.6.2.1 Origin of macrophages .....	14
1.6.2.2 Macrophages in Lung .....	15
1.6.2.3 Phenotypes of macrophages.....	16
1.6.2.3 Macrophages in cancer development.....	18
1.6.2.3.1 Activation of TAMs in the TME .....	19
1.6.2.3.2 Prognostic significance of lung cancer-associated TAMs at distinct tumor sites ...	22
1.6.3 Macrophage targeting in cancer .....	23
1.6.3.1 TAMs depletion.....	24
1.6.3.2 Inhibition of monocyte/macrophages recruitment.....	24
1.6.3.3 Reprogramming of TAMs .....	25
1.7 Wnt/ $\beta$ -catenin signaling in lung cancer .....	27
1.8 Wnt/ $\beta$ -catenin signaling in TAMs.....	30
1.8.1. Tumor cells – specific Wnt/ $\beta$ -catenin signaling influences macrophages infiltration and activation.....	31
1.8.2 TAMs-specific Wnt/ $\beta$ -catenin signaling induce malignancy in tumor cells.....	31
1.8.3 Crosstalk of tumor cell and TAMs via Wnt/ $\beta$ -catenin signaling.....	32
1.8.4 Role of tissue-resident macrophages – specific Wnt/ $\beta$ -catenin signaling .....	32
1.9 FOS Like 2 (FOSL2).....	33
1.9.1 Role of FOSL2 in cancer and macrophages.....	33
1.10 AT-Rich Interaction Domain 5A (ARID5A) .....	34
1.10.1 Role of ARID5A in cancer and macrophages .....	34
<b>2. AIMS OF THE STUDY .....</b>	<b>36</b>
<b>3. MATERIALS AND METHODS.....</b>	<b>37</b>
3.1 Experimental procedures – Cell culture .....	37

3.1.1 Cancer cell lines.....	37
3.1.2 Primary cancer cell culture.....	37
3.1.3 Generation of human macrophages from buffy coats.....	37
3.1.4 Generation of THP1-derived human macrophages .....	38
3.1.5 Generation of mouse macrophages from bone marrow-derived cells.....	38
3.1.6 Activation of M1 and M2 macrophages from undifferentiated M0 macrophages .....	39
3.1.7 Generation of <i>in-vitro</i> -trained TAMs.....	39
3.2 Experimental procedures – Cell isolation from human and mouse lung tissue .....	40
3.2.1 Human lung tissues .....	41
3.2.2 Mouse lung tissues .....	42
3.2.3 MACS sorting of <i>ex-vivo</i> TAMs from human lung tissues.....	42
3.2.3 MACS sorting of <i>ex vivo</i> TAMs from mouse lung tumor tissues.....	43
3.2.4 Flow cytometry and cell sorting.....	44
3.3 Experimental procedures – Treatment and transfection of cells.....	44
3.3.1 Treatment with XAV939.....	44
3.3.2 Transfection with siRNA and shRNA .....	44
3.3.3 Transfection with plasmids .....	45
3.4 Experimental procedures – Molecular Biology.....	46
3.4.1 RNA isolation, complementary DNA synthesis, and quantitative polymerase chain reaction (quantitative PCR).....	46
3.4.2 Western blotting .....	49
3.4.3 TCF/LEF luciferase activity assay .....	50
3.4.4 Chromatin immunoprecipitation (ChIP).....	51
3.5 Experimental procedures – Cellular functional Studies .....	53
3.5.1 Proliferation and apoptosis assay.....	53
3.5.2 Migration assay.....	53
3.6 Experimental procedures – Imaging .....	54
3.6.1 Immunofluorescence staining .....	54
3.7 Experimental procedures – <i>in vivo</i> .....	54
3.7.1 Animal experiments .....	54
3.7.2 Subcutaneous tumor model.....	55
3.7.3 Carcinogen-induced lung tumor model.....	55

3.7.4 Metastasis tumor model (tumor relapse model) .....	55
3.7.6 Bone marrow transplantation model .....	55
3.7.5 Treatment of tumor bearing mice with XAV939 .....	56
3.7.6 Hematoxylin and eosin staining .....	56
3.7.7 Lung tumor quantification.....	56
3.8 RNA sequencing .....	56
3.9 Statistical analysis .....	58
<b>4. RESULTS .....</b>	<b>59</b>
4.1 Wnt/ $\beta$ -catenin signaling upregulated in lung TAMs.....	59
4.2 Wnt/ $\beta$ -catenin signaling activated in <i>in-vitro-trained</i> M2-like TAMs .....	60
4.2.1 Establishment of “ <i>in-vitro-trained</i> ” TAMs model featuring tumor inhibiting M1-like TAMs and tumor promoting M2-like TAMs.....	60
4.2.2 Wnt/ $\beta$ -catenin signaling activated in <i>in-vitro-trained</i> M2-like TAMs .....	63
4.3 Inhibition of $\beta$ -catenin leads to a phenotypical and functional switch of tumor-promoting M2-like TAMs to tumor-inhibiting M1-like TAMs .....	66
4.3.1 Inhibition of $\beta$ -catenin in <i>in-vitro-trained</i> M2-like TAMs by sh_ $\beta$ -catenin .....	67
4.3.2 Inhibition of $\beta$ -catenin in human <i>ex vivo</i> TAMs by si_ $\beta$ -catenin.....	68
4.3.3 Inhibition of Wnt/ $\beta$ -catenin signaling in <i>ex vivo</i> TAMs and <i>in vitro</i> trained M2-like TAMs by XAV939.....	70
4.3.4 Effect of direct XAV939 treatment and CM from XAV939-treated M2-like TAMs ( <i>in-vitro-trained</i> ) on proliferation and apoptosis of tumor cells.....	73
4.4 Pharmacological ablation of $\beta$ -catenin suppresses primary and metastatic tumor growth by reprogramming TAMs into tumor-inhibiting M1-like TAMs.....	74
4.5 Macrophage-specific genetic ablation of $\beta$ -catenin reduces lung tumor development by inducing M1-like TAM-directed anti-tumor immunity in the TME .....	76
4.6 Inhibition of $\beta$ -catenin signaling, suppression of FOSL2 and activation of ARID5A leads to reprogramming of M2-like TAMs to M1-like TAMs; correlation of $\beta$ -catenin/FOSL2/ARID5A with survival of lung cancer patients.....	79
4.6.1 $\beta$ -catenin-mediated transcriptional regulation of FOSL2 and ARID5A may play a role in M2-like TAMs polarization.....	79
4.6.2 $\beta$ -catenin differentially regulates the transcription of FOSL2 and ARID5A in M2-like TAMs .....	83
4.6.3 Activation of FOSL2 induces lung tumorigenicity by triggering the pro-tumorigenic transcriptional program of M2-like macrophages.....	84

4.6.4 Repression of ARID5A contributes to the lung tumorigenicity of M2-like macrophages by suppressing the M1-like anti-tumorigenic transcriptional program .....	85
4.6.5 High expression of $\beta$ -catenin and FOSL2 and low expression of ARID5A correlated with poor survival in lung cancer patients.....	87
<b>5. DISCUSSION .....</b>	<b>88</b>
5.1 Anti-tumor M1-like TAMs undergo the phenotypic transition to pro-tumor M2-like TAMs, with the activation in Wnt/ $\beta$ -catenin signaling.....	88
5.2 Phenotypic and functional transition of M2-like TAMs to M1-like TAMs by inhibiting Wnt/ $\beta$ -catenin signaling .....	90
5.3 $\beta$ -catenin mediated FOSL2-activation and ARID5A-repression play a vital role in the phenotypic transition of M1-like to M2-like TAMs .....	93
5.4 Conclusion.....	96
5.5 Future outlook .....	97
<b>6. SUMMARY .....</b>	<b>99</b>
<b>7. ZUSAMMENFASSUNG .....</b>	<b>101</b>
<b>8. LIST OF ABBREVIATIONS .....</b>	<b>103</b>
<b>9. LIST OF FIGURES .....</b>	<b>106</b>
<b>10. LIST OF TABLES .....</b>	<b>109</b>
<b>11. REFERENCES .....</b>	<b>110</b>
<b>12. ERKLÄRUNG ZUR DISSERTATION .....</b>	<b>133</b>
<b>13. ACKNOWLEDGEMENT .....</b>	<b>134</b>

# 1. INTRODUCTION

## 1.1 General Introduction

Lung cancer is the most frequently diagnosed cancer (11.6% of the total cases) and the leading cause of mortality (18.4% of the total cancer deaths) in males and females (**Figure 1**). Lung cancer is the primary cause of death among males in Eastern Europe, Western Asia, Northern Africa, China, Myanmar, Philippines, and Indonesia. In 28 countries, lung cancer is the prominent cause of cancer death among females. The highest occurrence is seen in Hungary, Northern and Western Europe (notably in Denmark and the Netherlands), North America, and Australia/New Zealand (Bray, Ferlay et al. 2018).

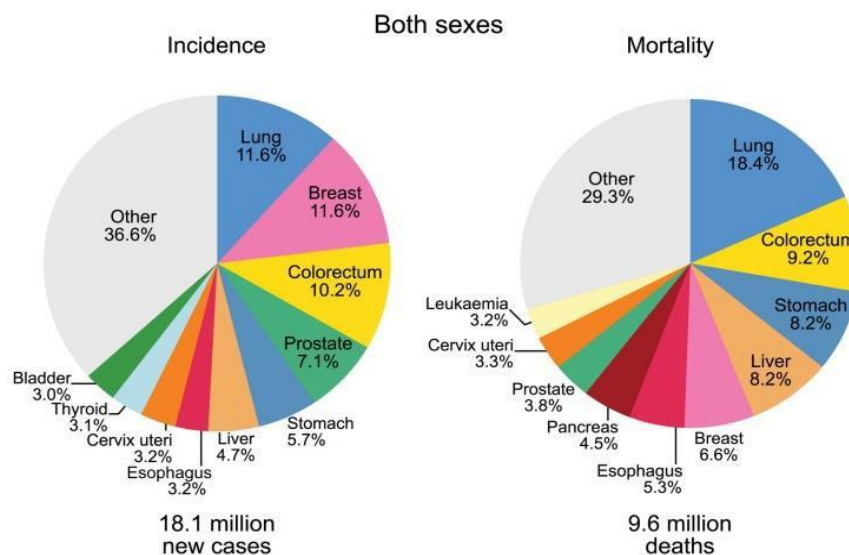


**Figure 1: Distribution of cases and deaths of the ten leading cancer types in 2018.** Pie charts represent the distribution of cancer cases and deaths for the ten most common cancers in 2018 for both males and females, and the area of the pie chart indicates the percentage of the total number of cases or deaths [(Bray, Ferlay et al. 2018) Reuse permission: License Number - 4934090226273]

The 5-year survival rate of lung cancer is 18.6%, which is lower than for many other commonly occurring cancers, such as colorectal (64.5%), breast (89.6%), and prostate (98.2%). The 5-year survival rate of primary lung cancer is 56%, while for metastatic lung cancer is only 5%. However, only 16% of lung cancer cases are diagnosed at a primary stage, and therefore more than half of the patients with lung cancer die within one year of diagnosis (Siegel, Miller et al. 2019).

## 1.2 Risk factors for lung cancer

## **1.2.1 Behavioral risk factors**

### **1.2.1.1 Tobacco Smoking**

Tobacco smoking is a primary risk factor in lung cancer development. Tobacco smoke produces free radicals in vapor and a particulate phase, which consists of as much as 60 potential carcinogens (e.g.- polycyclic aromatic hydrocarbons (PAH), including benzo[a]pyrene; nitrates; and tobacco-specific N-nitrosamines (TSNAs), such as 4-(methylnitrosamino)-1-(13-pyridyl-1-butanone) (NNK). The components from tobacco smoking and its metabolites induce carcinogenesis by formation of DNA adducts and by free radical damage. (Hecht 1998, Costa and Soares 2009, de Groot, Wu et al. 2018). Tobacco smoking induces premalignant histopathological changes in the lung, such as small tumor cells with the disturbed cell membrane and scanty cytoplasm in the cells of the proximal and small respiratory tract and tubular structure with high mucin content in the cells of the alveolar epithelium (Furrukh 2013).

### **1.2.1.2 Cannabis sativa**

The main psychoactive ingredient in cannabis,  $\Delta^9$ -tetrahydrocannabinol (THC), is not a carcinogen, but smoking marijuana combusts organic materials that have the potential to induce carcinogenesis. Because it produces a higher concentration of polyaromatic hydrocarbons when compared to tobacco smoke. The premalignant histopathological changes in bronchial epithelium by marijuana smoking are similar to that observed in tobacco smoking (Barsky, Roth et al. 1998, Aldington, Harwood et al. 2008).

### **1.2.1.3 Electronic nicotine delivery systems (ENDS)**

Electronic nicotine delivery systems (ENDS) came into the market in 2007. Although the vapors from an e-cigarette are different from traditional tobacco cigarettes, experimental studies strongly demonstrated that the concentration of formaldehyde, acetaldehyde, reactive oxygen species, polycyclic aromatic hydrocarbons, nitrosamines, and trace metals from ENDS consumption are sufficient to induce inflammatory damage to the airway and lung epithelium; inducing carcinogenesis. The particulate matter from ENDS, mainly deposits in the distal bronchioles or alveoli (Orr 2014, Dinakar and O'Connor 2016).

## **1.2.2 Environmental risk factors**

### **1.2.2.1 Radon**

Up till now, many studies established a relationship between mining and lung diseases (Samet 1991). Radon is a radioactive gas produced after uranium decay in mining. It is the second most common risk factor for lung cancer. Approximately 10% of cases of lung cancer resulted because of exposure to residential radon gas (Krewski, Lubin et al. 2005).

### **1.2.2.2 Asbestos**

The asbestos is widely used in the construction industry since the 19<sup>th</sup> century. Occupational exposure to asbestos was found to increase the risk of lung cancer by 5-fold. Asbestos exposure and tobacco smoking synergistically accelerate lung cancer development and progression (De Matteis, Consonni et al. 2008, Alberg, Brock et al. 2013).

### **1.2.2.3 Pollution and air quality**

The presence of carcinogens in the air due to pollution increases the risk of lung cancer in smokers as well as in non-smokers. For example, the combustion of fossil fuels in the trucking industry, the use of unprocessed fossil fuels such as soft coal and biomass fuels for heating and cooking, particulate matter in the air (Alberg, Brock et al. 2013). According to the International Agency for Research on Cancer (IARC), carcinogens are grouped as follows, Group 1: "Carcinogenic to humans", Group 2A: "Probably carcinogenic to humans", Group 2B: "Possibly carcinogenic to humans", Group 3: "Unclassifiable as to carcinogenicity in humans", Group 4: "Probably not carcinogenic to humans". Notably, particulate matter has been designated as a Group I carcinogen IARC (Hamra, Guha et al. 2014).

### **1.2.2.4 Infection**

The association of lung cancer with infections like tuberculosis (Brenner, McLaughlin et al. 2011) and human immunodeficiency viruses (HIV) (Engels, Biggar et al. 2008, Winstone, Man et al. 2013) was well established in past years. The prolonged inflammation in the lung by infection is implicated in carcinogenesis.

## **1.2.3 Genetic risk factors**

Inherited genetic mutations in tumor suppressor genes, oncogenes or DNA repair genes increases the potential risk of lung cancer. The positive family history potentiates lung cancer

risk by 1.7-fold (Lissowska, Foretova et al. 2010). The risk of lung cancer increases by 2 to 4-fold in first degree relatives but can be controlled by smoking status (Cote, Kardia et al. 2005). Genome-wide association studies (GWAS) demonstrated mutations in chromosome regions 5p15 (encodes telomerase reverse transcriptase/TERT, involved in cell replication) (Landi, Chatterjee et al. 2009), in region 15q25-26 (Thorgeirsson, Geller et al. 2008), in 6p21 (regulates G-protein signaling) (Yokota, Shiraishi et al. 2010) demonstrated markedly increased lung cancer risk in smokers and non-smokers (Schwartz and Cote 2016). Additionally, driver mutations in lung cells (e.g., genomic mutations in Epidermal Growth Factor Receptor/EGFR and KRAS, gene rearrangements in EML4-ALK Receptor Tyrosine Kinase/EML4-ALK, inactivation of tumor suppressor genes - p53, p16, Phosphatase And Tensin Homolog/PTEN by genetic and epigenetic modifications) potentiate the risk of lung cancer (Kristeleit, Enting et al. 2011).

### **1.3 Pathogenesis of lung cancer**

The repetitive insult of lung cells by one or more risk factors [*such as behavioral (e.g., tobacco smoking, marijuana smoking), occupational (e.g., radon, asbestos) environmental (e.g., air pollution) factors in combination with genetic, hormonal, and viral factors*] leads to lung tissue injury; inducing genetic and epigenetic changes [*such as mutations, loss of heterozygosity, and promoter methylation*] and global transcriptomic changes [*in inflammation and apoptosis pathways*]. The healthy cells are capable of repairing damaged DNA through various mechanisms, like cell cycle checkpoint activation, base or nucleotide excision repair, mismatch repair, etc. either to achieve a normal state of the cell or to undergo elimination by apoptosis; however, these mechanisms are ineffective in tumor cells. Chronic changes at DNA level for longer duration of time eventually lead to aberrant activation of multiple oncogenic pathways and inactivation of tumor-suppressor pathways; thereby leading to irreversible changes in cellular functions [*such as dysregulated proliferation, resistance to apoptosis, anoikis*] to produce premalignant changes, including dysplasia and clonal patches (*early-stage of lung cancer*). Further, the malignant growth of tumor cells is supported by additional changes [*such as co-occurring mutations, metabolic changes*] along with tumor microenvironment (TME)-mediated immune evasion, leading to invasion and metastasis of tumor cells (*advanced-stage of lung cancer*). The early and advanced stages of cancer share frequent molecular changes.

### **1.4 Classification of lung cancer**

Based on the histopathological changes, lung cancer is divided into three major subtypes, small cell lung cancer (SCLC), non small cell lung cancer (NSCLC), and neuroendocrine tumors. Each type of tumor shows distinct oncogenic changes.

### **1.4.1 Small cell lung cancer (SCLC)**

SCLC accounts for approximately 10%-15% of lung cancers. It is a very aggressive, fast-growing, and rapidly metastasizing cancer among all types of lung cancer. The occurrence of SCLC showed a strong relation with smoking. The significant histopathological changes observed in SCLC are - small tumor cells with distinct cytological features including ill-defined cell borders, scant cytoplasm and finely granular nuclear chromatin without visible nucleoli, smearing of nuclear chromatin and nuclear molding, high mitotic rate ( $\geq 11$  mitoses per 10 high power fields (HPF)), and extensive necrosis. Immunohistochemistry (IHC) markers are pan-cytokeratin, neuroendocrine markers (chromogranin, synaptophysin, and CD56), and Thyroid-Specific Enhancer-Binding Protein (TTF-1) and Ki-67 (Davidson, Gazdar et al. 2013). Frequent mutations in SCLCs are MYC Proto-Oncogene (MYC) amplification, RB Transcriptional Corepressor 1 (RB1) inactivation, gene mutations in fragile histidine triad di adenosine triphosphatase (FHIT), Ras association domain family member 1 (RASSF1A), p53, and BAX/BCL2 (apoptosis pathway-related genes) and loss of E-cadherin (epithelial-mesenchymal transition-related genes) (Kalari, Jung et al. 2013, Canadas, Rojo et al. 2014). EGFR mutations, ALK rearrangements, and Programmed Cell Death 1 (PD-L1) expression (approximately 10%) are rare characteristics in SCLCs (Nakamura, Tsuta et al. 2013, Toyokawa, Takenoyama et al. 2013, Lou, Yu et al. 2017, Tsuruoka, Horinouchi et al. 2017).

### **1.4.2 Non small cell lung cancer (NSCLC)**

NSCLC is the most commonly occurring lung cancer and accounts for approximately 85% of all lung cancer cases. It further divided into three major subtypes, such as

#### **1.4.2.1 Adenocarcinoma (ADC)**

ADC is histologically dominant among all types of lung cancer, accounting for approximately 40% of all lung cancers. It is most commonly seen in non-smokers, females, and Asians. The significant histopathological changes observed in ADC are - carcinoma with an acinar/tubular structure with mucin production, poorly differentiated carcinoma lacking light microscopic evidence of epithelial differentiation. IHC markers are "adenocarcinoma markers," such as Transcription Termination Factor 1 (TTF-1) and Napsin A (Davidson, Gazdar et al. 2013).

Based on the extent of invasiveness, 2015 WHO classification separates adenocarcinomas into adenocarcinoma *in situ*, minimally invasive adenocarcinoma, or invasive adenocarcinoma (Inamura 2017). The mutational spectrum observed in ADCs includes in KRAS, BRAF, EGFR, amplification of Erb-B2 receptor tyrosine kinase 2 (ERBB2), MET, Fibroblast Growth Factor Receptor (FGFR) -1 and FGFR-2, mutations in fusion oncogenes such as ALK, neuregulin 1 (NRG1), ROS1 receptor tyrosine kinase, RET and neurotrophic tyrosine kinase receptor type 1 (NTRK1).

### **1.4.2.2 Squamous cell carcinoma (SCC)**

The incidence of SCC has declined by 33% worldwide, mainly because of the change in the manufacturing of cigarettes. The new version of cigarettes has filter vents that allow the smokers deeper inhalation, which results in the deposition of particulate matter of the smoke in distal airways rather than in the proximal airway. The significant histopathological changes observed in SCC are (Davidson, Gazdar et al. 2013) - squamous differentiation with intercellular bridges, individual cell keratinization, squamous pearl formation. IHC markers are “SCC markers,” such as p40, CK5/6, and p63. In the new 2015 WHO classification, SCCs are classified into keratinizing SCC, non-keratinizing SCC, and basaloid SCC. Before this classification, basaloid SCC was categorized as a variant of large cell carcinoma. However, basaloid SCC immunohistochemically shows “SCC markers” (e.g., p40, CK5/6, and p63) and is therefore categorized as SqCC (Inamura 2017). The driver mutations in SCCs are gene mutations in the PI3K pathway, discoidin domain-containing receptor 2 (DDR2), and FGFR-1, FGFR-2, FGFR-3 (Weiss, Sos et al. 2010, Hammerman, Sos et al. 2011, Cancer Genome Atlas Research 2012, Guagnano, Kauffmann et al. 2012).

### **1.4.2.3 Large cell carcinoma (LCC)**

LCC is also known as undifferentiated carcinoma, and it is the least common type of NSCLC (approximately 3% of all lung cancers). It commonly spreads to lymph nodes and distant sites. LCC does not demonstrate morphological features of ADC, SCC, and SCLC. The significant histopathological changes observed in LCC are (Davidson, Gazdar et al. 2013) - large, partially necrotic tumors with sheets and nests of large polygonal cells with vesicular nuclei and prominent nucleoli. Electron microscopy, immunohistochemical studies, and next-generation sequencing suggested that LCC transforms into SCC, Large cell neuroendocrine carcinoma (LCNEC), SCLC, and ADC (Pelosi, Barbareschi et al. 2015).

## **1.4.3 Neuroendocrine Tumors (NETs)**

NETs account for approximately 20%-25% of lung cancers., A new category of “neuroendocrine tumors” was introduced in the 2015 WHO classification. SCLC is now included under this category, and other types are LCNEC and carcinoid tumor (typical/atypical). The clinical importance of diffuse idiopathic pulmonary neuroendocrine cell hyperplasia is low because it is infrequent and non-invasive. In contrast, the difference between high-grade neuroendocrine tumors (HGNET), comprising SCLC and LCNEC, and a carcinoid tumor are crucial in both clinical and pathological practice. HGNET is one of the most aggressive subtypes and positively associates with heavy smoking history, whereas carcinoid tumors usually carry a benign prognosis and frequently occur in patients with no history of smoking (Inamura 2017). The significant histopathological changes associated with SCLC described in section 1.4.1. and with LCNECs and carcinoids are as follows (Davidson, Gazdar et al. 2013).

LCNECs are also highly aggressive NETs, and the significant histopathological changes associated with LCNEC are - cytological features of NSCLC but with neuroendocrine architecture such as organoid nesting, palisading, trabecular growth and rosette-like structures high mitotic rate ( $\geq 11$  mitoses per 10 HPF). IHC markers are at least one neuroendocrine marker (chromogranin, synaptophysin, or CD56). Approximately 78% of LCNECs harbor a p53 mutation, other commonly altered genes include RB1, Serine/threonine Kinase 11 (STK11), Kelch like ECH associated protein 1 (KEAP1) and KRAS (Rekhtman, Pietanza et al. 2016).

Carcinoids are commonly occurring tumor types in children, accounting for 1% - 2% of all lung tumors. They are further divided into typical carcinoids (TC) and atypical carcinoids (AC). The significant histopathological changes associated with TC and AC are organoid, trabecular, insular, palisading, ribbon, rosette-like structures. TC has  $< 2$  mitoses per 10 HPF, and no necrosis, and AC has 2-10 mitosis per 10 HPF and shows necrosis (usually focal or punctate). Mutations in chromatin remodelers such as Menin 1 (MEN1), are frequently observed and restricted to carcinoid tumors (Fernandez-Cuesta, Peifer et al. 2014), while p53 mutations are occasional (Walter, Vollbrecht et al. 2016) and activating mutations of EGFR or KRAS genes are not found in carcinoid tumors (Rickman, Vohra et al. 2009).

## 1.5 Lung cancer treatment

### 1.5.1 Surgery

Types of lung cancer surgery are:

- *Lobectomy* – when one or more substantial parts of the lung (called lobes) are removed.

- *Pneumonectomy* – when the entire lung is removed. It is used when the cancer is located in the middle of the lung or has spread throughout the lung.
- *Wedge resection or segmentectomy* – when a small piece of the lung has been removed.

To date, surgery is the first choice of treatment, but most clinically detected cases are inoperable, and chances of missing micro-metastasis and recurrence are high (Lackey and Donington 2013).

### 1.5.2 Radiotherapy

Radiotherapy uses pulses of radiation to destroy tumor cells. There are three main ways of radiotherapy - conventional external beam radiotherapy (to direct the radiation beam at affected body parts), stereotactic radiotherapy (to distribute radiation to the tumor, while sparing the nearby healthy tissue), internal radiotherapy (a small portion of radioactive material is placed inside the catheter and located against the site of the tumor before removal). The treatment of lung cancer was carried out by different ways (Maciejczyk, Skrzypczynska et al. 2014) -

- *Radical radiotherapy* - to cure non-small-cell lung cancer if the person isn't healthy enough for surgery (Cole, Hanna et al. 2014)
- *Stereotactic radiotherapy* - to treat microscopic lung tumors (Yahya, Ghafoor et al. 2018)
- *Palliative radiotherapy* - to control the symptoms and slow the spread of lung cancer when a cure isn't possible (Nieder, Tollali et al. 2017)
- *Prophylactic Cranial Irradiation (PCI)* – It is used in the treatment of SCLC because of the risk of metastasizing to the brain (Yin, Yan et al. 2019).

### 1.5.3 Chemotherapy

Chemotherapy involves oral, intravenous, and intratracheal administration of low molecular weight drugs in different cycles. Chemotherapy is combined with other therapies for various purposes such as - to shrink a tumor before surgery, to avoid recurrence of tumor after surgery, to relieve symptoms, and to decelerate the proliferation of cancer when a cure is not possible. Chemotherapy and radiotherapy are the most considered options in the treatment of lung cancer, but these therapies have a devastating effect on healthy tissue homeostasis and reduce health-related quality of life (Zappa and Mousa 2016, Baxevanos and Mountzios 2018). The chemotherapeutic agents used in lung cancer treatment are Cisplatin, Carboplatin, Paclitaxel (Taxol), Albumin-bound paclitaxel (nab-paclitaxel, Abraxane), Docetaxel (Taxotere), Gemcitabine (Gemzar), Vinorelbine (Navelbine), Etoposide (VP-16), Pemetrexed (Alimta). The

complete list of the drugs approved by the Food and Drug Administration (FDA) for lung cancer treatment is available on the page <https://www.cancer.gov/about-cancer/treatment/drugs/lung>.

#### **1.5.4 Molecular targeted therapies**

The recent introduction of molecular targeted therapies, including activating mutations of EGFR and ALK translocation, led to improved treatment outcomes in selected subgroups of patients. However, for a large group of lung cancers, molecular alterations are not available to direct targeted therapies. Importantly, targeted therapies benefit only 15%–20% of lung cancer patients harboring drug-sensitive mutations. Even in these patients, the acquiring resistance is a significant impediment to a durable therapeutic response (Massarelli, Papadimitrakopoulou et al. 2014, Yang, Chen et al. 2016, Corrales, Scilla et al. 2018). For the lung cancer treatment, other molecular targeted therapies against HER2, MET, ROS1, NRTK1-3, SLK, BRAF and MEK are in different phases of clinical development (Schrank, Chhabra et al. 2018).

#### **1.5.5 Immunotherapy**

Historically, immunotherapy had marginal success in lung cancer, resulting in a common belief that lung cancer is poorly immunogenic. Advancement of immune checkpoint inhibitors targeting Cytotoxic T-Lymphocyte Associated Protein 4 (CTLA-4) and anti-PD-1 showed hope to target lung cancer by immunotherapy. Additional immunotherapeutic approaches (e.g., monoclonal antibodies, checkpoint inhibitors, therapeutic vaccines, adoptive T-cell transfer) are in different phases of clinical trials (Topalian, Hodi et al. 2012, Ock, Hwang et al. 2017, Chae, Arya et al. 2018, Seidel, Otsuka et al. 2018). Regardless of the promising results of certain immune checkpoint blockers, current immunotherapeutics has met a bottleneck concerning response rate, toxicity, and resistance in lung cancer. This attributable primarily to the fact that lung tumor cells acquire a large number of somatic mutations and, therefore, induce tumor immune evasion by suppressing immune cells-mediated immunosurveillance in multiple ways, such as - secretion of immunosuppressive cytokines, loss of major-histocompatibility-complex-antigen expression and expression of molecules that inhibit T-cell activation. Future studies should be oriented towards the analysis of tumor-infiltrating immune cells' landscape in tumor microenvironment, contributing to lung carcinogenesis to develop new immunotherapies.

#### **1.6. Lung tumor microenvironment**

The tumor microenvironment (TME) is heterogeneous not only because of tumor epithelial cells but also because of surrounding complex cellular ecology. TME consists of tumor cells, stromal cells, immune/ inflammatory cells (macrophages, neutrophils, mast cells, T lymphocytes, B cells, etc.). The tumor cells are closely associated with extracellular matrix (ECM), mesenchymal cells such as fibroblasts, infiltrating immune cells, and vasculature. ECM gives structural support to tumor cells and to tumor-associated fibroblasts (**Figure 2**). The tumor vasculature consists of blood and lymphatic vessels, which help in the homing of numerous blood cells and immune cells in the tumor. The infiltrated immune cells result in complex milieu of pro-inflammatory and anti-inflammatory cytokines in TME. The infiltrating immune cells not only support cancer progression and metastasis but also significantly influences the clinical outcome of patients depending on density and localization in lung tumor tissue.

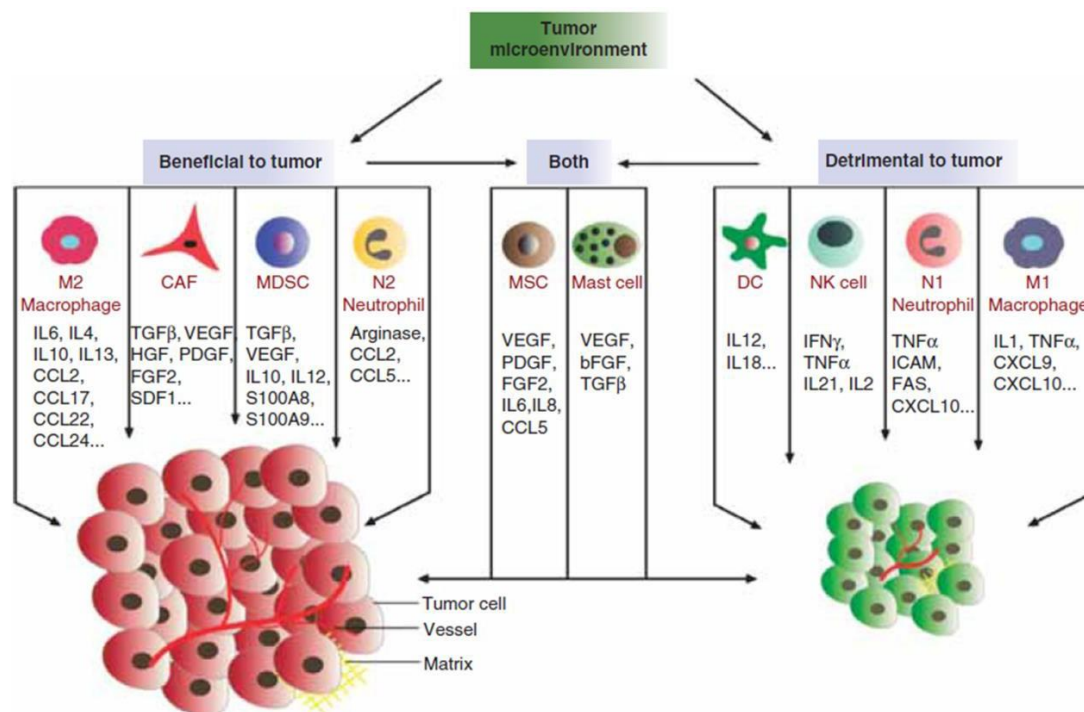


**Figure 2: Tumor Microenvironment.** The tumor microenvironment is composed of populations of stromal cells such as macrophages (M1 and M2), cancer-associated fibroblasts (CAF), myeloid-derived suppressor cells (MDSC), neutrophils (N1 and N2), mesenchymal stem cells (MSC), dendritic cells (DC), natural killer (NK) cells and mast cells. These can be beneficial or detrimental to tumor development by expressing and secreting specific cytokines, chemokines, and growth factors. [(Nikhely N et al., 2012) Reuse permission: Taylor & Francis is pleased to offer reuses of its content for a thesis or dissertation free of charge contingent on resubmission of permission request if work is published.]

## **1.6.1 Cellular composition of tumor microenvironment**

### **1.6.1.1 Cancer-Associated Fibroblasts (CAFs)**

CAFs display a specific subset of markers -  $\alpha$ -smooth muscle actin ( $\alpha$ -SMA), fibroblast-activating protein (FAP), fibroblast-specific protein-1 (FSP1), tenascin C, and neural-gial antigen. The stimulation of paracrine growth factors (PGF) by tumor cells (e.g., transforming growth factor- $\beta$ /TGF $\beta$ , platelet-derived growth factor/PDGF) induces activation of stromal fibroblast cells into CAFs (Shiga, Hara et al. 2015). On the other hands, CAFs also promote tumor cells growth and metastasis by secreting various growth factors, cytokines, and chemokines (e.g., TGF $\beta$ , stromal cell-derived factor-1 (SDF-1), CXCL1, tumor necrosis factor- $\alpha$  (TNF $\alpha$ ), as well as microRNAs and exosome). Moreover, CAFs also secrete different types of collagen to support the growth of ECM (Wang, Cao et al. 2017, Cruz-Bermudez, Laza-Briviesca et al. 2019, Hao, Zeltz et al. 2019). CAFs-derived platelet-derived growth factor receptor (PDGFR) family, CAF-markers like podoplanin and fibroblast activation protein (FAP), secreted factors (matrix metalloproteinases (MMPs) and, transcription factors (FoxF1), SPARC showed independent association with survival in lung cancer (Paulsson and Micke 2014).

### **1.6.1.2 Tumor-Associated Neutrophils (TANs)**

TANs are important tumor-infiltrating immune cells in lung cancer, grossly divided into two subtypes, N1 anti-tumoral or N2 pro-tumoral phenotype. TGF $\beta$  mediated signaling plays a crucial role in the polarization of N1 TANs, which secretes proteases, ROS, and RAN and thus induces cytotoxicity and restricts angiogenesis. On the other hand, in the polarization of N2 TANs, IFN $\beta$  plays a critical role, which then promotes angiogenesis, invasiveness, and metastasis of lung cancer cells. In general, TANs are widely characterized by CD66b<sup>+</sup> marker, which is stored in neutrophils granules (Hong 2017). A recent study by Rakaee et al. showed in 536 NSCLC patients of which 172 harbored lymph node metastases that CD66b<sup>+</sup> TANs are an independent, decisive prognostic factor for disease-free survival in SCC, while in AC it proved to be an independent negative prognostic factor (Rakaee, Busund et al. 2019). Additionally, few recent studies demonstrated that cross-talk of TANs with other tumor-infiltrating immune cells leads to phenotypic changes in TANs, which in advanced stages of lung cancer support growth and metastasis (Eruslanov, Bhojnagarwala et al. 2014, Eruslanov 2017, Teixeira and Rosell 2017).

### **1.6.1.3 Tumor-Associated Mast Cells (TAMCs)**

TAMCs identified in human lung cancer, but their contribution to tumor progression is not widely studied. Bone marrow released immature mast cell progenitors migrate into tissue and undergo division in two major subtypes: connective tissue mast cells and mucosal mast cells with tryptase secretion, which was also abundantly found in mucosa of the lungs (Shea- Donohue, Stiltz et al. 2010). Different studies demonstrated both the pro- and antitumorigenic role of TAMCs in lung cancer (Varricchi, Galdiero et al. 2017). Peritumoral but not intratumoral TAMCs (tryptase<sup>+</sup> chymase<sup>+</sup>) in stage I NSCLC (not in stage II) is an independent favorable prognostic factor (Soo, Chen et al. 2018).

### **1.6.1.4 Tumor-Infiltrating Dendritic cells (TIDCs)**

TIDCs are highly heterogeneous and highly plastic antigen-presenting immune cells, which in cancer engulf apoptotic and necrotic tumor fragments to present tumor-antigen to T cells. This interaction leads to the displacement of T-cell co-stimulatory molecules (CD40, CD86) that eventually potentiate cytotoxic T cell responses. Different studies in human lung cancer specimens suggest that a high density of mature and immature DCs positively correlate with cytotoxic T cell responses, improving patient survival (Goc, Germain et al. 2014). Conversely, other studies also demonstrated that TIDCs expressing PD-L1, PDL2 suppress T cell function by secreting arginase-1 or indoleamine 2,3-dioxygenase resulting in poor prognosis in lung cancer (Perrot, Blanchard et al. 2007, Pyfferoen, Brabants et al. 2017).

### **1.6.1.5 Tumor-Infiltrating Lymphocytes (TILs)**

TILs are a heterogeneous population of T lymphocytes and to a lesser extent, B lymphocytes, B cells, and NK cells. T cells are divided into different subtypes according to their cell surface markers such as CD8<sup>+</sup> cytotoxic T lymphocytes, CD4<sup>+</sup> T helper lymphocytes, and FOXP3 regulatory T cells. The widely accepted meta-analysis studies in lung cancer patients' by Geng et al. in 8600 NSCLC patients demonstrated that high density of TILs is associated with favorable progression-free survival (PFS) rather than overall survival (OS). Interestingly, high frequencies of CD8<sup>+</sup> T cells in tumor stroma (TS) and tumor nest (TN) correlates with better OS, but CD8<sup>+</sup> T cells in TN are prognostically more significant than those in TS (Geng, Shao et al. 2015). Another study by Schalper et al. reported that high infiltration of CD3<sup>+</sup> and CD8<sup>+</sup> T cells is associated with better outcome in NSCLC and that CD8<sup>+</sup> T cells density is an independent prognostic factor and stratified according to TNM stage (Schalper, Brown et al. 2015). The role of CD4<sup>+</sup> T cells in lung cancer is quite controversial; this is mainly because of

two subtypes of  $T_{H1}$  and  $T_{H2}$  cells.  $T_{H1}$  cells are mostly tumor-inhibiting cells as they play a role in enhancing antigen-presenting cells (APCs), prolonging  $CD8^+$  cells' cytotoxic response and secretion of IFN $\gamma$ , TNF $\alpha$ , and cytolytic granules. On the other hand,  $T_{H2}$  cells secrete pro-tumorigenic molecules like IL4, IL10, IL13, influence macrophage polarization, and thereby promote tumor progression and metastasis. A high ratio of  $T_{H2}$  to  $T_{H1}$  significantly correlates with poor patient outcomes in lung cancer (Wakabayashi, Yamazaki et al. 2003). Another subpopulation of TILs -  $CD4^+FoxP3^+$  T regulatory ( $T_{reg}$ ) cells influence lung tumor development by suppressing anti-tumor activities of  $CD8^+$  cytotoxic lymphocytes, NK-cells and DC, stimulating immunosuppressive cytokine profile, potentiating  $T_{H2}$  cells' response. FOXP3+ T cells in TS are a negative prognostic indicator in NSCLC (Kinoshita, Ishii et al. 2013).

### **1.6.1.6 Natural killer cells (NK)**

In lung cancer, peripheral NK cell cytotoxicity is reduced. The overexpression of T cell immunoglobulin and mucin-domain-containing molecule-3 (Tim3), on  $CD3^+ CD56^+$  NK cells and  $CD3^+ CD56^{dim}$  NK subsets is found to be positively associated with shorter OS in patients with LADC (Platonova, Cherfils-Vicini et al. 2011). The low expression of three NK isoforms receptors (NCR1/NKp46; NCR3/NKp30; NKp30) correlated with poor OS and PFS (Fend, Rusakiewicz et al. 2017).

### **1.6.1.7 Interleukins and chemokines**

In the TME, tumor cells crosstalk with other cells via chemokines and interleukins. An analysis of the expression level of these molecules in serum, bronchoalveolar lavage fluid (BALF), and lung tumor tissue served as an indicator of patient prognosis and survival. For example, low serum level of IL20, low BALF level of IL22 (Naumnik, Naumnik et al. 2016), high serum level of IL17 (Lin, Xue et al. 2015) correlates with worse outcome in patients with lung cancer. Not only interleukins but also the expression of chemokines correlates with outcome in lung cancer patients. For example, a low level of CCL2, CCL19, CXCL16, and a high level of CCL5, CXCL8, CXCR4 positively associated with worse patient survival (Rivas-Fuentes, Salgado- Aguayo et al. 2015). The "combined cytokine prognostic classifier" is a newly proposed diagnosis scheme in lung cancer treatment. For example, a high combined expression of IL8 with IL6 and IL6 with IL17 found to be a negative prognostic marker in stage I lung cancer (Ryan, Pine et al. 2014).

### **1.6.1.8 Extracellular Matrix (ECM)**

ECM is not an active cellular component of TME, but abnormalities in ECM such as disrupted organization, altered composition, changed topography found to be associated with cancer initiation, progression, angiogenesis, and metastasis (Levental, Yu et al. 2009). A study by Su Bin Lim et al. proposed a genomic tool, ECM-related prognostic, and predictive indicator (EPPI), to evaluate the biological and clinical contribution of different ECM components in lung tumor development. EPPI consist of following genes - [collagens (*COL10A1*, *COL11A1*), matrix metalloproteinases (*MMP1*, *MMP12*), secreted factors (*S100A2*), glycoproteins (*CTHRC1*, *SPP1*), and ECM-affiliated proteins, or genes encoding proteins affiliated structurally or functionally to ECM proteins (*GREM1*) and low expressions of surfactant proteins (*SFTPC*, *SFTPA2*, *SFTPD*), secreted proteins (*CHRDL1*, *WIFI*), ECM-regulated genes (*CPB2*, *MAMDC2*, *HHIP*, *LPL*, *CD36*, *ADAMTS8*), collagen (*COL6A6*), ECM-affiliated proteins (*FCN3*), ECM glycoproteins (*TNNC1*, *ABI3BP*), and proteoglycan (*OGM*)]. It will help to decide a better treatment regimen in lung cancer (Lim, Tan et al. 2017).

### **1.6.2 Tumor-Associated Macrophages (TAMs)**

Macrophages are a plastic, heterogeneous group of cells, which, aside from providing the first line of defense against invading pathogens, have a fundamental role in maintaining tissue integrity and homeostasis. Moreover, they have specified functions based on their locations and distinct gene expression profiles. Functional and/or phenotypic dysregulation have been linked with multiple chronic inflammatory and autoimmune diseases such as obesity, type II diabetes, atherosclerosis, asthma, fibrosis, inflammatory bowel disease, multiple sclerosis, rheumatoid arthritis, and cancer, suggesting that macrophages may serve as therapeutic targets (Schultze, Schmieder et al. 2015). For this purpose, a greater understanding of the differences in the development, phenotypes, and functions of macrophages is required (Murray and Wynn 2011).

#### **1.6.2.1 Origin of macrophages**

Van Furth and Cohn suggested that tissue-resident macrophages originate mainly from circulating adult, bone marrow-derived blood monocytes (Gordon and Martinez-Pomares 2017). However, in the last few years, this concept was drastically revised because a series of more definitive publications demonstrated that most mature tissue macrophages originate during embryonic development and not from circulating monocytes. In most adult tissues, tissue-resident macrophages derive from (i) fetal-generated macrophages that self-renew *in situ* and (ii) the engraftment of adult circulating macrophage progenitors (Epelman, Lavine et

al. 2014). The origin of macrophages occurs via following overlapping waves (Munro and Hughes 2017),

- *Wave 1* - The earliest macrophages originate from early and late erythro-myeloid progenitors (EMPs) produced in the extra-embryonic yolk sac for the duration of primitive hematopoiesis at E7.5 and E8.25. EMPs give rise to yolk sac-derived macrophages without going through a monocytic intermediate and are the seeded first in the fetal tissues following blood circulation initiation. In most of the fetal tissues, these macrophages are subsequently replaced either partially or entirely by fetal liver-derived monocytes, except microglial cells in the brain.
- *Wave 2* - Fetal liver monocytes generated from EMPs derived from hemogenic endothelium of yolk sac. Progenitors migrate to the fetal liver in two consecutive waves E9.5 (EMPs) and E10.5/E11 (immature and mature HSCs) followed by their expansion and differentiation into fetal liver monocytes, which then enter the circulation and differentiate into macrophages in peripheral tissues.
- *Wave 3* - In liver, lung, skin, spleen, and peritoneum, fetal liver monocyte-derived macrophages maintain their self-renew ability and create a population of tissue-resident macrophages. In dermis and gut, fetal liver monocyte-derived macrophages slowly substituted by the recruitment of bone marrow-derived monocytes derived from adult hematopoiesis beginning around E17.5

### 1.6.2.2 Macrophages in Lung

The lung has two different populations of resident macrophages, which are – (i) Alveolar macrophages that reside on alveolar septae in alveolar space and originate from fetal liver-derived monocytes. Markers of alveolar macrophages are CD11b/Integrin $\alpha$ M<sup>low/-</sup>, CD11c<sup>high</sup>, CD200 R1<sup>+</sup>, CD68/SR-D1<sup>+</sup>, Dectin-1<sup>+</sup>, DEC-205/CD205<sup>int</sup>, F4/80<sup>low</sup>, Galectin-3/Mac-2<sup>+</sup>, MHC class II<sup>low</sup>, MARCO<sup>+</sup>, MMR/CD206<sup>high</sup>, Siglec-F<sup>high</sup>, PPAR $\alpha$ <sup>+</sup>. They are specialized in the recycling of surfactant molecules, immune surveillance of inhaled pathogens, clearance of allergens, dust, and microorganisms, etc. (ii) Interstitial macrophages in the interstitium of lung that originate from fetal liver- and bone marrow-derived monocytes (Cortez-Retamozo, Etzrodt et al. 2012). Markers of interstitial macrophages are CD11b/Integrin $\alpha$ M<sup>int</sup>, CD11c<sup>-</sup>, CD68/SR-D1<sup>+</sup>, CD200 R1<sup>+/-</sup>, F4/80<sup>+</sup>, MHC class II<sup>+/-</sup>, Siglec-F<sup>-</sup>. They play a significant role in the function of dendritic cells (Kopf, Schneider et al. 2015, Schyns, Bureau et al. 2018).

### 1.6.2.3 Phenotypes of macrophages

Macrophages encounter diverse microenvironmental signal in general, which can alter their transcriptional programs leading to an activated state. An activation/polarization of macrophages is subdivided into two major types, classical (M1) macrophage activation, which promotes a pro-inflammatory response, and alternative (M2) macrophage activation, which stimulates an anti-inflammatory response (Martinez and Gordon 2014). However, this classical description of macrophage activation is currently under debate. To address the problems in classifying macrophage activation and in achieving experimental standards, Murray et al. described a set of standards encompassing three principles—the source of macrophages, the definition of the activators, and a consensus collection of markers to define the activation of macrophages (Murray, Allen et al. 2014). The framework for describing activated macrophages as suggested by Murray et al. is shown in **Figure 3A** (examples of widely used macrophage preparations), **Figure 3B** (marker systems for activated macrophages), **Figure 3C** (using genetics to aid in macrophage-activation studies).

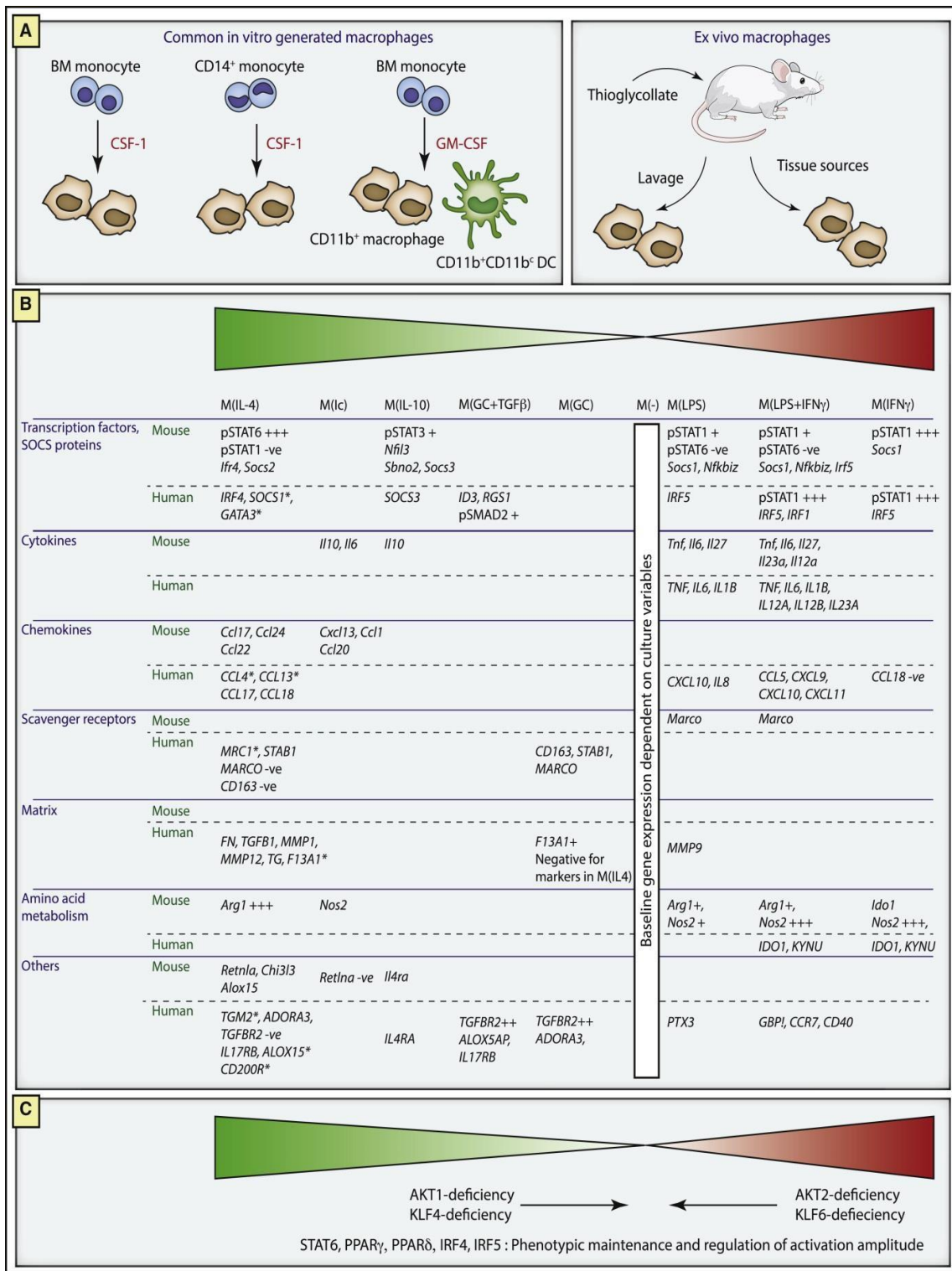


**Figure 3: Framework for classifying activated macrophages** [(Murray, Allen et al. 2014) Reuse permission: License Number - 4934090734990]

- A. Examples of widely used macrophage preparations – In vitro macrophages generated by CSF1-derived bone marrow (BM) monocytes, CSF1-derived CD14<sup>+</sup> monocytes, and GM-CSF-derived BM monocytes. GM-CSF-derived BM monocytes give rise to CD11b<sup>+</sup> macrophages and CD11b<sup>+</sup>CD11c<sup>+</sup> dendritic cells (DCs). Ev-vivo macrophages from the

mouse generated by thioglycollate injection, followed by peritoneal lavages or by isolating macrophages from various tissues or organs.

- B. *Marker systems for activated macrophages* – Red gradient indicate a subdivision of M1 macrophages [LPS, LPS, and IFN- $\gamma$ , and IFN- $\gamma$  alone] and green gradients indicate a subdivision of M2 macrophages [IL-4, immune complexes (Ic), IL-10, glucocorticoids (GC) + transforming growth factor  $\beta$  (TGF- $\beta$ ), glucocorticoids alone]. For each type of human and mouse macrophages, transcription factors, cytokines, chemokines, scavenger receptors, matrix, amino acid metabolism are mentioned.
- C. *Using genetics to aid in macrophage-activation studies* - Mutations in AKT1 and KLF4 switch M1 (LPS) - and M2 (IFN- $\gamma$ )-related gene expression, while mutations in AKT2 and KLF6 show the reversal in phenotype. Mutations in STAT6, PPARG, IRF4, and IRF5 depletion implicated in the preservation and scale of activation.

With the increasing knowledge of macrophage biology, even this expanded model of macrophage activation is considered too simplistic to define phenotypes of macrophages observed in different homeostatic and pathological conditions. On this note, recently, a new multidimensional model of macrophage activation (based on extensive gene expression analysis) was proposed. This model suggests that a scale of activation states covering the M1/M2 states can occur in response to various signals, including ontogeny-related signals, tissue-specific signals, and stress signals, which are integrated to determine the macrophage response (Li, Menoret et al. 2019).

### **1.6.2.3 Macrophages in cancer development**

The complex cellular microenvironment of tumors establishes and supports the destructive nature of cancer. In the TME, innate immune cells predominating, among which macrophages are highly represented cells (Cassetta and Pollard 2018). Generally, macrophages are considered to have anti-tumor functions, but there is considerable clinical and experimental evidence to suggest that in the majority of cases, these tumor-associated macrophages (TAMs) are pro-tumorigenic in nature. At the primary site, TAMs support tumor-associated angiogenesis, promote tumor cell invasion, migration, and intravasation, as well as regulating pro-tumor immune réponses. TAMs also potentiate the seeding and establishment of metastatic cells and play a role in tumor initiation at a secondary site. Additionally, TAMs can antagonize, augment, or suppress anti-tumor effects of cytotoxic agents, tumor irradiation therapies, anti-angiogenic/vascular damaging agents, and checkpoint inhibitors (Conway, Pikor et al. 2016, Yang, McKay et al. 2018). TAMs promote cancer development in multiple ways, such as -

- TAMs promote tumor cell proliferation and survival by secreting Insulin Like Growth Factor 1 (IGF1), Fibroblast Growth Factor (FGF) -1, -2, PDGF, and TGF $\alpha$  and  $\beta$  (Hao, Lu et al. 2012).
- TAMs-derived migration inhibitory factor (MIF) induce DNA damage and immune escape by suppressing p53 activity (Hudson, Shoaibi et al. 1999).
- TAMs in hypoxic regions adapt to low oxygen tension by expressing Hypoxia Inducible Factor 1 Subunit Alpha (HIF1 $\alpha$ ) and subsequently secrete angiogenic factors, [like Vascular Endothelial Growth Factor A (VEGF), IL8, Cyclooxygenase (COX)-2, and matrix metalloproteinase (MMP) -9] (Nishida, Yano et al. 2006).
- To support invasion and metastasis of tumor cells, TAMs induce epithelial-mesenchymal transition (EMT) in tumor cells via secretion of MMPs (Wang, Zhang et al. 2011).
- TAMs establish a pro-tumor anti-inflammatory environment by the recruitment of Th2 cells and regulatory T cells (Mantovani, Sica et al. 2004).
- TAMs play a part in T cell anergy and inhibition of the activation and growth of naïve T cells. (Rodriguez, Quiceno et al. 2004, Johnson and Munn 2012).
- TAMs induced autocrine IL10 signaling pathway drives M2-like TAMs polarization to suppress anti-tumor response in TME (Sica, Saccani et al. 2000).
- TAMs induce intrinsic activation of the immune checkpoint protein PDL1, which by binding to PD1 on T cells leads to cytotoxic T cells senescence, exhaustion, and apoptosis (Kuang, Zhao et al. 2009)

Until now, a large body of experimental, pathological, and clinical evidence confirmed that a high density of TAMs at tumor sites plays a significant role in cancer development and progression. But the future research on the topic of “TAMs in cancer development” needs an comprehensive understanding of the activation of TAMs by tumor cells and their role in specific tumor areas. Increasing clinical evidence is strengthening the fact that not only the numbers but also the particular phenotype of TAMs in specific tumor areas correlates with relapse-free survival (RFS) and overall survival (OS) in human cancer patients.

### **1.6.2.3.1 Activation of TAMs in the TME**

TAMs exhibit a functional heterogeneity ranging from pro-inflammatory, immune activatory, and anti-tumoral responses to anti-inflammatory, regulatory, and pro-tumoral activities. The functional heterogeneity in TAMs is reflected by phenotypic subsets – grossly subdivided as tumor-inhibiting M1-like TAMs and tumor-promoting M2-like TAMs. Although, there is no clear phenotypic definition of TAMs as they are composed of several distinct macrophage subpopulations, which often share standard features of classically activated M1 and alternatively activated M2 macrophages (**Figure 4**).

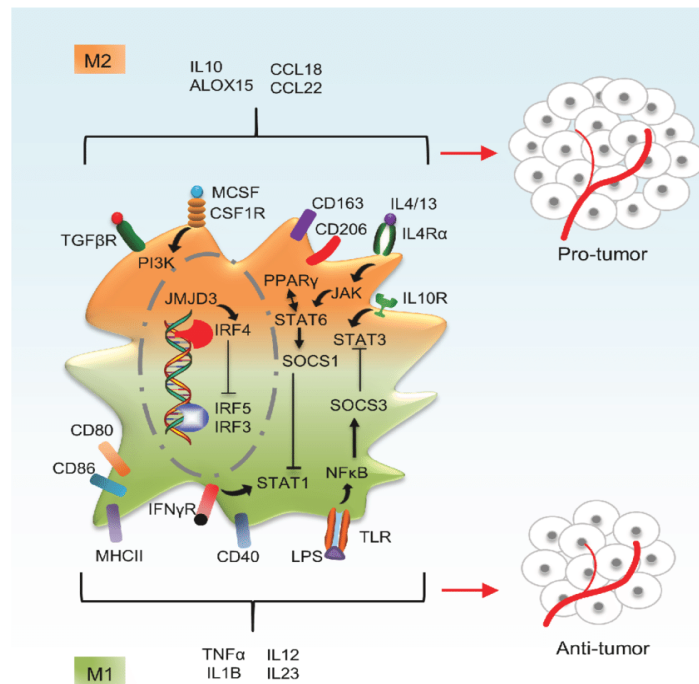


**Figure 4: Distinct activation mechanisms in M1-like and M2-like macrophages.** Macrophages are stimulated either classically (M1) or alternatively (M2). M2 macrophages express high levels of CD206, CD163, and TGFβR, whereas M1 macrophages express high levels of CD40, CD80, and CD86 on the cell membrane. STAT1 and STAT3 are highly activated in the M1 phenotype and STAT6 in the M2 phenotype. IRF3, 5, and 7 are activated in the M1 phenotype, whereas IRF4 is enabled in the M2 macrophages. Cytokines and chemokines such as TNFα, IL1B, and IL12 observed in the M1 and factors such as IL10, ALOX15, and CCL18 are highly expressed in the M2 phenotype. Abbreviations: ALOX15, Arachidonate 15-Lipoxygenase; CCL18, C-C Motif Chemokine Ligand; IL, Interleukin; IRF, Interferon Regulatory Factor; STAT, Signal Transducer And Activator Of Transcription; TGFβR, Transforming Growth Factor Beta Receptor; TNF, Tumor Necrosis Factor. *[(Zheng X et.al.2017) Reuse permission: Distributed under the terms of the Creative Commons Attribution 3.0 License]*

Distinct signals and molecular pathways are responsible for M1-like macrophages (M1) and M2-like macrophage (M2) activation. For example, activation of NFKB1, STAT1, IRF3, IRF5, and IRF7 promotes M1 activation while STAT3, STAT6, and IRF4 promote M2 macrophages. M1 express high levels of CD40, CD80, and CD86, while M2 express high levels of CD206, CD163, and TGFβR on the cell surface. The secretome profile from differentiated M1 and M2 macrophages has distinct functions. Remarkably, the molecules primarily responsible for M1 and M2 activities repress each other's responses. High levels of the pro-inflammatory cytokines and chemokines such as TNF, IL1B, IL6 and IL12 are observed in M1, and anti-inflammatory factors such as IL4, IL10, IL13, ALOX15 and CCL18 are highly expressed in M2 [35-37]. In the context of tumor biology, M1-like macrophages (M1-like TAMs) induce a tumor-inhibiting inflammatory response by activation of NK and T<sub>H</sub>1 cell responses and by presenting

antigen to phagocytic cells. However, M2-like macrophages (M2-like TAMs) promote tumor growth, angiogenesis, invasion, metastasis, and therapy-resistance by activating T<sub>H2</sub> immune responses.

The majority of the lung cancer – associated TAMs express high levels of M2-like TAMs' markers, such as - IL10, IL1 receptor antagonist, CCL22, CCL18, CD209, and CD163 antigen [38, 39]. Aberrant accumulation of M2-like TAMs in TME mainly depends differentiation of monocyte-to-macrophages, activation of different macrophage phenotypes, inter-conversion within these phenotypes, and migration from other sites [40-42]. The cellular and molecular mechanisms responsible for TME-mediated accumulation and activation of M2-like TAMs are just beginning to be understood and seem to be greatly influenced by crosstalk with tumor cells. Currently, researches are working on various different hypothesis to explain the activation of M2-like TAMs by tumor cells, such as-

- The driver mutations in tumor cells influence the activation of TAMs. For example, – driver mutations in lung cancer are gene mutations in EGFR and KRAS, EML4-ALK rearrangements, and altered MET signaling (Sanchez-Vega, Mina et al. 2018). The extensive immunogenic analysis of more than 10,000 TCGA samples comprising 33 diverse cancer types displayed a more prominent M2-like TAMs signature with Th1 suppressed responses in tumors with gene mutations in EGFR, KRAS, and KRAS G12 (Thorsson, Gibbs et al. 2018).
- The secretome of TME shifts transcriptional program responsible for M1-like TAMs activation (NFKB1, STAT1, IRF3, IRF5, and IRF7) to M2-like TAMs (STAT3, STAT6, and IRF4). For example - tumor cell-secreted CSF1 regulates recruitment of macrophages in tumor stroma. Other cytokines like TNF $\alpha$  and IL6 are also linked to the accumulation/recruitment of macrophages to the tumor periphery. The tumor stromal cells produce chemokines such as Colony Stimulating Factor (CSF) -1, CCL2, CCL3, CCL5, and placental growth factor which recruits macrophages to the tumor surroundings and provides a microenvironment for activation of macrophages, in which macrophages produce high levels of IL10, TGF $\beta$ , Arginase 1 (ARG1), VEGF and low levels of IL12, TNF $\alpha$ , and IL6 (Lin and Pollard 2007).
- The apoptosis and necrosis of tumor cells induce activation of M2-like TAMs. For example, - tumor cell apoptosis-derived Sphingosine-1-Phosphate (S1P) contributes to macrophage polarization (Weigert, Tzieply et al. 2007).
- Hypoxic environments in tumors attract monocyte/macrophages followed by differentiation and production of HIF1 $\alpha$  and HIF2 $\alpha$ , which regulate the transcription of genes associated with tumor promotion such as angiogenesis. For example, - Neuropilin

1 (Nrp-1) plays critical roles in hypoxic TME-induced activation and pro-tumoral effects of TAMs in cervical cancer (Chen, Wu et al. 2019).

- The tumor cell-mediated metabolic shift in macrophages phenotype activates M2-like TAMs in TME. For example – reduced glycolysis via Mechanistic Target Of Rapamycin Kinase (mTOR) inhibition in hypoxic TAMs increases endothelial glucose availability and disturbs the formation of an organized tumor vasculature, which helps tumor cells to undergo metastasis (Wenes, Shang et al. 2016).
- TAMs maintain an immunosuppressive phenotype by receiving polarization signals from tumor cells. IL1R and MYD88 mediated inhibitor of nuclear factor kappa B kinase subunit beta (IKBKB) and NFKB1 signaling cascade maintain M2-like phenotype in TAMs (Hagemann, Lawrence et al. 2008).

#### **1.6.2.3.2 Prognostic significance of lung cancer-associated TAMs at distinct tumor sites**

As cancer progresses, macrophages differentiate, activate, and migrate into distinct tumor sites by exposing themselves to different microenvironmental signals that “educate” them to perform functions that are required by tumor cells in those areas. Tumor sites are mainly divided as follows (Yang, McKay et al. 2018),

- *Invasive margin* – There are three main sites where the invasive behaviors of cancer are seen. (i) around preinvasive lesions where the aberrant proliferation of newly altered, neoplastic cells leads to their invasion through the membrane into the surrounding healthy parenchyma to form a carcinoma, (ii) in established tumors, at the “tumor-stroma border (TSB)” between cancer cell nests and the stroma within the tumor mass and (iii) at the “invasive margin” where cancer cells invade into surrounding healthy tissues.
- *Tumor nest* - This is the area of high cancer cell density. In this area, TAMs are close to tumor cells.
- *Stroma* - In this area, cancer cells are often sparse or absent. It comprises of a network of macromolecules in the extracellular matrix (ECM) such as collagen fibrils, tenascin C fibronectin, laminin, and hyaluronic acid (HA) and nonmalignant cell populations including fibroblasts, endothelial cells, pericytes, lymphocytes, and myeloid cells. Many studies have shown that ECM components and their proteolytic products regulate the phenotype of macrophages.
- *Perivascular (PV) niche* - A subset of TAMs lies close to blood vessels in mouse and human tumors. These PV cells express high levels of the M2 markers, TEK Receptor Tyrosine Kinase (TIE2, a receptor for angiopoietins), CD206, and CD163.
- *Hypoxic/necrotic tumor areas* - Hypoxic areas are located more than 150  $\mu\text{m}$  away from tumor blood vessels and have low oxygen tensions (below 10 mm Hg). High numbers of

hypoxic TAMs are associated with elevated levels of tumor angiogenesis, metastasis, poor recurrence-free survival (RFS), and reduced overall survival in various cancers.

**Table 1** summarises functions of TAMs in different sites of human lung tumors and their correlation with clinic pathological features (Carus, Ladekarl et al. 2013, Wu, Wu et al. 2016, Yang, McKay et al. 2018).

Tumor sites					
Tumor type	Invasive front	Tumor nests	Stroma	Peri-vascular	Hypoxic /necrotic area
Non-small-cell lung cancer (NSCLC)	ND	High CD163 <sup>+</sup> TAM density correlates with increased LNM (but not OS)	High CD163 <sup>+</sup> TAM density correlates with increased LNM (but not OS)	ND	ND
Lung (meta-analysis of 21 studies)	ND	High TAM density correlates with better 3-year OS but not 5-year OS; specifically, high M1(*)-TAMs associated with better 3- and 5-year OS. M2(*)-TAMs was not associated with 3- or 5-year OS	High TAM density correlates with worse 3- and 5-year OS; specifically, high M2-TAMs was associated with reduced 5-year (but not 3-year) OS	ND	ND

**Table 1: TAMs in different areas of human lung cancer: correlation with prognosis and overall survival** (adapted from Ming Y. et al., 2018). "High TAMs," high number of TAMs in a given area. \*M1-like: CD68<sup>+</sup>HLA<sup>-</sup>DR<sup>+</sup> cells; M2-like: CD163<sup>+</sup> alone, CD204<sup>+</sup> alone, CD68<sup>+</sup>CD163<sup>+</sup>, CD68<sup>+</sup>CD206<sup>+</sup>, or CD68<sup>+</sup>IL10<sup>+</sup> cells. CD68 used for immunolabeling TAMs in tumor sections unless otherwise stated. Abbreviations: **ND**, not determined; **LNM**, lymph node metastases.

### 1.6.3 Macrophage targeting in cancer

A large body of clinical and experimental evidences suggests that TAMs, especially M2-like TAMs, play a critical role in all stages of tumor development and frequently antagonize the response to therapy. Therefore, immunotherapies directed towards TAMs represent a

promising cancer therapeutic approach. The different immunotherapeutic strategies to target TAMs are depletion, inhibition of monocyte/macrophage recruitment, and reprogramming of TAMs.

### 1.6.3.1 TAM depletion

Following targeting, approaches are in different phases of the clinical trial to interfere with TAMs survival.

- *Clodronate liposomes approach* - Macrophages ingest and digest clodronate (non-toxic bisphosphonate) liposomes and intracellularly release clodronate. Upon a specific intracellular concentration of clodronate, macrophages undergo apoptosis (Schmall, Al-Tamari et al. 2015).
- *Bisphosphonate agonists* – Phagocytosis of bisphosphonates by macrophages offers another TAMs' depletion strategy. Based on their structure and mechanism of action, bisphosphonates are mainly divided into two groups; the first group includes clodronate, etidronate, and tiludronate, while alendronate, ibandronate, pamidronate, risedronate, and zolenodrate belong to the second group.
- *Legumain, CD204, CD124, Folate receptor  $\beta$  blockers* – Depleting pro-tumoral M2-like TAMs rather than all subsets of TAMs is a much-considered option. Targeting of molecules expressed explicitly by M2-like TAMs (e.g., Legumain, CD204, CD124, Folate receptor  $\beta$ ) are under pre-clinical evaluation (Luo, Zhou et al. 2006, Bak, Walters et al. 2007, Nagai, Tanaka et al. 2009, Roth, De La Fuente et al. 2012).
- *CSF1-CSF1R axis antagonists* – The crucial role of the CSF1-CSF1R axis in macrophage differentiation makes it an attractive target to deplete TAMs in TME selectively. Small molecules (LX3397, JNJ-40346527, PLX7486, ARRY-382, and BLZ945) and monoclonal antibodies (RG7155, IMC-CS4 and FPA008) targeting the CSF1-CSF1R axis are showing promising results in pre-clinical studies and clinical trials (Yan, Kowal et al. 2017).
- *Caspase 8 activators* – Trabectedin mainly activates caspase 8 to induce monocyte apoptosis, while sparing neutrophils, and T cells (Moreau, Guillet et al. 2007, Rogers and Holen 2011, Van Acker, Anguille et al. 2016).

### 1.6.3.2 Inhibition of monocyte/macrophage recruitment

Accumulation of TAMs in TME is primarily dependent on the recruitment of monocyte and macrophages to the site of the tumor. Therefore, targeting molecules or signaling pathways responsible for monocyte/macrophage recruitment are under critical evaluation. For example,

- *CCL2-CCR2 axis antagonists* – Tumor cells secrete CCL2 (chemoattractant for monocyte, T cells, NK cells), which specifically recruit CCR2-expressing monocytes to the tumor sites. This bidirectional interaction plays a role in all stages of lung tumor development. Carlumab (CNTO 888), anti-CCL2 mAb, and small molecule inhibitor PF-04136309 targeting CCR2 are currently under investigation (Deshmane, Kremlev et al. 2009, Sandhu, Papadopoulos et al. 2013, Hitchcock and Watson 2015, Schmall, Al-Tamari et al. 2015, Fang, Yao et al. 2016, Nywening, Wang-Gillam et al. 2016).
- *CSF1R antagonists* – Targeting CSF1R is also under clinical investigation because of its involvement in monocyte/macrophage recruitment.

Results from the ongoing clinical trials pointed out the fact that targeting monocyte and macrophages recruitment needed much more biological knowledge to achieve sufficient inhibition, because compensatory mechanisms by tissue-resident macrophages and ligand-receptor concentration-dependent recruitment of monocyte/macrophage may reduce the efficacy of such strategies.

### 1.6.3.3 Reprogramming of TAMs

The inter-conversion of TAMs from anti-tumoral to pro-tumoral phenotypes suggests that manipulation of the plasticity of macrophages to re-activate anti-tumor immunity in TAMs is possible. Unlike other TAMs targeting strategies, reprogramming of TAMs will induce anti-tumor immunity in TME by rebalancing microenvironmental immune infiltrates, while sparing other subtypes of macrophages like anti-tumoral M1-like TAMs and tissue-resident macrophages. It can also enhance the efficacy of checkpoint inhibitors. Many different methods are currently under pre-clinical and clinical investigations,

- *Anti-CD47 antibodies* – Interaction of CD47 with thrombospondin 1 and signal regulatory protein  $\alpha$  (mainly expressed by DCs and macrophages) results in “do not eat me” signals. This mechanism tightly regulated and mainly activated in pro-inflammatory conditions (Brown and Frazier 2001). Many tumors overexpress CD47 which is involved in tumor invasion, metastasis, and immune evasion by interacting with SIRP $\alpha$ . Inhibition of CD47 restricts tumor growth by inducing macrophage-mediated phagocytosis of tumor cells (Zhang, Lu et al. 2015, Zhao, Wang et al. 2016). Currently, two anti-CD47 mAbs (Hu5F9-G4 and CC-90002) and one soluble recombinant SIRP $\alpha$ -crystallizable fragment (Fc) fusion protein (TTI-621) are in phase I clinical trials of different malignancies (Gholamin, Mitra et al. 2017, Sikic, Lakhani et al. 2019).
- *Toll-like receptor (TLRs) agonist* – The fundamental role of TLRs in the activation of innate immune response makes them an attractive target to induce reprogramming of macrophages towards pro-inflammatory anti-tumor phenotypes (Kaczanowska, Joseph

- et al. 2013, Le Mercier, Poujol et al. 2013, Singh, Khong et al. 2014). Two TLR7 ligands (imiquimod and 852A) and one TLR9 ligand (IMO-2055) are in different phases of clinical trials (Dudek, Yunis et al. 2007, Smith, Conkling et al. 2014).
- *Anti-CD40 antibodies* – The interaction of CD40 (expressed by APCs such as monocytes, macrophages, dendritic cells, and B cells) with its ligand CD40L (expressed by CD4<sup>+</sup> T cells, basophils, and mast cells) induces production of pro-inflammatory cytokines like IL12 and prime CD4<sup>+</sup>, CD8<sup>+</sup> T cells anti-tumoral responses by upregulating expression of MHC molecules (van Kooten and Banchereau 2000, Khalil and Vonderheide 2007). Two agonistic anti-CD40 antibodies (CP-870,893 and RO7009789) are in clinical trials (Vonderheide, Flaherty et al. 2007).
  - *Histone deacetylase (HDAC) inhibitors* – HDACs play a crucial role in the expression of genes. HDACs from different families regulate the expression of various genes. For example, a specific inhibitor of class IIA HDACs, TMP195 modifying the epigenetic profile of monocytes and macrophages, resulting in induction of CCL1, CCL2-producing pro-inflammatory phenotype of macrophages (Arrowsmith, Bountra et al. 2012, Guerriero, Sotayo et al. 2017).
  - *Anti-MARCO antibody therapy* – Macrophages exclusively express macrophage receptor with collagenous structure (MARCO). Its high expression is linked to poor prognosis in different malignancies like breast cancer and metastatic melanoma. In various preclinical studies, anti-MARCO therapy showed an anti-tumor effect and improved efficacy of anti-CTLA4 immunotherapy (Li and Ravetch 2011).
  - *PI3Ky inhibitors* – Class IB PI3Ky are mainly expressed by hematopoietic cells, and it acts as a critical regulator of tumor immune suppression exerted by TAMs. Genetic and pharmacological inhibition of PI3Ky increased expression of MHCII molecules and of IL12, decreased expression of IL10 to re-activate anti-tumor immunity in TME (Kaneda, Messer et al. 2016).
  - *Inhibition of microRNA activity* – The regulation transcription of genes by MicroRNAs (miR) mediated through RNase-III enzyme DICER. Inhibition of DICER induced the expression of IFN $\gamma$ -STAT1 signatures in TAMs (Baer, Squadrito et al. 2016). The expression of miR by M1 and M2 macrophages differ from each other - M1 macrophages produce miR-125, miR-155, and miR-378, while miR-9, miR-21, miR-146, miR-147, miR-187 and miR-511-3p are expressed by M2 macrophages. Therefore, targeting a specific miR can induce anti-tumor immunity in TME (Squadrito, Etzrodt et al. 2013).

Although reactivation of immunosurveillance in TME via reprogramming of tumor-promoting TAMs is the wave of future, a thorough understanding of immune cells mediated molecular pathways is required to improve immune-therapeutic modalities.

## 1.7 Wnt/ $\beta$ -catenin signaling in lung cancer

Multiple studies strongly demonstrated the role of Wnt signaling in the development of lung-associated diseases, mainly focusing on  $\beta$ -catenin-mediated canonical Wnt signaling. The inherited and sporadic mutations in the tumor suppressor adenomatous polyposis coli (APC) and  $\beta$ -catenin are not common in lung cancer (Sequist, Heist et al. 2011, Coscio, Chang et al. 2014). Nevertheless, Wnt/ $\beta$ -catenin signaling (hereafter referred to as Wnt signaling) was found to be activated in 50% of human lung cancer cell lines and lung cancer resected samples (Akiri, Cherian et al. 2009). Wnt signaling is best described in the absence (off state) and in the presence of (on state) Wnt ligand, as shown in **Figure 5**.

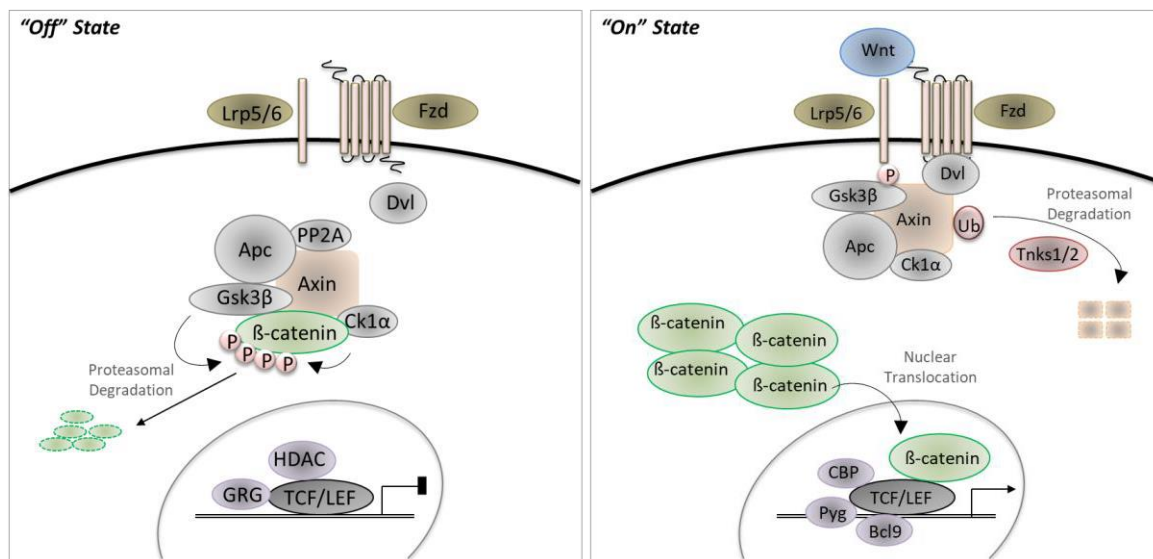


**Figure 5: Wnt/ $\beta$ -catenin signaling pathway.** In the absence of Wnt ligands (off state),  $\beta$ -catenin levels are regulated by a destruction complex of Apc and Axin, Ser/Thr kinases Ck1 $\alpha$  and Gsk3 $\beta$ , which phosphorylate  $\beta$ -catenin followed by ubiquitination and proteasomal degradation. In the presence of Wnt ligands (on state), Wnts bind to Fzd receptors and interact with adjacent Lrp5/6 co-receptors, the above complex recruits Dvl to the cytoplasmic tail of Fzd receptors, and Dvl recruits the destruction complex to the Fzd/Lrp5/6 complex and associated Ser/Thr kinases. Additionally, cytoplasmic Tnks1/2 ubiquitinates Axin, targeting it for proteasomal degradation to disrupt the  $\beta$ -catenin destruction complex, followed by its translocation to the nucleus. This translocation leads to the displacement of the co-repressor GRG on the TCF/LEF transcription factor by  $\beta$ -catenin and the recruitment of co-activators such as BCL9, CBP, and Pyg to regulate transcription of target genes. Abbreviations: Apc, adenomatous polyposis coli; Bcl9, B-cell CLL/lymphoma 9 protein; CBP, CREB-binding protein; Ck1 $\alpha$ , casein kinase 1 $\alpha$ ; Dvl, disheveled; Fzd, Frizzled; Gsk3 $\beta$ , glycogen synthase kinase 3; GRG, Groucho; HDAC, histone deacetylases; LRP5/6, low-density lipoprotein receptor-related protein 5/6; PP2A, phosphatase A2Pyg, Pygopus; TCF/LEF, T-cell factor/lymphoid enhancer factor; Tnks1/2, tankyrase-1/2.

In the off state (absence of Wnt ligands), cytoplasmic  $\beta$ -catenin forms a complex with Axin, Apc, Gsk3 $\beta$  and CK1 $\alpha$ , and is then phosphorylated by CK1 $\alpha$  and subsequently by Gsk3 $\beta$ . Phosphorylated  $\beta$ -catenin is recognized by the E3 ubiquitin ligase  $\beta$ -Trcp, which leads to its proteasomal degradation. In the nucleus, Wnt target genes are repressed by TCF-LEF1/GRG and HDAC. In contrast, in the on state (presence of Wnt ligands),  $\beta$ -catenin levels in the cytoplasm are upregulated through the following steps - (i) Wnts binds to cognate Fzd receptors and interacts with adjacent Lrp 5/6 co-receptors. (ii) The resulting complex is recruit Dvl to the cytoplasmic tail of Fzd receptors. (iii) The destruction complex recruits to the Fzd/Lrp5/6 complex and Gsk3 $\beta$  by Dvl to change the localization of the complex. Moreover, cytoplasmic Tnks1/2 ubiquitinates Axin, targeting it for proteasomal degradation and causing disruption of the  $\beta$ -catenin destruction complex. (iv) Stabilized cytosolic  $\beta$ -catenin then accumulates in the nucleus. (v) Nuclear translocation displaces co-repressor GRG from the TCF/LEF transcription factor and recruits co-activators such as Bcl9, CBP, and Pyg to result in the transcription of target genes. The list of  $\beta$ -catenin-target genes is continuously growing, yet many are subject to complex, context-dependent regulation and are expressed in a cell or tissue-specific or temporally restricted manner. The transcriptional regulation via the  $\beta$ -catenin/TCF complex is very diverse because accumulating evidence suggests that it not only activates but can also repress the target genes (MacDonald, Tamai et al. 2009, Valenta, Hausmann et al. 2012).

The master regulator of activated Wnt signaling – “ $\beta$ -catenin” is clinically associated with the size, stage, grade of lung tumors, prognosis, and survival of lung cancer patients (Kren, Hermanova et al. 2003, Jin, Zhan et al. 2017). An activation of Wnt signaling in lung cancer is the result of co-occurring genetic, epigenetic, and expression alterations in Wnt signaling components and aberrant expression of molecules associated with Wnt signaling activity. For example - (i) upregulation (Wnt1, 2, 3, 5A, 7B, 11) and downregulation (Wnt7A) of Wnt ligands; (ii) increased expression of membrane receptors (Fzd8, Lrp5/6, ROR2); (iii) increased expression of cytoplasmic stimulatory modifications of Wnt signaling (Dvl1, 2, 3); (iv) deregulation in membranous and cytoplasmic inhibitory alterations of Wnt signaling due to epigenetic changes (e.g. sFRPs, WIF1, DKKs, Axin2, Apc); (v) upregulation (AEG-1, ARMC8 $\alpha$ , DEPDC1B, Porcupine, RNF146; etc) or downregulation (EMX2, Fibulin3, ING4, LKB1; etc.) of molecules associated with Wnt signaling activity (Stewart 2014, Yang, Chen et al. 2016, Rapp, Jaromi et al. 2017).

Aberrant upregulation of Wnt signaling is an essential element of lung tumorigenesis, controlling not just the tumorigenesis, but also tumor vascularisation and metastasis (Imielinski, Berger et al. 2012, Nakata, Yoshida et al. 2015). Wnt signaling plays a cardinal role

in maintaining therapy-surviving cancer stem cell populations, and therefore, plays a vital role in drug resistance and tumor relapse (He, Barg et al. 2005, Stewart 2010, Takebe, Miele et al. 2015). As one of the best-established therapeutic targets of cancer, significant efforts are being made to develop potential modulators to understand the fundamentals of the pathway and to target its various components for cancer treatment. **Table 2** summarizes the Wnt signaling antagonists targeting different parts of the signaling, which are (i) in different phases of clinical trials (indicated by Clinicaltrials.Gov identifier number), (ii) drugs approved to treat other diseases that have been recently found to inhibit Wnt signaling (shown by Abbreviated New Drug Application Identification Number/ ANDA) and (ii) drugs in the preclinical studies (Kahn 2014, Harb, Lin et al. 2019) (Krishnamurthy and Kurzrock 2018) (Roos, Grosch et al. 2016).

<b>Drugs targeting Wnt signaling under clinical trial</b>				
<b>Agents</b>	<b>Target</b>	<b>Clinical trial stage</b>	<b>Clinicaltrials.Gov identifier</b>	<b>Diseases</b>
OMP-54F28	Wnt	Phase 1B	NCT02092363	Refractory solid tumors, ovarian cancers
OMP-18R5	Fzd	Phase 1B	NCT01973309, NCT02005315	Mammary, pancreatic cancers
ETC-159	Porcupine	Phase 1A/B	NCT02521844	Advanced solid tumors
LGK974	Porcupine	Phase 1	NCT01351103	Pancreatic, melanoma, mammary, head and neck, cervical, and respiratory cancers
PRI-724	CBP	Phase 1	NCT01764477	Pancreatic cancers
CWP232291	$\beta$ -catenin /TCF	Phase 1A/B	NCT02426723	Relapsed or refractory multiple myeloma,
<b>Drugs approved to treat other diseases that have been recently found to inhibit Wnt signaling</b>				
<b>Agents</b>	<b>Target</b>	<b>Abbreviated New Drug Application (ANDA)</b>		<b>Diseases</b>
Ethacrynic acid	$\beta$ -catenin /LEF	016092		Leukemia, hepatic cancers
Pimozide	CK1 $\alpha$	017473		Colorectal cancers

Celecoxib	GSK3	204590	Familial adenomatous polyposis, colorectal, mammary cancers
Pyrvinium	CK1 $\alpha$	011964	Mammary, epithelial, melanoma, myeloma cancers
Sulindac	Dsh	073262	Familial adenomatous polyposis, colorectal cancers
Niclosamide	Dsh	018669	Colorectal, prostatic, and ovarian

#### Drugs in preclinical studies

Agents	Target	Current state
XAV939	Tankyrase	In vivo (mouse models)
JW55	Tankyrase	In vivo (mouse models)
BC21	$\beta$ -Catenin /TCF	In vitro (HCT116 cell line)
iCRT3, iCRT5	$\beta$ -Catenin /TCF	In vitro (colon cancer cell lines)
iCRT14	$\beta$ -Catenin /TCF	In vivo (mouse models)

**Table 2: Selected Wnt signaling inhibitors, their targets and current stage of development,** adapted from (updated from Ross J. et al. 2016 and Harb J et al. 2019)

Until now, Wnt signaling antagonism is focused mainly on tumor cells. Although recent studies reported the molecular footprint of activated Wnt signaling not only in tumor cells but also in tumor-infiltrating immune cells; indicating its bidirectional role in tumor-immunity cycle (Yeo, Cassetta et al. 2014, Finkernagel, Reinartz et al. 2016, Pai, Carneiro et al. 2017, Zhan, Rindtorff et al. 2017, Yang, Ye et al. 2018).

### 1.8 Wnt/ $\beta$ -catenin signaling in TAMs

Ongoing research in Wnt signaling suggests that not only tumor cell-specific Wnt signaling plays a pivotal role in tumorigenesis and tumor progression, but also that TME-mediated Wnt signaling governs the balance between activation/suppression of tumor-immune responses. Accumulating experimental evidence demonstrated that cross-talk of tumor cells with tumor-

infiltrating immune cells via Wnt signaling modulates the immune response of dendritic cells, CD4 T regulatory cells, cytotoxic CD8+ T cells, and NK cells; shifting their immunosurveillance function to immune evasion. Additionally, some studies reported immune exclusion mechanisms through T cells, dendritic cell - specific Wnt signaling in various cancers. A small number of cancer studies reported a role of TAMs-specific Wnt signaling in tumor-immunity cycle, which were mainly focused on the following hypothesis.

### **1.8.1. Tumor cells – specific Wnt/ $\beta$ -catenin signaling influences macrophages infiltration and activation**

Yang Y et al. demonstrated that mRNA expression of Wnt ligand (Wnt2, 3, 3a, 4, 10b, and 16) is more in hepatic tumor cells (Hepa1-6) compared to TAMs. Henceforth, crosstalk of hepatic tumor cells with macrophage induces malignancy via promoting M2-like TAMs activation through c-Myc (Yang, Ye et al. 2018). Specifically, induction of IL10 and inhibition of the classical TLR4-NF- $\kappa$ B signaling in monocytes/macrophages by Wnt 5a induces M2-like TAMs phenotype in sepsis and breast cancer (Bergenfelz, Medrek et al. 2012). Tumor cells and myeloid cells – secreted CCL2 induces infiltration and production of Wnt 1 in CD206<sup>+</sup>/Tie2<sup>+</sup> macrophages (M2-like TAMs) that in turn downregulates E-cadherin junctions in the HER2<sup>+</sup> tumor cells; inducing early dissemination and metastasis of breast cancer cells (Linde, Casanova-Acebes et al. 2018). Lui et al. showed a non-Wnt ligand-dependent pathway to activate Wnt signaling in lung cancer. Overexpression of MORC Family CW-Type Zinc Finger 2 (MORC2) activates Wnt signaling in cancer cells, and MORC2-overexpressing tumors showed significant increase in CD206<sup>+</sup> macrophage (M2-like TAMs) infiltration via increased expression of CSF-1 and CCL2/5 (Liu, Liu et al. 2015). Cathelicidin, an antimicrobial peptide produced by macrophages, also activates Wnt signaling in colon tumor cells by inducing PTEN phosphorylation, leading to PI3K/Akt signaling activation followed by GSK3 $\beta$  phosphorylation; resulting in stabilization and nuclear translocation of  $\beta$ -catenin (Li, Liu et al. 2015). In osteosarcoma, SPARCL1 [a member of the SPARC (secreted protein acidic and rich in cysteine) family] - mediated Wnt signaling activation promotes infiltration of macrophages by increasing CCL5 production in human OS cells (Zhao, Jiang et al. 2017).

### **1.8.2 TAMs-specific Wnt/ $\beta$ -catenin signaling induce malignancy in tumor cells**

Not only tumor cells but also macrophages are known to secrete the Wnt ligand. In breast cancer, macrophage-derived Wnt5a induces invasion of tumor cells (Pukrop, Klemm et al. 2006), while Wnt 7b mediates the angiogenic switch and metastasis (Yeo, Cassetta et al. 2014). In human colorectal cancer, upregulation in the expression of Wnt2 and 5a in

macrophages is seen in the development from normal to adenoma to carcinoma (Smith, Bui et al. 1999). Additionally, a study by Ojalvo et al. reported a prominent signature of activated Wnt signaling in TAMs from invasive tumor area of breast cancer. Invasive TAMs are known to play a role in angiogenesis and metastasis of breast cancer and this may be linked to their activated status of Wnt signaling. Not only primary TAMs from breast cancer but also from ovarian cancer showed a prominent intrinsic signature of activated Wnt signaling (Ojalvo, Whittaker et al. 2010). Infiltrating macrophages are a vital source of steatosis-induced Wnt expression; thus, selective depletion of these macrophages leads to a reduction of Wnt and suppresses liver tumor development (Debebe, Medina et al. 2017). Not only tumor cells but also cancer stem cells (CSCs) are affected by macrophage-initiated Wnt signaling. Interaction of CSCs with macrophages through Wnt signaling plays a role in development and maintenance of pro-tumoral and malignant phenotypes in 3D engineered microenvironments of ovarian cancer (Raghavan, Mehta et al. 2019).

### **1.8.3 Crosstalk of tumor cell and TAMs via Wnt/ $\beta$ -catenin signaling**

TAMs-secreted interleukin-1 $\beta$  (IL1 $\beta$ ) stabilizes cytoplasmic  $\beta$ -catenin through phosphorylation of GSK3 $\beta$  in colon cancer cells (Kaler, Augenlicht et al. 2009). Interestingly, transcriptionally active  $\beta$ -catenin activates snail (soluble factor product of a Wnt-regulated gene), thereby stimulating IL-1 $\beta$  production in TME of colon cancer (Kaler, Augenlicht et al. 2012). These studies demonstrated an exciting bidirectional role of Wnt signaling in tumor cells – TAMs crosstalk. Another study by Loilome et al., showed that crosstalk of cholangiocarcinoma cells with Wnt-secreting inflammatory TAMs maintains activated state of Wnt signaling in tumor cells (Loilome, Bungkanjana et al. 2014). Macrophage-specific RelA/p65 induced TNF- $\alpha$  promotes Wnt signaling in gastric and lung tumor cells through inhibition of GSK3 $\beta$ , which may contribute to tumorigenesis (Oguma, Oshima et al. 2008, Li, Beisswenger et al. 2013).

### **1.8.4 Role of tissue-resident macrophages – specific Wnt/ $\beta$ -catenin signaling**

TAMs have resulted from the differentiation of bone marrow monocytes to macrophages (BMDMs) and the expansion of tissue-resident macrophages. Both the TAMs play a significant role in cancer development. The genetic ablation of myeloid-specific recombination signal binding protein-Jk (RBPj)-mediated Notch signaling attenuates differentiation of BMDMs, but TAM populations with kupffer cells-like phenotype (liver tissue-resident macrophages) are expanded via proliferation and constituted an another source of M2-like TAMs to facilitate tumor growth and metastasis in hepatocellular carcinoma (HCC) (Zhao, Huang et al. 2016). Yu-Chen et al. showed that lack of RBPj- mediated Notch signaling activates Wnt signaling in

kupffer cells, regulating the expansion of these kupffer cells -like TAMs in HCCs (Ye, Zhao et al. 2019). Brain tissue-resident macrophages - microglia also promote invasion and colonization of brain tissue by breast cancer cells in a Wnt-dependent way, serving both as active transporters and guiding rails (Pukrop, Dehghani et al. 2010).

The above mentioned experimental studies have demonstrated the immunomodulatory role of tumor cell and TAMs-specific Wnt signaling in various cancer, but the transcriptional regulation of  $\beta$ -catenin mediated Wnt signaling in TAMs' activation and immune evasion resulting in cancer development is still unanswered. Unraveling the transcriptional role of  $\beta$ -catenin in TAMs' biology is needed to develop a safe and effective immuno-therapeutic approach targeting Wnt signaling.

## **1.9 FOS Like 2 (FOSL2)**

The Fos gene family comprises of 4 members: FOS, FOSB, FOSL1, and FOSL2; these leucine zipper proteins dimerize with JUN family proteins, thereby forming the transcription factor complex AP-1. FOS proteins are implicated as regulators of cell proliferation, differentiation, and transformation. Gene Ontology (GO) annotations related to FOSL2 include *DNA-binding transcription factor activity* and *RNA polymerase II regulatory region sequence-specific DNA binding*. FOSL2 (FOS Like 2, AP-1 Transcription Factor Subunit) found to be associated with diseases such as lipodystrophy and congenital generalized, Type 3. FOSL2 is also actively involved in IL1 family signaling pathways (Acuner Ozbabacan, Gursoy et al. 2014).

### **1.9.1 Role of FOSL2 in cancer and macrophages**

Until now, very few studies reported the role of FOSL2 in cancer development and progression. The overexpression of FOSL2 correlates with poor prognosis of breast, colon, and tongue cancer (Langer, Singer et al. 2006, Gupta, Kumar et al. 2015, Li, Fang et al. 2018). In NSCLC, FOSL2 positively regulates TGF $\beta$  signaling, thereby increasing growth and metastasis (Wang, Sun et al. 2014). FOSL2 is also found to upregulate CCR4 expression in adult T cell leukemia resulting in increased proliferation (Nakayama, Hieshima et al. 2008). Some studies reported inhibition of FOSL2 by miRNAs such as – (i) FOSL2 is downregulated by miR-597, resulting in inhibition of proliferation, migration, and invasion of breast tumor cells (He, Mai et al. 2017); (ii) miR-124-3p suppress aggressiveness of glioma (Luo, Chi et al. 2018); (iii) miR-143-3p restricts the proliferation, migration, and invasion of osteosarcoma by downregulating FOSL2 (Sun, Dai et al. 2018); and (iv) in hepatocellular carcinoma FOSL2 inhibited by miR-133a thereby regulating oncogenic potential of TGF $\beta$  signaling.

In the context of macrophages, the analysis of transcriptional landscapes of the macrophages associated with inflammatory bowel disease (Baillie, Arner et al. 2017), *Mycobacterium tuberculosis* infection (Roy, Schmeier et al. 2018) and skeletal muscle regeneration (Varga, Mounier et al. 2016) reported the transcriptional role of FOSL2 in genes responsible for inflammation, resolution and tissue repair. The deepCAGE transcriptome analysis of M1 and M2 macrophages (mice BM-derived macrophages) predicted that FOSL2 plays a significant role in the activation of M2 macrophage genes. Recently, Masuda *et al.* demonstrated an expression correlation between FOSL2 and mesenchymal genes in the TME of glioblastoma (Cooper, Gutman et al. 2012). However, the transcriptional regulation and role of FOSL2 in various malignancies is still poorly understood.

### **1.10 AT-Rich Interaction Domain 5A (ARID5A)**

ARID5A is a member of the ARID protein family (contains 7 subfamilies and 15 members), which have diverse functions in development, tissue-specific gene expression, and regulation of cell growth. Gene Ontology (GO) annotations related to ARID5A include *chromatin binding* and *transcription regulatory region DNA binding*. ARID5A binds to AT-rich stretches in the modulator region upstream of the human cytomegalovirus significant intermediate early gene enhancer and may act as a repressor and downregulate enhancer-dependent gene expression (Huang, Oka et al. 1996). ARID5A is implicated in positive regulation of chondrocyte-specific transcription such as of COL2A1 in collaboration with SOX9. This mechanism leads to stimulation of early-stage chondrocyte differentiation and inhibition of later stage differentiation. It is also proposed that it acts as a corepressor for selective nuclear hormone receptors via repression of ESR1-mediated transcriptional activation (Georgescu, Li et al. 2005)

#### **1.10.1 Role of ARID5A in cancer and macrophages**

Accumulating evidence suggested that ARID family members show high mutations, differential expression, and involvement in cancer-related signaling pathways; because of their ability to regulate transcription of the genes associated with cell differentiation and proliferation. The members of ARID family acts as a tumor suppressor (e. g. ARID1, ARID2), tumor promotor (e. g. ARID3, JAIRD2), or as both (e.g., ARID4, JAIRD1) (Lin, Song et al. 2014).

ARID5A and ARID5B are members of subfamily ARID5. The precise role of both the members in cancer development is unknown. Some studies reported mutations and single nucleotide polymorphisms in ARID5B in the case of acute lymphoblastic leukemia in childhood and adults

(Peyrouze, Guihard et al. 2012, Xu, Cheng et al. 2012, Linabery, Blommer et al. 2013, Rudant, Orsi et al. 2013), however, until now the role of ARID5A in cancer has not been reported. Recent studies in inflammatory diseases like autoimmune diseases and septic shock provided insight into the role of macrophage-specific ARID5A in promotion of inflammatory processes via its RNA-binding capacity. ARID5A stabilizes inflammation-related mRNAs, such as IL6, STAT3, and TBX21, to potentiate the inflammatory response (Masuda, Ripley et al. 2013, Higa, Oka et al. 2018, Masuda and Kishimoto 2018, Wammers, Schupp et al. 2018). However, the transcriptional regulation and the roles of ARID5A under various physiological and pathological conditions are still unknown.

## 2. AIMS OF THE STUDY

The interaction of tumor cells with tumor-infiltrating immune cells ultimately determines whether a tumor progresses, metastasizes, responds to therapy, or acquires drug resistance. Among tumor-infiltrating immune cells, M2-like Tumor-Associated Macrophages (TAMs) play a critical role in all stages of tumor development and frequently antagonize the response to therapy. Different mechanisms are involved in the accumulation of TAMs at the tumor sites such as - TME-mediated monocyte to macrophage differentiation, polarization into different TAMs' subsets, and inter-conversion within the subgroups. The phenotypic transition of tumor-inhibiting M1-like TAMs to tumor-promoting M2-like TAMs is one of the crucial events responsible for activation of pro-tumor macrophages in TME, but the underlying molecular mechanisms remain poorly characterized.

The present study has performed to decipher the TAMs-specific signal transduction pathways responsible for phenotypic switch of M2-like TAMs into M1-like TAMs. We set the following central aims to conduct this study:

1. Establishment and characterization of tumor cells-macrophages *in vitro* co-culture models to mimic the phenotypic switches within TAMs in the presence of tumor cells
2. Identification and validation of lung TAMs-specific signal transduction pathways
3. *In vitro* manipulation of the identified targets by different genetic and pharmacological strategies
4. To test the *in vivo* relevance of manipulation of identified targets by different genetic (macrophage-specific knockout mice) and pharmacological (small molecule inhibitors) strategies
5. Elucidation of molecular mechanisms regulated by the identified therapeutic targets
6. Determination of the clinical relevance of the study

These aims were accomplished using *ex vivo* TAMs from human lung cancer patients, co-culture models for *in vitro* training of TAMs, pathway-specific inhibitors, RNA-interference tools, and pathway-specific macrophage-specific knockout mice.

### **3. MATERIALS AND METHODS**

#### **3.1 Experimental procedures – Cell culture**

##### **3.1.1 Cancer cell lines**

Human lung cancer cell lines A549 (ATCC® CRL-5800™), A427 (ATCC® HTB-53™), H1650 (ATCC® CRL-5883™), human monocyte cell line THP1 (ATCC® TIB-202™) and mouse lung cancer cell line LLC1 (ATCC® CRL-1642™) were purchased from the American Type Culture Collection (ATCC, Manassas, USA) and cultured according to the manufacturer's instructions. Dulbecco's Modified Eagle Medium F12 (DMEM, 41965-039), Roswell Park Memorial Institute 1640 (21875-034), HEPES (15630), trypsin 10× (25200056), fetal calf serum (FCS, 10500-064), 0.1 mg/ml penicillin (100U/ml) /streptomycin (P/S, 15140-122), , phosphate-buffered saline (PBS, 14190-094) and all cell culture materials (e.g. cell culture flasks) were purchased from Gibco® life technologies, Grand Island, USA. Trypan blue (T6146), DMSO (D2438) was purchased from Sigma-Aldrich, St. Louis, USA.

A549, A427 cells were cultured in DMEM supplemented with 10% FCS and 1% P/S. THP1, H1650, LLC1 cells were cultured in RPMI supplemented with 10% FCS, 1% P/S, and 5% HEPES. LLC1 cells cultured in RPMI supplemented with 10% FCS and 1% P/S. For *in vitro* and *in vivo* experiments, cells were trypsinized by 1X trypsin and then resuspended in respective fresh medium. The cell viability was analyzed by trypan blue staining. The cells were counted by cell counter (TC20™ automated cell counter, Bio-rad, Steenvoorde, France), and the seeding density was adjusted according to an experiment by dilution with the necessary amount of fresh media.

##### **3.1.2 Primary cancer cell culture**

The University of Giessen Biobank provided lung tumors. The primary tumor cells were isolated, characterized, and maintained by our lab. Cells were grown in DMEM medium supplemented with sodium selenite, ethanolamine, phosphoryl ethanolamine, sodium pyruvate, adenine, and HEPES. They were kept for a maximum of 7–8 passages.

##### **3.1.3 Generation of human macrophages from buffy coats**

Human macrophages were differentiated from peripheral blood mononuclear cells (PBMCs), isolated from buffy coats obtained from the blood bank of the Universities of Giessen and Marburg Lung Center using Ficoll gradient centrifugation. The Lucosep tubes (227290, Sarstedt, Nümbrecht, Germany) filled with 15mL of Ficoll (L6115, BIOCROLL Biochrom AG, Berlin, Germany), and then approximately 40 mL blood overlaid. After centrifugation without a break for 30 min at 440g, the interphase of white blood cells was transferred in a new 50mL falcon and centrifuged for 8 min at 1600rpm to pellet down. The pellet was resuspended in 50 mL 1X red blood cells (RBC) lysis Buffer (555899, BD Biosciences, Tullastraße, Heidelberg) and centrifuged for 8 min at 1600rpm. The pellet washed with thrice with 50 mL 1X PBS by centrifuging at for 8 min at 1600rpm. The pellet from 1 buffy coat was resuspended in 150mL of RPMI supplemented with 1% P/S and seeded in tissue culture-treated 6-well plates or 10cm<sup>2</sup> dishes (83.3920.300, Sarstedt, Nümbrecht, Germany). After culturing the PBMCs for 1 h, non-adherent cells were removed, and cells were cultured in macrophage medium (RPMI-1640 medium supplemented with 2% human serum and 1% P/S) for seven days to allow differentiation from monocytes to macrophages. The medium changed on alternate days with the RPMI medium supplemented with macrophage medium. The density of macrophages was roughly  $1 \times 10^5$  cells per well in six-well dishes.

### **3.1.4 Generation of THP1-derived human macrophages**

THP1 cells were treated with 10 ng/mL phorbol 12-myristate-12 acetate (PMA, P1585, Sigma-Aldrich, St. Louis, USA) for 24 h, then removed for 24 h before differentiation.

### **3.1.5 Generation of mouse macrophages from bone marrow-derived cells**

For mouse macrophages, tibia and femurs were dissected from 5 to 7-week old mice, and each bone was subsequently flushed thrice with 5 mL RPMI-1640 medium supplemented with 1% P/S. The RBC-depleted cells were passed through a 40- $\mu$ M cell strainer (CLS431750-50EA, Merck, Darmstadt, Germany), centrifuged, and resuspended in RPMI medium supplemented with 10% FCS, 1% P/S, and 20 ng/mL mouse macrophage-colony stimulating factor (M-CSF, 416-ML, R and D Systems, Minneapolis, USA) and plated in six-well plate. The medium changed on alternate days with RPMI medium supplemented with 10% FCS, 1% P/S, and 20 ng/mL mouse M-CSF until undifferentiated macrophages obtained.

### 3.1.6 Activation of M1 and M2 macrophages from undifferentiated M0 macrophages

Human, THP1-derived, and mouse macrophages (M0) activated or polarised by cytokine stimulations. M1 macrophages were obtained through M0 stimulation with 100 ng/mL lipopolysaccharide (LPS, L5418, Sigma-Aldrich, St. Louis, USA) and 100 U/mL interferony (IFN $\gamma$ , 285-IF, R and D Systems, Minneapolis, USA) for 24 h, whereas M2 macrophages were stimulated with 20 ng/mL IL4 (204-IL, R and D Systems, Minneapolis, USA) for 24 h (Schmall, Al-Tamari et al. 2015, Pullamsetti, Kojonazarov et al. 2017).

### 3.1.7 Generation of *in-vitro*-trained TAMs

Cancer cells were harvested with trypsin, washed once with tumor cell medium (supplemented with 10% FCS and 1% P/S), and subsequently resuspended in macrophage medium. Macrophages and tumor cells were cultured in a 1:1 ratio in macrophage medium for 72 h. Then, the medium in the culture dish discarded. The remaining tumor cells were detached using trypsin and removed from the culture dish. The macrophages in the wells were washed thrice with macrophage medium, and further incubated in macrophage medium for 1 h at 37°C. Subsequently, new tumor cells added to the culture dish containing macrophages (previously cultured with tumor cells for 48 h) in a 1:1 ratio for further 48 h (**Figure 6A**). The medium in the culture dish discarded to obtain pure macrophages at the end of the co-culture. The remaining tumor cells were detached using trypsin and removed from the culture dish (Weichand, Popp et al. 2017, Ringleb, Strack et al. 2018).

Co-culture was performed with M0 macrophages labeled with Red PKH dye (PKH26, PKH26GL, Sigma-Aldrich, St. Louis, USA) and tumor cells with Green PKH dye (PKH267, PKH67GL, Sigma-Aldrich, St. Louis, USA) to check the efficiency of trypsinization to yield pure macrophages after co-culture. Labelling was done as per the manufacturer's protocol. In brief, cells were resuspended in diluent C (500 $\mu$ L/5 million cells) to make 2x cell suspension. Similarly, the 2X dye solution was prepared by mixing PKH dye and diluent C. Cell suspension and dye solution mixed and incubated for 5 min at RT in darkness. 1 mL media with BSA (A9478, Sigma-Aldrich, St. Louis, USA) 5% was added and incubated for 1 min to stop the reaction of labeling. Cells were washed with medium for 3 times. The cells were co-cultured for the time points mentioned above. Followed by co-culture, macrophages, and tumor cells were separated from each other by 5 mins of trypsinization. As shown in **Figure**, trypsinization yielded around 90-95%

pure macrophages, but tumor cells were mixed with macrophages, which was then confirmed by FACS (**Figure 6B, 6C**).

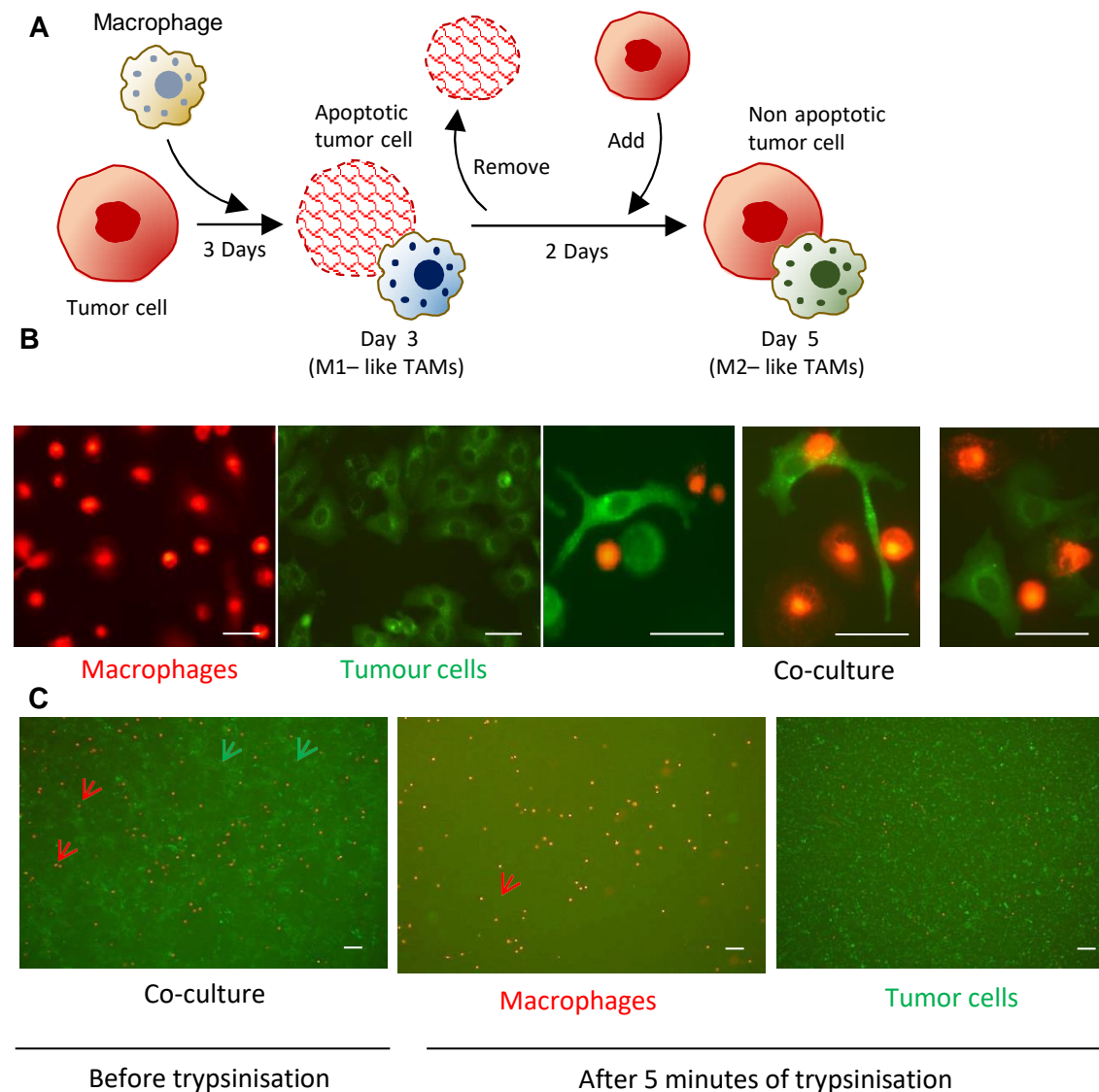


**Figure 6: Generation of *in vitro* trained TAMs and efficiency of trypsinization to yield pure macrophages from the co-culture. (A)** Schematic experimental plan showing the generation of TAMs *in vitro*. M1-like TAMs generated by directly co-culturing undifferentiated PBMC-derived macrophages (M0) and A549 cells for 72 h (3 days), followed by removal of apoptotic cancer cells and addition of new A549 cells. Co-culture continued for the next 48 h (5 days), which found to generate M2-like TAMs (“training”). **(B)** Red PKH26 dye labeled-macrophages and Green PKH67 dye labeled-tumor cells co-cultured for a specified time point (Scale bar: 10µM for macrophages and tumor cells and 20µM for co-culture). **(C)** Representative images were showing the co-culture of macrophages and tumor cells before trypsinization and after trypsinization (Scale bar: 5µM).

### 3.2 Experimental procedures – Cell isolation from human and mouse lung tissue

### 3.2.1 Human lung tissues

Lung tissue specimens obtained in the RPMI medium supplemented with 10 µg/mL cycloheximide (C4859, Sigma-Aldrich, St. Louis, USA) from the Institute for Pathology (Giessen, Germany). Tissue specimens were stored at 4°C on the day of collection and processed on the following day. The study protocol for tissue donation was approved by the ethics committee (“Ethik Kommission am Fachbereich Humannmedizin der Justus Liebig Universität Giessen”) of the University Hospital Giessen (Giessen, Germany), by national law and “Good Clinical Practice/International Conference on Harmonisation” guidelines. A written informed consent provided by each patient or the patient’s next of kin (AZ 58/15). Patient characteristics are shown in **Table 3**.

<b>Samples</b>	<b>Primary tissue</b>	<b>Histology-reduced (WHO categories based on diagnosis reported in surgical pathology report)</b>	<b>Sex</b>	<b>Age at Surgery (Years)</b>	<b>Tumor Stage</b>
1	Lung	Squamous cell carcinoma G3	M	65	pM1 R0
2	Lung	Squamous cell carcinoma G3	F	78	pT3, N0(0/13) L0 V1 R0
3	Lung	Squamous cell carcinoma G3	F	64	pT4 N0(0/21) L0 V0 R0
4	Lung	Squamous cell carcinoma G2	M	76	pT2a N0(0/13) L0 V0 R0
5	Lung	Squamous cell carcinoma G2	M	60	pM1 (PUL, LYM) L0 V0
6	Lung	Bronchopulmonary adenocarcinoma G3	F	64	pT2b N0(0/29) L1 V0 Rx
7	Lung	Bronchopulmonary adenocarcinoma G3	M	63	pT3 n1 (1/16) LX V0 R0
8	Lung	Bronchopulmonary adenocarcinoma G2	F	75	pT2a N0 (0/19) L0 V0 R0
9	Lung	Squamous cell carcinoma G2	F	73	pT2b N0 (0/21) L0 V0 R0

10	Lung	Squamous cell carcinoma G3	M	75	pT2a N3 (6/6) LX V0 R0
11	Lung	Bronchopulmonary adenocarcinoma G2	M	61	pT3 N1 (5/5) L0 V0 R0
12	Lung	Squamous cell carcinoma G2	F	74	pT2a N0(0/20) L0 V0 R0

**Table 3: Patients characteristics.**

### 3.2.2 Mouse lung tissues

Mouse LLC1 cells ( $1 \times 10^6$ ) were intravenously injected (24g needle, 0.55 × 25 mm, Neolus, Terumo Europe, Leuven, Belgium) into C57BL/6 mice. On day 20, the mice sacrificed, and lung harvested as previously described (Schmall, Al-Tamari et al. 2015).

### 3.2.3 MACS sorting of *ex-vivo* TAMs from human lung tissues

Human lung tumor single-cell suspensions were prepared using the Tumor Dissociation Kit (130-095-929, Miltenyi Biotec, Bergisch Gladbach, Germany) according to the manufacturer's instructions as follows,

Tissue (g)	Enzyme mix			
	0.05 – 0.2 g	2.2 mL RPMI 1640	100 $\mu$ L Enzyme H	50 $\mu$ L Enzyme R
0.2 – 1.0 g	4.7 mL RPMI 1640	200 $\mu$ L Enzyme H	100 $\mu$ L Enzyme R	25 $\mu$ L Enzyme A

**Table 4: Volume of enzyme mix components according to the weight of tissue**

The enzyme mix prepared according to **table 4** into gentleMACS™ C Tube (130-093-237, Miltenyi Biotec, Bergisch Gladbach, Germany). Fat, fibrous areas were removed from the tumor sample and chopped into small pieces of 2–4 mm and transferred into gentleMACS™ C Tube. Tubes kept on gentleMACS Dissociator (Miltenyi Biotec, Bergisch Gladbach, Germany) upside down. First, the gentleMACS program h\_tumor\_01 was run, followed by incubation of sample for 20 minutes at 37 °C under continuous rotation using the MACSmix™ Tube Rotator (Miltenyi Biotec, Bergisch Gladbach, Germany). Then, gentleMACS Program h\_tumor\_02 was run, followed by

short centrifugation and application of samples to a MACS SmartStrainer (30  $\mu\text{m}$ , 130-098-458, Miltenyi Biotec, Bergisch Gladbach, Germany) placed on a 50 mL tube. MACS SmartStrainer washed with 20 mL of RPMI. Cells were collected with centrifugation at 300 $\times$ g for 7 minutes. RBC was lysed by 1X RBC Lysis Solution for 15 min and centrifugation at 300 $\times$ g for 7 minutes. The cell pellet washed with 20 mL of RPMI 1640 and resuspended as required for further applications.

Macrophages from single-cell suspensions magnetically sorted by primary antibody, CD68-PE human (130-096-807, Miltenyi Biotec, Bergisch Gladbach, Germany) and secondary antibody, Anti-PE MicroBeads (130-048-801, Miltenyi Biotec, Bergisch Gladbach, Germany) according to the instructions provided by the manufacturer. In brief,  $10^7$  cells were washed by adding 1–2 mL of buffer and centrifugation at 300 $\times$ g for 10 min. Cells pellet was resuspended in 100  $\mu\text{L}$  of buffer and add 10 $\mu\text{L}$  of CD68-PE antibody and incubated for 10 min in the dark in the refrigerator (2-8°C). 1-2mL of buffer per  $10^7$  cells were added and centrifuged at 300 $\times$ g for 10 min to remove unbound primary antibody. Then cell pellet resuspended as 80 $\mu\text{L}$  and 20 $\mu\text{L}$  Anti-PE microbeads of buffer per  $10^7$  cells and incubated for 15 min in the dark in the refrigerator (2-8°C). Again, to remove unbound antibody, 1-2mL of buffer per  $10^7$  cells were added and centrifuged at 300 $\times$ g for 10 min. Pellet was resuspended as required for further applications.

### **3.2.3 MACS sorting of *ex vivo* TAMs from mouse lung tumor tissues**

Mouse tumor tissues were fragmented in small pieces, followed by digestion with collagenase (5  $\mu\text{g}/\mu\text{L}$ , C9891, Sigma-Aldrich, St. Louis, USA) supplemented with DNase (10  $\mu\text{g}/\mu\text{L}$ , 04536282001, Roche Diagnostics GmbH, Mannheim, Germany) for 30 min at 37°C. Further tissue extract passed through the cell strainer and treated with red bloodcell lysis buffer. Subsequently, cells were centrifuged and suspended in MACS buffer [by diluting MACS BSA (130-091-376) 1:20 with autoMACS™ Rinsing Solution (130-091-222)], supplemented with 5% BSA. Macrophages from single-cell suspensions were magnetically sorted using primary antibody F4/80-PE mouse (130-102-422, Miltenyi Biotec, Bergisch Gladbach, Germany) and secondary antibody Anti-PE MicroBeads (Miltenyi Biotec, Bergisch Gladbach, Germany), according to the manufacturer' instructions described in 3.2.3.

### 3.2.4 Flow cytometry and cell sorting

Single-cell suspensions were blocked with FcR blocking reagent (Human – 130-059-901, Mouse – 130-092-575, Miltenyi Biotec, Bergisch Gladbach, Germany) in 0.5% PBS-BSA for 20 min, stained with fluorochrome-conjugated antibodies, and analyzed on a LSR II/Fortessa flow cytometer or sorted using a FACS Aria III cell sorter (BD Biosciences, California, USA). Data were analyzed using FlowJo V10. All antibodies and secondary reagents were titrated to determine optimal concentrations. Comp-Beads (552843, BD Biosciences) used for single-color compensation to create multicolor compensation matrices. For gating, fluorescence minus one control used. Instrument calibration was controlled daily using Cytometer Setup and Tracking beads (BD Biosciences, California, USA). Anti-CD206-FITC (51135, BD Biosciences) antibody used for characterization and sorting of human macrophages, single-cell suspensions were stained with the following antibodies: anti-CD33-BV510 (744351, BD Biosciences), anti-CD45-AlexaFluor700 (560510, BD Biosciences), anti-CD64-BV605 (740406, BD Biosciences), anti-CD83-BV711 (740802, BD Biosciences), and anti-CD163-PE (326505, BioLegend, Koblenz, Germany), anti-CD206-PE-Cy7 (141719, BioLegend), and anti-CD326-FITC (324203, BioLegend,). For the exclusion of dead cells, 7-AAD used.

### 3.3 Experimental procedures – Treatment and transfection of cells

#### 3.3.1 Treatment with XAV939

In this project, we different type of cells were treated with varying concentrations of XAV939 (3748, Tocris, Wiesbaden-Nordenstadt, Germany) - (i) *in-vitro trained M1- like TAMs and M2-like TAMs* treated with 5 $\mu$ M of XAV939 for 24 hours; (ii) *ex vivo TAMs from human and mouse lung tumor tissues* treated with 5 $\mu$ M of XAV939 for 24 hours; (iii) to study effect of different concentrations of XAV939 directly on A549 cells and of CM from XAV939 treated M2-like TAMs, A549 cells treated with 1, 2, 4, 8, 16, 32, 64, 128  $\mu$ M and *in-vitro trained M2-like TAMs* 1, 2, 4, 8  $\mu$ M for 24 hours as per previous studies (Li, Zheng et al. 2018, Stakheev, Taborska et al. 2019) for 24 h at 37°C.

#### 3.3.2 Transfection with siRNA and shRNA

Macrophages were transfected with different siRNA using Hiperfect Transfection Reagent (371707, Qiagen, Hilden, Germany) in OPTI-MEM serum-free medium (11058021, Sigma-Aldrich, St. Louis, USA).  $\beta$ -catenin siRNA, FOSL2 siRNA, and all-star

negative siRNA as non-silencing control obtained from Qiagen (Qiagen, Hilden, Germany) (**Table 5**). According to the protocol provided by the manufacturer, the cells were transfected with siRNAs for 6 h in a serum-free medium. After 6 h, the cells cultured in serum-containing macrophage medium for 24 h.

Gene	Product	Catalogue number	Target sequence
$\beta$ -catenin	Hs_CTNNB1_9	SI04379662	CAGGATGAATCCTAGCTATCGT
FOSL2	Hs_FOSL2_5	SI02780379	GCGGATCATGTACCAGGATTA

**Table 5: siRNA details**

For shRNA, macrophages were transfected with different shRNA using the jetPEI™-Macrophag kit (103-05N, Polyplus Transfection, Illkirch-Graffenstaden, France).  $\beta$ -catenin shRNA, EG5 positive control shRNA, and non-silencing shRNA obtained from GE Dharmacon (Lafayette, CO, USA) (**Table 6**). According to the protocol provided by the transfection manufacturer, shRNA (1.5  $\mu$ g) and transfection reagent (3  $\mu$ L) mixed in one well of a six-well plate and incubated for 30 min at room temperature to form complexes. Subsequently, serum-containing medium added dropwise to the mixture and incubated for 24 h at 37°C to transfect the cells.

Gene	Product Name	Catalog number	Company
$\beta$ -catenin	GIPZ Human CTNNB1 shRNA (Glycerol stock)	RHS4430	GE Dharmacon
EG5	GIPZ EG5 Lentiviral shRNA Positive Control (Glycerol stock)	RHS4480	GE Dharmacon
NS	GIPZ Non-silencing Lentiviral shRNA Control (Glycerol stock)	RHS4346	GE Dharmacon

**Table 6: shRNA details**

### 3.3.3 Transfection with plasmids

M2-like TAMs were transfected with different plasmids ( $\beta$ -catenin, ARID5A) using the Viromer® RED kit (VR-01LB-00, Lipocalyx, Halle, Germany). The  $\beta$ -catenin, ARID5A, and negative plasmid obtained from GeneCopoeia (Rockville, MD, USA) (**Table 7**). Before transfection, cells were serum-starved for 24 h. According to the protocol provided by the manufacturer, plasmid (2  $\mu$ g) and transfection reagent (2.4  $\mu$ L) mixed in a six-well

plate and incubated for 30 min at room temperature to form complexes. Subsequently, serum-containing medium added dropwise to the transfection mixture and incubated for 24 h at 37°C (Ringleb, Strack et al. 2018).

Gene	Product Name	Catalog number	Company
$\beta$ -catenin	ORF expression clone for CTNNB1 (NM_001330729.1) (Purified plasmid)	EX-I4822-M03	Gene Copeia
ARID5A	ORF expression clone for ARID5A (NM_001319092.1) (Purified plasmid)	EX-Y5502-M03	Gene Copeia
NS	Empty control vector for pReceiver-M03	EX-NEG-M03	Gene Copeia

**Table 7: Plasmid details**

### 3.4 Experimental procedures – Molecular Biology

#### 3.4.1 RNA isolation, complementary DNA synthesis, and quantitative polymerase chain reaction (quantitative PCR)

Total mRNA was extracted from cells utilizing the miRNeasy Micro Kit (217084, Qiagen, Hilden, Germany). Further, RNA was subsequently transcribed into complementary DNA using the Applied Biosystem' kit according to the manufacturer's instructions. Quantitative PCR performed with SYBER Green Supermix (A25742, Thermo Fisher Scientific GmbH, Dreieich, Germany). Intron-spanning human and mouse-specific primers genes designed using sequence information from the National Center for Biotechnology Information database and purchased from Sigma-Aldrich, St. Louis, USA. Expression was determined using the  $\Delta$ Ct method. The Ct values were normalized to the housekeeping gene encoding HPRT using equation  $\Delta$ Ct = Ct<sub>reference</sub> - Ct<sub>target</sub> and expressed as  $\Delta$ Ct. The primer sequences used in the study shown in **Tables 8 and 9**.

Gene		Sequence (5'–3')	Accession No.
HPRT	FP	TGACACTGGCAAACAATGCA	NM_000194
	RP	GGTCCTTTTCACCAGCAAGCT	
WNT1	FP	GCGTCTGATACGCCAAAATC	NM_005430
	RP	GGATTTCGATGGAACCTTCTG	

WNT 4	FP	CCTTCGTGTACGCCATCTCT	NM_030761
	RP	GCCTCATTGTTGTGGAGGTT	
WNT5A	FP	CCACATGCAGTACATCGGAG	NM_003392
	RP	CACTCTCGTAGGAGCCCTTG	
WNT7A	FP	AGTACAACGAGGCCGTTTAC	NM_00462
	RP	GCACGTGTTGCACTTGACAT	
WNT7B	FP	AAGCTCGGAGCACTGTCATC	NM_058238
	RP	CCCTCGGCTTGGTTGTAGTA	
WNT10B	FP	GCAAGAGTTTCCCCACTCT	NM_003394
	RP	GATTGCGGTTGTGGGTATC	
WNT11	FP	TTGCTTGACCTGGAGAGAGG	NM_004626
	RP	GACGAGTTCCGAGTCCTTCA	
FZD1	FP	GTGAGCCGACCAAGGTGTAT	NM_003505
	RP	CAGCCGGACAAGAAGATGAT	
FZD2	FP	GCGTCTTCTCCGTGCTCTAC	NM_001466
	RP	CTGTTGGTGAGGCGAGTGTA	
FZD4	FP	AACCTCGGCTACAACGTGAC	NM_012193
	RP	GTTGTGGTCGTTCTGTGGTG	
FZD5	FP	CTTGTTTCAAAGTCCAATCAAGTG	NM_003468
	RP	GCCTACTCTTACCCTTCTTTAACG	
FZD6	FP	ATTTTGGTGTCCAAGGCATC	NM_003506
	RP	TATTGCAGGCTGTGCTATCG	
FZD8	FP	TCTTGTCGCTCACATGGTTC	NM_031866
	RP	GTAGAGCACGGTGAACAGG	
FZD9	FP	CGCTGGTCTTCTACTGCTC	NM_003508
	RP	AGAAGACCCCGATCTTGACC	
DVL1	FP	GCTGACGGTGAAGAGTGA	NM_001330311
	RP	GCATTGGCGATGGTGAT	
DVL2	FP	GCCTATCCAGGTTCCCTCCTC	NM_004422
	RP	AGAGCCAGTCAACCACATCC	
DVL3	FP	CACAGCGAAGGCAGTCGG	NM_004423
	RP	TGCTCACATCACATCCACAAAG	
TNKS1	FP	ATGCCCCAGAGGCCTTAC	NM_003747
	RP	GGTGGATGCTGGTGAGATCA	
TNKS2	FP	ATCTGCTCTGCCCTCTTGTTACAA	NM_025235

	RP	GCTAAAATCTACTCCTGGAACCTC	
CCND1	FP	TATTGCGCTGCTACCGTTGA	NM_053056
	RP	CCAATAGCAGCAAACAATGTGAAA	
TNF $\alpha$	FP	GAGGCCAAGCCCTGGTATG	NM_000594
	RP	CGGGCCGATTGATCTCAGC	
IL1B	FP	CTAAACAGATGAAGTGCTCC	NM_000576
	RP	GGTCATTCTCCTGGAAGG	
IL8	FP	ACAGCAGAGCACACAAGCTTC	NM_000584
	RP	ATCAGGAAGGCTGCCAAGAG	
CCR7	FP	GCTGGTGGTGGCTCTCCTT	NM_001838
	RP	GTAATCGTCCGTGACCTCATCTT	
ALOX15	FP	CTTCAAGCTTATAATTCCCCAC	NM_001140
	RP	GATTCCTTCCACATACCGATAG	
IL10	FP	GAGGCTACGGCGCTGTCA	NM_000572
	RP	TCCACGGCCTTGCTCTTG	
IL1R1	FP	CCTGCTATGATTTTCTCCCAATAAA	NM_000877
	RP	CACAAAATATCACAGTCAGAGGTAGAC	
CD163	FP	AGCATGGAAGCGGTCTCTGTGATT	NM_003416
	RP	AGCTGACTCATTCCCACGACAAGA	
CD206	FP	ACAACAAAAGCTGACACAAGGA	NM_002438.4
	RP	AGGACAGACCAGTACAATTCAG	
TGFB1	FP	GCAGCACGTGGAGCTGTA	NM_000660
	RP	CAGCCGGTTGCTGAGGTA	
FOSL2	FP	GCCCAGTGTGCAAGATTAGC	NM_005253.4
	RP	GGGCTCCTGTTTCACCACTA	
ARID5A	FP	GTCTTGGGCCAGTAAGGAGTG	NM_001319092.1
	RP	AGGACCAGCCTCTCGTAGT	

Table 8: Sequence of human primers

Gene		Sequence (5'–3')	Accession No.
HPRT	FP	GCTGACCTGCTGGATTACAT	NM_013556
	RP	TTGGGGCTGTACTGCTTAAC	
CCND1	FP	GGGCAGCCCCAACAACCTTCC	NM_007631
	RP	TCCTCAGTGGCCTTGGGGTC	

TNF $\alpha$	FP	CATCTTCTCAAATTCGAGTGACAA	NM_013693
	RP	TGGGAGTAGACAAGGTACAACCC	
IL1B	FP	ACCCCAAAGATGAAGGGCTG	NM_008361
	RP	TACTGCCTGCCTGAAGCTCT	
iNOS	FP	CACCAAGCTGAACTTGAGCG	NM_001313922
	RP	CCATAGGAAAAGACTGCACCG	
IL10	FP	CAGAGAAGCATGGCCCAGA	NM_010548
	RP	TGCTCCACTGCCTTGCTCTTA	
Arginase1	FP	GGTTCTGGGAGGCCTATCTT	NM_007482
	RP	CACCTCCTCTGCTGTCTTCC	
Chitinase 1	FP	CCCTGGGTCTCGAGGAAGCCC	NM_009892
	RP	GCAGCCTTGAATGTCTTTCTCCAC	
FOSL2	FP	CCAGCAGAAGTTCCGGGTAG	NM_008037
	RP	GTAGGGATGTGAGCGTGGATA	
ARID5A	FP	CAGCACCTCCGGCCAAA	NM_001290726
	RP	CTTGAAGCCAAGATGGGGCA	
FOXJ3	FP	GCGGCCCCGGATGTT	NM_172699
	RP	GGAGTTGAGGCCCGTTCTAC	
TFEC	FP	AGGTTATGAGACGAGGGGCT	NM_031198
	RP	CCTGGACCAGCACTGATTGG	
PRDM1	FP	TGCTTATCCCAGCACCCC	NM_007548
	RP	CTTCAGGTTGGAGAGCTGACC	
RBPJ	FP	ATCCATCTCTTGGACGACGAC	NM_001359152
	RP	CTGCATGTCACACCTGCACT	
TFEB	FP	GCAGAAGAAAGACAATCACAA	NM_001161723
	RP	GCCTTGGGGATCAGCATT	
RELB	FP	CTTTGCCTATGATCCTTCTGC	NM_001290457
	RP	GAGTCCAGTGATAGGGGCTCT	
BATF	FP	CTGGCAAACAGGACTCATCTG	NM_016767
	RP	GGGTGTCGGCTTTCTGTGTC	

Table 9: Sequence of mouse primers

### 3.4.2 Western blotting

Cells were lysed in radioimmunoprecipitation assay lysis buffer (RIPA, R0278, Sigma-Aldrich, St. Louis, USA) containing protease and phosphatase inhibitors. Subsequently, the lysate cleared through high-speed centrifugation. Proteins separated using 10% polyacrylamide gels and transferred to polyvinylidene difluoride membranes (PVDF, 1620177, Bio-Rad, California, USA). After blocking with 5% milk, the membranes incubated with one of the following primary antibodies overnight at 4°C on a rotating platform. After washing with Tris-buffered saline and Tween 20, the blots incubated with secondary antibodies conjugated to horseradish peroxidase. Bound protein-antibody conjugates detected using an enhanced chemiluminescence detection system. The details of the antibodies shown in **Table 10**.

Antibody	Host	Catalog number	Company	Dilution
ACTB\β-actin	Mouse	8227	Abcam	1:5000
CTNNB1 \ β-catenin	Rabbit	9582	Cell signaling	1:1000
TNKS12	Rabbit	Sc-8337	Santa cruz	1:500
GSK3	Mouse	Sc-7297	Santa cruz	1:500
CCND1	Rabbit	2978	Cell signaling	1:1000
MYC	Rabbit	5605	Cell signaling	1:1000
p-GSK3 <sup>S9</sup>	Rabbit	9336	Cell signaling	1:1000
MET	Rabbit	8198	Cell signaling	1:1000
CD68	Mouse	Ab-955	Abcam	1:100
ARID5A	Rabbit	HPA023879	Sigma	1:1000
FOSL2	Rabbit	HPA004817	Sigma	1:1000
Anti-mouse IgG, HRP-linked Antibody	Anti-Mouse	W4018	Promega	1:2000
Anti-rabbit IgG, HRP-linked Antibody	Anti-Rabbit	W4028	Promega	1:2000
Anti-goat IgG, HRP- linked Antibody	Anti-Goat	sc-2378	Santa cruz	1:1000

**Table 10: List of antibodies**

### 3.4.3 TCF/LEF luciferase activity assay

Macrophages (M0, M1-like TAMs, M2-like TAMs) in six-well plates were co-transfected with TCF/LEF Luciferase construct (0.3 µg/well, from Dobrev lab) and Renilla luciferase

construct (10 ng/well; Promega) using Lipofectamine 2000 transfection reagent (11668, Thermo Fisher Scientific GmbH, Dreieich, Germany) for 6 h in serum-free optimum medium. After 6 h, cells incubated with a serum-containing medium for 24 h at 37°C. Luciferase activities were quantified using the Dual-Luciferase® Reporter Assay System (E1910, Promega GmbH, Mannheim, Germany) according to the instructions provided by the manufacturer, and a spectrofluorometer (Tecan Infinite M200 PRO plate reader). The ratio of luciferase signal-to-Renilla signal for each well calculated as previously described (Pullamsetti, Banat et al. 2013).

### 3.4.4 Chromatin immunoprecipitation (ChIP)

Approximately  $10 \times 10^6$  macrophages (THP1-derived M2 macrophages) were treated with XAV939 (5  $\mu$ M) for 24 h and assessed through ChIP. Cells were cross-linked by adding the one-tenth volume of cross-linking solution (11% formaldehyde, 0.1 M sodium chloride, 1 mM EDTA, 0.5 mM egtazic acid, 50 mM HEPES at pH 8) overnight at 4°C. The following day, the reaction terminated by adding 0.125 M glycine. Cells washed thrice with ice-cold PBS for 5 min, and the nuclear cell fraction obtained through sequential lysis with L1 lysis buffer and L2 nuclear resuspension buffer. The cell lysate in L2 buffer sonicated using a Diagenode Bioruptor (Bioruptor™ Pico, Seraing, Belgium) for 3x30 s pulses (30 s pause between pulses). Cell debris removed through high-speed centrifugation. The resulting chromatin extract, containing DNA fragments with an average size of 500 bp, was immunoprecipitated overnight at 4°C using Salmon Sperm DNA/Protein A Agarose beads (16-157 Merk Millipore, Darmstadt, Germany), that had been pre-incubated with 5  $\mu$ g of the appropriate antibody. The following day, after washing (Low Salt washing buffer, High Salt washing buffer, LiCl washing buffer), elution (C1 DNA elution buffer), and reverse cross-linking, DNA was purified using a PCR purification kit (Qiagen). Purified DNA quantified via SYBR Green real-time PCR (StepOnePlus, Bio-Rad, California, USA) using specific primers (Table 1). Data are expressed as a percentage of input, calculated from the formula: percentage of Input is equal to  $2^{-(dCt)}$ , dCt is Ct ChIP – (Ct Input –  $\log_2$  dilution factor). The compositions of solutions are as shown in **Table 11**, and the sequence of ChIP primers listed in **Table 12**.

Reagents	Composition
L1 lysis buffer	50 mM Tris.HCl pH 8.0, 2 mM EDTA pH 8.0, 0.1 % NP40, 10 % glycerol
L2 nuclear resuspension buffer	50 mM Tris.HCl pH 8.0, 5 mM EDTA pH 8.0, 1 % SDS
DB-dilution buffer	50 mM Tris.HCl pH 8.0, 5 mM EDTA pH 8.0, 0.5 % NP40, 0.2 M NaCl
Low Salt washing buffer	20 mM Tris.HCl pH 8.0, 2 mM EDTA pH 8.0, 1 % NP40, 0.1 % SDS, 0.15 M NaCl
High Salt washing buffer	20 mM Tris.HCl pH 8.0, 2 mM EDTA pH 8.0, 1 % NP40, 0.1 % SDS, 0.5 M NaCl
LiCl washing buffer	10 mM Tris.HCl pH 8.0, 1 mM EDTA pH 8.0, 1 % NP40, 1% Na-deoxycholate, 0.25 M LiCl
TE buffer	10 mM Tris.HCl pH 8.0, 1 mM EDTA pH 8.0
C1 DNA elution buffer	10 mM Tris.HCl pH 8.0, 1 mM EDTA pH 8.0, 0.1 M NaHCO <sub>3</sub> , 1 % SDS
DNA elution TE buffer	25 mM Tris.HCl, 1 mM EDTA pH 10.0

Table 11: Compositions of solutions used in ChIP

Gene		Sequence
CCND1	FP	CCTCCCGCTCCCATTCTCTGT
	RP	CAAACTCCCCTGTAGTCCGTG
Myc	FP	AGGCAACCTCCCTCTCGCCTA
	RP	AGCAGCAGATACCGCCCCTCCT
IL10	FP	AGTCTTGGGTATTCATCCCAGGT
	RP	GAGCTCCTCCTTCTCTAACCTC
FUSL2	FP	GGCCGGAATGTCTTGACTGG
	RP	GGCTGGCCTGCCTATTTTTTC
ARID5A	FP	GCACAGGGCCACTTTCAAATC
	RP	AGGC AAAACTAGAGCCTTGGA

Table 12: Sequence of ChIP primers

### 3.5 Experimental procedures – Cellular functional Studies

#### 3.5.1 Proliferation and apoptosis assay

A549, primary tumor, or LLC1 cells ( $1 \times 10^4$  cells/well) seeded in a 96-well plate for 24 h, followed by serum starvation for 24 h. Then, the cells treated with different CM for 24 h. A549 cells were treated with CM from M0 macrophages, *in-vitro*- trained M1-like TAMs, M2-like TAMs, M2-like TAMs treated with DMSO, 5  $\mu$ M XAV939, M2-like TAMs transfected with EG5 shRNA, NS shRNA,  $\beta$ -catenin shRNA, M2-like TAMs transfected with all-star negative siRNA, FOSL2 siRNA, negative plasmid, ARID5A, and  $\beta$ -catenin plasmids. Primary tumor cells were treated with CM from M0 macrophages, *in-vitro*-trained M1-like TAMs, M2-like TAMs, human *ex-vivo* TAMs treated with DMSO, 5  $\mu$ M XAV939, human *ex-vivo* TAMs transfected with AllStars negative siRNA, and  $\beta$ -catenin siRNA. LLC1 cells treated with CM from mouse *ex-vivo* TAMs treated with DMSO and 5  $\mu$ M XAV939. The following day, proliferation and apoptosis were assessed using the bromodeoxyuridine cell proliferation assay kit (11647229001, Roche Diagnostics GmbH, Mannheim, Germany) and cell death detection kit (11920685001, Roche Diagnostics GmbH, Mannheim, Germany), respectively (Savai, Al-Tamari et al. 2014, Schmall, Al-Tamari et al. 2015, Pullamsetti, Kojonazarov et al. 2017).

#### 3.5.2 Migration assay

A549 cells' migration after different CM treatment quantified using a Boyden chamber transwell assay. CM (700  $\mu$ L/well) added in 24-well companion plate with 8  $\mu$ m pore size insert (83.3930.800, Sarstedt, Nümbrecht, Germany).  $5 \times 10^4$  cells/300  $\mu$ L medium were seeded in the upper part of each insert and incubated for 6 h at 37°C. Subsequently, transwell inserts washed with PBS and placed in methanol for fixation, followed by 10-min crystal violet staining. After washing with distilled water, each membrane mounted on slides with Pertex (41-4011-00, Medite GmbH, Burgdorf, Switzerland). The slides scanned with Nanozoomer 2.0 HT digital slide scanner C9600 (Hamamatsu Photonics Deutschland GmbH, Herrsching am Ammersee, Germany). The number of migrated cells per membrane was quantified using the ImageJ software as previously described (Savai, Al-Tamari et al. 2014, Schmall, Al-Tamari et al. 2015, Pullamsetti, Kojonazarov et al. 2017)

### 3.6 Experimental procedures – Imaging

#### 3.6.1 Immunofluorescence staining

The lung tissue microarray LUC1501 contains 150 cores from tissue samples consisting of normal/benign (n = 2) and cancer (n = 70, graded by the Tumor, Node, Metastasis staging system) cases, with duplicated cores for each case (Pantomics, Inc. Cat no. LUC1501, Richmond, CA, USA). The slide with the lung tissue microarray (LUC1501) was deparaffinized by heating at 60°C for 1 h and immersion in xylol (CN80.2, Roth) for 30 min. Tissues were rehydrated sequentially using 99% (K928.4, Roth), 96% (T171.4, Roth), and 70% (T913.3, Roth) ethanol, and iso-propanol (6752.4, Roth). Antigen retrieval was performed by heating in citrate buffer for 30 min, followed by washing with 1×PBS and blocking in 5% BSA at room temperature for 1 h. The slides were subsequently washed thrice with 1× PBS, and incubated overnight at 4°C with primary antibodies for  $\beta$ -catenin (1:100; Millipore; 06-734) and CD68 (1:100; Abcam; ab-955). The slides were washed thrice with 1×PBS and incubated at RT with secondary antibodies Alexa Fluor 488 goat anti-rabbit IgG (1:1000; Invitrogen; A11008) and Alexa Fluor 555 goat anti-mouse IgG (1:1000; Invitrogen; A21422) for 1 h. The slides were re-washed thrice with 1×PBS and incubated with DAPI (1:100) at RT for 15 min to stain the nuclei, followed by a 5-min wash with 1×PBS and mounting with DAKO (S3023, Agilent, CA, USA) tissue-mounting medium. The slides were visualized with a confocal microscope (Zeiss LSM 710) and the Zen 2011 software.

### 3.7 Experimental procedures – *in vivo*

#### 3.7.1 Animal experiments

All mice maintained under specific-pathogen-free conditions and handled by the guidelines of the European Union Commission on Laboratory animals. C57BL/6, *Catnb<sup>ff</sup>* (B6.129-Ctnnb1tm2Kem/KnwJ), and *Lysm<sup>Cre</sup>* (B6.129P2-Lyz2tm1(cre)lfo/J) mice were purchased from Jackson Laboratory (Bar Harbor, ME, USA). *Catnb<sup>ff</sup>Lysm<sup>Cre</sup>* mice generated by crossbreeding *Catnb<sup>ff</sup>* mice with *Lysm<sup>Cre</sup>* mice. All the animal experiments were performed at the Max Planck Institute for Heart and Lung Research (Bad Nauheim, Germany), which were approved by local authorities in Regierungspräsidium Darmstadt, Hessen, Germany (Animal proposal no. B2/1088) and at the University of Patras (Patras, Greece).

### 3.7.2 Subcutaneous tumor model

Mouse LLC1 cells ( $1 \times 10^6$ ) were subcutaneous (s.c.) injected (24g needle, 0.55 × 25 mm, Neolus, Terumo Europe, Leuven, Belgium) into C57BL/6 mice, followed by 25 mg/kg XAV939 treatment. Tumor growth measured every 4 days with digital calipers. On day 20, the mice sacrificed, and tumors, lung, livers, and spleen harvested as previously described (Schmall, Al-Tamari et al. 2015).

### 3.7.3 Carcinogen-induced lung tumor model

Lung adenocarcinoma`s were chemically induced in C57BL/6 and transgenic mice (Catnb<sup>ff</sup>Lysm<sup>Cre</sup>, Catnb<sup>ff</sup>, and Lysm<sup>Cre</sup>) by 10 consecutive weekly intraperitoneal exposures to 1 g/Kg urethane (U2500, Sigma-Aldrich, St. Louis, USA) for 5 months, followed by 25 mg/kg XAV939 treatment and mice were sacrificed on 26<sup>th</sup> day following the first injection of XAV939 (Stathopoulos, Sherrill et al. 2007).

### 3.7.4 Metastasis tumor model (tumor relapse model)

Primary tumor growth initiated in C57BL/6 mice through s.c. injection of  $1 \times 10^6$  LLC1 cells. On day 10, the s.c. tumors were resected, followed by wound closure and 25 mg/kg XAV939 treatment. All mice carefully examined each day for 20–32 consecutive days (Schmall, Al-Tamari et al. 2015).

### 3.7.6 Bone marrow transplantation model

C57BL/6 mice lethally irradiated after total body irradiation (1100 Rad). Twelve hours post-irradiation, the C57BL/6 mice were reconstituted with bone marrow transplants (BMT) from transgenic mice (Catnb<sup>ff</sup>Lysm<sup>Cre</sup>, Catnb<sup>ff</sup>, and Lysm<sup>Cre</sup>) by receiving  $1 \times 10^7$  bone marrow cells retro-orbitally. At day 30 after transplantation, full bone marrow reconstitution was completed (Agalioti, Giannou et al. 2017), and  $1 \times 10^6$  LLC1 cells were intratracheally injected into mice as previously described (Schmall, Al-Tamari et al. 2015). On day 16, lungs photographed. The right lung was used to prepare single-cell suspension for FACS analysis and MACS sorting of F4/80 positive macrophages, while the left lung was immersed in 4% paraformaldehyde followed by embedding in paraffin for histological examination.

### **3.7.5 Treatment of tumor-bearing mice with XAV939**

The mice were treated intraperitoneally with XAV939 (25 mg/kg) on every third day until the endpoints mentioned above of respective tumor models were reached. The s.c. tumors or lungs were photographed. Notably, s.c. tumor (0.4 gm) or right lung was used to prepare single-cell suspension for FACS analysis and MACS sorting of F4/80<sup>+</sup> macrophages. The remaining s.c. tumor or left lung was immersed in 4% paraformaldehyde, followed by embedding in paraffin for histological examination.

### **3.7.6 Hematoxylin and eosin staining**

Tissue sections were deparaffinized by heating at 60°C for 1 h, and immersion in xylol for 30 min. Tissues rehydrated sequentially by 99%, 96%, and 70% ethanol, and isopropanol. The sections were immersed in hematoxylin (254766.1611, PanReac AppliChem, Darmstadt, Germany) for 20 min, followed by washing with distilled water and immersion in acidified eosin solution (H110132, Sigma-Aldrich, St. Louis, USA) for 4 min. After the final wash with distilled water, the sections dehydrated sequentially through immersion in 96% and 99% ethanol and xylene, followed by mounting with Pertex (41-4011-00, Medite GmbH, Burgdorf, Switzerland ).

### **3.7.7 Lung tumor quantification**

At the end of the animal experiment, the mice euthanized. Their lungs collected and processed for histopathology, as previously described (Savai, Schermuly et al. 2007). Briefly, tissue blocks from all left lung lobes dissected and embedded in paraffin. From each tissue block, serial sections of 50–80 µm were produced. These sections stained with hematoxylin and eosin and analyzed under a Leica light microscope for the presence of tumor cell clusters. The analysis performed in a blinded fashion (Savai, Schermuly et al. 2007).

### **3.8 RNA sequencing**

For RNA sequencing, RNA isolated from primary macrophages (NMs and TAMs from human lung tissue; n = 2), *in-vitro*-trained TAMs (A549 *in-vitro*-trained M1-like TAMs and M2-like TAMs; n = 3) and  $\beta$ -catenin knockdown M2-like TAMs (M2-like TAMs transfected with control\_shRNA and  $\beta$ -catenin\_shRNA; n = 3) using the miRNeasy Micro Kit

(Qiagen) with on-column DNase digestion (DNase-Free DNase Set; Qiagen) to avoid genomic DNA contamination. RNA and library preparation integrity verified with a BioAnalyzer 2100 (Agilent) or LabChip Gx Touch 24 (Perkin Elmer). For *in-vitro*-trained TAMs and  $\beta$ -catenin knockdown M2-like TAMs, total RNA (3  $\mu$ g) used as input for the preparation of the Truseq Stranded mRNA Library following the low sample protocol (Illumina). Total RNA (1  $\mu$ g) from primary macrophages used as input for SMARTer Stranded Total RNA Sample Prep Kit - HI Mammalian (Clontech). Sequencing was performed on the NextSeq500 instrument (Illumina) using v2 chemistry with a 1x75-bp single end setup.

The resulting raw reads assessed for quality, adapter content, and duplication rates with FastQC (at <http://www.bioinformatics.babraham.ac.uk/projects/fastqc>). Trimmomatic version 0.36 employed to trim reads after a reduction in quality below a mean of Q15 in a window of five nucleotides (Bolger, Lohse et al. 2014). It only reads longer than 15 nucleotides cleared for further analysis. Trimmed and filtered reads were aligned versus the Ensembl human genome version hg38 (GRCh38.27) using STAR 2.5.4b with the parameter “--outFilterMismatchNoverLmax 0.1” to increase the maximum ratio of mismatches to mapped length to 10% (Dobin, Davis et al. 2013). The number of reads aligning to genes was counted using the featureCounts 1.6.0 tool from the Subread package (Liao, Smyth et al. 2014). Only reads mapping at least partially inside exons admitted and aggregated per gene. Reads multiple overlapping genes or aligning to various regions were excluded. Differentially expressed genes were identified using DESeq2 version 1.14.1 (Love, Huber et al. 2014). The Ensembl annotation enriched with Universal Protein Resource (UniProt) data based on Ensembl gene identifiers. In this project we

1. *For the RNA sequencing of primary macrophages*, genes were classified as significantly differentially expressed at an average count  $>5$ ,  $P < 0.05$ , and  $-0.59 \leq \log_2FC \leq +0.59$ .
2. *For the RNA sequencing of in-vitro-trained TAMs*, the raw count matrix was normalized using DESeq2 version 1.18.1 (Love et al.). Since strong biological biases could not be adequately standardized using batch correction algorithms,  $\log_2$  transformed fold changes independently computed for each biological replicate and contrast. Genes assumed to be differentially expressed when all three biological replicates showed a  $\log_2$  fold change  $\geq 0.585$  or  $\leq -0.585$ , and the mean normalized expression was  $\geq 30$ .

3. For the RNA sequencing of  $\beta$ -catenin knockdown M2-like TAMs, Reaper version 13-100 was employed to trim reads after a reduction in quality below a mean of Q20 in a window of 20 nucleotides (Davis et al.). Genes were classified as significantly differentially expressed at an average count  $>5$ , with Benjamini–Hochberg corrected  $P < 0.05$ .

### **3.9 Statistical analysis**

All data were analyzed using Prism 5.0 and Prism 6.0 (GraphPad Software). Statistical comparisons within two groups performed using Student's t-test. For comparisons between more than two groups, one-way analysis of variance performed, followed by Tukey's post-test. All data expressed as mean $\pm$ standard error of the mean. A  $p \leq 0.05$  denoted statistical significance.

## 4. RESULTS

### 4.1 Wnt/ $\beta$ -catenin signaling upregulated in lung TAMs

A flow cytometry sorting protocol, based on 8-fluorochrome cell staining, was developed to precisely delineate the molecular signature of TAMs obtained from lung cancer patients, and of non-tumor macrophages (NMs) obtained from matched control tissue (**Figure 7A**). RNA sequencing of fluorescence-activated cell sorting (FACS)-sorted macrophages revealed differential gene expression between TAMs and NMs (**Figure 7B**). Importantly, the panther pathway analysis identified the Wnt signaling pathway as one of the most enriched pathways in the TAMs (**Figure 7C**).

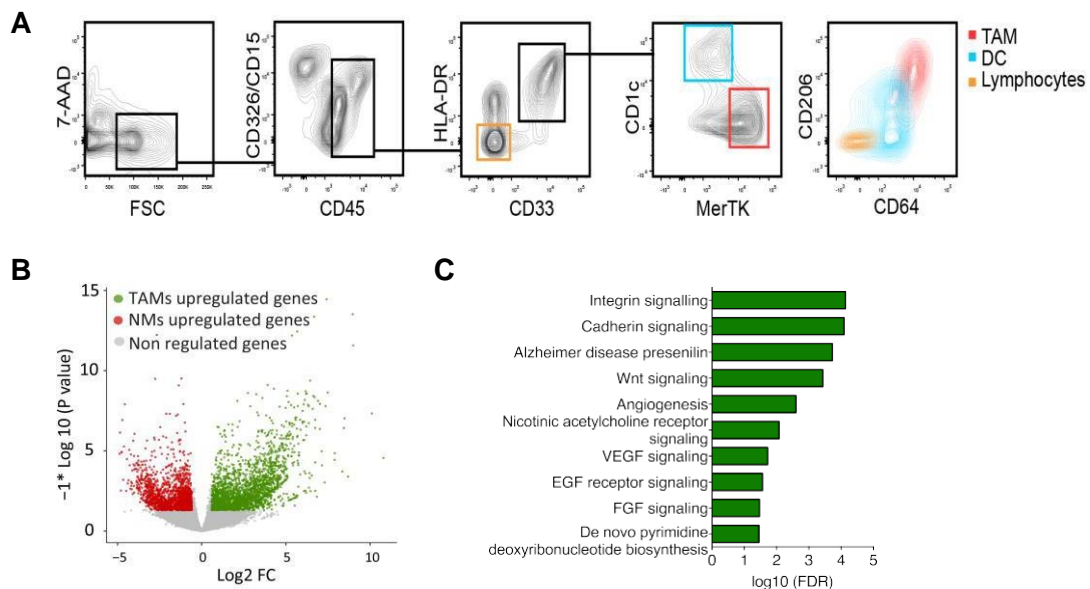


**Figure 7: Wnt/ $\beta$ -catenin signaling upregulated in primary TAMs isolated from patients with lung cancer. (A)** Representative FACS plot demonstrating macrophages (CD15<sup>+</sup>, CD45<sup>+</sup>, CD33<sup>+</sup>, HLA-DR<sup>+</sup>, CD1c<sup>+</sup>, MerTK<sup>+</sup>, CD64<sup>+</sup>, CD206<sup>+</sup>, CD326<sup>-</sup>) in freshly isolated human lung cancer tissues (n=12). **(B)** Volcano plot showing differentially expressed genes (DEGs) in TAMs versus NMs, n = 5. FC, fold change. **(C)** Top 10 panther pathways in TAMs—up-regulated DEGs. VEGF, vascular endothelial growth factor; EGF, epidermal growth factor; FGF, fibroblast growth factor. [(Sarode P et.al. 2020) Reuse permission: Distributed under the terms of the Creative Commons Attribution-NonCommercial license]

In accordance, protein expression analysis of Wnt signaling components ( $\beta$ -catenin, Tankyrase (TNKS 1/2, p-GSK3B), and its target genes (CCND1, MYC, MET) in TAMs and NMs confirmed Wnt/ $\beta$ -catenin signaling activation in TAMs (**Figure 8A**). Furthermore, co-immunostaining of  $\beta$ -catenin and a macrophage marker (CD68) in a microarray of human lung tissue revealed that  $\beta$ -catenin expressed in tumor cells, but also highly expressed in TAMs

**(Figure 8B).** Collectively, these results indicate that Wnt/ $\beta$ -catenin signaling is significantly upregulated in TAMs of lung cancer patients.

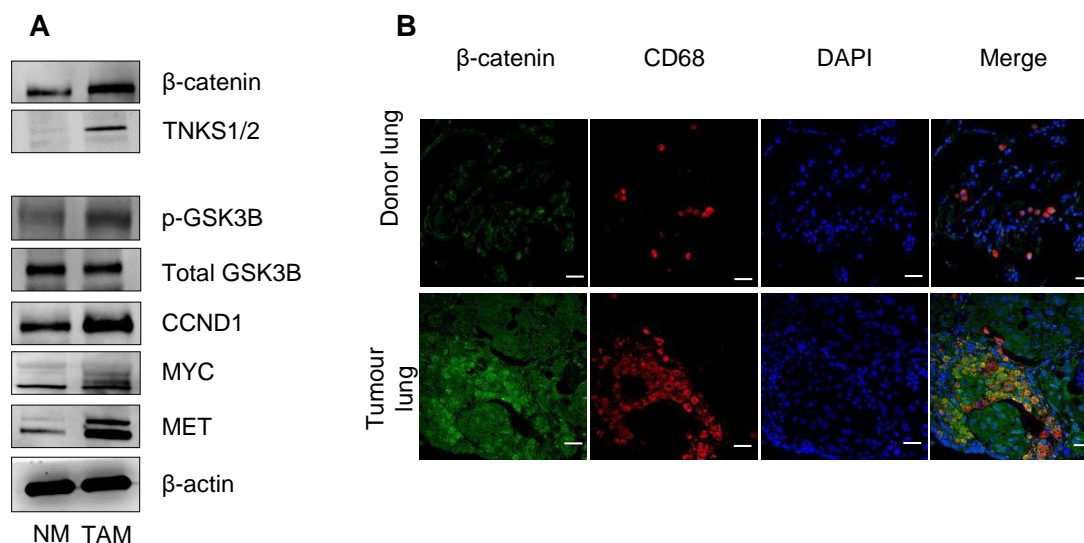


**Figure 8: Wnt/ $\beta$ -catenin signaling is activated in primary TAMs isolated from lung cancer patients. (A)** TAMs and NMs sorted from fresh human lung tumor tissue and its matched control, respectively, through a limited selection of CD68<sup>+</sup> antigen using the magnetic-activated cell sorting (MACS) system. Western blotting analysis of Wnt/ $\beta$ -catenin signaling ( $\beta$ -catenin, TNKS1/2, p-GSK3B, Total GSK3B), its target genes (CCND1, MYC, MET), and  $\beta$ -actin (loading control) in TAMs and NMs (n = 3). **(B)** Representative immunofluorescence images of tissue sections from donor and lung cancer tissue. The lung tissue microarray stained with  $\beta$ -catenin (green) and CD68 (macrophage marker, red); nuclei counterstained with DAPI (blue). Scale bars, 50  $\mu$ M. The images are representative of n = 70 tumor tissues and n = 2 donor tissues. [(Sarode P et.al. 2020) Reuse permission: Distributed under the terms of the Creative Commons Attribution-NonCommercial license]

## 4.2 Wnt/ $\beta$ -catenin signaling activated in *in-vitro*-trained M2-like TAMs

A large body of evidence has shown that the cross-talk between tumor cells and TAMs in spatial proximity leads to a phenotypic shift of anti-tumor M1-like TAMs to pro-tumor M2-like TAMs (Yuan, Hsiao et al. 2015). However, the lack of an *in-vitro* model to study this time-dependent shift is a significant hurdle in delineating the underlying molecular mechanisms. Therefore, an *in-vitro* co-culture model, featuring both M1-like and M2-like TAMs, was developed to study this phenotypic plasticity in TAMs (**Figure 9A**) (Weigert, Tzieply et al. 2007).

### 4.2.1 Establishment of “*in-vitro*-trained” TAMs model featuring tumor-inhibiting M1-like TAMs and tumor-promoting M2-like TAMs

Undifferentiated PBMC-trained macrophages (M0) were directly co-cultured with A549 cells for five days. The CM from the three days of co-culture strongly induced apoptosis of A549 cells, with minor impact on proliferation and migration, as compared to the CM from M0. Therefore, macrophages from the three-day co-culture were termed M1-like TAMs (**Figure 9B, C**). Subsequently, apoptotic and remaining tumor cells were extracted and were replaced with new A549 cells. Conversely, the CM from the five-day co-culture did not induce apoptosis; however, it sharply increased A549 cells' proliferation and migration, as compared to M0 and M1-like TAM states. Therefore, macrophages from the five-day co-culture were termed M2-like TAMs (**Figure 9B, C**).

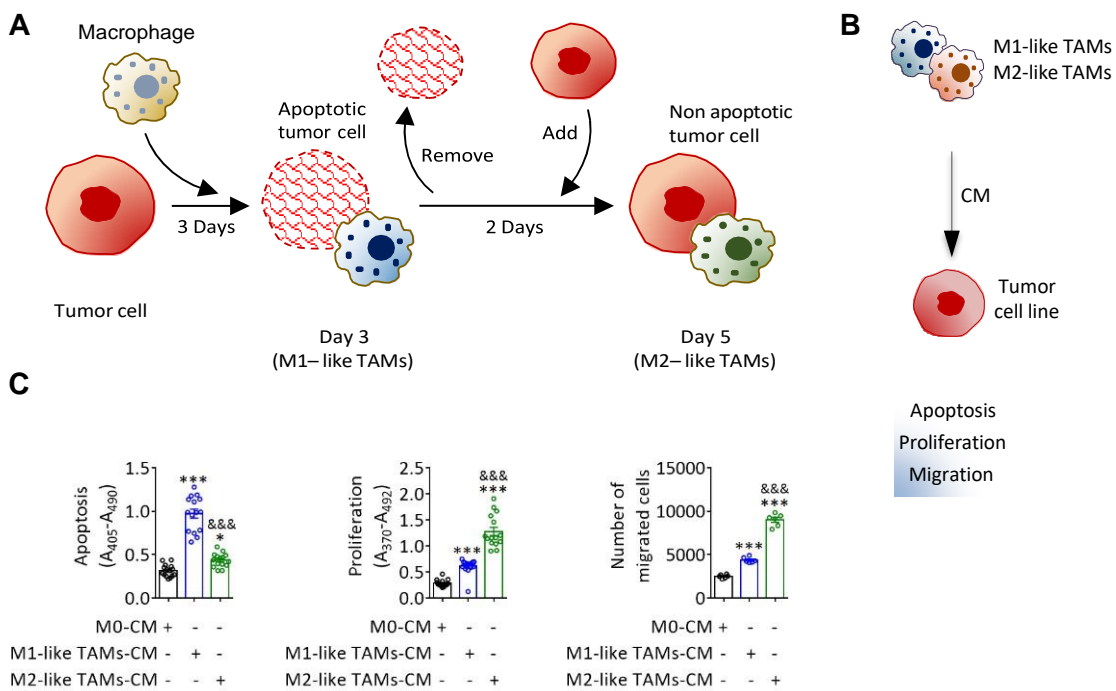


**Figure 9: Tumor cell – macrophages crosstalk simultaneously generates *in-vitro*-trained M1-like and M2-like TAMs. (A)** Schematic experimental plan showing the generation of TAMs *in vitro*. M1-like TAMs produced by directly co-culturing undifferentiated PBMC-derived macrophages (M0) and A549 cells for 72 h (3 days), followed by removal of apoptotic cancer cells and addition of new A549 cells. Co-culture was continued for the next 48 h (5 days), which found to generate M2-like TAMs (“training”). **(B)** Schematic experimental plan showing the treatment of the A549 or primary tumor cells in the presence of conditioned medium (CM) from tumor cell line-trained or primary tumor cell-trained M1-like TAMs and M2-like TAM, respectively. **(C)** Quantification of apoptosis, proliferation, and migration of A549 cells. n = 3 biological replicates, 3 technical replicates. \*\*\*P < 0.001, \*\*\*\*P < 0.0001 compared with M0-CM; &&&P < 0.001, &&&&P < 0.0001 compared with the CM of M1-like TAMs. [(Sarode P et.al. 2020) Reuse permission: Distributed under the terms of the Creative Commons Attribution-NonCommercial license]

Similar to A549 cells, human primary lung tumor cells treated with CM from M2-like TAMs (*in-vitro* trained by co-culturing with primary tumor cells) did not show change in apoptosis but

displayea significant increase in proliferation and migration as compared to their M1 counterparts (**Figure 10A**). Further, to confirm that the established *in vitro* co-culture model is not cancer cell line-specific, two other lung-cancer-cell lines (A427 and H1650) were co-cultured with M0 macrophages, and functional studies were carried out. Notably, CM from A427 and H1650 derived M2-like TAMs did not show apoptosis but showed increased proliferation and migration of A427 and H1650 cells, respectively (**Figure 10B, C**).

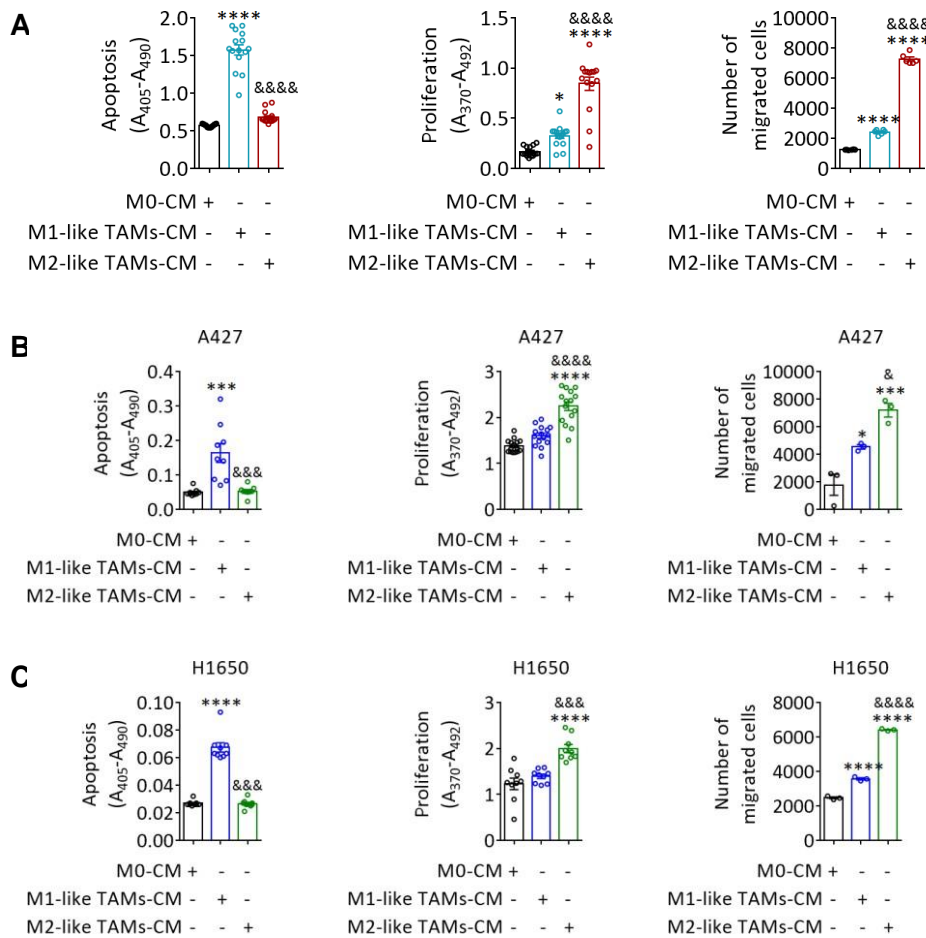


**Figure 10: Tumor cell – macrophages crosstalk functionally switch M1-like and M2-like TAMs.** Quantification of apoptosis, proliferation, and migration of **(A)** primary tumor cells **(B)** A427 cells **(C)** H1650 cells in the presence of CM from M0 macrophages and primary tumor cell-trained, A427 trained and H1650 trained M1-like TAMs and M2-like TAMs; n = 3 biological replicates, 5 (for Apoptosis, Proliferation) or 2 (for Migration) technical replicates. \*\*\*P < 0.001, \*\*\*\*P < 0.0001 compared with M0-CM; &&&P < 0.001, &&&&P < 0.0001 compared with the CM of M1-like TAMs. [(Sarode P et.al. 2020) Reuse permission: Distributed under the terms of the Creative Commons Attribution-NonCommercial license]

Notably, mRNA expression profiling of macrophage markers revealed that M1-like TAMs mainly expressed M1-macrophage markers (*TNF*, *IL1B*, *IL8*), while M2-like TAMs expressed M2-macrophage markers (*IL10*, *CD163*, *ALOX15*) (**Figure 11A, B**). The high expression of cell surface markers of M2 macrophages (CD163, CD206) further confirmed the presence of

the M2-like TAM phenotypic profile at five days of the co-culture (**Figure 11C**). Collectively, these results indicate that M1-like TAMs undergo a phenotypic and functional switch to M2-like TAMs when in spatial proximity to tumor cells for several days.

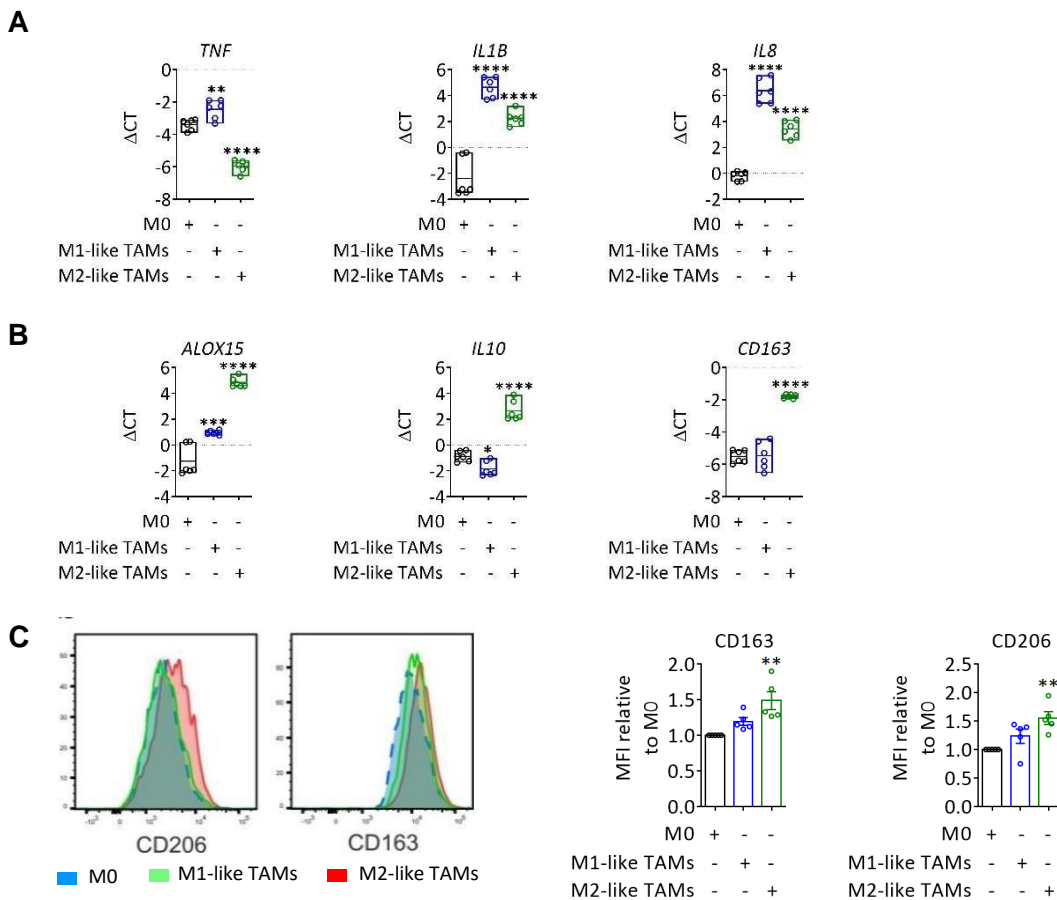


**Figure 11: *In-vitro*-trained M1-like TAMs expressed more M1 markers, while M2-like TAMs expressed more M2 markers.** Relative mRNA expression of (A) M1 macrophage markers (*TNF*, *IL1B*, *IL8*) and (B) M2 macrophage markers (*IL10*, *CD163*, *ALOX15*) in M0 and tumor cell line-trained M1-like TAMs and M2-like TAMs;  $n = 3$  biological replicates, 2 technical replicates. \* $P < 0.05$ , \*\* $P < 0.01$ , \*\*\* $P < 0.001$ , \*\*\*\* $P < 0.0001$  compared with M0. (C) FACS analysis of CD163, CD206 cell surface markers on M0 macrophages (blue), M1-like TAMs (green), and M2-like TAMs (red); and quantification of the mean fluorescence intensity (MFI) of CD163, CD206 in M0 macrophages and tumor cell line-trained M1-like TAMs and M2-like TAMs;  $n = 5$  biological replicates. \*\* $P < 0.01$ , compared with M0. [(Sarode Pet.al. 2020) Reuse permission: Distributed under the terms of the Creative Commons Attribution-NonCommercial license]

#### 4.2.2 Wnt/ $\beta$ -catenin signaling activated in *in-vitro*-trained M2-like TAMs

The analysis of Wnt/ $\beta$ -catenin signaling via nuclear  $\beta$ -catenin activity (TCF/LEF-reporter based) (**Figure 12A**), nucleo-cytoplasmic extraction of  $\beta$ -catenin (**Figure 12B**), western blotting ( $\beta$ -catenin, TNKS1/2, p-GSK3B) and its target genes (CCND1, MYC, MET) (**Figure**

**12C)** confirmed the translocation of  $\beta$ -catenin in the nucleus, alongside with activation of Wnt target genes.

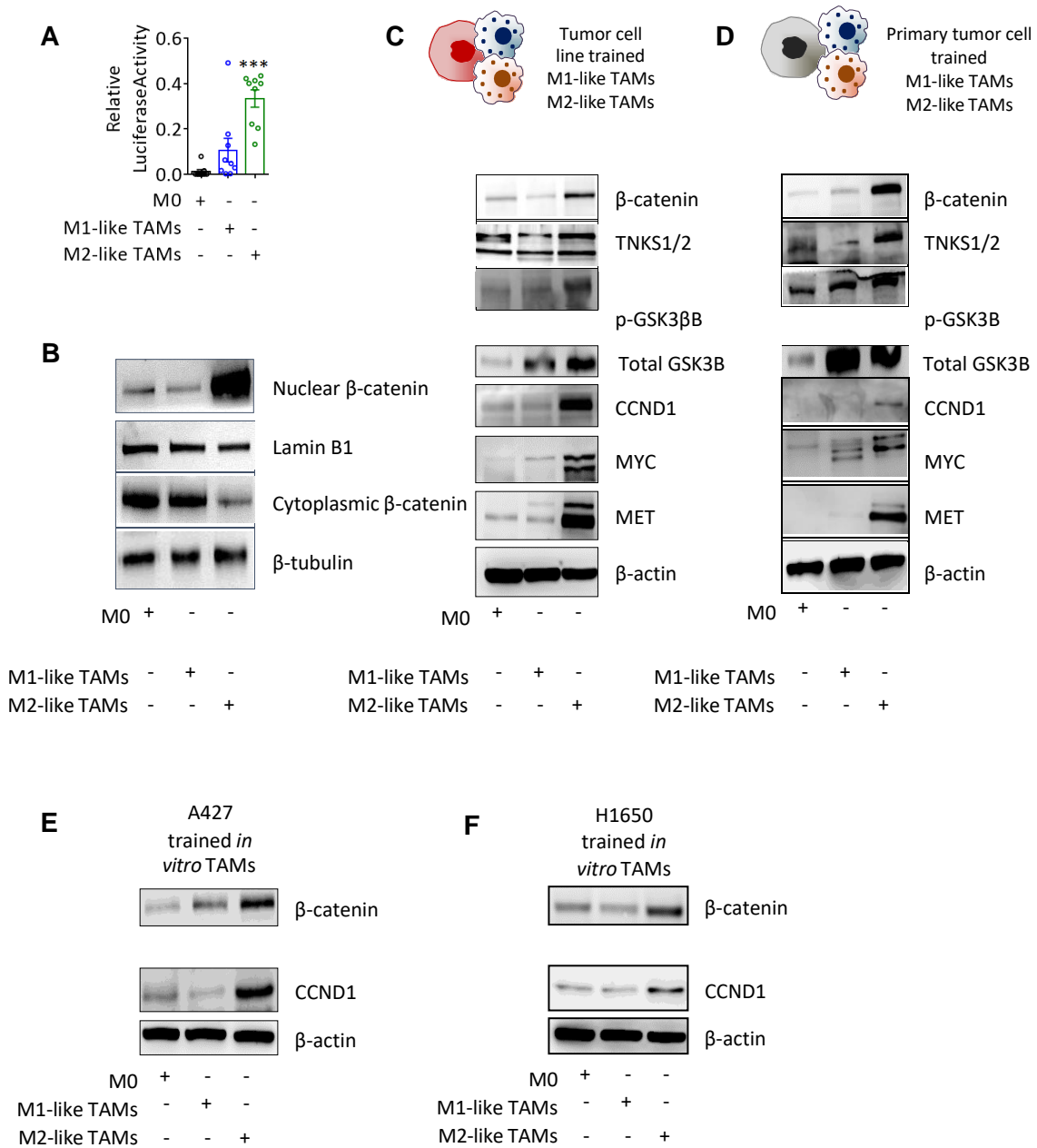


**Figure 12: Wnt/ $\beta$ -catenin signaling activated in *in-vitro*-trained M2-like TAMs. (A) Relative TCF/LEF luciferase activity in M0 macrophages and A549-trained M1-like TAMs and M2-like TAMs; n = 3 biological replicates, 3 technical replicates. \*\*\*P < 0.001 compared with M0 macrophages and &&&P < 0.001 compared with M1-like TAMs. Western blotting analysis of (B) nuclear and cytoplasmic  $\beta$ -catenin, Lamin B1 (nuclear protein control),  $\beta$ -tubulin (cytoplasmic protein control) in A549-trained TAMs; Wnt/ $\beta$ -catenin signaling ( $\beta$ -catenin, TNKS1/2, p-GSK3B, Total GSK3B), its target genes (CCND1, MYC, MET), and  $\beta$ -actin (loading control) in (C) A549-trained TAMs (D) in primary tumor cell-trained TAMs;  $\beta$ -catenin and its target gene (CCND1) in (E) A427-trained TAMs (F) H1650-trained TAMs. n = 3. M0 macrophages as a control in all experiments. [(Sarode P et.al. 2020) Reuse permission: Distributed under the terms of the Creative Commons Attribution-NonCommercial license]**

Moreover, TAMs trained through co-culture with primary lung tumor cells activated Wnt/ $\beta$ -catenin signaling in M2-like TAMs versus M1-like TAMs (**Figure 12D**). Additionally, protein expressions of  $\beta$ -catenin and its target gene (CCND1) showed upregulation on A427, and H1650 derived M2-like TAMs when compared to their M1 counterparts (**Figure 12E, F**).

Besides, RNA sequencing analysis of M1-like TAMs and M2-like TAMs confirmed the M1 and M2 macrophage marker expression profiles, respectively (**Figure 13A, B**). RNA sequencing data also revealed that most common stimulatory modifications of Wnt/ $\beta$ -catenin signaling (*WNTs*, *DVLs*, *LEF1*, etc.) (**Figure 13C**) and its target genes (*CCND1*, *MYC*, *IDs*, etc.) (**Figure 13D**) upregulated in M2-like TAMs versus M1-like TAMs.

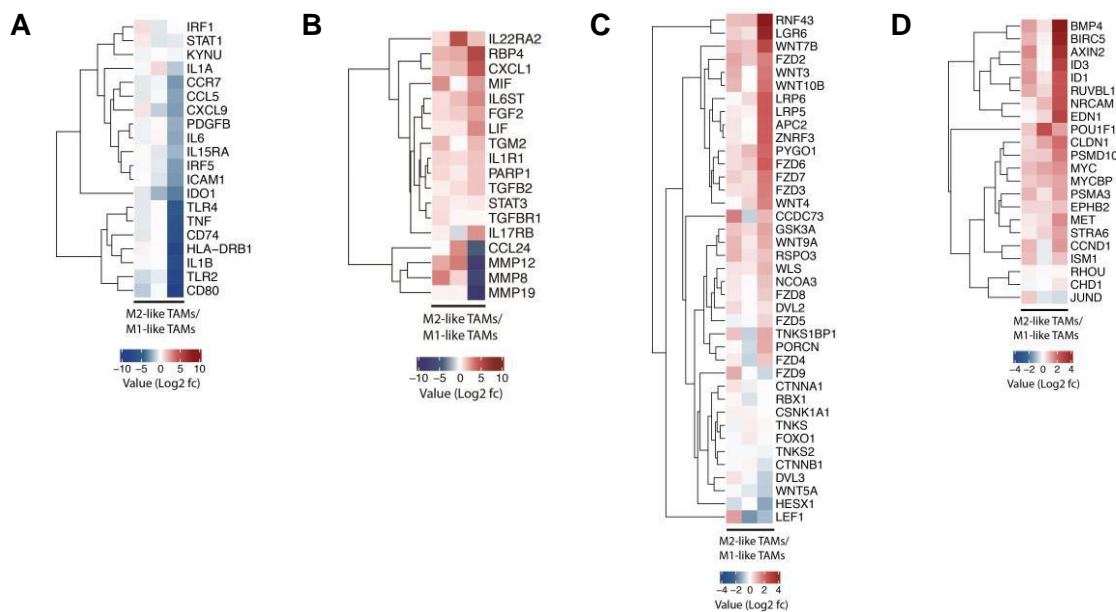


**Figure 13: RNA sequencing in *in-vitro*-trained M2-like TAMs identifies upregulated Wnt/ $\beta$ -catenin signaling.** M1-like TAMs and M2-like TAMs generated by directly co-culturing M0 macrophages and A549 cells. Heatmaps display the expression of genes encoding **(A)** M1 macrophage markers, **(B)** M2 macrophage markers, **(C)** Wnt/ $\beta$ -catenin pathway genes, and **(D)** target genes of Wnt/ $\beta$ -catenin signaling in M1-like TAMs and M2-like TAMs, assessed by RNA sequencing;  $n = 3$ . [(Sarode P et al. 2020) Reuse permission: Distributed under the terms of the Creative Commons Attribution-NonCommercial license]

Additionally, mRNA expression profiling of Wnt molecules confirmed the upregulation of WNT ligands (*WNT5A*, *WNT 7B*, *WNT 11*), frizzled receptors (*FZD4*, *FZD5*, *FZD6*, *FZD8*, *FZD9*), disheveled (*DVL2*, *DVL 3*), and *TNKS1/2* exclusively in M2-like TAMs (**Figure 14**). Collectively, these results show the significant activation of Wnt/ $\beta$ -catenin signaling in *in-vitro*-trained M2-like TAMs, indicating that it may be the underlying molecular mechanism responsible for the transition of M1-like TAMs to M2-like TAMs.

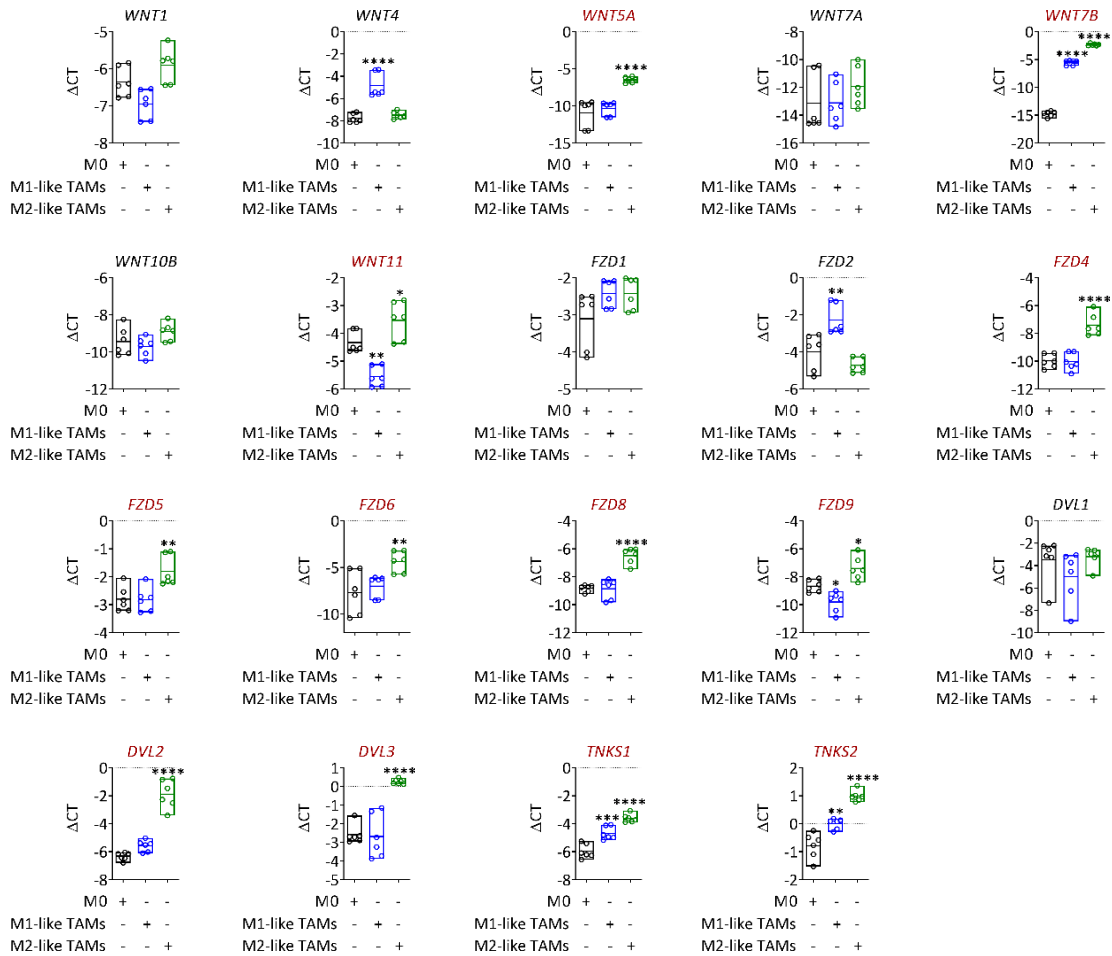


**Figure 14: Upregulation of different components of Wnt/β-catenin signaling in M2-like TAMs.** Relative mRNA expression of WNT ligands (*WNT1*, *WNT4*, *WNT5A*, *WNT7A*, *WNT7B*, *WNT10B*, *WNT11*), frizzled receptors (*FZD1*, *FZD2*, *FZD4*, *FZD5*, *FZD6*, *FZD8*, *FZD9*), disheveled (*DVL1*, *DVL2*, *DVL3*), and tankyrases (*TNKS1/2*) in M0 macrophages, M1-like TAMs, and M2-like TAMs *in-vitro*-trained by co-culturing M0 macrophages with A549 cells; n = 3 biological replicates, 2 technical replicates. \*P < 0.05, \*\*P < 0.01, \*\*\*P < 0.001, \*\*\*\*P < 0.0001 compared with M0 macrophages. [(Sarode P et.al. 2020) Reuse permission: Distributed under the terms of the Creative Commons Attribution-NonCommercial license]

### 4.3 Inhibition of β-catenin leads to a phenotypal and functional switch of tumor-promoting M2-like TAMs to tumor-inhibiting M1-like TAMs

To test whether Wnt/β-catenin signaling is a crucial molecular mechanism responsible for the phenotypic and functional shift in TAMs, different strategies (β-catenin shRNA, β-catenin siRNA, pharmacological inhibitor - XAV939) were used to manipulate Wnt/β-catenin signaling in various *in vitro* models of M2-like TAMs (*in vitro* trained M2-like TAMs, *ex vivo* TAMs from human and mouse lung tumor).

### 4.3.1 Inhibition of $\beta$ -catenin in *in-vitro*-trained M2-like TAMs by sh\_ $\beta$ -catenin

M2-like TAMs were transfected with  $\beta$ -catenin short hairpin RNA (shRNA; sh\_ $\beta$ -catenin) for 24 h to specifically knockdown  $\beta$ -catenin-dependent signaling *in vitro* trained M2-like TAMs (**Figure 15A**). Protein expression profiling of Wnt/ $\beta$ -catenin signaling ( $\beta$ -catenin, TNKS1/2, and p-GSK3B) and its target genes (CCND1, MYC, MET) confirmed downregulation of nuclear  $\beta$ -catenin activity in M2-like TAMs transfected with sh\_ $\beta$ -catenin (**Figure 15B**).

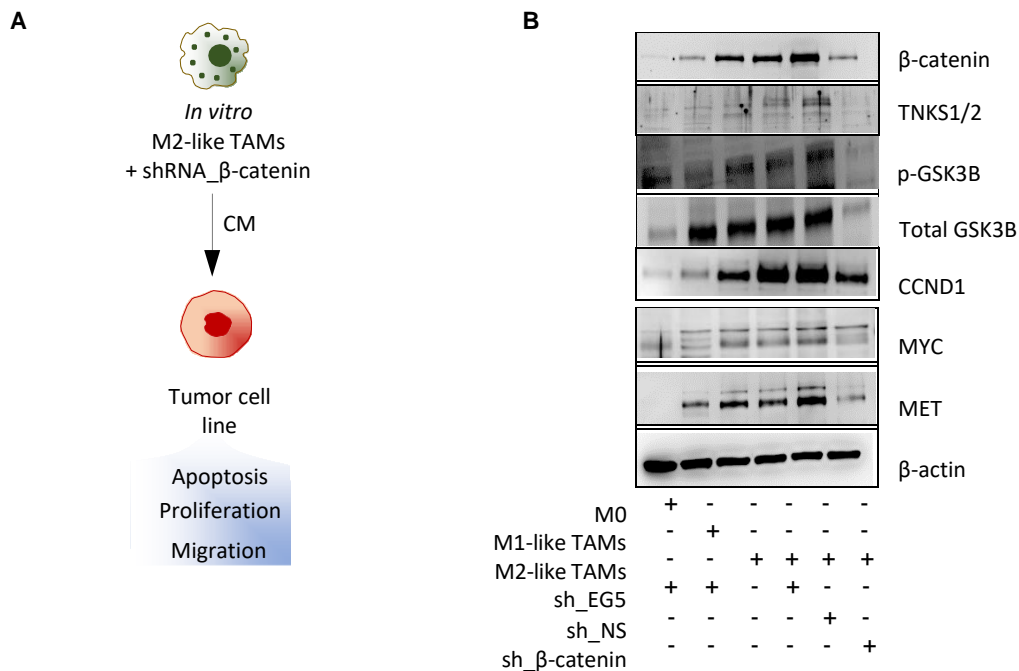


**Figure 15: Genetic ablation of  $\beta$ -catenin in *in-vitro*-trained TAMs downregulates Wnt/ $\beta$ -catenin signaling.** (A) Schematic experimental plan showing the treatment of A549 cells in the presence of CM from M2-like TAMs transfected with sh\_ $\beta$ -catenin concerning tumor cell apoptosis, proliferation, and migration. (B) Western blotting analysis of Wnt/ $\beta$ -catenin signaling ( $\beta$ -catenin, TNKS1/2, p-GSK3B, Total GSK3B), its target genes (CCND1, MYC, MET), and  $\beta$ -actin (loading control) in M0 macrophages, M1-like TAMs, M2-like TAMs, and M2-like TAMs transfected with sh\_NS, sh\_EG5, and sh\_ $\beta$ -catenin for 24 h. [(Sarode P et.al. 2020) Reuse permission: Distributed under the terms of the Creative Commons Attribution-NonCommercial license]

Notably, the mRNA expression of M1 macrophage markers were upregulated, whereas that of M2 macrophage markers was downregulated in M2-like TAMs transfected with sh\_ $\beta$ -catenin, demonstrating M2-like TAMs' phenotypic transition to M1-like TAMs (**Figure 16A, B**). In addition, treatment of A549 cells with CM from M2-like TAMs transfected with sh\_ $\beta$ -catenin showed increased apoptosis and reduction in proliferation and migration, further confirming the functional transition of M2-like TAMs to M1-like TAMs (**Figure 16C**).

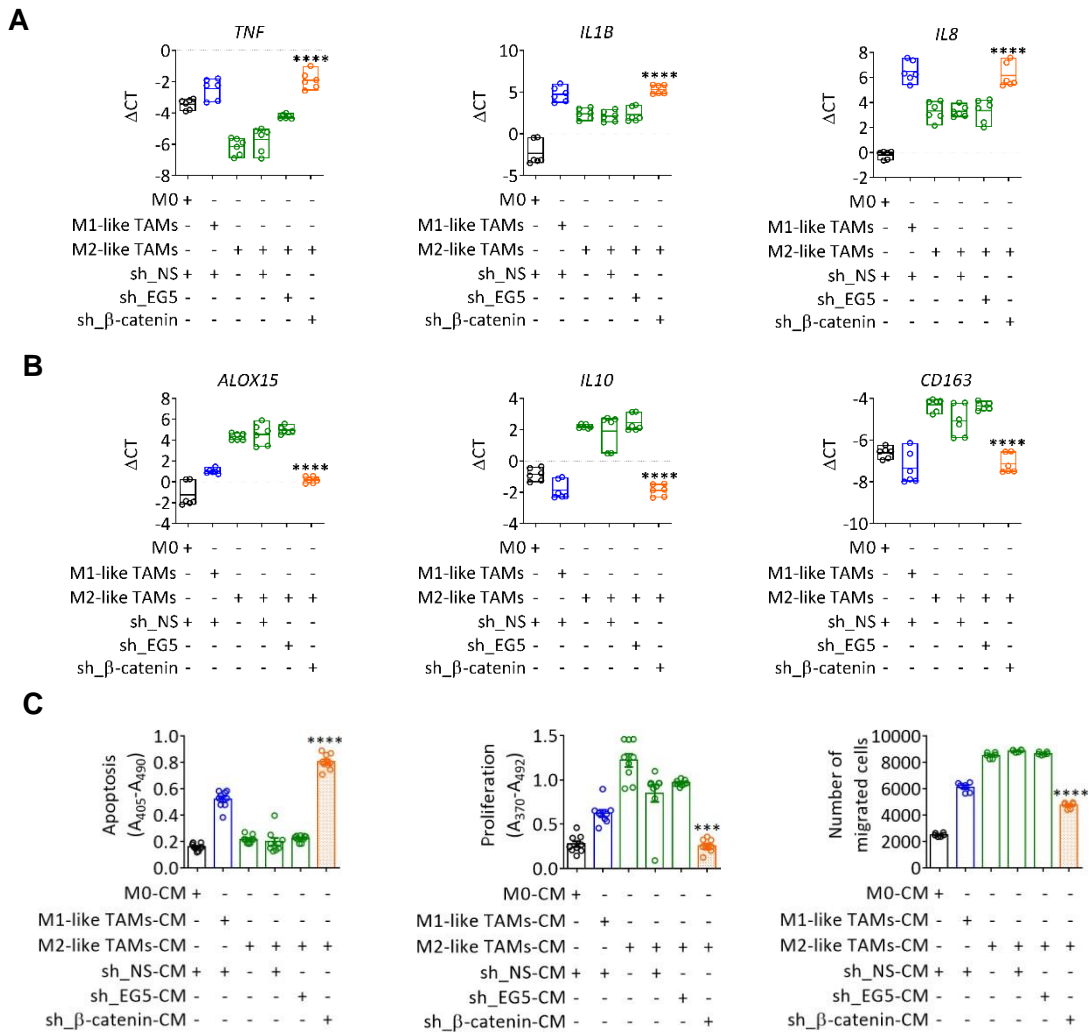


**Figure 16: Genetic ablation of  $\beta$ -catenin in *in-vitro*-trained TAMs switches M2-like TAMs to M1-like TAMs phenotype.** Relative mRNA expression of (A) M1 macrophage markers (*TNF*, *IL1B*, *IL8*) and (B) M2 macrophage markers (*IL10*, *CD163*, *ALOX15*) in M0 macrophages, M1-like TAMs, M2-like TAMs, and M2-like TAMs transfected with sh\_NS, sh\_EG5, and sh\_β-catenin for 24 h; n = 3 biological replicates, 2 technical replicates. \*P < 0.05, \*\*P < 0.01, \*\*\*P < 0.001 compared with sh\_NS. (C) Quantification of apoptosis, proliferation, and migration of A549 cells in the presence of CM from M0 macrophages, M1-like TAMs, M2-like TAMs, and M2-like TAMs transfected with sh\_NS, sh\_EG5, sh\_β-catenin for 24 h; n = 3 biological replicates, 3 (for apoptosis, proliferation) or 2 (for migration) technical replicates. \*\*\*P < 0.001, \*\*\*\*P < 0.0001 compared with sh\_NS. [(Sarode P et.al. 2020) Reuse permission: Distributed under the terms of the Creative Commons Attribution-NonCommercial license]

#### 4.3.2 Inhibition of $\beta$ -catenin in human *ex vivo* TAMs by si\_β-catenin

In TME, TAMs are composed of different phenotypes. Therefore, to understand the effect of  $\beta$ -catenin inhibition on primary TAMs from human lung tissue, small-interfering RNA (siRNA)-

mediated knockdown of  $\beta$ -catenin performed in *ex-vivo* TAMs obtained from human lung tumors for 24 h (**Figure 17A**). *si* $\beta$ -catenin mediated knockdown in *ex-vivo* TAMs downregulated the mRNA expression of *CCND1* (**Figure 17B**).

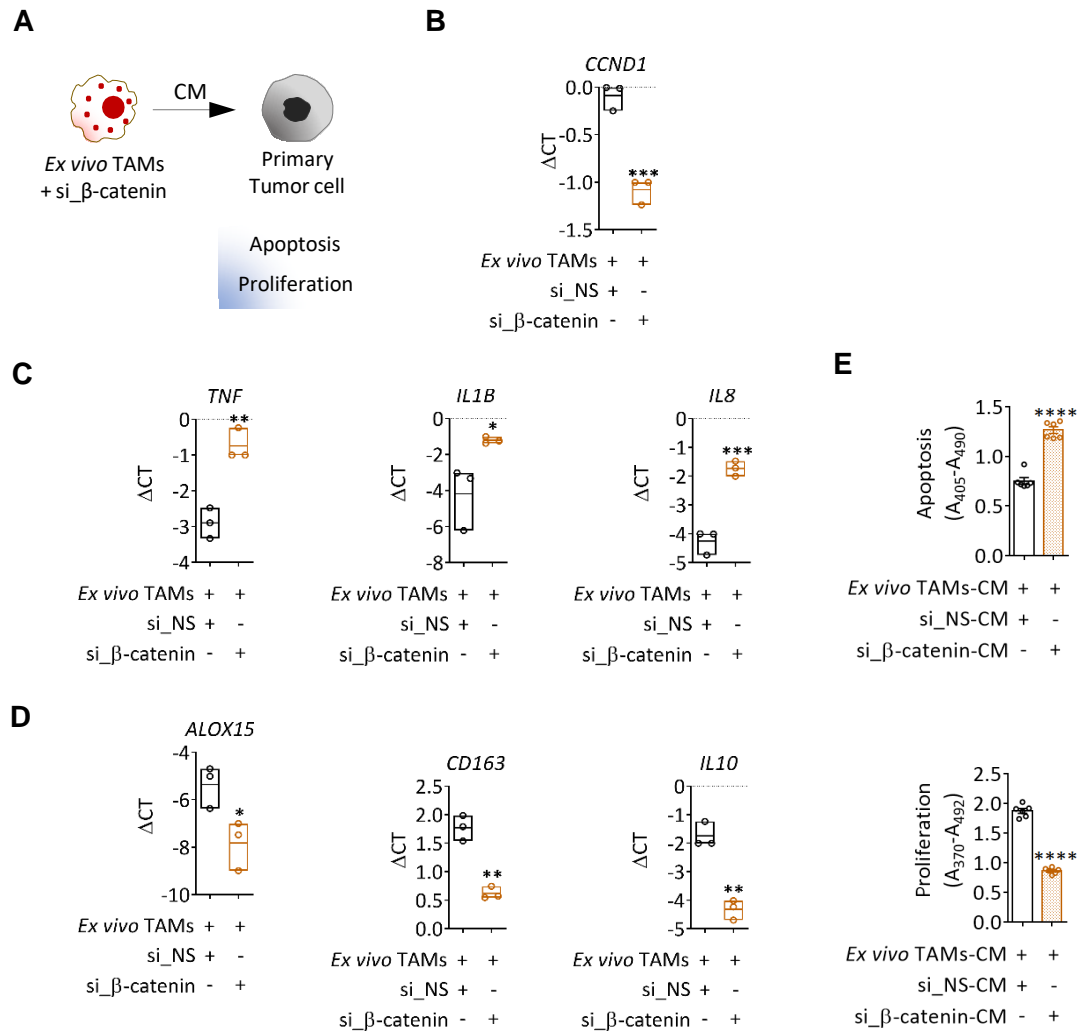


**Figure 17: Genetic ablation of  $\beta$ -catenin in human *ex-vivo* TAMs reprograms to M1-like TAMs phenotype.** (A) Schematic experimental plan showing the treatment of primary tumor cells in the presence of CM from *ex-vivo* TAMs transfected with *si* $\beta$ -catenin in terms of primary tumor cell apoptosis and proliferation. Relative mRNA expression of (B)  $\beta$ -catenin target gene (*CCND1*), (C) M1 macrophage markers (*TNF*, *IL1B*, *IL8*), and (D) M2 macrophage markers (*IL10*, *CD163*, *ALOX15*) in *ex-vivo* TAMs transfected with *si*\_NS and *si* $\beta$ -catenin for 24 h; n = 3 biological replicates. \*\*P < 0.01, \*\*\*P < 0.001 compared with *si*\_NS. (E) Quantification of apoptosis and proliferation of primary tumor cells in the presence of CM from *ex-vivo* TAMs transfected with *si*\_NS and *si* $\beta$ -catenin for 24 h. n = 3 biological replicates, 2 technical replicates. \*\*\*\*P < 0.0001 compared with *si*\_NS-CM. [(Sarode P et.al. 2020) Reuse permission: Distributed under the terms of the Creative Commons Attribution-NonCommercial license]

Similar to M2-like TAMs, *ex-vivo* TAMs transfected with *si* $\beta$ -catenin showed increased

expression of M1 and decreased expression of M2 macrophage markers (**Figure 17C, D**). In addition, their CM sharply decreased primary tumor cells' survival and proliferation (**Figure 17E**).

### 4.3.3 Inhibition of Wnt/ $\beta$ -catenin signaling in *ex vivo* TAMs and *in vitro* trained M2-like TAMs by XAV939

Similar to  $\beta$ -catenin's genetic ablation, pharmacological blockade using a cell-permeable small molecule inhibitor (XAV939) performed in *ex-vivo* TAMs obtained from human lung tumors (**Figure 18A**) and *ex-vivo* TAMs from mouse lung tumors (**Figure 18E**). XAV939 is a potent tankyrase (TNKS) inhibitor, which antagonizes Wnt/  $\beta$ -catenin signaling via stimulation of  $\beta$ -catenin degradation and stabilization of axin.

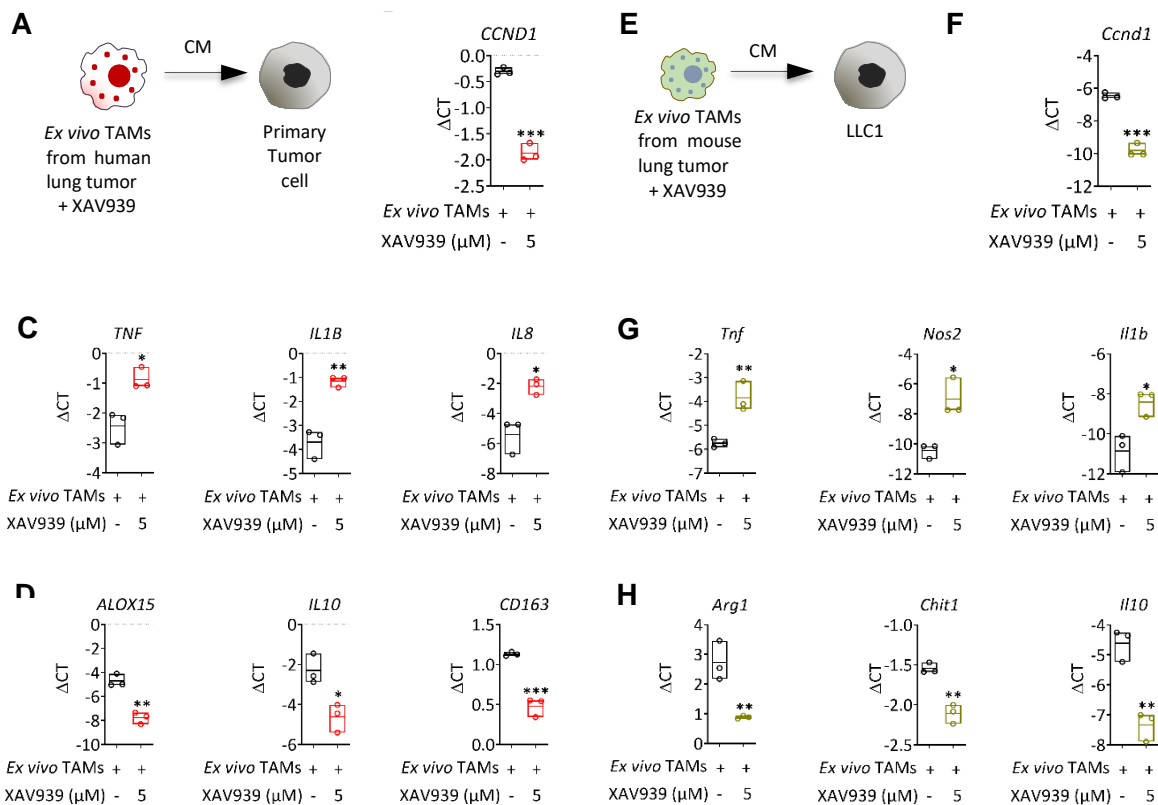


**Figure 18: Pharmacological ablation of  $\beta$ -catenin in primary TAMs reprograms to M1-like phenotype. (A)** Experimental plan showing human *ex-vivo* TAMs treated with XAV939 (5  $\mu$ M) for 24 h followed by conditioned medium (CM) treatment to the primary tumor cell. Relative mRNA expression of **(B) *CCND1*** **(C)** M1 macrophage markers (*TNF*, *IL1B*, *IL8*) **(D)** M2 macrophage markers (*IL10*, *CD163*, *ALOX15*) in human *ex-vivo* treated and untreated TAMs. **(E)** Experimental plan showing mouse *ex-vivo* TAMs treated with XAV939 (5  $\mu$ M) for 24 h followed by CM treatment to LLC1. Relative mRNA expression of **(F) *Ccnd1*** **(G)** M1 macrophage markers (*Tnf*, *Il1b*, *Il8*) **(H)** M2 macrophage markers (*Il10*, *Arg1*, *Chit1*) in mouse *ex-vivo* treated and untreated TAMs. n = 3 biological replicates. \*P < 0.05, \*\*P < 0.01, \*\*\*P < 0.001, \*\*\*\*P < 0.0001 compared with *ex-vivo* TAMs. [(Sarode P et.al. 2020)]

The downregulation of *Ccnd1* (**Figure 18B, F**) confirms that nuclear  $\beta$ -catenin activity was reduced after treatment with XAV939 in all types of TAMs. The downregulation of nuclear  $\beta$ -catenin activity in TAMs resulted consistently in upregulation of M1 macrophage markers and downregulation of M2 macrophage markers (**Figure 18C, D, G, H**)

Furthermore, treatment of human primary lung tumor cells and mouse-lung cancer cell lines, with CM from XAV939-treated human *ex-vivo* TAMs and mouse *ex-vivo* TAMs decreased survival and proliferation (**Figure 19A, B**). Additionally, CM from XAV939-treated M2-like TAMs (trained *in vitro* by co-culturing with A427, H1650) decreased survival and proliferation of A427, H1650 cells when compared that from untreated M2-like TAMs (**Figure 19C, D**).

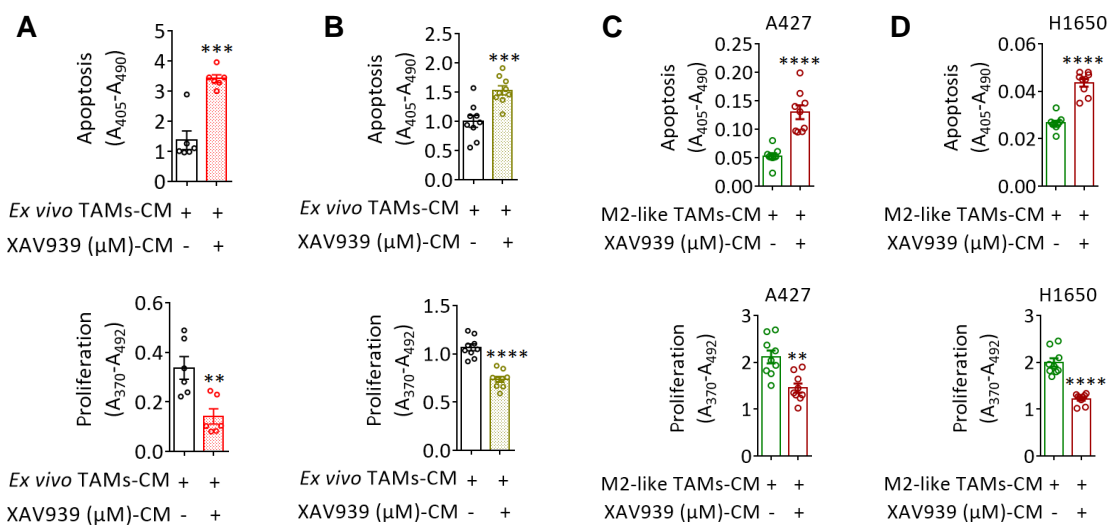


**Figure 19: Pharmacological ablation of  $\beta$ -catenin in primary TAMs and *in-vitro*-trained TAMs functionally switches M2-like TAMs to the M1-like TAMs phenotype.** Quantification of apoptosis and proliferation of (A) primary tumor cells in the presence of CM from *ex-vivo* TAMs treated with XAV939 for 24 h. n = 3 biological replicates, 2 technical replicates. \*\*P < 0.01, \*\*\*P < 0.001 compared with the CM of *ex-vivo* TAMs (B) LLC1 cells in presence of CM from *ex vivo* TAMs treated with XAV939 for 24 h. n=3 biological replicates, 3 technical replicates. \*\*P<0.01, \*\*\*P<0.001 compared with *Ex vivo* TAMs-CM (C) A427 presence of CM from A427-trained M2-like TAMs treated with XAV939 for 24 h (D) H1650 cells in the presence of CM from M2-like TAMs trained H1650-trained M2-like TAMs treated with XAV939 for 24 h; n = 3 biological replicates, 3 technical replicates. \*\*\*P < 0.001, \*\*\*\*P < 0.0001 compared with M2-like TAMs. [(Sarode P et.al. 2020) Reuse permission: Distributed under the terms of the Creative Commons Attribution-NonCommercial license]

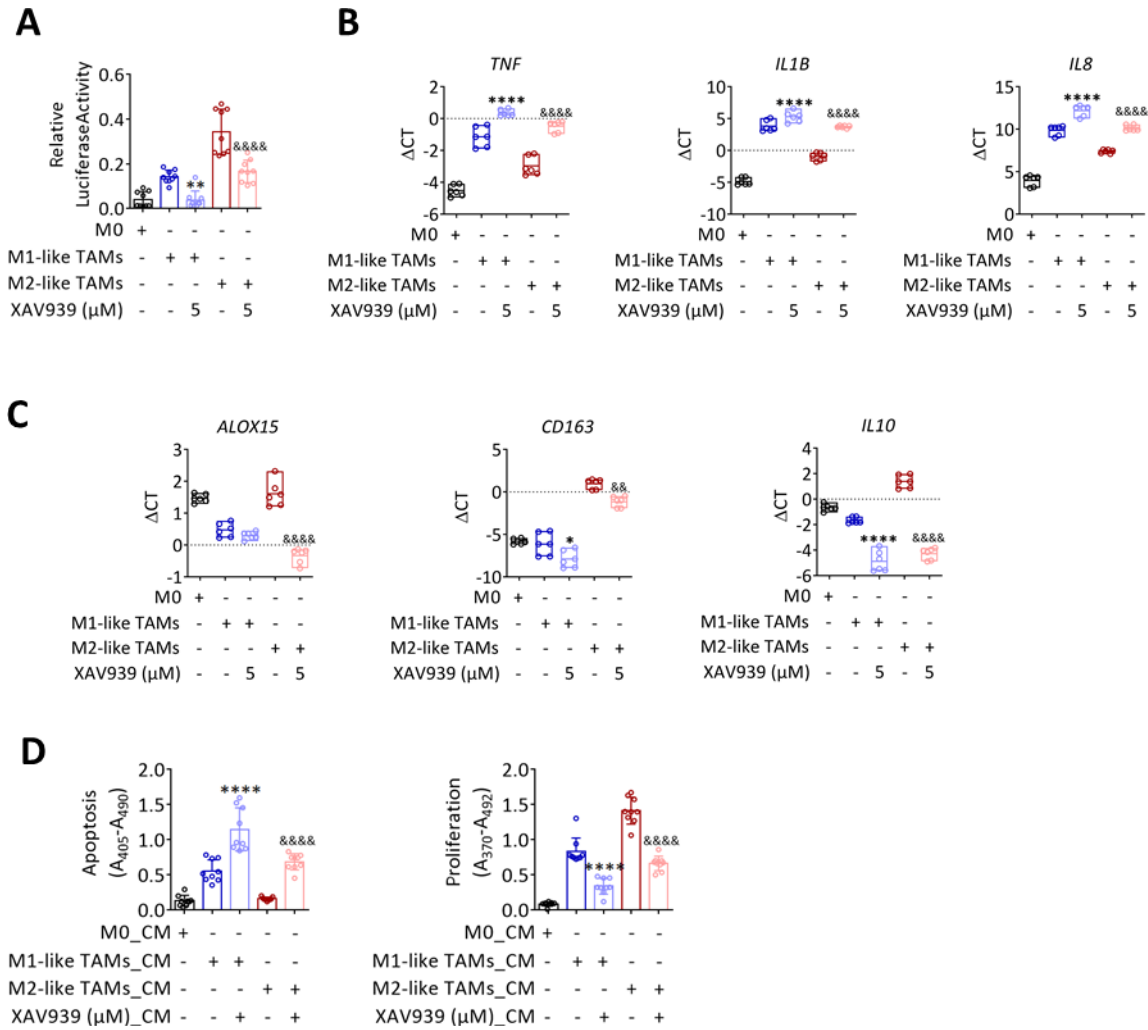


**Figure 20: Pharmacological inhibition of  $\beta$ -catenin in M1-like TAMs improves its anti-tumor effects.** M1-like TAMs and M2-like TAMs generated by directly co-culturing M0 macrophages and A549 cells. (A) Relative TCF/LEF luciferase activity in M0, M1-like TAMs, M2-like TAMs, and M1-like TAMs, M2-like TAMs treated with 5 $\mu$ M XAV939 for 24 hours; n = 3 biological replicates, 3 technical replicates. \*\*P < 0.01 compared with M1-like TAMs with M1-like TAMs\_5 $\mu$ M XAV939, &&&&P < 0.0001 compared with M2-like TAMs with M2-like TAMs\_5 $\mu$ M XAV939. Relative mRNA expression of (B) M1 macrophage markers (*TNF*, *IL1B*, *IL8*), and (C) M2 macrophage markers (*IL10*, *CD163*, *ALOX15*) in M0, M1-like TAMs, M2-like TAMs, and M1-like TAMs, M2-like TAMs treated with 5 $\mu$ M XAV939 for 24 h; n = 3 biological replicates, 2 technical replicates. \*\*P < 0.01, \*\*\*\*P < 0.0001 compared with M1-like TAMs with M1-like TAMs\_5 $\mu$ M XAV939, &&P < 0.001, &&&&P < 0.0001 compared with M2-like TAMs with M2-like TAMs\_5 $\mu$ M XAV939. (D) Quantification of apoptosis and proliferation of A549 cells in the presence of CM from M0, M1-like TAMs, M2-like TAMs and M1-like TAMs, M2-like TAMs treated with 5 $\mu$ M XAV939 for 24 h; n = 3 biological replicates, 3 technical replicates. \*\*\*\*P < 0.0001 compared with CM\_M1-like TAMs with CM\_M1-like TAMs\_5 $\mu$ M XAV939, &&&&P < 0.0001 compared with CM\_M2-like TAMs with CM\_M2-like TAMs\_5 $\mu$ M XAV939. [(Sarode P et.al. 2020) Reuse permission: Distributed under the terms of the Creative Commons Attribution-NonCommercial license]

As a control, M1-like TAMs treated with XAV939 for 24 hours, followed by mRNA expression profiling of macrophage markers and functional studies on A549 cells. Nuclear  $\beta$ -catenin activity (TCF/LEF activity-based) and expression of M2 macrophage markers decreased while that of M1-macrophage markers further increased in XAV939-treated M1-like TAMs (**Figure 20A - C**). CM from XAV939 treated M1-like TAMs reduced proliferation and survival in A549 cells (**Figure 20D**). Collectively, these results strongly demonstrated that the genetic and pharmacological ablation of  $\beta$ -catenin shifts tumor-promoting M2-like TAMs to tumor-inhibiting M1-like TAMs.

#### 4.3.4 Effect of direct XAV939 treatment and CM from XAV939-treated M2-like TAMs (*in-vitro-trained*) on proliferation and apoptosis of tumor cells

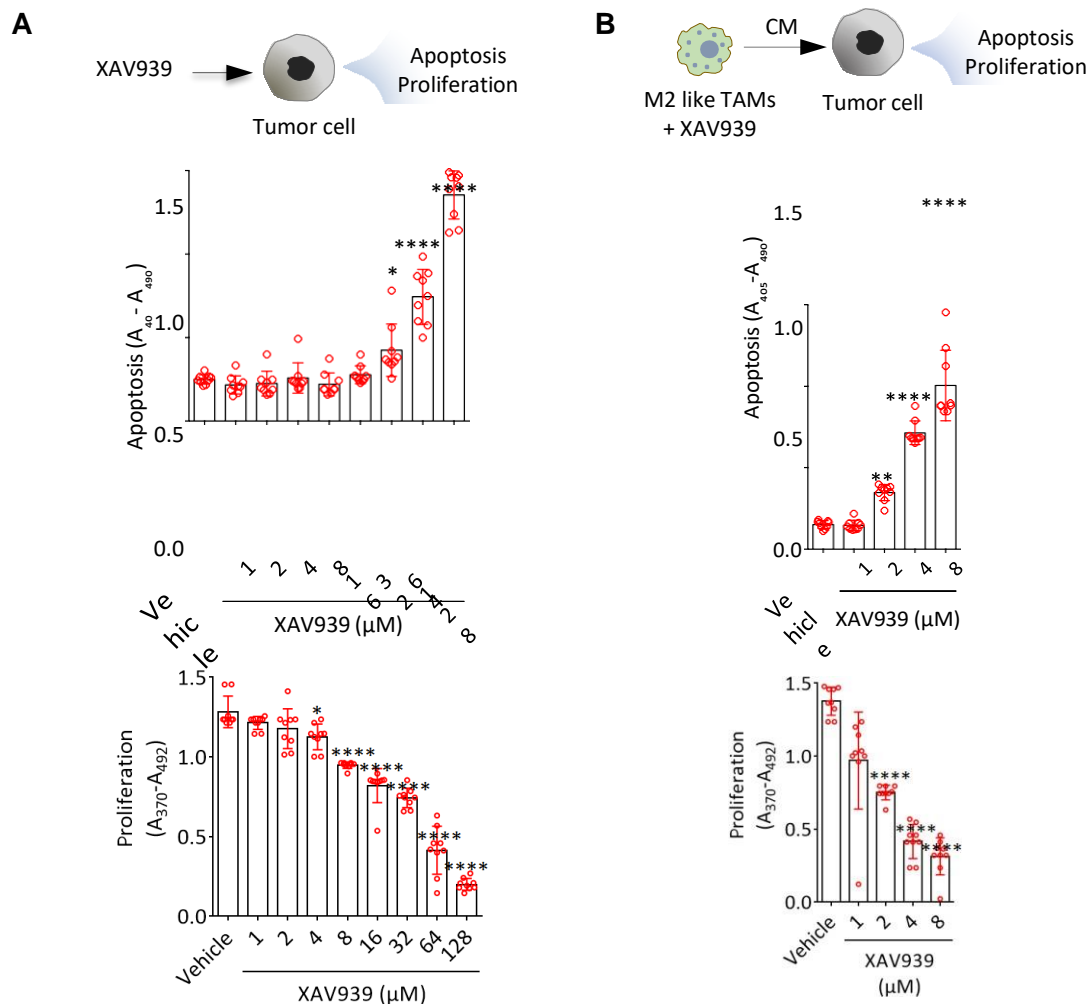


**Figure 21: Low dose of XAV939 was required to induce M1-like TAM anti-tumor immunity compared with direct treatment.** Quantification of apoptosis and proliferation of A549 cells treated (**A**) directly with XAV939 (1, 2, 4, 8, 16, 32, 64, 128  $\mu$ M) and (**B**) with CM from XAV939 (1, 2, 4, 8  $\mu$ M)-treated M2-like TAMs; n = 3 biological replicates, 3 technical replicates. \*P < 0.5, \*\*P < 0.01, \*\*\*\*P < 0.0001 compared with vehicle. [(Sarode P et.al. 2020) Reuse permission: Distributed under the terms of the Creative Commons Attribution-NonCommercial license]

A549 cells were treated with various concentrations of XAV939 (0, 1, 2, 4, 8, 16, 32, 64, 128  $\mu\text{M}$ ) or CM from XAV939 (0, 1, 2, 4, 8  $\mu\text{M}$ )-treated M2-like TAMs, to compare the effects of direct versus indirect (via TAM manipulation)  $\beta$ -catenin blockade on the tumorigenicity of A549 cells. In the first constellation, 32-64  $\mu\text{M}$  of XAV939 was required to reduce survival and proliferation in A549 cells by approximately 50–60% (**Figure 21A**). In contrast, a corresponding downregulation of A549 survival and proliferation was induced by the CM from M2-like TAMs, which were treated with only 4–8  $\mu\text{M}$  XAV939 (**Figure 21B**). These results demonstrated that re-activating TME's anti-tumor immunity by inhibiting TAM-specific Wnt/ $\beta$ -catenin might require a significantly lower amount of drug as compared to directly targeting the cancer cells by this inhibitor approach.

#### 4.4 Pharmacological ablation of $\beta$ -catenin suppresses primary and metastatic tumor growth by reprogramming TAMs into tumor-inhibiting M1-like TAMs

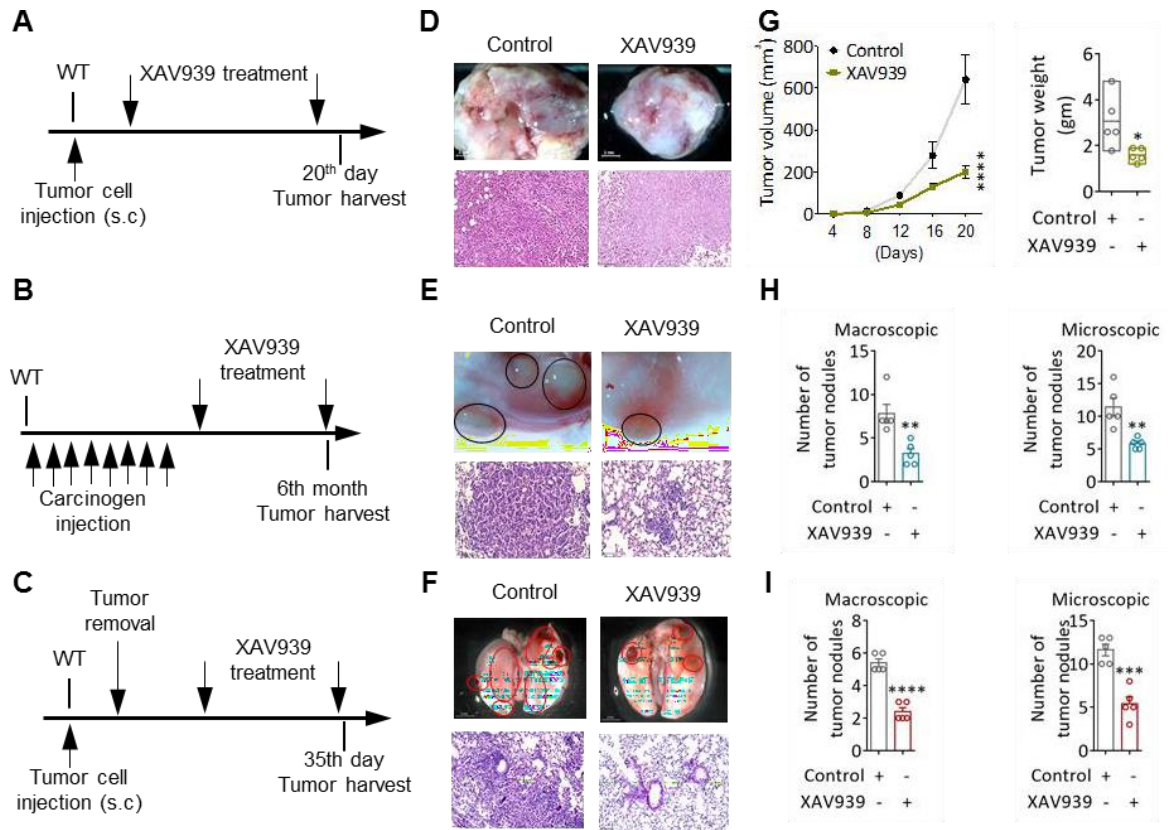


**Figure 22: Pharmacological ablation of  $\beta$ -catenin restricts tumor growth *in vivo*.** Experimental plan of the (A) subcutaneous (s.c.) tumor model; (B) Carcinogen-induced lung tumor model; (C) Metastasis lung tumor model; n = 5 per group. Representative pictures and images of hematoxylin and eosin (H&E)-stained sections of tumor from (D) s.c., (E) carcinogen-induced and (F) metastasis lung tumor models, scale bar = 20  $\mu$ M. (G) Quantification of tumor size on days 4–20 and tumor weight on day 20 to assess s.c. tumor growth, macroscopic and microscopic lung tumor nodules to be assessed in the (H) carcinogen-induced and (I) metastasis lung tumor models; \*P < 0.05, \*\*P < 0.01, \*\*\*P < 0.001, \*\*\*\*P < 0.0001 compared with control. [(Sarode P et.al. 2020) Reuse permission: Distributed under the terms of the Creative Commons Attribution-NonCommercial license]

To determine the functional role of  $\beta$ -catenin inhibition *in vivo*, we used XAV939 (25 mg/kg, intraperitoneally) in three different tumor models: (i) subcutaneous (s.c.) tumors (**Figure 22A**), (ii) carcinogen-induced lung tumors (**Figure 22B**), and (iii) metastatic lung tumors (**Figure 22C**). Treatment with XAV939 significantly reduced the growth of primary (s.c. and carcinogen-induced) and metastatic (macroscopic and microscopic) lung tumors *in vivo* (**Figure 22D–I**).

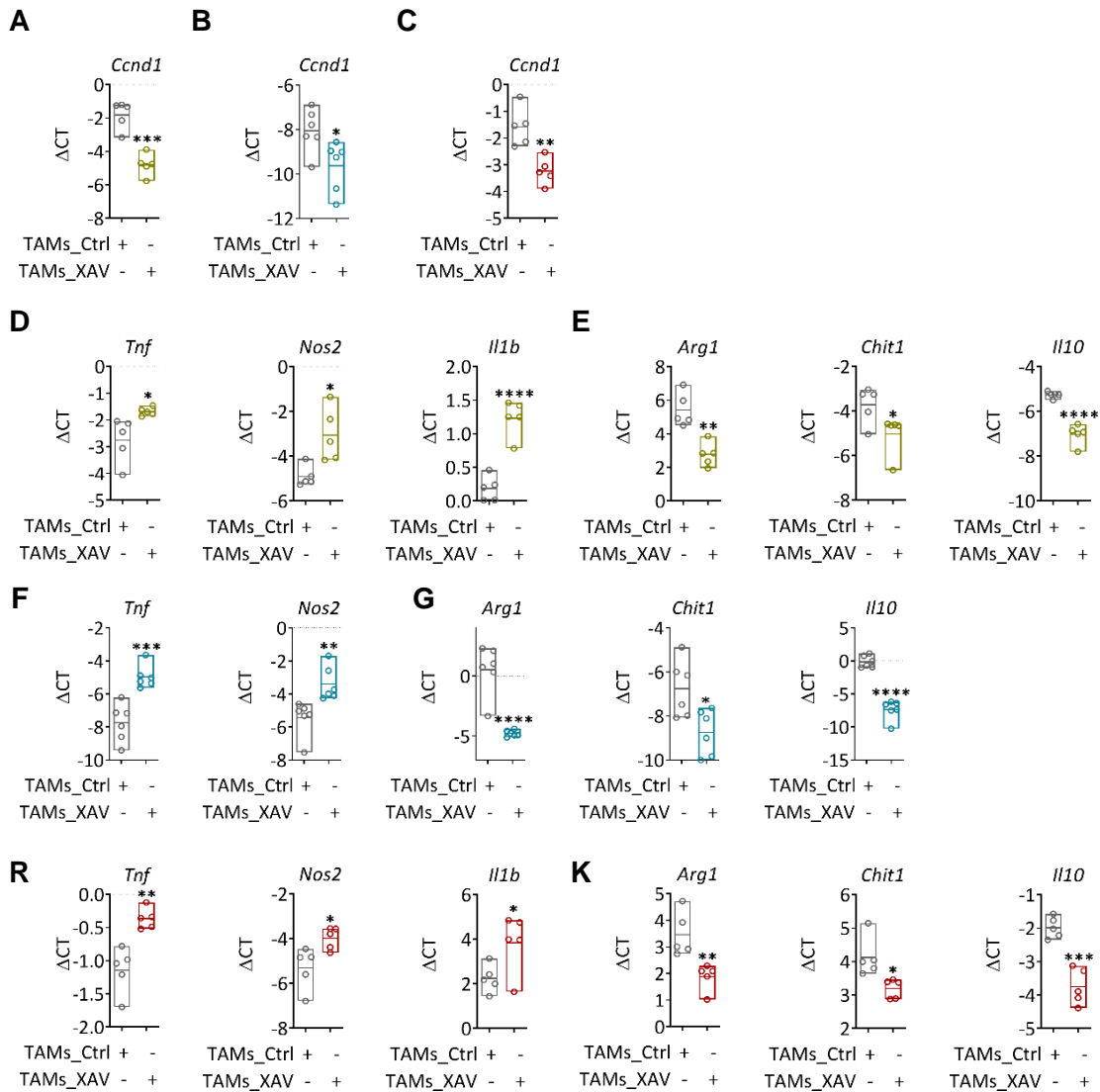


**Figure 23: Pharmacological ablation of  $\beta$ -catenin restricts tumor growth *in vivo* by phenotypically switching M2-like TAMs to M1-like TAMs.** Relative mRNA expression of (**A–C**) *Ccnd1*, (**D–F**) M1 (*Tnf*, *Nos*, *Il1b*), (**G–I**) M2 (*Il10*, *Arg1*, *Chit1*) macrophage markers in TAMs sorted from mice tumor tissue treated with control (DMSO; TAM\_Ctrl) and XAV939 (TAMs\_XAV) in the (**A, D, E**) s.c., (**B, F, G**) carcinogen-induced, and (**C, H, I**) metastasis lung tumor models; n = 5 biological replicates, \*\*P < 0.05, \*\*P < 0.01, \*\*\*P < 0.001, \*\*\*\*P < 0.0001 compared with TAMs\_Ctrl. [(Sarode P et.al. 2020) Reuse permission: Distributed under the terms of the Creative Commons Attribution-NonCommercial license]

To delineate the TAM' molecular signature of the control (dimethyl sulfoxide: DMSO) versus the XAV939-treated groups, primary TAMs were isolated using F4/80 antibody-linked magnetic beads, followed by mRNA expression profiling. The reduced mRNA expression of *Ccnd1* in TAMs isolated from the XAV939 treated animals confirmed the downregulation of nuclear  $\beta$ -catenin activity in these *in vivo* studies (**Figure 23A–C**). Notably, TAMs isolated from the XAV939 group showed increased M1 expression (*Tnf*, *Nos2*, *Il1b*) and decreased expression of M2 macrophage markers (*Il10*, *Arg1*, *Chit1*) (**Figure 23D–I**).

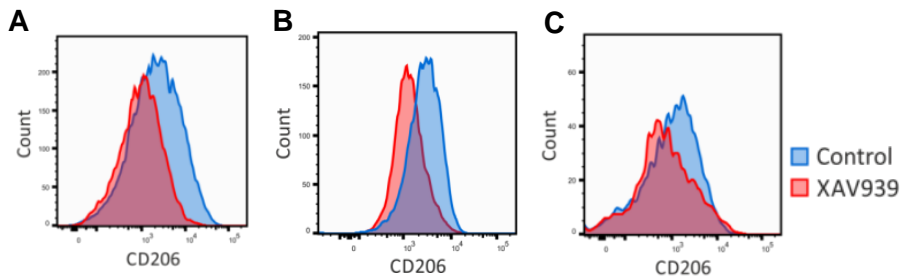


**Figure 24: Pharmacological ablation of  $\beta$ -catenin restricts tumor growth *in vivo* by reducing CD206 macrophage infiltration.** FACS histograms indicate the mean fluorescence intensity of CD206<sup>+</sup> macrophages in control (blue) and XAV939 (red)-treated tumor tissue from (A) s.c., (B) carcinogen-induced, and (C) metastasis lung tumor models. [(Sarode P et.al. 2020) Reuse permission: Distributed under the terms of the Creative Commons Attribution-NonCommercial license]

Moreover, treatment with XAV939 significantly reduced the number of CD206-positive M2-like TAMs in the TME (**Figure 24A–C**). Collectively, these results indicate that inhibiting  $\beta$ -catenin restricts tumor growth *in vivo*. Importantly,  $\beta$ -catenin downregulation in TAMs induces their phenotypical switch into tumor-inhibiting M1-like TAMs in the TME in different lung cancer models.

#### 4.5 Macrophage-specific genetic ablation of $\beta$ -catenin reduces lung tumor development by inducing M1-like TAM-directed anti-tumor immunity in the TME

We hypothesized that inactivating TAM'  $\beta$ -catenin switches the phenotype to that of M1-like TAMs, thereby inducing functional anti-tumor immunity in the lung TME. Transgenic mice with macrophage-specific  $\beta$ -catenin depletion (*Catnb*<sup>ff</sup>*Lysm*<sup>Cre</sup>) were developed. We subsequently used two different approaches to induce lung tumors in these transgenic mice. In a first approach, a carcinogen-induced model, *Catnb*<sup>ff</sup>*Lysm*<sup>Cre</sup>, *Catnb*<sup>ff</sup>, and *Lysm*<sup>Cre</sup> mice intraperitoneally treated with urethane for six months (**Figure 25A**). In the second approach, bone marrow cells from *Catnb*<sup>ff</sup>*Lysm*<sup>Cre</sup>, *Catnb*<sup>ff</sup>, and *Lysm*<sup>Cre</sup> mice were transplanted into these lethally irradiated wild-type mice, followed by intratracheal injection of Lewis lung

carcinoma (LLC1) cells (**Figure 25B**). In both models, mice with  $\beta$ -catenin-deficient macrophages ( $Catnb^{ff}/Lysm^{Cre}$ ) showed a significant reduction of macroscopic and microscopic lung tumor burden versus wild-type mice ( $Catnb^{ff}$ , and  $Lysm^{Cre}$ ) (**Figure 25C–F**).

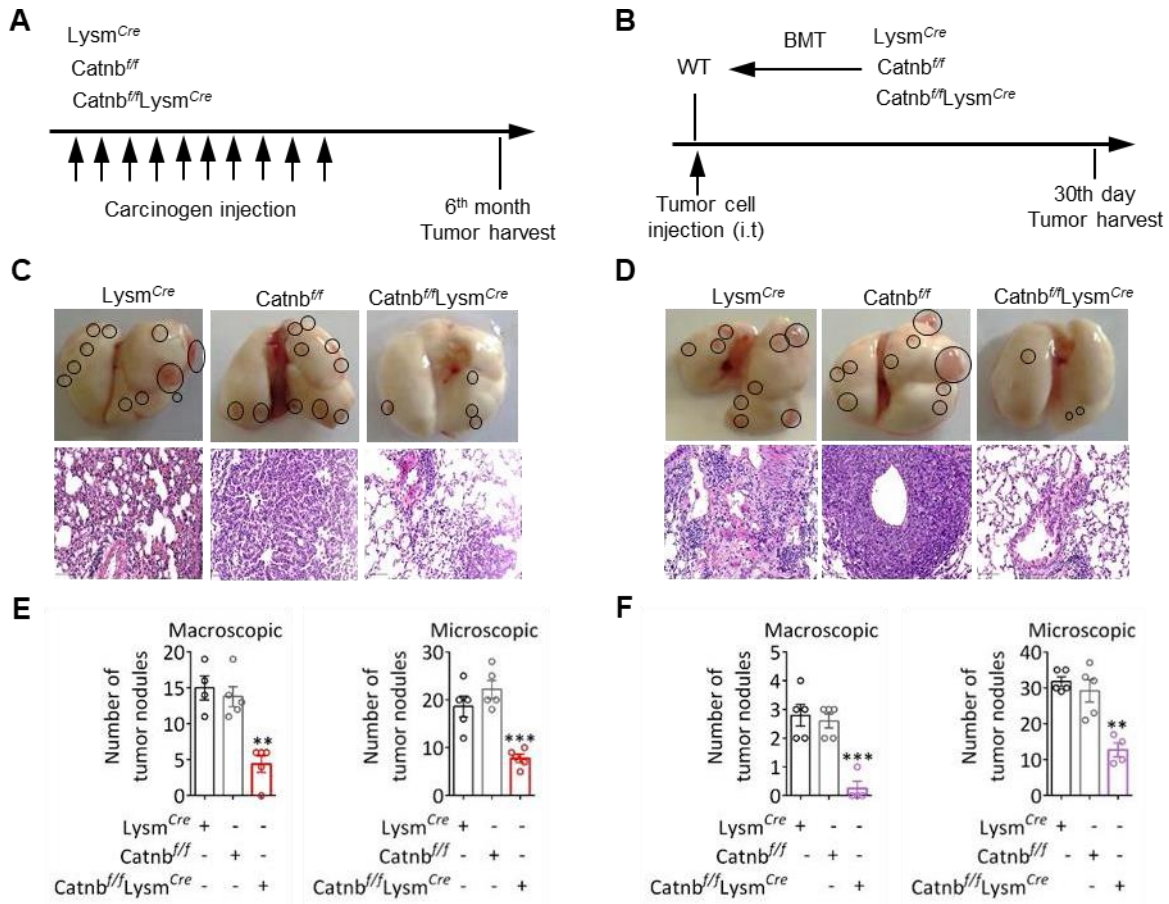


**Figure 25: Macrophage-specific genetic ablation of  $\beta$ -catenin reduces the development of lung tumors.** Experimental plan of the **(A)** carcinogen-induced lung tumor model ( $Catnb^{ff}/Lysm^{Cre}$ ,  $Catnb^{ff}$ , and  $Lysm^{Cre}$ ) mice intraperitoneally treated with urethane for 6 months). **(B)** Bone marrow transplantation model (BMT); bone marrow cells from  $Catnb^{ff}/Lysm^{Cre}$ ,  $Catnb^{ff}$ , and  $Lysm^{Cre}$  were transplanted into lethally irradiated C57BL/6, and after 1 month of bone marrow reconstitution, LLC1 cells intratracheally injected into mice. **(C, D)** Representative pictures and images of H&E stained sections of lungs from the **(C)** carcinogen-induced lung tumor model and **(D)** BMT lung tumor model, Scale bar=20 $\mu$ m. **(E, F)** Quantification of macroscopic and microscopic lung tumor nodules for the assessment of tumor burden in the **(E)** carcinogen-induced and **(F)** bone marrow transplantation models; \*\*P < 0.01, \*\*\*P < 0.001 compared with  $Catnb^{-/-}$ . [(Sarode P et.al. 2020) Reuse permission: Distributed under the terms of the Creative Commons Attribution-NonCommercial license]

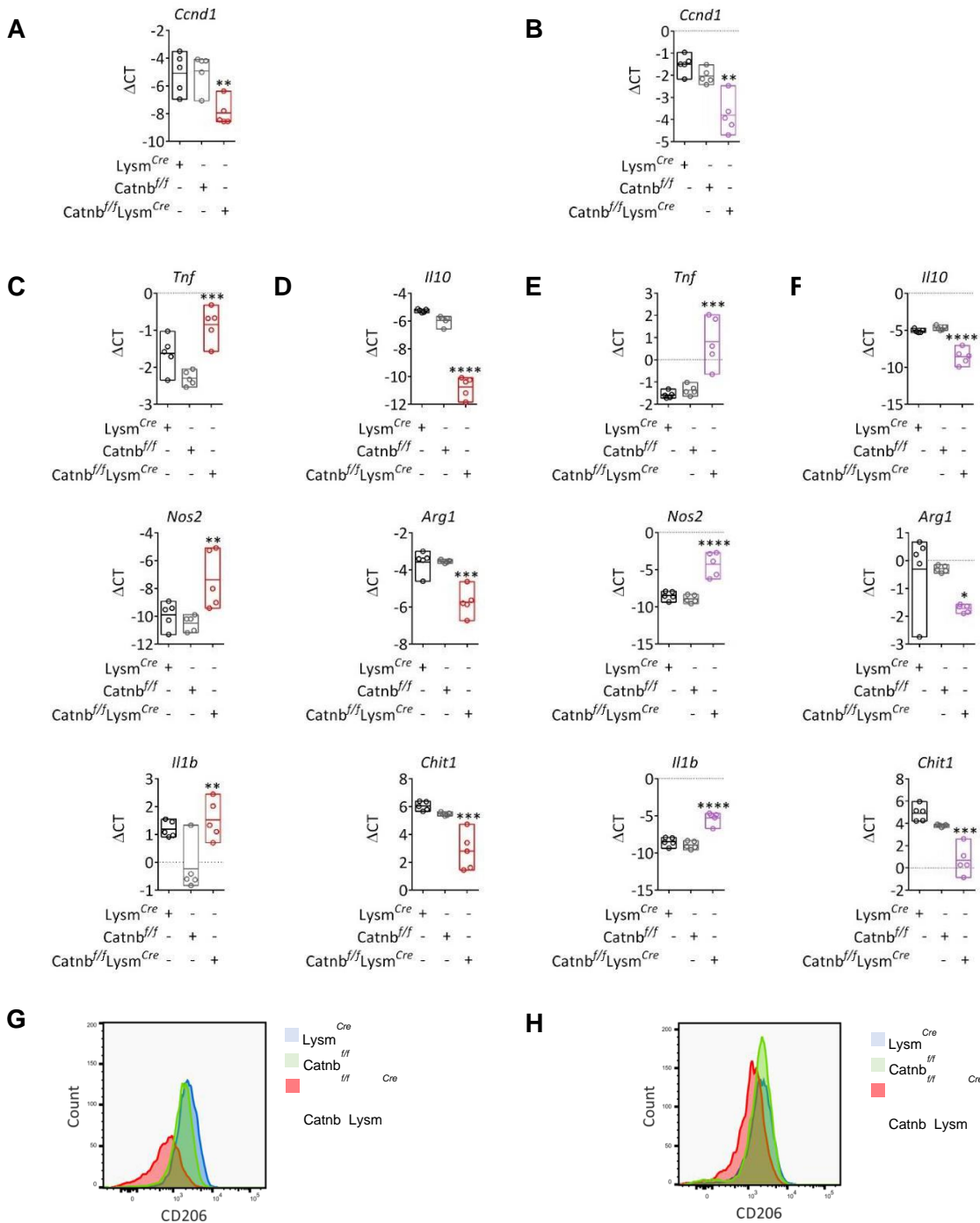


**Figure 26: Macrophage-specific genetic ablation of  $\beta$ -catenin leads to induction of M1-like TAM-directed anti-tumor immunity in the TME.** Relative mRNA expression of **(A, B) *Ccnd1*** **(C, E) *Tnf***, ***Nos2***, ***Il1b*** **(D, F) *Il10***, ***Arg1***, ***Chit1*** in TAMs sorted from macrophage-specific  $\beta$ -catenin-deficient tumors (TAMs\_Catnb<sup>ff/ff</sup>Lysm<sup>Cre</sup>) and wild-type tumors (TAMs\_Lysm<sup>Cre</sup> and TAMs\_Catnb<sup>ff/ff</sup>) in the **(A, C, E)** carcinogen-induced, **(B, D, F)** BMT lung tumor models; n = 5 biological replicates, \*\*P < 0.05, \*\*P < 0.01, \*\*\*P < 0.001, \*\*\*\*P < 0.0001 compared with TAMs\_Ctrl. **(G, H)** FACS histograms indicate the MFI of CD206<sup>+</sup> macrophages in Catnb<sup>ff/ff</sup>Lysm<sup>Cre</sup> (red) and Lysm<sup>Cre</sup> (blue) and Catnb<sup>ff/ff</sup> (green) from the **(G)** carcinogen-induced and **(H)** BMT lung tumor models. n = 5. [(Sarode P et.al. 2020)]

Reduced *Ccnd1* mRNA expression confirmed the downregulation of nuclear  $\beta$ -catenin activity in  $\beta$ -catenin-deficient TAMs (**Figure 26A, B**). Notably, TAMs\_ *Catnb*<sup>ff</sup>/*Lysm*<sup>Cre</sup> showed increased expression of M1 and decreased expression of M2 macrophage markers (**Figure 26C–F**). The tumors from mice bearing  $\beta$ -catenin-deficient macrophages also showed a significant reduction of CD206-positive M2-like TAM infiltration (**Figure 26G, H**). Collectively, these results indicate that inhibiting macrophage-specific  $\beta$ -catenin reduced lung tumorigenesis by inducing M1-like TAMs anti-tumor response in the TME.

#### **4.6 Inhibition of $\beta$ -catenin signaling, suppression of FOSL2 and activation of ARID5A leads to reprogramming of M2-like TAMs to M1-like TAMs; correlation of $\beta$ -catenin/FOSL2/ARID5A with survival of lung cancer patients**

##### **4.6.1 $\beta$ -catenin-mediated transcriptional regulation of FOSL2 and ARID5A may play a role in M2-like TAMs polarization.**

To uncover the molecular mechanism behind the robust phenotypic and functional switch of M2-like TAMs to M1-like TAMs after  $\beta$ -catenin inhibition *in vitro* and in *in vivo* experiments, RNA sequencing of M2-like TAMs transfected with control shRNA, and  $\beta$ -catenin shRNA was performed. As shown in **Figure 27A**, the majority of M1 macrophages markers were upregulated and M2 macrophages markers was downregulated in M2-like TAMs transfected with  $\beta$ -catenin shRNA compared to M2-like TAMs transfected with scramble shRNA.  $\beta$ -catenin is a transcription factor known to interact with the promoter of individual genes and with other transcription factors to regulate a wide range of genes. We performed a 2-step analysis to find whether  $\beta$ -catenin directly interacts with transcription factors involved in macrophage polarization. (i) RNA sequencing revealed 109 transcription factors (TFs) differentially regulated after inhibition of Wnt/ $\beta$ -catenin signaling in M2-like TAMs. Depending upon the stimulus,  $\beta$ -catenin binds to its specific transcriptional co-factors to regulate transcription of the target gene. The most common transcriptional co-factors of  $\beta$ -catenin are from the TCFs\LEF family, which possess nearly identical conserved  $\beta$ -catenin interaction domains near the N-terminus (<sup>A</sup>/<sup>A</sup><sub>T</sub>/TCAAAG). Therefore, we analyzed <sup>A</sup>/<sup>A</sup><sub>T</sub>/TCAAAG domain in differentially regulated TFs. *In-silico* analysis of the TCF-binding motif (<sup>A</sup>/<sup>A</sup><sub>T</sub>/TCAAAG) in these TFs predicted that  $\beta$ -catenin can bind to the promoter of FOSL2, RBPJ, PRDM1, KLF9, TFEC, MGA, FOXJ3, KFL12, CREB5 (downregulated TFs in M2-like TAMs transfected with sh\_ $\beta$ -catenin) and TFEB, USF1, ARID5A, RELB, BATF (upregulated TFs in M2-like TAMs transfected with sh\_ $\beta$ -catenin). (**Figure 27B**). (ii) TF binding site motif enrichment scanning performed in the promoter sequences of M1 and M2 macrophage genes to uncover the role of these TFs in the macrophage transcriptional program. Notably, in comparison with other TFs, FOSL2 and

ARID5A exhibited the most significant enrichment of transcription factor binding sites (TFBS) in the promoter of M2 and M1 macrophage genes, respectively (**Figure 27C**).

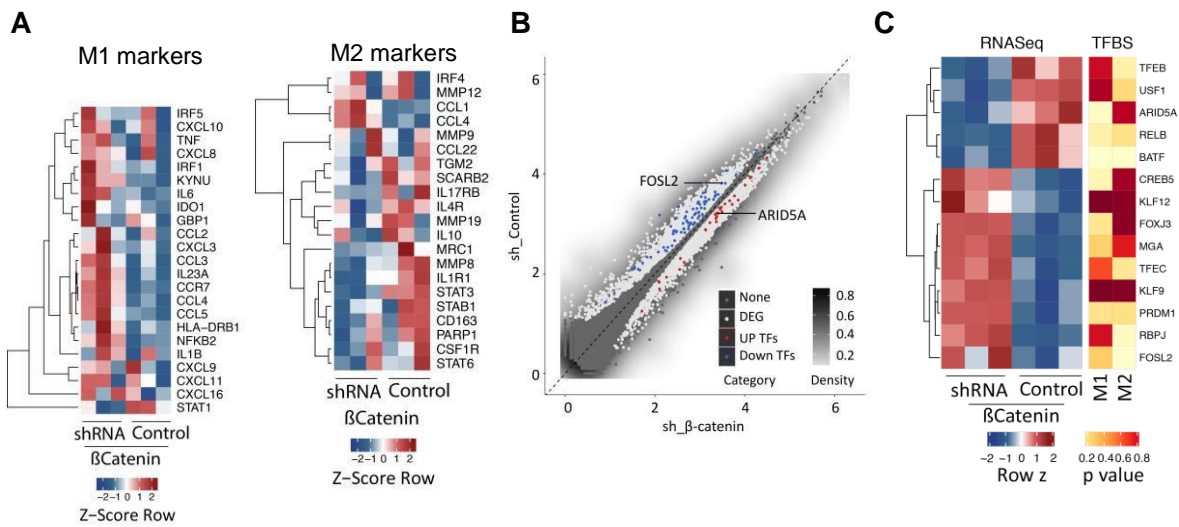


**Figure 27: Differential regulation of transcription factors in M2-like TAMs after inhibition of  $\beta$ -catenin.** M2-like TAMs were transfected with shRNA Control and sh $\beta$ -catenin and assessed using RNA sequencing. **(A)** The heatmaps show the expression of genes encoding M1 and M2 macrophage markers in M2-like TAMs transfected with shRNA Control and sh $\beta$ -catenin,  $n = 3$ . **(B)** DESeq normalized read count averages of genes were log<sub>10</sub>-transformed and compared between sh $\beta$ -catenin and shRNA Control. DEGs (FDR < 0.05, light grey), DEGs annotated as a transcription factor by the Jaspas vertebrate database (blue, red), and non-differential genes (dark grey) depicted as points. The grey shading represents the estimation of kernel density. **(C)** The heatmap displays the transcription factor-binding site (TFBS) enrichment analysis. The M1 and M2 macrophage marker genes (25 each) submitted to the TFBS enrichment analysis. 14 genes were found to be significantly differentially expressed between sh $\beta$ -catenin and shRNA Control (FDR < 0.05 annotated as transcription factors by Jaspas). The left heatmap depicts a row-wise Z-score of RNASeq DESeq normalized expression values, while the right heatmap shows the Pscan TFBS enrichment P-value. Overrepresentation of the respective binding motif of the TFs in the promoters of the 25-macrophage marker genes of either M1 or M2 compared with the background of all protein-coding genes' promoters. [(Sarode P et.al. 2020) Reuse permission: Distributed under the terms of the Creative Commons Attribution-NonCommercial license]

The mRNA and protein expression analyzed in unstimulated bone marrow-derived macrophages from Catnb<sup>fl/fl</sup>Lysm<sup>Cre</sup>, Catnb<sup>fl/fl</sup>, and Lysm<sup>Cre</sup> mice, to investigate the possibility that ARID5A and FOSL2 expression may be  $\beta$ -catenin dependent.

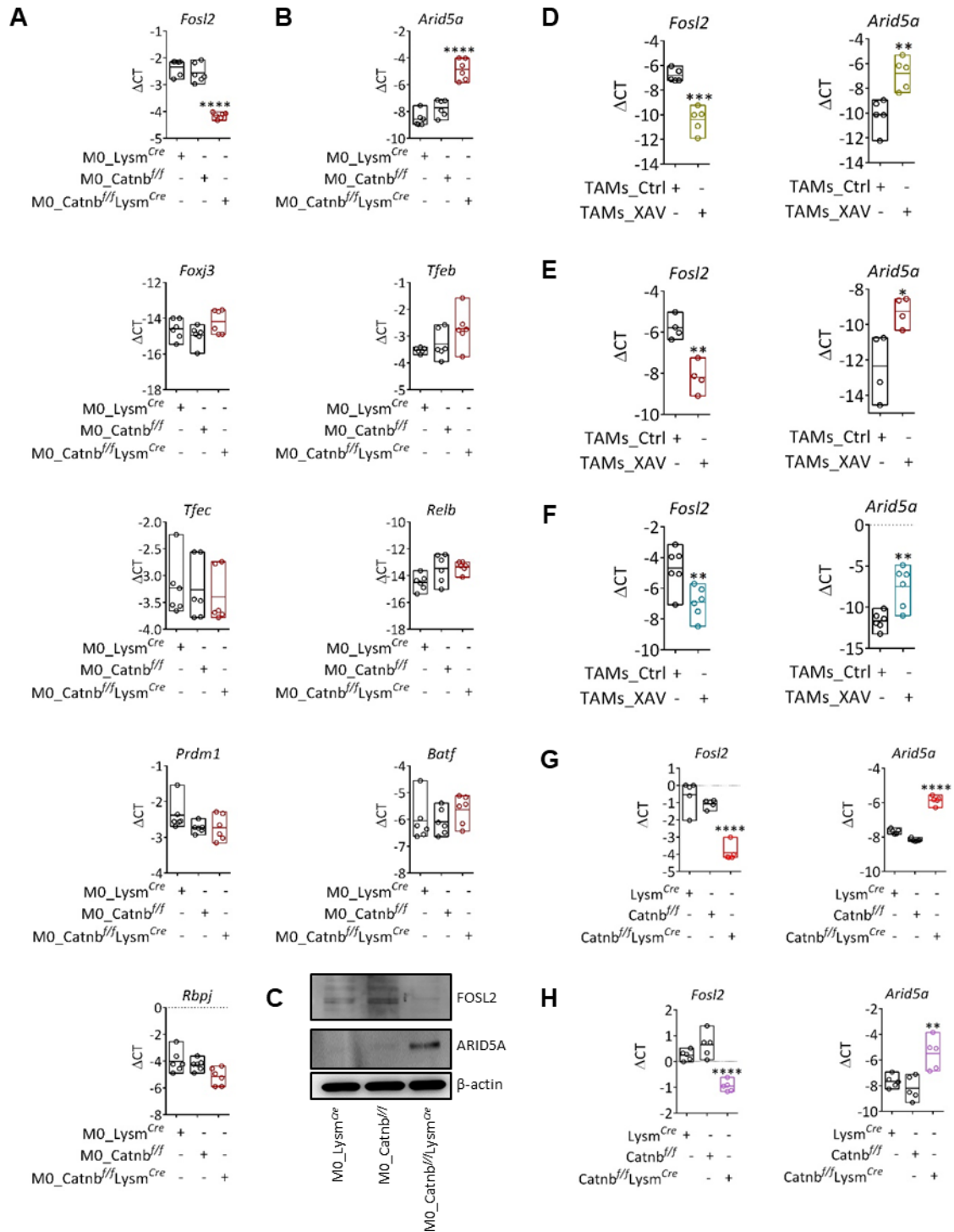


**Figure 28:  $\beta$ -catenin reciprocally regulates transcription of FOSL2 and ARID5A in M2-like TAMs.**

Relative mRNA expression of **(A)** *Fosl2*, *Foxj3*, *Tfec*, *Prdm1*, *Rbpj*, **(B)** *Arid5a*, *Tfeb*, *Relb*, and *Batf* **(C)** Western blotting analysis of *Fosl2*, *Arid5a*, and  $\beta$ -actin in undifferentiated BMDMs (M0) from Catnb<sup>f/f</sup>Lysm<sup>Cre</sup>, Catnb<sup>f/f</sup>, and Lysm<sup>Cre</sup> mice; n = 6. mRNA expression of *Fosl2* and *Arid5a* in TAMs sorted from **(D)** s.c., **(E)** carcinogen-induced, **(F)** metastasis lung tumor models, **(G)** carcinogen-induced and **(H)** BMT lung tumor models n = 5 biological replicates. \*P < 0.05, \*\*P < 0.01, \*\*\*P < 0.001, \*\*\*\*P < 0.0001 compared with TAM\_Ctrl.or TAMs\_Catnb<sup>f/f</sup> [(Sarode P et.al. 2020) Reuse permission: Distributed under the terms of the Creative Commons Attribution-NonCommercial license]

The mRNA expression profiling of these TFs in undifferentiated bone marrow-derived macrophages (M0) from *Catnb<sup>ff/Lysm<sup>Cre</sup></sup>*, *Catnb<sup>ff</sup>*, and *Lysm<sup>Cre</sup>* mice showed significant downregulation of *Fosl2* and upregulation of *Arid5a* in  $\beta$ -catenin-deficient M0 (M0\_ *Catnb<sup>ff/Lysm<sup>Cre</sup></sup>*) versus other TFs (**Figure 28A, B**). Corresponding effects were observed for the FOSL2 and ARID5A at protein levels (**Figure 28C**). Interestingly,  $\beta$ -catenin-deficient M1-like TAMs, isolated from five different *in-vivo* tumor models (TAMs from XAV393 and TAMs from *Catnb<sup>ff/Lysm<sup>Cre</sup></sup>*), also showed downregulation of *Fosl2* and upregulation of *Arid5a* at the mRNA level (**Figure 28D–H**).

Furthermore, analysis of mRNA and protein expression in M1 macrophages (induced via lipopolysaccharide+interferon gamma), M2 macrophages (induced via IL4), M1-like TAMs, and M2-like TAMs confirmed higher expression of FOSL2 in M2 macrophages and M2-like TAMs, and ARID5A in M1 macrophages and M1-like TAMs (**Figure 29A–D**).

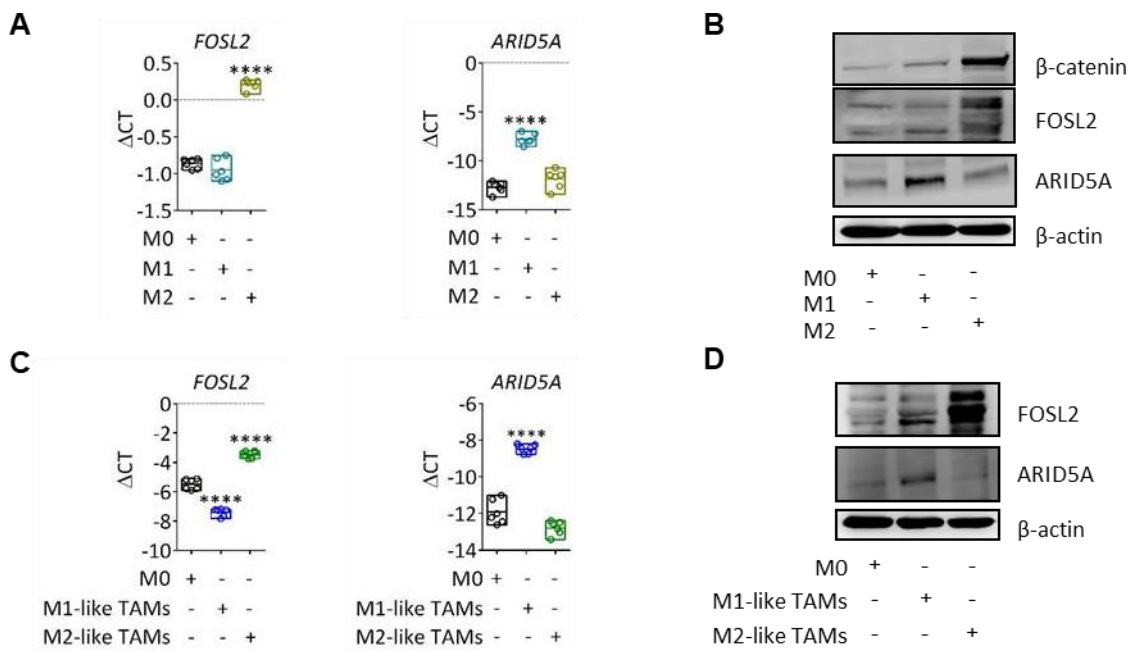


**Figure 29: Expression of FOSL2 and ARID5A increased and decreased, respectively, in M2 macrophages and M2-like TAMs. (A)** Relative mRNA expression **(B)** Western blotting analysis of  $\beta$ -catenin, *FOSL2* and *ARID5A* in **(A)** M0 macrophages, M1 macrophages, and M2 macrophages; **(C)** Relative mRNA expression **(D)** Western blotting analysis of  $\beta$ -catenin, *FOSL2* and *ARID5A* in **(A)** M0 macrophages, M1-like TAMs, and M2-like TAMs. n = 3 biological replicates, 2 technical replicates. \*\*\*\*P < 0.0001 compared with M0. [(Sarode P et.al. 2020) Reuse permission: Distributed under the terms of the Creative Commons Attribution-NonCommercial license]

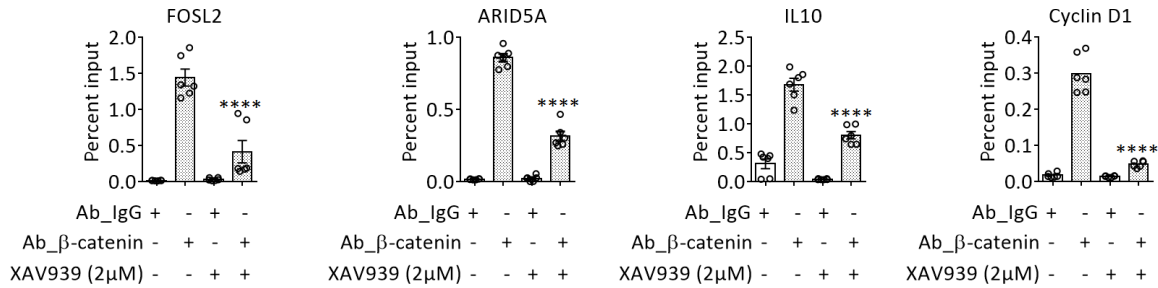


**Figure 30: β-catenin directly bound to the promoter of FOSL2 and ARID5A.** The real-time PCR analysis of β-catenin ChIP assays performed in M2 macrophages treated with control (DMSO) and XAV939 (2μM) for 24 h. Specific oligonucleotides for FOSL2, ARID5A, IL10, and CCND1 were used to detect β-catenin binding in chromatin enriched with β-catenin antibody (Ab\_β-catenin) and with isotype control antibody (IgG); n = 3 biological replicates, 2 technical replicates. \*\*\*\*P < 0.0001 compared with Ab\_β-catenin. [(Sarode P et.al. 2020) Reuse permission: Distributed under the terms of the Creative Commons Attribution-NonCommercial license]

Promoter occupancy by β-catenin was determined through ChIP using a β-catenin antibody in M2 macrophages treated with control (DMSO) and XAV939 to identify whether β-catenin directly binds to the promoter of FOSL2 and ARID5A. Strong enrichment of β-catenin observed at the promoter regions of FOSL2 and ARID5A, as well as known β-catenin target genes (IL10, CCND1) in M2 macrophages. XAV939 significantly impaired binding of β-catenin to the promoters of target mentioned above genes (**Figure 30**). Collectively, these results indicate that β-catenin-induced transcriptional regulation may play a role in M2-like TAMs polarization.

#### 4.6.2 β-catenin differentially regulates the transcription of FOSL2 and ARID5A in M2-like TAMs

β-catenin gain (OE\_β-catenin) and loss (si\_β-catenin) of function were performed in M2-like TAMs to explore the β-catenin-mediated transcriptional regulation of the TFs FOSL2 and ARID5A. The mRNA and protein expression of FOSL2 was found to be upregulated in M2-like TAMs overexpressing β-catenin. In contrast, FOSL2 expression was downregulated in M2-like TAMs transfected with si\_β-catenin. ARID5A behaved in the opposite direction in each of these studies. These findings demonstrated that β-catenin acts as a transcriptional activator and repressor of FOSL2 and ARID5A, respectively (**Figure 31A–D**).

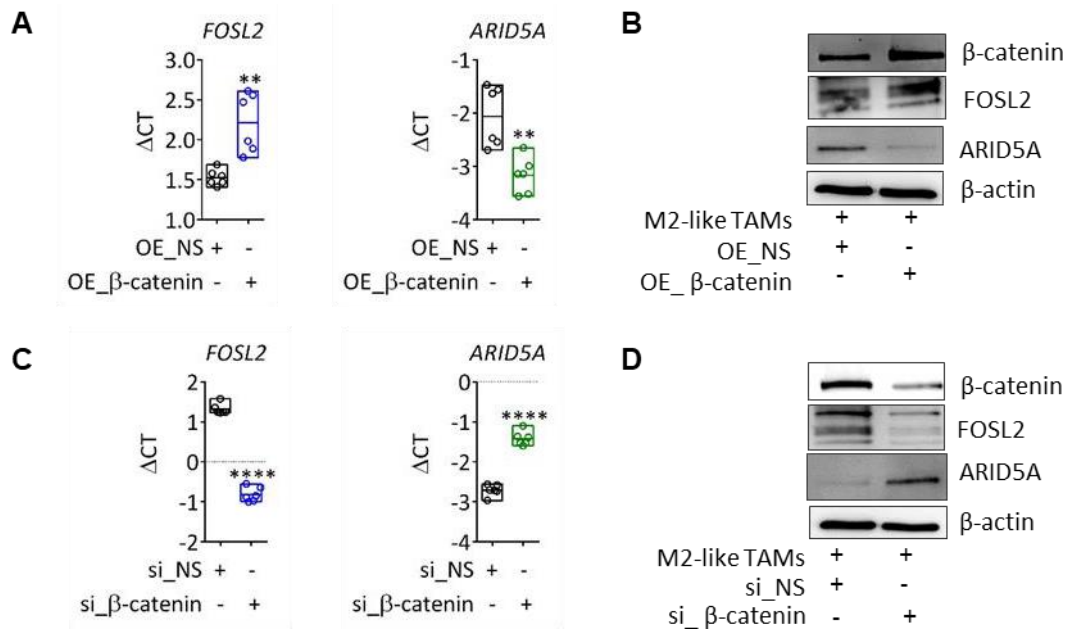


**Figure 31: β-catenin acted as a transcriptional activator and repressor of FOSL2 and ARID5A, respectively, in M2-like TAMs.** Relative mRNA expression and western blot analysis of FOSL2 and ARID5A in M2-like TAMs transfected with **(A, B)** OE\_NS, OE\_β-catenin; **(C, D)** si\_NS and si\_β-catenin for 24 h; n = 3 biological replicates, 2 technical replicates. \*\*P < 0.01, \*\*\*\*P < 0.0001 compared with si\_NS or OE\_NS. [(Sarode P et.al. 2020) Reuse permission: Distributed under the terms of the Creative Commons Attribution-NonCommercial license]

#### 4.6.3 Activation of FOSL2 induces lung tumorigenicity by triggering the pro-tumorigenic transcriptional program of M2-like macrophages.

The siRNA-mediated knockdown of FOSL2 was performed in M2-like TAMs to further probe FOSL2's transcriptional role in the polarization of M2-like TAMs **(Figure 32A–C)**. The mRNA expression of various M2 macrophage markers (*CD163*, *CD206*, *IL1R1*, *TGFB1*) was significantly downregulated, whereas that of certain M2 (*IL10*, *ALOX15*) and M1 macrophage markers (*IL1B*, *IL8*, *CCR7*) remained unchanged in M2-like TAMs transfected with si\_FOSL2 **(Figure 32D, E)**. The treatment of A549 cells with CM from M2-like TAMs transfected with si\_FOSL2 led to a decrease in survival and proliferation **(Figure 32F)**. This indicates that β-catenin-mediated activation of FOSL2 induces lung tumorigenicity by triggering the pro-tumorigenic transcriptional program of M2-like macrophages.

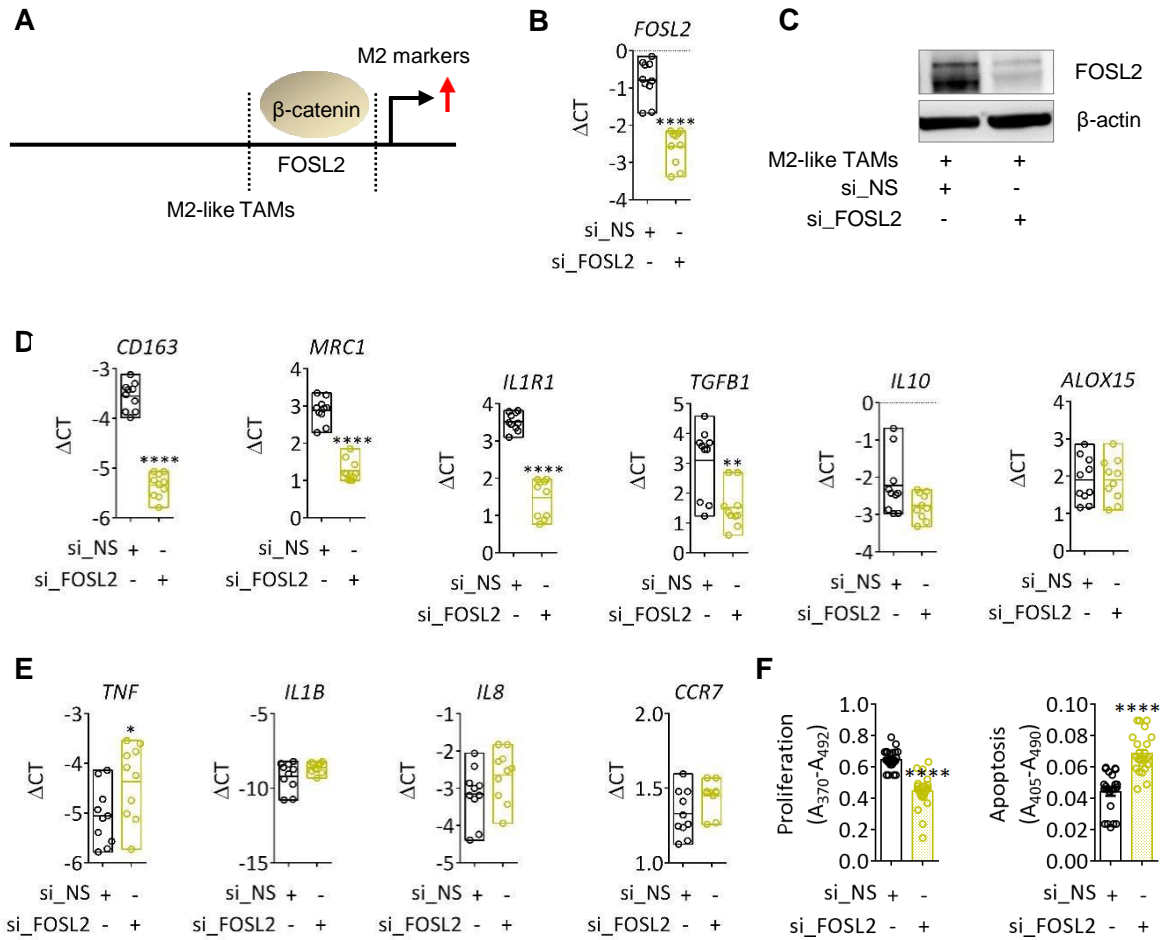


**Figure 32: Activation of FOSL2 leads to upregulation of M2-like macrophages' transcriptional program.** (A)  $\beta$ -catenin acts as a transcriptional activator of FOSL2. (B) Relative mRNA expression (C) western blot analysis of FOSL2; Relative mRNA expression of (D) M2, (E) M1 macrophage markers in M2-like TAMs transfected with si\_NS and si\_FOSL2 for 24 h. \*\*\*P < 0.001 compared with si\_NS. (F) Quantification of apoptosis and proliferation of A549 cells in the presence of CM from M2-like TAMs transfected with si\_NS and si\_FOSL2 for 24 h. \*\*\*P < 0.001, \*\*\*\*P < 0.0001 compared with si\_NS-CM. [(Sarode P et.al. 2020) Reuse permission: Distributed under the terms of the Creative Commons Attribution-NonCommercial license]

#### 4.6.4 Repression of ARID5A contributes to the lung tumorigenicity of M2-like macrophages by suppressing the M1-like anti-tumorigenic transcriptional program.

To ascertain the role of ARID5A repression in the polarization of M2-like TAMs, cells were transfected with an ARID5A overexpression plasmid (OE\_ARID5A) (Figure 33A–C). Notably, the mRNA expression of M1 macrophage markers (*TNF*, *IL8*, *CCR7*, *IL6*) was significantly upregulated by this intervention, whereas that of certain M1 (*IL1B*) and M2 macrophage

markers (*IL10*, *CD163*, *ALOX15*) remained unchanged (**Figure 33D, E**). The CM from M2-like TAMs transfected with OE\_ARID5A led to decreased survival and proliferation of A549 cells (**Figure 33F**). This finding indicates that  $\beta$ -catenin-mediated repression of ARID5A contributes to the lung tumorigenicity of M2-like macrophages by suppressing the M1-like anti-tumorigenic transcriptional program.

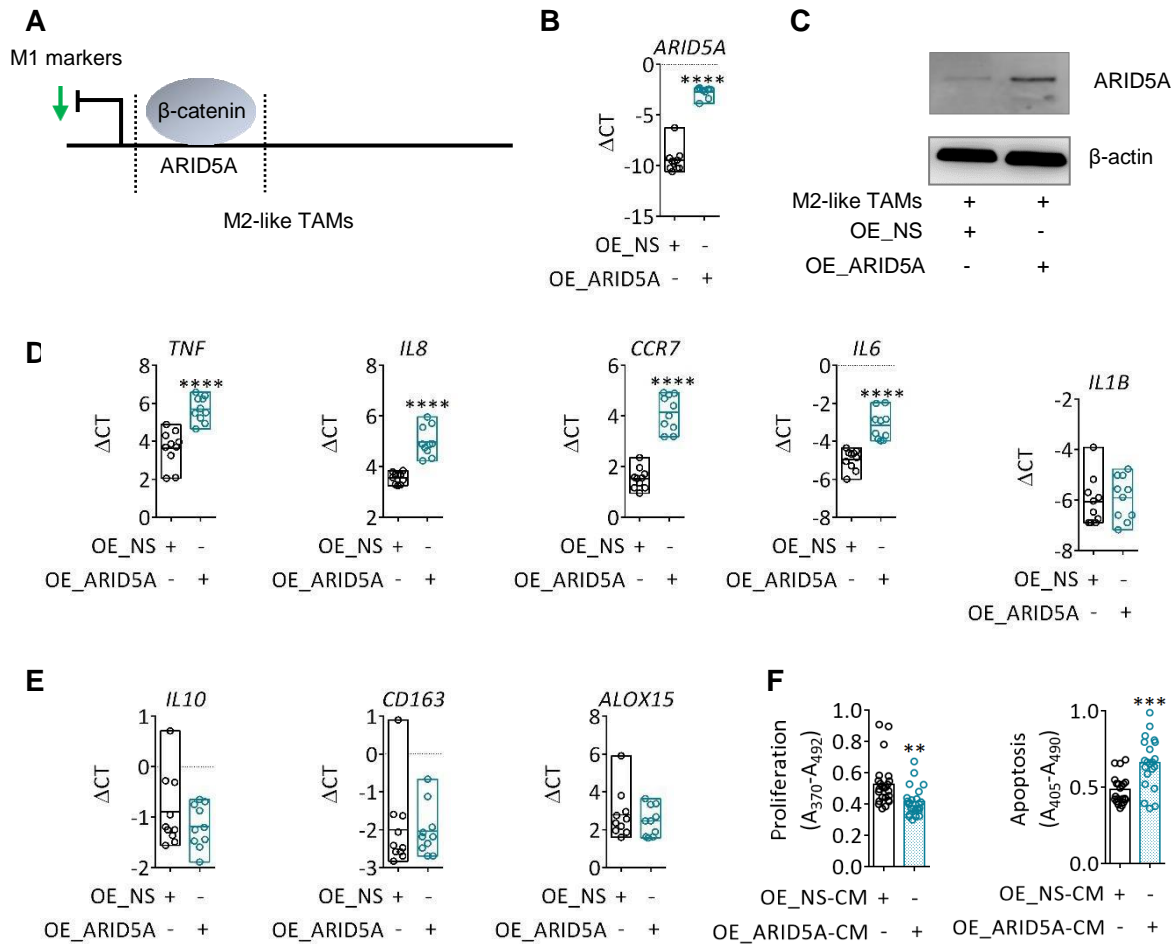


**Figure 33: Activation of ARID5A leads to upregulation of M1-like macrophages' transcriptional program.** (A)  $\beta$ -catenin acts as a transcriptional repressor of ARID5A. (B) Relative mRNA expression (C) Western blot analysis of ARID5A; Relative mRNA expression of (D) M1 (E) M2 macrophage markers in M2-like TAMs transfected with OE\_NS and OE\_ARID5A for 24 h. \*\*\*P < 0.001 compared with OE\_NS. (F) Apoptosis and proliferation of A549 cells in the presence of CM from M2-like TAMs transfected with OE\_NS and OE\_ARID5A for 24 h. \*\*\*P < 0.001, \*\*\*\*P < 0.0001 compared with OE\_NS-CM. [(Sarode P et.al. 2020) Reuse permission: Distributed under the terms of the Creative Commons Attribution-NonCommercial license]

#### 4.6.5 High expression of $\beta$ -catenin and FOSL2 and low expression of ARID5A correlated with poor survival in lung cancer patients

A survival analysis, using transcriptomic data of lung cancer patients, was performed to understand the clinical significance of  $\beta$ -catenin, FOSL2, and ARID5A expression in the lung TME (Gyorffy, Surowiak et al. 2013). Notably, Kaplan–Meier curves illustrated that low expression of  $\beta$ -catenin and FOSL2 in lung cancer patients; results in improved patient survival (Figure 34).

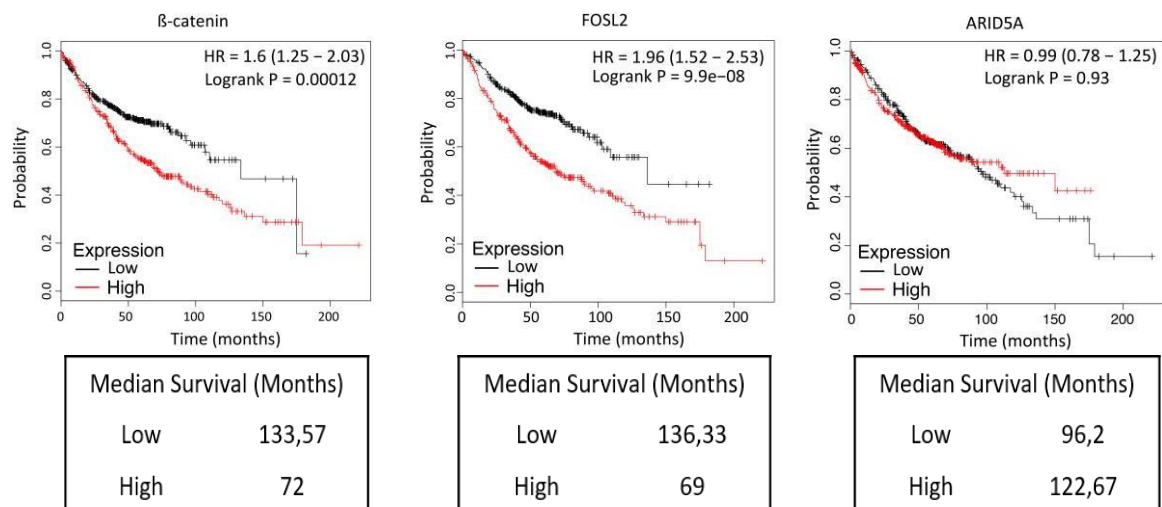


**Figure 34: Correlation of  $\beta$ -catenin/FOSL2/ARID5A with the survival of lung cancer patients.** Kaplan–Meier survival analysis of patients with human lung adenocarcinoma ( $n = 720$ ) stratified by the average expression of  $\beta$ -catenin, FOSL2, and ARID5A. Data obtained from <http://kmplot.com/> (Gyorffy et al., 2013). Parameters set to perform KM analysis are – Survival (OS), Split Patients by (Median), Probe set option (only JetSet best probe set), Array quality control (exclude biased arrays). [(Sarode P et.al. 2020) Reuse permission: Distributed under the terms of the Creative Commons Attribution-NonCommercial license]

Altogether, this study strongly supports the relevance of the previously unacknowledged role of  $\beta$ -catenin-mediated transcriptional regulation of the TFs, FOSL2, and ARID5A in the phenotypic transition of TAMs in the lung TME, thereby impacting tumor biology. Therefore, targeting  $\beta$ -catenin and specific downstream TFs offers a novel therapeutic concept to efficiently reprogram M2-like TAMs to M1-like TAMs, thereby repressing the transcriptional program of pro-tumorigenic M2 macrophages, activating the anti-tumorigenic transcriptional program of M1 macrophages, and reducing lung tumor growth and metastasis.

## 5. DISCUSSION

The present study provides strong evidence that  $\beta$ -catenin-mediated transcription plays a central role in the transition of tumor-inhibiting M1-like TAMs to tumor-promoting M2-like TAMs. Therefore, targeting  $\beta$ -catenin in TAMs may offer a new immunotherapeutic option to reactivate anti-tumor immunity in the lung TME. This concept is based on the following key findings: (i) Wnt/ $\beta$ -catenin signaling (expression, nuclear  $\beta$ -catenin activity) is activated in TAMs isolated from patients with lung cancer and in M2-like TAMs “trained” by co-culturing with primary lung cancer cells or 3 different lung cancer cell lines, as compared to their M1 counterparts; (ii) Genetic and/or pharmacological ablation of nuclear  $\beta$ -catenin activity in primary TAMs isolated from human and mouse lung tumors, as well as in *in-vitro*-trained M2-like TAMs, phenotypically and functionally “re- programs” M2-like TAMs to M1-like TAMs; (iii) Pharmacological and macrophage-specific genetic ablation of  $\beta$ -catenin in five different *in-vivo* lung tumor models reduces primary and metastatic lung tumor growth, together with re-activating M1-like TAMs anti-tumor immunity in the lung TME; (iv)  $\beta$ -catenin-mediated transcriptional activation of FOSL2 (TF regulating the M2 macrophage-specific gene signature), and repression of ARID5A (TF regulating the M1 macrophage-specific gene signature) play a prominent role in TAM’ phenotypic transition.

### 5.1 Anti-tumor M1-like TAMs undergo the phenotypic transition to pro-tumor M2-like TAMs, with the activation in Wnt/ $\beta$ -catenin signaling

The CIBERSORT analysis of tissue microarray data sets of human tumors revealed that immune infiltrates in TME vary according to the cancer type. However, TAMs represent the significant infiltrating population in most human cancers (Cassetta and Pollard 2018). Several histopathological and experimental studies reported a prominent signature and prognostic importance of macrophages in the lung TME (Banat, Tretyn et al. 2015, Schmall, Al-Tamari et al. 2015, Weichand, Popp et al. 2017, Catacchio, Scattone et al. 2018, Jackute, Zemaitis et al. 2018, Rakae, Busund et al. 2019). Macrophages are divided into two subtypes: classically activated M1 macrophages and alternatively activated M2 macrophages. However, this dualistic definition of M1/M2 macrophages is limited and may not be applicable to TAMs, which are present in spatial proximity to tumor cells and other tumor-infiltrating immune cells in the TME, and therefore receive a multitude of activating signals (Chittezhath, Dhillon et al. 2014, Finkernagel, Reinartz et al. 2016, Cassetta, Fragogianni et al. 2019). To this end, we used two different

approaches to identify critical signal transduction pathways which are deregulated in TAMs in lung TME – (i) In the *first approach*, to precisely delineate the molecular signature of TAMs (from human lung cancer patients) and non-tumor macrophages (NMs, from its matched control tissue), a flow cytometric sorting was developed. Further, RNA sequencing of FACS sorted TAMs and NMs was performed. (ii) In the *second approach*, we established an *in-vitro* “training” protocol for macrophages (by co-culturing human-derived macrophages with lung tumor cell lines and primary lung tumor cells) to induce TAMs development in a dish. This approach nicely reproduced the phenotypic (*upregulation of M2 macrophage markers with simultaneous downregulation of M1 macrophage markers*) and functional transition (*reduced apoptosis and increased proliferation and migration of tumor cells*) of M1-like TAMs to M2-like TAMs, allowing the analysis of the underlying transcriptional changes by RNA sequencing. The advantages of the established model are – (i) Classically, *in vitro* macrophages are generated by M-CSF stimulation which, drives macrophage transcriptional program to M2 phenotype. Although this method is well accepted in the field, the major shortcoming is that macrophages acquire an M2-like phenotype before interacting with tumor cells, which is not the case in *in vivo tumor progression*. The model established in this study overcomes the above-mentioned shortcoming, as monocyte to macrophage differentiation is done by human serum which resembles physiological condition; (ii) Previously, work from our group, and others demonstrated that co-culture of M-CSF derived macrophages with tumor cells with cell membrane insert (the cells are not in direct contact with each other), polarize macrophages to M2-phenotype within 24 hours. The time window to study gene regulation responsible for the phenotypic transition in macrophages is too short. On the other hand, the co-culture method in this study is done without cell membrane insert (to mimic spatial proximity contact within the cells as seen *in vivo*), which nicely showed the changes in macrophage and tumor cells phenotype over the longer time. These advantages allowed us to study differential gene regulation in M1-like TAMs and M2-like TAMs and to reveal the underlying signaling pathways.

RNA sequencing of both primary TAMs and *in vitro* trained TAMs disclosed that Wnt/ $\beta$ -catenin signaling is a crucial pathway upregulated in M2-like TAMs. To validate RNA sequencing data, we performed, (i) Co-immunostaining of  $\beta$ -catenin and CD68 in human lung tissue microarray. CD68 is a glycoprotein that expressed by macrophages and is associated with lysosomes, and importantly it is widely used as an immunohistochemical marker to distinguish macrophages from other stromal and immune cells (Barros, Hauck et al. 2013); (ii) Assessment of nuclear  $\beta$ -catenin activity by nuclear/cytoplasmic fractionation and by TCF/LEF luciferase activity assay. Upon stabilization in cytoplasm

and translocation in the nucleus,  $\beta$ -catenin binds to TCF/LEF transcription factors to regulate transcription and expression of Wnt-responsive genes. The TCF/LEF luciferase activity assay was designed for monitoring the activity of Wnt/ $\beta$ -catenin signaling pathway in the cultured cells; (iii) Protein expression analysis of Wnt/ $\beta$ -catenin signaling ( $\beta$ -catenin, TNKS1/2, pGSK3B) and its target genes (CCND1, MYC, MET) in three different *in-vitro* TAM models. The Wnt/ $\beta$ -catenin signaling has many target genes but the most accepted canonical targets include CCND1, MYC, MET, JUN and MMP7 (Brabletz, Jung et al. 1999, Mann, Gelos et al. 1999, Shtutman, Zhurinsky et al. 1999, Wilkins and Sansom 2008, Zeilstra, Joosten et al. 2008, Clevers and Nusse 2012). These investigations demonstrated that Wnt/ $\beta$ -catenin signaling is strongly activated in M2-like as compared to M1-like TAMs. The two significant findings from the co-culture model strongly predicted that, Wnt/ $\beta$ -catenin signaling pathway might play a potential role in phenotypic transition to M2-like TAMs when macrophages comes in contact with tumor cells for longer duration, which are – (i) When naïve macrophages (M0) comes in contact with tumor cells, they undergo transition from M1-like TAMs to M2-like TAMs; and (ii) Wnt/ $\beta$ -catenin signaling upregulated over the time in the co-culture model. The hypothesis was tested – (i) *In vitro*: by blocking the signaling in M2-like TAMs followed by analyzing macrophage polarization markers and functional effects on tumor cells (here we used various *in vitro* and *ex vivo* models of M2-like TAMs and various genetic and pharmacological tools to inhibit  $\beta$ -catenin); (ii) *In vivo*: by blocking the signaling in lung tumor models (subcutaneous, metastasis, carcinogen-induced, bone marrow transplantation model) with pharmacological and genetic ablation of  $\beta$ -catenin, followed by analyzing macrophage polarization markers in the TAMs sorted from the tissue, and infiltration of macrophages.

## **5.2 Phenotypic and functional transition of M2-like TAMs to M1-like TAMs by inhibiting Wnt/ $\beta$ -catenin signaling**

The alterations in developmental signal transduction pathways at varying frequencies and combinations across the different organs and tissues by tumor cells and other tumor-infiltrating cells are very well established in tumor biology. Therefore, the biggest challenge in onco-therapeutics development is targeting them with no or negligible devastating effects on healthy tissue homeostasis (Sanchez-Vega, Mina et al. 2018). The Wnt/ $\beta$ -catenin signaling is one such crucial oncogenic pathway, which remained undruggable because of its involvement in embryology and developmental biology. However, decades of enormous research in Wnt/ $\beta$ -catenin signaling has paved the way for addressing various issues that must be well thought out in the development of Wnt/ $\beta$ -

catenin signaling-modulators in the treatment of cancers; which are – (i) the aberrant expression of Wnt/ $\beta$ -catenin signaling not found to correlate with reduced patient survival in all cancer types — for example, increased Wnt/ $\beta$ -catenin signaling in tumors correlated with poor prognosis in colorectal cancer, ovarian cancer, etc. (Takada, Yagi et al. 2004, Lugli, Zlobec et al. 2007), while in melanoma it is correlated with favorable prognosis (Bachmann, Straume et al. 2005). Therefore, it is a crucial step to check the co-relation of Wnt/ $\beta$ -catenin signaling with patient survival in the respective cancer before developing and using Wnt/ $\beta$ -catenin signaling therapeutics in its treatment; (ii) The alterations responsible for aberrant expression of  $\beta$ -catenin are not common in all cancer types. Therefore, the efficacy of the therapeutic approach is highly dependent on where it is acting - upstream of Wnt signaling responsible for cytoplasmic stabilization of  $\beta$ -catenin (e.g., LGK974, OMP18R5) or downstream of  $\beta$ -catenin-mediated transcription (e.g., PRI-724) in cancer under treatment. For example, upstream targeting agents are not effective in colorectal cancer, as APC mutation leads to constitutive translocation of  $\beta$ -catenin in the nucleus, thereby upregulating the signaling (Kwong and Dove 2009). On the other hand, upstream targeting agents are found to be effective in pancreatic cancer carrying mutation in ring finger protein 43 (RNF43) (Jiang, Hao et al. 2013); (iii) Tumor and tumor-infiltrating cells acquire multiple genomic and expression alterations in Wnt signaling components, and importantly, co-occurrence of such various changes indicates functional synergies to activate the pathway and, importantly this might reflect the resistance to therapies targeting a single modification; (iv) Wnt/ $\beta$ -catenin signaling has high cellular and temporal specificity. Therefore, targeted therapy will be the best approach to avoid deleterious effect on healthy tissue homeostasis; (v) Until now the main focus of Wnt/ $\beta$ -catenin signaling therapeutics is on tumor cells but accumulating clinical and pathological evidence suggests that this is one of the essential immunomodulatory pathways in cancer (Kahn 2014, Wang, Tian et al. 2018).

The preliminary literature screening of Wnt/ $\beta$ -catenin signaling in lung cancer highlighted that high expression of  $\beta$ -catenin in lung cancer significantly correlated with poor patient survival (Stewart 2014, Rapp, Jaromi et al. 2017). A large body of evidence also suggests that tumor cells and tumor-infiltrating immune cells like TAMs may share similar oncogenic signal transduction pathways to preserve malignancy and the deregulation of these pathways in immune cells leading to tumorigenesis and tumor development by inducing tumor immunogenicity, making them difficult to target by first-line cancer therapy (Blankenstein, Coulie et al. 2012, Imielinski, Berger et al. 2012, Pai, Carneiro et al. 2017, Zakiryanova, Wheeler et al. 2018). Therefore, the treatment of such cancers needs urgent development of immunotherapeutics activating anti-tumor immunity in TME.

In previous studies, Wnt/ $\beta$ -catenin signaling interference was mainly considered to directly affect the tumor cells (Valenta, Hausmann et al. 2012, Kahn 2014, Krishnamurthy and Kurzrock 2018, Dangaj, Barras et al. 2019). To investigate TAM based Wnt/ $\beta$ -catenin signaling, genetic and pharmacological ablation of  $\beta$ -catenin in primary TAMs (isolated from human and mouse lung tumors), and in *in-vitro*-trained M2-like TAMs was undertaken. This intervention resulted in markedly increased expression of M1 macrophage genes (TNF, IL1B, IL8, IL6, CCR7, etc.), whereas M2 macrophage genes (IL10, CD163, CD206, ALOX15, IL1R1, TGFB1, etc.) were downregulated. Furthermore, the CM from these manipulations sharply increased apoptosis and decreased the proliferation and migration of primary lung tumor cells and lung tumor cell lines (human and mouse). These data strongly support the concept that TAMs-specific Wnt/ $\beta$ -catenin signaling plays a crucial role in the phenotypic transition of TAMs and M2-like TAMs-driven tumorigenesis.

The postulated central role of Wnt/ $\beta$ -catenin signaling in the activation of M2-like TAMs is further supported by *in vivo* studies. In 3 different tumor models, inhibition of Wnt/ $\beta$ -catenin signaling significantly reduced primary and metastatic lung tumor growth by reprogramming TAMs into the M1-like TAMs phenotype. These results confirmed that  $\beta$ -catenin inhibition not only affects tumor cells but also switches TAMs phenotype *in vivo*. Furthermore, to precisely investigate the contribution of macrophage-specific  $\beta$ -catenin to experimental lung tumorigenesis, we used two approaches to induce lung tumor development in macrophage-specific  $\beta$ -catenin knockout mice ( $Catnb^{ff/Lysm^{Cre}}$ ) – (i) carcinogen-induced lung tumor model, (ii) LLC1 induced lung tumor model after bone marrow transplantation. In both of these models, targeted depletion of  $\beta$ -catenin in macrophages reduced lung tumor development, and more interestingly,  $\beta$ -catenin\_KO\_TAMs possess M1-like TAMs phenotype. These results indicate that macrophage-specific  $\beta$ -catenin antagonism is sufficient to restrict lung tumor development. Spranger et al. demonstrated that in human melanoma tumors, activation of  $\beta$ -catenin prevents CCL4 gene expression, which further leads to T-cell exclusion (Spranger, Bao et al. 2015). The RNA sequencing data from this study revealed the increased mRNA expression of CCL4 upon inhibition of  $\beta$ -catenin in M2-like TAMs, postulating that interference in TAMs-specific Wnt/ $\beta$ -catenin signaling may recruit antigen-presenting cells in TME to overcome immune evasion.

Interestingly, *in vitro* study showed that 32 to 64  $\mu$ M concentration of XAV939 is needed to reduce survival and proliferation of tumor cells by approximately 50 to 60%, while to unleash the anti-tumor response in M2-like TAMs and to achieve the effect of similar

magnitude on tumor cells requires less concentration of XAV939 (4 to 8  $\mu$ M). These results indicated that TAMs-specific targeting might reduce the dose of Wnt/ $\beta$ -catenin signaling-inhibitors, which will eventually reduce the associated side effects on healthy tissue homeostasis. However, follow up *in vivo* studies should be done with series of XAV939 doses to compare the impact of TAMs-specific targeting (by liposomes or nanoparticle encapsulated XAV939) vs. direct treatment of XAV939 in the experimental lung tumorigenesis.

The present study also demonstrated that like lung tumor cells, primary TAMs, and *in vitro* trained M2-like TAMs have co-occurrence of multiple expression alterations in upstream Wnt signaling components. For example, upregulation of WNT ligands (5A, 7B, 11), frizzled receptors (FZD 4, 5, 6, 8, 9), dishevelled (DVL 2, 3) and tankyrases (TNKS 1, 2) while downregulation of DKKs, sFRPs, etc.; leading to cytoplasmic stabilization of  $\beta$ -catenin followed by its nuclear translocation. A recent paper by Sanchez-Vega F et al. described that co-occurrence of multiple alterations indicates functional synergies to activate the pathway, and, importantly, this may reflect the resistance to therapies targeting a single alteration (Nissan, Pratilas et al. 2014). Therefore, the concluding molecular mechanism responsible for the phenotypic transition of TAMs needs to be investigated to develop therapeutic agents.

### **5.3 $\beta$ -catenin mediated FOSL2-activation and ARID5A-repression play a vital role in the phenotypic transition of M1-like to M2-like TAMs**

To pinpoint pivotal molecular alterations or mechanism responsible for phenotypic transition in TAMs upon  $\beta$ -catenin inhibition, RNA sequencing of M2-like TAMs transfected with  $\beta$ -catenin shRNA ( $\beta$ -catenin\_KD\_M2-like TAMs) was performed. The results from RNA-sequencing indicate that the  $\beta$ -catenin-mediated transcriptional landscape is a potential molecular mechanism responsible for the transition of M1-like to M2-like TAMs. Upon nuclear translocation,  $\beta$ -catenin mainly binds to its transcription co-factors from the TCF family to regulate a plethora of target genes, including individual genes or transcription factors regulating the family of genes. *In silico* analysis of TCF binding domain in differentially regulated TFs demonstrated that 14 differentially regulated TFs in  $\beta$ -catenin\_KD\_M2-like TAMs have the  $\beta$ -catenin binding site. The expression analysis in  $\beta$ -catenin\_KO\_M0 and  $\beta$ -catenin\_KO\_TAMs showed that among these TFs, FOSL2 is significantly downregulated while ARID5A is upregulated in  $\beta$ -catenin-deficient macrophages. Furthermore, promotor occupancy assay in M2 macrophages after  $\beta$ -catenin pulldown and  $\beta$ -catenin gain and loss of function in M2-like

TAMs demonstrated that  $\beta$ -catenin directly regulates transcription of FOSL2 and ARID5A, although in opposite ways. These results strongly forecasted that  $\beta$ -catenin-mediated transcriptional activation of FOSL2 and repression of ARID5A might play a central role in the phenotypic and functional transition of tumor-inhibiting M1-like TAMs to tumor-promoting M2-like TAMs.

The deepCAGE transcriptome analysis of M1 and M2 macrophages (mice BM-derived macrophages) predicted that FOSL2 plays a significant role in the activation of M2 macrophage genes, while ARID5A has a similar role in M1 macrophage genes (Roy, Schmeier et al. 2015). Therefore, to test whether FOSL2 and ARID5A have binding sites in promoters of human M1 and M2 macrophage genes, transcription factor binding site motif scanning (TFBS) was performed in promotor sequence of 50 most validated M1 and M2 macrophage genes. Interestingly, these macrophage genes also showed differential expression after genetic ablation of  $\beta$ -catenin in M2-like TAMs.

The loss of function of FOSL2 in M2-like TAMs demonstrated its transcriptional role in the activation of M2 macrophage genes (CD163, CD206, IL1R1, TGFB1). In corroboration with the present study, the analysis of the transcriptional landscapes of the macrophages associated with inflammatory bowel disease (Baillie, Arner et al. 2017), *Mycobacterium tuberculosis* infection (Roy, Schmeier et al. 2018) and skeletal muscle regeneration (Varga, Mounier et al. 2016) reported the transcriptional role of FOSL2 in genes responsible for pro-inflammation, resolution and tissue repair. Another study by Masuda et al. in the TME of glioblastoma demonstrated an expression correlation between FOSL2 and mesenchymal genes (Cooper, Gutman et al. 2012). Several other studies shown the oncogenic potential of FOSL2 in growth and metastasis of tumor cells (Mangone, Brentani et al. 2005, Langer, Singer et al. 2006, Milde-Langosch, Janke et al. 2008, Nakayama, Hieshima et al. 2008, Wang, Sun et al. 2014, Gupta, Kumar et al. 2015, He, Mai et al. 2017, Li, Fang et al. 2018, Luo, Chi et al. 2018, Sun, Guo et al. 2018, Sun, Dai et al. 2018, Gao, Guo et al. 2019), but no study, to our knowledge as yet, has experimentally demonstrated the transcriptional role of macrophage-specific FOSL2 mediated by  $\beta$ -catenin in the activation of M2-like TAMs in TME.

Furthermore, the gain of function of ARID5A in M2-like TAMs demonstrated its transcriptional role in the activation of M1 macrophage genes (TNF, IL1B, CCR7, IL6). Recent studies in inflammatory diseases like autoimmune diseases and septic shock provided insight into the role of macrophage-specific ARID5A in promotion of inflammatory transcriptional programs via mechanisms like inhibition of the destabilizing

effect of Regnase-1 on IL-6 mRNA, hinting in the direction of our findings (Masuda, Ripley et al. 2013, Higa, Oka et al. 2018, Masuda and Kishimoto 2018, Wammers, Schupp et al. 2018). Interestingly, we also observed that loss of function of FOSL2 did not change expression of M1 macrophage markers while that of M2 macrophage markers did not change upon the gain of function of ARID5A in M2-like TAMs; indicating that in comparison with FOSL2 and ARID5A,  $\beta$ -catenin has a dual transcriptional role in the activation of M2-like TAMs. However, the transcriptional function of FOSL2 and ARID5A is limited to genes of only one subtype of macrophage, the CM from M2-like TAMs manipulated by FOSL2-knockdown and ARID5A-overexpression significantly decreased survival and proliferation of lung tumor cells. Therefore, apart from  $\beta$ -catenin, the present study also highlights potential novel targets (FOSL2 and ARID5A) to unleash anti-tumor M1-like TAMs responses in lung TME.

The survival analysis in transcriptomic data of human lung cancer patients co-related the low expression of  $\beta$ -catenin and FOSL2 and high expression of ARID5A to better patient survival. However, future studies should assess clinical outcomes based on TAMs-specific  $\beta$ -catenin/FOSL2/ARID5A expression to evaluate a survival advantage provided by a TAM-specific inhibitor of  $\beta$ -catenin and its transcriptional targets (FOSL2 and ARID5A) in the treatment of lung cancer. Many inhibitors targeting Wnt/ $\beta$ -catenin signaling are in different phases of clinical trials (Harb, Lin et al. 2019); still, no safe and effective inhibitor moved to bedside. The major obstacles for  $\beta$ -catenin inhibitor entering clinical use are not only common issues of bioactivity and safety of new drug development but also strategies used for its targeting. An absence of ligand binding pocket in  $\beta$ -catenin makes it undruggable, but, given the fact that activation of  $\beta$ -catenin in TAMs is triggered by alterations in membranous and cytoplasmic components of Wnt signaling and not by intrinsic mutations, there may be an opportunity to use Wnt/ $\beta$ -catenin signaling inhibitors in the modulation of TAMs (Wang, Tian et al. 2018).

## 5.4 Conclusion

Based on **Figure 35**, we conclude that TAM-specific  $\beta$ -catenin drives a transcriptional switch from M1-like to M2-like TAMs in the lung tumor microenvironment, thereby promoting tumor progression and metastasis. Inhibition of Wnt/ $\beta$ -catenin signaling in TAMs may offer a potential immunotherapeutic option to reduce lung tumor progression by reactivating anti-tumor M1-like TAM activity in the tumor microenvironment.

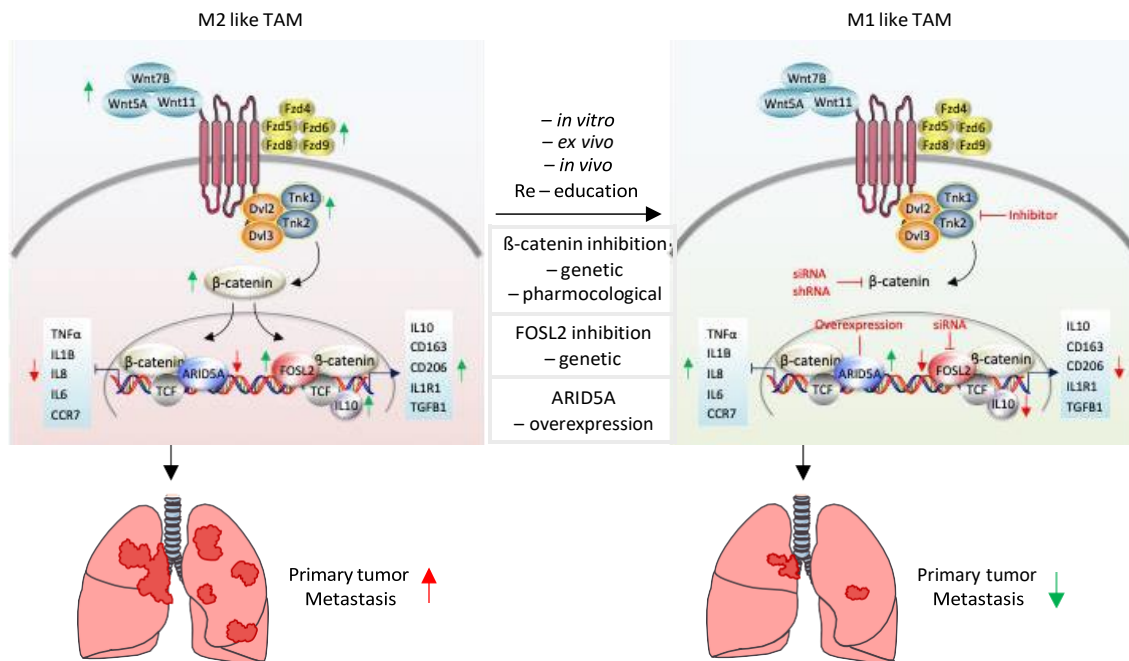


**Figure 35: Proposed mechanism of reprogramming of tumor-promoting M2-like TAMs to tumor-inhibiting M1-like TAMs via TAM-specific inhibition of Wnt/ $\beta$ -catenin signaling.** In comparison with M1-like TAMs, M2-like TAMs show significant upregulation of WNT ligands (5A, 7B, 11), frizzled receptors (FZD 4, 5, 6, 8, 9), disheveled (DVL 2,3), and TNKS (1,2); resulting in cytoplasmic stabilization of  $\beta$ -catenin, followed by its nuclear translocation. In the nucleus,  $\beta$ -catenin activates the transcription of M2 macrophage genes by directly binding to their promoter (e.g., IL10) and the transcription factor FOSL2, activating M2 macrophage genes, (i.e., CD163, CD206, IL1R1, TGFB1). Additionally,  $\beta$ -catenin represses the transcription of M1 macrophage genes by binding to transcription factor ARID5A, which regulates M1 macrophage genes (TNF $\alpha$ , IL8, CCR7, IL6). Therefore, *in-vitro*-trained, *ex-vivo* cultured, and *in-vivo*  $\beta$ -catenin-KO M2-like TAMs reprogrammed into M1-like TAMs by genetic and pharmacological inhibition of  $\beta$ -catenin, knockdown of FOSL2 and overexpression of ARID5A; resulting in the re-activation of anti-tumor immunity in the TME to restrict primary and metastatic lung tumor growth. [(Sarode P et.al. 2020) Reuse permission: Distributed under the terms of the Creative Commons Attribution-NonCommercial license]

## 5.5 Future outlook

The future investigations should focus on following central questions,

### 1. How do tumor cells induce Wnt/ $\beta$ -catenin signaling in M2-like TAMs?

Activation of canonical Wnt/ $\beta$ -catenin signaling in any cells mainly carried out by specific membrane-complex of Wnt and Fzd. We observed in this study, Wnt (7B, 5A, 11) and Fzd (4, 5, 6,8, 9) exclusively upregulated in M2-like TAMs compared to M1-like TAMs. Therefore, follow up studies should identify which cells (tumor cells or macrophages) specifically secrete these ligands by mRNA, protein, and secretome analysis, followed by their blocking by blocking peptides. Additionally, blocking of individual Fzd receptor by RNA-interference tools on M2-like TAMs will answer which Wnt-Fzd membrane-complex is involved in activation of the signaling. Moreover, secreted cytokines and chemokines can also activate Wnt/ $\beta$ -catenin signaling. Analysis of exclusive tumor cells' secretome by cytokine array, mass-spectrometry, followed by identification, validation, and blocking of a potential target in M2-like TAMs will answer Wnt-independent activation of Wnt/ $\beta$ -catenin signaling in M2-like TAMs by tumor cells.

### 2. How does $\beta$ -catenin regulate simultaneous activation of FOSL2 and repression of ARID5A in M2-like TAMs?

To confirm  $\beta$ -catenin-mediated dual transcriptional regulation, follow up studies should perform rescue experiments. For this experiment, M1 and M2 macrophage markers should be analyzed by overexpressing FOSL2 (by plasmid) and knocking down ARID5A (by RNA-interference tools) in  $\beta$ -catenin\_KD\_M2-like TAMs. The upregulation of M2 markers and downregulation of M1 markers will confirm the simultaneous activation of FOSL2 and repression of ARID5A in M2-like TAMs by  $\beta$ -catenin.

### 3. How does $\beta$ -catenin induce transcriptional repression of ARID5A?

The role of  $\beta$ -catenin as transcriptional activator is very well documented in the literature, but  $\beta$ -catenin mediated simultaneous transcriptional activation and repression is only just beginning to be understood and seems diverse (Valenta, Hausmann et al. 2012).  $\beta$ -catenin regulates transcription of any gene by binding to

its co-factors. The most common co-activators of  $\beta$ -catenin are from TCF7, TCF7L2, and LEF1, while co-repressor is TCF7L1. Interestingly, these co-factors regulate similar and distinct family of genes. Therefore, selective manipulation of each TCFs by RNA-interference tools will identify whether differential regulation of FOSL2 and ARID5A by  $\beta$ -catenin uses different TCFs to bind at their promoters.

4. Is the  $\beta$ -catenin-FOSL2-ARID5A axis macrophage-specific?

The transcriptional activity of  $\beta$ -catenin is highly dependent on the cell type. Therefore, to check the specificity of the  $\beta$ -catenin-FOSL2-ARID5A axis, manipulation of  $\beta$ -catenin should be done in tumor cells, followed by expression analysis of FOSL2 and ARID5A. Absence of expressional changes in this experiment will confirm macrophage-specificity of the  $\beta$ -catenin-FOSL2-ARID5A axis. Additionally, these results will forecast the need for cell-specific targeting of Wnt/ $\beta$ -catenin signaling.

5. How to achieve TAMs-specific targeting of  $\beta$ -catenin, FOSL2, and ARID5A?

Future studies should assess the safety and efficacy of TAMs-targeted liposomal or nanoparticle formulations (Zhu, Niu et al. 2013, Binnemars-Postma, Storm et al. 2017, Ma, Bygd et al. 2017, Ngambenjawong, Gustafson et al. 2017, Qian, Qiao et al. 2017, Scodeller, Simon-Gracia et al. 2017, Cassetta and Pollard 2018) of Wnt/ $\beta$ -catenin signaling inhibitors, FOSL2 and ARID5A-modulators in the treatment of lung cancer.

## 6. SUMMARY

Lung cancer is regarded as the most devastating type of cancer because of its high incidence, reduced health-related quality of life, late diagnosis, and importantly low response rate, high toxicity, and resistance to available therapeutic options. The high density of TAMs, especially M2-like TAMs in lung cancer patients, positively co-relates with poor prognosis and survival. The phenotypic transition of tumor-inhibiting M1-like TAMs to tumor-promoting M2-like TAMs is one of the crucial events responsible for activation of pro-tumor macrophages, but the underlying molecular mechanisms remain poorly characterized.

Through high-throughput transcriptome analysis of isolated TAMs from human lung tumor tissue compared to control, we found Wnt/ $\beta$ -catenin signaling is among the top up-regulated signal transduction pathways in TAMs. Additionally, to mimic the spatial proximity relationship of tumor cells and TAMs, as seen in TME, we established a new *in vitro* co-culture model featuring both anti-tumor M1-like TAMs and pro-tumor M2-like TAMs. Here we substantiated the crucial characteristics of tumor-promoting M2-like TAMs: enhancement of tumor cell proliferation, migration, reduction of apoptosis and notably, activated Wnt/ $\beta$ -catenin signaling in *in-vitro*-trained M2-like TAMs compared to M1-like TAMs.

Genetic ablation (by shRNA and siRNA mediated knockdown of  $\beta$ -catenin) and pharmacological inhibition (by XAV939 treatment) of  $\beta$ -catenin in primary TAMs (isolated from human and mouse lung tumors) and in *in-vitro*-trained M2-like TAMs phenotypically (upregulation and downregulation of M1 and M2 macrophage markers, respectively) and functionally (increased apoptosis and decreased proliferation and migration of tumor cell lines and primary tumor cells) switched M2-like TAMs to M1-like TAMs.

A series of *in-vivo* studies further support this concept. In three different tumor models, inhibition of Wnt/ $\beta$ -catenin signaling using XAV939 significantly reduced the growth of primary and metastatic lung tumors, in companion with the reprogramming of TAMs into tumor-inhibiting M1-like TAMs. Two findings document the causality between these observations. *First*, *in vitro* studies showed that any direct impact of XAV939 on lung tumor cell growth demands its concentrations be more than one order of magnitude higher than those affecting the TAM M2-M1 phenotypic switch. And *second*, the targeted depletion of  $\beta$ -catenin in macrophages to prevent M2 phenotype development

(*Catnb<sup>fl/fl</sup>Lysm<sup>Cre</sup>* combined with bone marrow transplantation) was similarly effective in suppressing lung cancer growth as the employment of the pharmacological inhibitor XAV939.

However, the  $\beta$ -catenin-mediated transcriptional landscape that drives reprogramming of TAMs remains unexplored. To the best of our knowledge, this study provides the first evidence that  $\beta$ -catenin-mediated transcriptional activation of FOSL2 (TF involved in M2 macrophage polarization) and repression of ARID5A (TF involved in M1 macrophage polarization) play a central role in the phenotypic and functional transition of tumor-inhibiting M1-like TAMs to tumor-promoting M2-like TAMs, thereby promoting lung tumor progression and metastasis. Moreover, high expression of  $\beta$ -catenin and FOSL2 and low expression of ARID5A found to correlate with poor prognosis in lung cancer patients.

In conclusion, this study demonstrated that TAM-specific antagonism of  $\beta$ -catenin and selective manipulation of FOSL2 and ARID5A leads to phenotypical and functional reprogramming of tumor-promoting M2-like TAMs to tumor-inhibiting M1-like TAMs. Restricting the anti-Wnt/ $\beta$ -catenin intervention to TAMs may offer a novel immunotherapeutic option to suppress lung tumor progression by unleashing anti-tumor M1-like TAM activity in the tumor microenvironment, with confined pharmacological action to avoid side effects of broad Wnt/ $\beta$ -catenin interference.

## 7. ZUSAMMENFASSUNG

Lungenkrebs wird als der verheerenste Krebstyp angesehen, wegen seiner weiten Verbreitung, erniedrigten Lebensqualität, oft erst späten Diagnose und nicht zuletzt wegen der niedrigen Anschlagsquote, hohen Toxizität und Resistenzen gegenüber bisher verfügbaren Therapien. In Lungenkrebspatienten korreliert eine erhöhte Dichte an Tumor-assoziierten Makrophagen (TAMs), besonders M2 TAMs, mit einer erniedrigten Überlebensrate und einer schlechteren Prognose. Der phänotypische Wechsel von Tumor-inhibierenden M1-ähnlichen (*like*) TAMs zu Tumor-fördernden M2-like TAMs ist eines der entscheidenden Ereignisse in der Umgehung der Immunantwort während des Tumorwachstums. Der zugrundeliegende molekulare Mechanismus ist jedoch noch nicht vollständig charakterisiert.

In aus humanem Lungentumorgewebe isolierten TAMs konnten wir mittels *high-throughput* Transkriptomanalyse den Wnt/ $\beta$ -catenin Signalweg unter den am stärksten hochregulierten Signaltransduktionswegen im Vergleich zum Kontrollgewebe identifizieren. Zusätzlich waren wir in der Lage ein neues *in vitro* Ko-Kultur Modell zu etablieren, das die räumliche Nähe von TAMs und Tumorzellen im TME nachahmt und Tumor-inhibierende M1-like sowie Tumor-fördernde M2-like TAMs aufweist. Mithilfe dieses Modells konnten wir die grundlegenden Charakteristika von M2-like TAMs feststellen: erhöhte Tumorzellproliferation und -migration, niedrigere Apoptose Rate sowie vor allem ein aktivierter Wnt/ $\beta$ -catenin Signalweg in den *in vitro* erzeugten M2-like TAMs verglichen zu M1-like TAMs.

Genetisches Ausschalten (*knock down* mittels shRNA oder siRNA) und pharmakologische Inhibition (durch XAV939 Behandlung) von  $\beta$ -catenin in primären TAMs (isoliert aus humanen und murinen Lungentumoren) sowie in *in vitro* erzeugten M2-like TAMs führte zu einem phänotypischen (Hoch- und Herunterregulation von M1 und M2 Makrophagen Markern) und funktionellen (erhöhte Apoptose, erniedrigte Proliferation und Migration von Tumorzelllinien und primären Tumorzellen) Wechsel der M2-like TAMs zu M1-like TAMs.

Dieses Konzept wird zusätzlich unterstützt von einer Serie an *in vivo* Studien. Drei verschiedene Tumormodelle zeigten signifikant reduziertes Tumorwachstum in Primärtumoren sowie metastasierenden Lungentumoren nach Inhibition des Wnt/ $\beta$ -catenin Signalwegs mittels XAV939. Die Tumorreduktion ging einher mit

Reprogrammierung der TAMs zu Tumor-inhibierende M1-like TAMs. Dass hinter diesen beiden Beobachtungen im Zusammenhang stehen ist durch zwei Ergebnisse zu begründen. Erstens zeigten *in vitro* Studien, dass ein direkter Einfluss von XAV939 auf die Proliferation der Tumorzellen selbst eine mehr als zehnfach höhere Konzentration benötigt, als diese, die für den phänotypischen M2-zu-M1-Wechsel eingesetzt wurde. Zweitens zeigte eine gezielte Depletion von  $\beta$ -catenin in Makrophagen zur Verhinderung der Entwicklung zum M2 Phänotyp ( $Catnb^{ff/Lysm^{Cre}}$  kombiniert mit Knochenmarkstransplantation) eine ähnlich effektive Unterdrückung der Lungenkrebs Entwicklung wie die Gabe des pharmakologischen Inhibitors XAV939.

Dennoch ist der Einfluss von  $\beta$ -catenin auf das Transkriptom, das die Reprogrammierung von TAMs beeinflusst, noch nicht vollständig aufgeklärt. Diese Studie zeigt erste Hinweise darauf, dass  $\beta$ -catenin-vermittelte transkriptionelle Aktivierung von FOSL2 (Transkriptionsfaktor in der M2 Polarization) und Repression von ARID5A (Transkriptionsfaktor in der M1 Polarization) eine zentrale Rolle im phänotypischen und funktionellen Wechsel der Tumor-inhibierenden M1-like TAMs zu Tumor-fördernden M2-like TAMs spielt und dadurch Tumorwachstum, Tumorprogression und Metastasierung fördert. Zusätzlich korreliert hohe Expression von  $\beta$ -catenin und FOSL2 sowie niedrige Expression von ARID5A mit einer schlechten Prognose in Lungenkrebs Patienten.

Schlussendlich konnte gezeigt werden, dass TAM-spezifische Inhibition von  $\beta$ -catenin und selektive Manipulation von FOSL2 und ARID5A zu einem phänotypischen und funktionellen Wechsel von Tumor-fördernden M2-like TAMs zu Tumor-inhibierenden M1-like TAMs führt. Eine Beschränkung der anti-Wnt/ $\beta$ -catenin Behandlungen auf TAMs könnte eine neuartige Möglichkeit in der Immuntherapie bieten, um die Progression von Lungenkrebs durch Freisetzung des anti-Tumor-Effekts von M1-like TAMs in der Tumormikroumgebung einzudämmen und gleichzeitig die Nebenwirkungen einer globalen Wnt/ $\beta$ -catenin Inhibition zu vermeiden.

## 8. LIST OF ABBREVIATIONS

-/-	Homozygous Knockout of the indicated gene
+/-	Heterozygous Knockout of the indicated gene
AC	Adenocarcinoma
ALK	Anaplastic lymphoma kinase
ALOX15	Arachidonate 15-Lipoxygenase
APC	Antigen presenting cell
ARID5A	AT-Rich Interaction Domain 5A
BAC	Bronchoalveolar carcinoma
BATF	Basic Leucine Zipper ATF-Like Transcription Factor
BRaf	v-Raf murine sarcoma viral oncogene homolog B1
CAF	Cancer associated fibroblast
CCL	C-C Motif Chemokine Ligand
CCR	Chemokine (C-C motif)-receptor
CD	Cluster of differentiation
CM	Conditioned media
CREB5	CAMP Responsive Element Binding Protein 5
CSF1	Colony Stimulating Factor 1
CSFR1	Colony-stimulating factor receptor 1
CTLA4	Cytotoxic T-Lymphocyte Associated Protein 4
CTNNB1	$\beta$ -catenin
CXCL	C-X-C Motif Chemokine Ligand
DC	Dendritic cell
DMSO	Dimethyl sulfoxide
ECM	Extracellular matrix
EGFR	Epidermal growth factor receptor
ENDS	Electronic nicotine delivery systems
FACS	Fluorescence-Activated Cell Sorting
FCS	Fetal calf serum
FOSL2	FOS Like 2, AP-1 Transcription Factor Subunit
FOXJ3	Forkhead Box J3
GOI	Gene of interest
GWAS	Genome wide association studies
HEGNET	High-Grade Neuroendocrine Tumor
IARC	International Agency for Research on Cancer

## List of abbreviations

---

IFN $\gamma$	Interferon $\gamma$
IL	Interleukin
IL-1RA	Interleukin 1 receptor antagonist
iNOS	Inducible nitric oxide synthases
IRF	Interferon Regulatory Factor
KLF	Kruppel Like Factor
KO	Knockout
KRas	V-Ki-ras2 Kirsten rat sarcoma viral oncogene homolog
LCNEC	Large Cell Neuroendocrine Carcinoma
LLC1	Lewis Lung Carcinoma 1
LPS	Lipopolysaccharide
M0	Undifferentiated Macrophages
M1	Macrophage with M1-phenotype
M2	Macrophage with M2-phenotype
MAG	MAX Dimerization Protein MAG
MARCO	Macrophage receptor with collagenous structure
M-CSF	Macrophage colony-stimulating factor
MET	Proto-oncogene encoding for hepatocyte growth factor receptor
MHC-II	Major histocompatibility complex Class II
MIA	Minimally invasive adenocarcinoma
miR	MicroRNA
MMP	Matrix metalloproteinase
NF- $\kappa$ B	Nuclear factor kappa-light-chain-enhancer of activated B cells
NK-Cells	Natural killer cells
NMK	4-(methylnitrosamino)-1-(13-pyridyl)-1-butanone
NMs	Non-tumor Macrophages
NSCLC	Non-small cell lung cancer
PAH	Polycyclic Aromatic Hydrocarbons
PBMCs	Peripheral Blood Mononuclear Cells
PBS	Phosphate buffered saline
PCI	Prophylactic Cranial Irradiation
PMA	Phorbol 12-myristate-12 acetate
PRDM1	PR/SET Domain 1
RBPJ	Recombination Signal Binding Protein For Immunoglobulin Kappa J Region
RELB	RELB Proto-Oncogene, NF- $\kappa$ B Subunit
SCC/SqCC	Squamous-cell carcinoma

## List of abbreviations

---

SCLC	Small cell lung cancer
STAT	Signal transducers and activators of transcription
TAM	Tumor associated macrophage
TAMCs	Tumor Associated Mast cells
TAN	Tumor associated neutrophil
TCGA	The Cancer Genome Atlas
TERT	Telomerase Reverse Transcriptase
TF	Transcription Factor
TFBS	Transcription Factor Binding Sites
TFEB	Transcription Factor EB
TFEC	Transcription Factor EC
TGF $\beta$	Transforming growth factor $\beta$
TH	T-helper cell
THC	$\Delta$ 9-tetrahydrocannabinol
TIDCs	Tumor Infiltrating Dendritic cells
TILs	Tumor Infiltrating Lymphocytes
TLRs	Toll-like receptor
TME	Tumor Microenvironment
TN	Tumor Nest
TNF $\alpha$	Tumor necrosis factor $\alpha$
TREG	Regulatory T-cell
TS	Tumor Stroma
TSNA	tobacco-specific N-nitrosamines
USF1	Upstream Transcription Factor 1
VEGF	Vascular endothelial growth factor
WHO	World Health Organisation
Wnt	Wingless-Type MMTV Integration Site Family
WT	Wildtype
$\Delta$ Ct	Threshold-cycle difference (HPRT-GOI)

## 9. LIST OF FIGURES

Figure	From	Title of the Figure	Page
1	Bray et al., A Cancer Journal for Clinicians, 2018	Distribution of cases and deaths of the 10 leading cancer types in 2018	1
2	El-Nikhely N et al., Expert Opinion on Investigational Drugs, 2012	Tumor Microenvironment	10
3	Murray et al., Immunity, 2014	Framework for describing activated macrophages	16
4	Zheng et al., Oncotarget, 2017	Distinct polarization mechanism in M1 and M2 macrophages	19
5		Wnt/ $\beta$ -catenin signaling pathway	26
6		Generation of <i>in vitro</i> trained TAMs and efficiency of trypsinization to yield pure macrophages from the co-culture	39
7	Sarode et al., Science Advances, 2020	Wnt/ $\beta$ -catenin signaling upregulated in primary TAMs isolated from patients with lung cancer	58
8	Sarode et al., Science Advances, 2020	Wnt/ $\beta$ -catenin signaling activated in primary TAMs isolated from lung cancer patients.	59
9	Sarode et al., Science Advances, 2020	Tumor cell – macrophages crosstalk simultaneously generates <i>in-vitro</i> -trained M1-like and M2-like TAMs	60
10	Sarode et al., Science Advances, 2020	Tumor cell – macrophages crosstalk functionally switch M1-like and M2-like TAMs	61
11	Sarode et al., Science Advances, 2020	<i>In-vitro</i> -trained M1-like TAMs expressed more M1 markers, while M2-like TAMs expressed more M2 markers	62
12	Sarode et al., Science Advances, 2020	Wnt/ $\beta$ -catenin signaling activated in <i>in- vitro</i> -trained M2-like TAMs	63
13	Sarode et al., Science Advances, 2020	RNA sequencing in <i>in-vitro</i> -trained M2-like TAMs identifies upregulated Wnt/ $\beta$ -catenin signaling	64
14	Sarode et al., Science Advances, 2020	Upregulation of different components of Wnt/ $\beta$ -catenin signaling in M2-like TAMs	65

---

15	Sarode et al., Science Advances, 2020	Genetic ablation of $\beta$ -catenin in <i>in-vitro</i> - trained TAMs downregulates Wnt/ $\beta$ -catenin signaling	66
16	Sarode et al., Science Advances, 2020	Genetic ablation of $\beta$ -catenin in <i>in-vitro</i> - trained TAMs switches M2-like TAMs to M1-like TAMs phenotype	67
17	Sarode et al., Science Advances, 2020	Genetic ablation of $\beta$ -catenin in human <i>ex- vivo</i> TAMs reprograms to M1-like TAMs phenotype	68
18	Sarode et al., Science Advances, 2020	Pharmacological ablation of $\beta$ -catenin in primary TAMs reprograms to M1-like phenotype	69
19	Sarode et al., Science Advances, 2020	Pharmacological ablation of $\beta$ -catenin in primary TAMs and <i>in-vitro</i> -trained TAMs functionally switches M2-like TAMs to the M1-like TAMs phenotype	70
20	Sarode et al., Science Advances, 2020	Pharmacological inhibition of $\beta$ -catenin in M1-like TAMs improves its anti-tumor effects	71
21	Sarode et al., Science Advances, 2020	A low dose of XAV939 was required to induce M1-like TAM anti-tumor immunity compared with direct treatment	72
22	Sarode et al., Science Advances, 2020	Pharmacological ablation of $\beta$ -catenin restricts tumor growth <i>in vivo</i>	73
23	Sarode et al., Science Advances, 2020	Pharmacological ablation of $\beta$ -catenin restricts tumor growth <i>in vivo</i> by phenotypically switching M2-like TAMs to M1-like TAMs	74
24	Sarode et al., Science Advances, 2020	Pharmacological ablation of $\beta$ -catenin restricts tumor growth <i>in vivo</i> by reducing CD206 macrophage infiltration	75
25	Sarode et al., Science Advances, 2020	Macrophage-specific genetic ablation of $\beta$ - catenin reduces the development of lung tumors	76
26	Sarode et al., Science Advances, 2020	Macrophage-specific genetic ablation of $\beta$ - catenin leads to induction of M1-like TAM- directed anti-tumor immunity in the TME	77
27	Sarode et al., Science Advances, 2020	Differential regulation of transcription factors in M2-like TAMs after inhibition of $\beta$ - catenin	79
28	Sarode et al., Science Advances, 2020	$\beta$ -catenin reciprocally regulate transcription of FOSL2 and ARID5A in M2-like TAMs	80
29	Sarode et al., Science Advances, 2020	Expression of FOSL2 and ARID5A increased and decreased, respectively, in M2 macrophages and M2-like TAMs	81

## List of figures

---

30	Sarode et al., Science Advances, 2020	$\beta$ -catenin directly bound to the promoter of FOSL2 and ARID5A	81
31	Sarode et al., Science Advances, 2020	$\beta$ -catenin acted as a transcriptional activator and repressor of FOSL2 and ARID5A, respectively, in M2-like TAMs	82
32	Sarode et al., Science Advances, 2020	Activation of FOSL2 leads to upregulation of M2-like macrophages' transcriptional program	83
33	Sarode et al., Science Advances, 2020	Activation of ARID5A leads to upregulation of M1-like macrophages' transcriptional program	84
34	Sarode et al., Science Advances, 2020	Correlation of $\beta$ -catenin/FOSL2/ARID5A with survival of lung cancer patients	85
35	Sarode et al., Science Advances, 2020	Proposed mechanism of re-education of tumor-promoting M2-like TAMs to tumor- inhibiting M1-like TAMs via TAM-specific inhibition of Wnt/ $\beta$ -catenin signaling	94

**10. LIST OF TABLES**

Table	Title of the table	Page
1	TAMs in different areas of human lung cancer: correlation with prognosis and overall survival	22
2	Selected Wnt signaling inhibitors, their targets and current stage of development	29
3	Patients characteristics	40
4	The volume of enzyme mix components according to the weight of tissue	41
5	siRNA characteristics	44
6	shRNA characteristics	44
7	Plasmid characteristics	45
8	Sequence of human primers	45
9	Sequence of mouse primers	47
10	List of antibodies	49
11	Compositions of solutions used in ChIP	51
12	Sequence of ChIP primers	51

## 11. REFERENCES

Acuner Ozbabacan, S. E., A. Gursoy, R. Nussinov and O. Keskin (2014). "The structural pathway of interleukin 1 (IL-1) initiated signaling reveals mechanisms of oncogenic mutations and SNPs in inflammation and cancer." *PLoS Comput Biol* **10**(2): e1003470.

Agalioti, T., A. D. Giannou, A. C. Krontira, N. I. Kanellakis, D. Kati, M. Vreka, M. Pepe, M. Spella, I. Lilis, D. E. Zazara, E. Nikolouli, N. Spiropoulou, A. Papadakis, K. Papadia, A. Voulgaridis, V. Harokopos, P. Stamou, S. Meiners, O. Eickelberg, L. A. Snyder, S. G. Antimisiaris, D. Kardamakis, I. Psallidas, A. Marazioti and G. T. Stathopoulos (2017). "Mutant KRAS promotes malignant pleural effusion formation." *Nat Commun* **8**: 15205.

Akiri, G., M. M. Cherian, S. Vijayakumar, G. Liu, A. Bafico and S. A. Aaronson (2009). "Wnt pathway aberrations including autocrine Wnt activation occur at high frequency in human non-small-cell lung carcinoma." *Oncogene* **28**(21): 2163-2172.

Alberg, A. J., M. V. Brock, J. G. Ford, J. M. Samet and S. D. Spivack (2013). "Epidemiology of lung cancer: Diagnosis and management of lung cancer, 3rd ed: American College of Chest Physicians evidence-based clinical practice guidelines." *Chest* **143**(5 Suppl): e1S-e29S.

Aldington, S., M. Harwood, B. Cox, M. Weatherall, L. Beckert, A. Hansell, A. Pritchard, G. Robinson, R. Beasley, Cannabis and G. Respiratory Disease Research (2008). "Cannabis use and risk of lung cancer: a case-control study." *Eur Respir J* **31**(2): 280-286.

Arrowsmith, C. H., C. Bountra, P. V. Fish, K. Lee and M. Schapira (2012). "Epigenetic protein families: a new frontier for drug discovery." *Nat Rev Drug Discov* **11**(5): 384-400.  
Bachmann, I. M., O. Straume, H. E. Puntervoll, M. B. Kalvenes and L. A. Akslen (2005). "Importance of P-cadherin, beta-catenin, and Wnt5a/frizzled for progression of melanocytic tumors and prognosis in cutaneous melanoma." *Clin Cancer Res* **11**(24 Pt 1): 8606-8614.

Baer, C., M. L. Squadrito, D. Laoui, D. Thompson, S. K. Hansen, A. Kiialainen, S. Hoves, C. H. Ries, C. H. Ooi and M. De Palma (2016). "Suppression of microRNA activity amplifies IFN-gamma-induced macrophage activation and promotes anti-tumour immunity." *Nat Cell Biol* **18**(7): 790-802.

Baillie, J. K., E. Arner, C. Daub, M. De Hoon, M. Itoh, H. Kawaji, T. Lassmann, P. Carninci, A. R. Forrest, Y. Hayashizaki, F. Consortium, G. J. Faulkner, C. A. Wells, M. Rehli, P. Pavli, K. M. Summers and D. A. Hume (2017). "Analysis of the human monocyte-derived macrophage transcriptome and response to lipopolysaccharide provides new insights into genetic aetiology of inflammatory bowel disease." *PLoS Genet* **13**(3): e1006641.

Bak, S. P., J. J. Walters, M. Takeya, J. R. Conejo-Garcia and B. L. Berwin (2007). "Scavenger receptor-A-targeted leukocyte depletion inhibits peritoneal ovarian tumor progression." *Cancer Res* **67**(10): 4783-4789.

Banat, G. A., A. Tretyn, S. S. Pullamsetti, J. Wilhelm, A. Weigert, C. Olesch, K. Ebel, T. Stiewe, F. Grimminger, W. Seeger, L. Fink and R. Savai (2015). "Immune and Inflammatory Cell Composition of Human Lung Cancer Stroma." *PLoS One* **10**(9): e0139073.

- Barros, M. H., F. Hauck, J. H. Dreyer, B. Kempkes and G. Niedobitek (2013). "Macrophage polarisation: an immunohistochemical approach for identifying M1 and M2 macrophages." PLoS One **8**(11): e80908.
- Barsky, S. H., M. D. Roth, E. C. Kleerup, M. Simmons and D. P. Tashkin (1998). "Histopathologic and molecular alterations in bronchial epithelium in habitual smokers of marijuana, cocaine, and/or tobacco." J Natl Cancer Inst **90**(16): 1198-1205.
- Baxevasos, P. and G. Mountzios (2018). "Novel chemotherapy regimens for advanced lung cancer: have we reached a plateau?" Ann Transl Med **6**(8): 139.
- Bergenfelz, C., C. Medrek, E. Ekstrom, K. Jirstrom, H. Janols, M. Wullt, A. Bredberg and K. Leandersson (2012). "Wnt5a induces a tolerogenic phenotype of macrophages in sepsis and breast cancer patients." J Immunol **188**(11): 5448-5458.
- Binnemars-Postma, K., G. Storm and J. Prakash (2017). "Nanomedicine Strategies to Target Tumor-Associated Macrophages." Int J Mol Sci **18**(5).
- Blankenstein, T., P. G. Coulie, E. Gilboa and E. M. Jaffee (2012). "The determinants of tumour immunogenicity." Nat Rev Cancer **12**(4): 307-313.
- Bolger, A. M., M. Lohse and B. Usadel (2014). "Trimmomatic: a flexible trimmer for Illumina sequence data." Bioinformatics **30**(15): 2114-2120.
- Brabletz, T., A. Jung, S. Dag, F. Hlubek and T. Kirchner (1999). "beta-catenin regulates the expression of the matrix metalloproteinase-7 in human colorectal cancer." Am J Pathol **155**(4): 1033-1038.
- Bray, F., J. Ferlay, I. Soerjomataram, R. L. Siegel, L. A. Torre and A. Jemal (2018). "Global cancer statistics 2018: GLOBOCAN estimates of incidence and mortality worldwide for 36 cancers in 185 countries." CA Cancer J Clin **68**(6): 394-424.
- Brenner, D. R., J. R. McLaughlin and R. J. Hung (2011). "Previous lung diseases and lung cancer risk: a systematic review and meta-analysis." PLoS One **6**(3): e17479.
- Brown, E. J. and W. A. Frazier (2001). "Integrin-associated protein (CD47) and its ligands." Trends Cell Biol **11**(3): 130-135.
- Canadas, I., F. Rojo, A. Taus, O. Arpi, M. Arumi-Uria, L. Pijuan, S. Menendez, S. Zazo, M. Domine, M. Salido, S. Mojal, A. Garcia de Herreros, A. Rovira, J. Albanell and E. Arriola (2014). "Targeting epithelial-to-mesenchymal transition with Met inhibitors reverts chemoresistance in small cell lung cancer." Clin Cancer Res **20**(4): 938-950.
- Cancer Genome Atlas Research, N. (2012). "Comprehensive genomic characterization of squamous cell lung cancers." Nature **489**(7417): 519-525.
- Carus, A., M. Ladekarl, H. Hager, H. Pilegaard, P. S. Nielsen and F. Donskov (2013). "Tumor-associated neutrophils and macrophages in non-small cell lung cancer: no immediate impact on patient outcome." Lung Cancer **81**(1): 130-137.
- Cassetta, L., S. Fragkogianni, A. H. Sims, A. Swierczak, L. M. Forrester, H. Zhang, D. Y. H. Soong, T. Cotechini, P. Anur, E. Y. Lin, A. Fidanza, M. Lopez-Yrigoyen, M. R. Millar, A. Urman, Z. Ai, P. T. Spellman, E. S. Hwang, J. M. Dixon, L. Wiechmann, L. M. Coussens, H. O. Smith and J. W. Pollard (2019). "Human Tumor-Associated Macrophage and Monocyte Transcriptional Landscapes Reveal Cancer-Specific

Reprogramming, Biomarkers, and Therapeutic Targets." Cancer Cell **35**(4): 588-602 e510.

Cassetta, L. and J. W. Pollard (2018). "Targeting macrophages: therapeutic approaches in cancer." Nat Rev Drug Discov.

Catacchio, I., A. Scattone, N. Silvestris and A. Mangia (2018). "Immune Prophets of Lung Cancer: The Prognostic and Predictive Landscape of Cellular and Molecular Immune Markers." Transl Oncol **11**(3): 825-835.

Chae, Y. K., A. Arya, W. Iams, M. R. Cruz, S. Chandra, J. Choi and F. Giles (2018). "Current landscape and future of dual anti-CTLA4 and PD-1/PD-L1 blockade immunotherapy in cancer; lessons learned from clinical trials with melanoma and non-small cell lung cancer (NSCLC)." J Immunother Cancer **6**(1): 39.

Chen, X. J., S. Wu, R. M. Yan, L. S. Fan, L. Yu, Y. M. Zhang, W. F. Wei, C. F. Zhou, X. G. Wu, M. Zhong, Y. H. Yu, L. Liang and W. Wang (2019). "The role of the hypoxia-Nrp-1 axis in the activation of M2-like tumor-associated macrophages in the tumor microenvironment of cervical cancer." Mol Carcinog **58**(3): 388-397.

Chittezhath, M., M. K. Dhillon, J. Y. Lim, D. Laoui, I. N. Shalova, Y. L. Teo, J. Chen, R. Kamaraj, L. Raman, J. Lum, T. P. Thamboo, E. Chiong, F. Zolezzi, H. Yang, J. A. Van Ginderachter, M. Poidinger, A. S. Wong and S. K. Biswas (2014). "Molecular profiling reveals a tumor-promoting phenotype of monocytes and macrophages in human cancer progression." Immunity **41**(5): 815-829.

Clevers, H. and R. Nusse (2012). "Wnt/beta-catenin signaling and disease." Cell **149**(6): 1192-1205.

Cole, A. J., G. G. Hanna, S. Jain and J. M. O'Sullivan (2014). "Motion management for radical radiotherapy in non-small cell lung cancer." Clin Oncol (R Coll Radiol) **26**(2): 67-80.

Conway, E. M., L. A. Pikor, S. H. Kung, M. J. Hamilton, S. Lam, W. L. Lam and K. L. Bennewith (2016). "Macrophages, Inflammation, and Lung Cancer." Am J Respir Crit Care Med **193**(2): 116-130.

Cooper, L. A., D. A. Gutman, C. Chisolm, C. Appin, J. Kong, Y. Rong, T. Kurc, E. G. Van Meir, J. H. Saltz, C. S. Moreno and D. J. Brat (2012). "The tumor microenvironment strongly impacts master transcriptional regulators and gene expression class of glioblastoma." Am J Pathol **180**(5): 2108-2119.

Corrales, L., K. Scilla, C. Caglevic, K. Miller, J. Oliveira and C. Rolfo (2018). "Immunotherapy in Lung Cancer: A New Age in Cancer Treatment." Adv Exp Med Biol **995**: 65-95.

Cortez-Retamozo, V., M. Etzrodt, A. Newton, P. J. Rauch, A. Chudnovskiy, C. Berger, R. J. Ryan, Y. Iwamoto, B. Marinelli, R. Gorbатов, R. Forghani, T. I. Novobrantseva, V. Koteliansky, J. L. Figueiredo, J. W. Chen, D. G. Anderson, M. Nahrendorf, F. K. Swirski, R. Weissleder and M. J. Pittet (2012). "Origins of tumor-associated macrophages and neutrophils." Proc Natl Acad Sci U S A **109**(7): 2491-2496.

Coscio, A., D. W. Chang, J. A. Roth, Y. Ye, J. Gu, P. Yang and X. Wu (2014). "Genetic variants of the Wnt signaling pathway as predictors of recurrence and survival in early-stage non-small cell lung cancer patients." Carcinogenesis **35**(6): 1284-1291.

- Costa, F. and R. Soares (2009). "Nicotine: a pro-angiogenic factor." Life Sci **84**(23-24): 785-790.
- Cote, M. L., S. L. Kardia, A. S. Wenzlaff, J. C. Ruckdeschel and A. G. Schwartz (2005). "Risk of lung cancer among white and black relatives of individuals with early-onset lung cancer." JAMA **293**(24): 3036-3042.
- Cruz-Bermudez, A., R. Laza-Briviesca, R. J. Vicente-Blanco, A. Garcia-Grande, M. J. Coronado, S. Laine-Menendez, C. Alfaro, J. C. Sanchez, F. Franco, V. Calvo, A. Romero, P. Martin-Acosta, C. Salas, J. M. Garcia and M. Provencio (2019). "Cancer-associated fibroblasts modify lung cancer metabolism involving ROS and TGF-beta signaling." Free Radic Biol Med **130**: 163-173.
- Dangaj, D., D. Barras and G. Coukos (2019). "Tumor Landscapes: beta-Catenin Drives Immune Desertification." Clin Cancer Res **25**(10): 2943-2945.
- Davidson, M. R., A. F. Gazdar and B. E. Clarke (2013). "The pivotal role of pathology in the management of lung cancer." J Thorac Dis **5 Suppl 5**: S463-478.
- de Groot, P. M., C. C. Wu, B. W. Carter and R. F. Munden (2018). "The epidemiology of lung cancer." Transl Lung Cancer Res **7**(3): 220-233.
- De Matteis, S., D. Consonni and P. A. Bertazzi (2008). "Exposure to occupational carcinogens and lung cancer risk. Evolution of epidemiological estimates of attributable fraction." Acta Biomed **79 Suppl 1**: 34-42.
- Debebe, A., V. Medina, C. Y. Chen, I. M. Mahajan, C. Jia, D. Fu, L. He, N. Zeng, B. W. Stiles, C. L. Chen, M. Wang, K. R. Aggarwal, Z. Peng, J. Huang, J. Chen, M. Li, T. Dong, S. Atkins, Z. Borok, W. Yuan, K. Machida, C. Ju, M. Kahn, D. Johnson and B. L. Stiles (2017). "Wnt/ $\beta$ -catenin activation and macrophage induction during liver cancer development following steatosis." Oncogene **36**: 6020.
- Deshmane, S. L., S. Kremlev, S. Amini and B. E. Sawaya (2009). "Monocyte chemoattractant protein-1 (MCP-1): an overview." J Interferon Cytokine Res **29**(6): 313-326.
- Dinakar, C. and G. T. O'Connor (2016). "The Health Effects of Electronic Cigarettes." N Engl J Med **375**(26): 2608-2609.
- Dobin, A., C. A. Davis, F. Schlesinger, J. Drenkow, C. Zaleski, S. Jha, P. Batut, M. Chaisson and T. R. Gingeras (2013). "STAR: ultrafast universal RNA-seq aligner." Bioinformatics **29**(1): 15-21.
- Dudek, A. Z., C. Yunis, L. I. Harrison, S. Kumar, R. Hawkinson, S. Cooley, J. P. Vasilakos, K. S. Gorski and J. S. Miller (2007). "First in human phase I trial of 852A, a novel systemic toll-like receptor 7 agonist, to activate innate immune responses in patients with advanced cancer." Clin Cancer Res **13**(23): 7119-7125.
- Engels, E. A., R. J. Biggar, H. I. Hall, H. Cross, A. Crutchfield, J. L. Finch, R. Grigg, T. Hylton, K. S. Pawlish, T. S. McNeel and J. J. Goedert (2008). "Cancer risk in people infected with human immunodeficiency virus in the United States." Int J Cancer **123**(1): 187-194.
- Epelman, S., K. J. Lavine and G. J. Randolph (2014). "Origin and functions of tissue macrophages." Immunity **41**(1): 21-35.

- Eruslanov, E. B. (2017). "Phenotype and function of tumor-associated neutrophils and their subsets in early-stage human lung cancer." Cancer Immunol Immunother **66**(8): 997-1006.
- Eruslanov, E. B., P. S. Bhojnagarwala, J. G. Quatromoni, T. L. Stephen, A. Ranganathan, C. Deshpande, T. Akimova, A. Vachani, L. Litzky, W. W. Hancock, J. R. Conejo-Garcia, M. Feldman, S. M. Albelda and S. Singhal (2014). "Tumor-associated neutrophils stimulate T cell responses in early-stage human lung cancer." J Clin Invest **124**(12): 5466-5480.
- Fang, W. B., M. Yao, G. Brummer, D. Acevedo, N. Alhakamy, C. Berkland and N. Cheng (2016). "Targeted gene silencing of CCL2 inhibits triple negative breast cancer progression by blocking cancer stem cell renewal and M2 macrophage recruitment." Oncotarget **7**(31): 49349-49367.
- Fend, L., S. Rusakiewicz, J. Adam, B. Bastien, A. Caignard, M. Messaoudene, C. Iribarren, I. Cremer, A. Marabelle, C. Borg, M. Semeraro, L. Barraud, J. M. Limacher, A. Eggermont, G. Kroemer and L. Zitvogel (2017). "Prognostic impact of the expression of NCR1 and NCR3 NK cell receptors and PD-L1 on advanced non-small cell lung cancer." Oncoimmunology **6**(1): e1163456.
- Fernandez-Cuesta, L., M. Peifer, X. Lu, R. Sun, L. Ozretic, D. Seidal, T. Zander, F. Leenders, J. George, C. Muller, I. Dahmen, B. Pinther, G. Bosco, K. Konrad, J. Altmuller, P. Nurnberg, V. Achter, U. Lang, P. M. Schneider, M. Bogus, A. Soltermann, O. T. Brustugun, A. Helland, S. Solberg, M. Lund-Iversen, S. Ansen, E. Stoelben, G. M. Wright, P. Russell, Z. Wainer, B. Solomon, J. K. Field, R. Hyde, M. P. Davies, L. C. Heukamp, I. Petersen, S. Perner, C. Lovly, F. Cappuzzo, W. D. Travis, J. Wolf, M. Vingron, E. Brambilla, S. A. Haas, R. Buettner and R. K. Thomas (2014). "Frequent mutations in chromatin-remodelling genes in pulmonary carcinoids." Nat Commun **5**: 3518.
- Finkernagel, F., S. Reinartz, S. Lieber, T. Adhikary, A. Wortmann, N. Hoffmann, T. Bieringer, A. Nist, T. Stiewe, J. M. Jansen, U. Wagner, S. Muller-Brusselbach and R. Muller (2016). "The transcriptional signature of human ovarian carcinoma macrophages is associated with extracellular matrix reorganization." Oncotarget **7**(46): 75339-75352.
- Furrukh, M. (2013). "Tobacco Smoking and Lung Cancer: Perception-changing facts." Sultan Qaboos Univ Med J **13**(3): 345-358.
- Gao, L., Y. N. Guo, J. H. Zeng, F. C. Ma, J. Luo, H. W. Zhu, S. Xia, K. L. Wei and G. Chen (2019). "The expression, significance and function of cancer susceptibility candidate 9 in lung squamous cell carcinoma: A bioinformatics and in vitro investigation." Int J Oncol **54**(5): 1651-1664.
- Geng, Y., Y. Shao, W. He, W. Hu, Y. Xu, J. Chen, C. Wu and J. Jiang (2015). "Prognostic Role of Tumor-Infiltrating Lymphocytes in Lung Cancer: a Meta-Analysis." Cell Physiol Biochem **37**(4): 1560-1571.
- Georgescu, S. P., J. H. Li, Q. Lu, R. H. Karas, M. Brown and M. E. Mendelsohn (2005). "Modulator recognition factor 1, an AT-rich interaction domain family member, is a novel corepressor for estrogen receptor alpha." Mol Endocrinol **19**(10): 2491-2501.
- Gholamin, S., S. S. Mitra, A. H. Feroze, J. Liu, S. A. Kahn, M. Zhang, R. Esparza, C. Richard, V. Ramaswamy, M. Remke, A. K. Volkmer, S. Willingham, A. Ponnuswami, A. McCarty, P. Lovelace, T. A. Storm, S. Schubert, G. Hutter, C. Narayanan, P. Chu, E. H. Raabe, G. t. Harsh, M. D. Taylor, M. Monje, Y. J. Cho, R. Majeti, J. P. Volkmer, P. G. Fisher, G. Grant, G. K. Steinberg, H. Vogel, M. Edwards, I. L. Weissman and S. H.

- Cheshier (2017). "Disrupting the CD47-SIRPalpha anti-phagocytic axis by a humanized anti-CD47 antibody is an efficacious treatment for malignant pediatric brain tumors." Sci Transl Med **9**(381).
- Goc, J., C. Germain, T. K. Vo-Bourgais, A. Lupo, C. Klein, S. Knockaert, L. de Chaisemartin, H. Ouakrim, E. Becht, M. Alifano, P. Validire, R. Remark, S. A. Hammond, I. Cremer, D. Damotte, W. H. Fridman, C. Sautes-Fridman and M. C. Dieu-Nosjean (2014). "Dendritic cells in tumor-associated tertiary lymphoid structures signal a Th1 cytotoxic immune contexture and license the positive prognostic value of infiltrating CD8+ T cells." Cancer Res **74**(3): 705-715.
- Gordon, S. and L. Martinez-Pomares (2017). "Physiological roles of macrophages." Pflugers Arch **469**(3-4): 365-374.
- Guagnano, V., A. Kauffmann, S. Wohrle, C. Stamm, M. Ito, L. Barys, A. Pornon, Y. Yao, F. Li, Y. Zhang, Z. Chen, C. J. Wilson, V. Bordas, M. Le Douget, L. A. Gaither, J. Borawski, J. E. Monahan, K. Venkatesan, T. Brummendorf, D. M. Thomas, C. Garcia-Echeverria, F. Hofmann, W. R. Sellers and D. Graus-Porta (2012). "FGFR genetic alterations predict for sensitivity to NVP-BGJ398, a selective pan-FGFR inhibitor." Cancer Discov **2**(12): 1118-1133.
- Guerriero, J. L., A. Sotayo, H. E. Ponichtera, J. A. Castrillon, A. L. Pourzia, S. Schad, S. F. Johnson, R. D. Carrasco, S. Lazo, R. T. Bronson, S. P. Davis, M. Lobera, M. A. Nolan and A. Letai (2017). "Class IIa HDAC inhibition reduces breast tumours and metastases through anti-tumour macrophages." Nature **543**(7645): 428-432.
- Gupta, S., P. Kumar, H. Kaur, N. Sharma, D. Saluja, A. C. Bharti and B. C. Das (2015). "Selective participation of c-Jun with Fra-2/c-Fos promotes aggressive tumor phenotypes and poor prognosis in tongue cancer." Sci Rep **5**: 16811.
- Gyorffy, B., P. Surowiak, J. Budczies and A. Lanczky (2013). "Online survival analysis software to assess the prognostic value of biomarkers using transcriptomic data in non-small-cell lung cancer." PLoS One **8**(12): e82241.
- Hagemann, T., T. Lawrence, I. McNeish, K. A. Charles, H. Kulbe, R. G. Thompson, S. C. Robinson and F. R. Balkwill (2008). "'Re-educating' tumor-associated macrophages by targeting NF-kappaB." J Exp Med **205**(6): 1261-1268.
- Hammerman, P. S., M. L. Sos, A. H. Ramos, C. Xu, A. Dutt, W. Zhou, L. E. Brace, B. A. Woods, W. Lin, J. Zhang, X. Deng, S. M. Lim, S. Heynck, M. Peifer, J. R. Simard, M. S. Lawrence, R. C. Onofrio, H. B. Salvesen, D. Seidel, T. Zander, J. M. Heuckmann, A. Soltermann, H. Moch, M. Koker, F. Leenders, F. Gabler, S. Querings, S. Ansen, E. Brambilla, C. Brambilla, P. Lorimier, O. T. Brustugun, A. Helland, I. Petersen, J. H. Clement, H. Groen, W. Timens, H. Sietsma, E. Stoelben, J. Wolf, D. G. Beer, M. S. Tsao, M. Hanna, C. Hatton, M. J. Eck, P. A. Janne, B. E. Johnson, W. Winckler, H. Greulich, A. J. Bass, J. Cho, D. Rauh, N. S. Gray, K. K. Wong, E. B. Haura, R. K. Thomas and M. Meyerson (2011). "Mutations in the DDR2 kinase gene identify a novel therapeutic target in squamous cell lung cancer." Cancer Discov **1**(1): 78-89.
- Hamra, G. B., N. Guha, A. Cohen, F. Laden, O. Raaschou-Nielsen, J. M. Samet, P. Vineis, F. Forastiere, P. Saldiva, T. Yorifuji and D. Loomis (2014). "Outdoor particulate matter exposure and lung cancer: a systematic review and meta-analysis." Environ Health Perspect **122**(9): 906-911.

- Hao, J., C. Zeltz, M. Pintilie, Q. Li, S. Sakashita, T. Wang, M. Cabanero, S. N. Martins-Filho, D. Y. Wang, E. Pasko, K. Venkat, J. Joseph, V. Raghavan, C. Q. Zhu, Y. H. Wang, N. Moghal, M. S. Tsao and R. Navab (2019). "Characterization of Distinct Populations of Carcinoma-Associated Fibroblasts from Non-Small Cell Lung Carcinoma Reveals a Role for ST8SIA2 in Cancer Cell Invasion." Neoplasia **21**(5): 482-493.
- Hao, N. B., M. H. Lu, Y. H. Fan, Y. L. Cao, Z. R. Zhang and S. M. Yang (2012). "Macrophages in tumor microenvironments and the progression of tumors." Clin Dev Immunol **2012**: 948098.
- Harb, J., P. J. Lin and J. Hao (2019). "Recent Development of Wnt Signaling Pathway Inhibitors for Cancer Therapeutics." Curr Oncol Rep **21**(2): 12.
- He, B., R. N. Barg, L. You, Z. Xu, N. Reguart, I. Mikami, S. Batra, R. Rosell and D. M. Jablons (2005). "Wnt signaling in stem cells and non-small-cell lung cancer." Clin Lung Cancer **7**(1): 54-60.
- He, J., J. Mai, Y. Li, L. Chen, H. Xu, X. Zhu and Q. Pan (2017). "miR-597 inhibits breast cancer cell proliferation, migration and invasion through FOSL2." Oncol Rep **37**(5): 2672-2678.
- Hecht, S. S. (1998). "Biochemistry, biology, and carcinogenicity of tobacco-specific N-nitrosamines." Chem Res Toxicol **11**(6): 559-603.
- Higa, M., M. Oka, Y. Fujihara, K. Masuda, Y. Yoneda and T. Kishimoto (2018). "Regulation of inflammatory responses by dynamic subcellular localization of RNA-binding protein Arid5a." Proc Natl Acad Sci U S A **115**(6): E1214-E1220.
- Hitchcock, J. R. and C. J. Watson (2015). "Anti-CCL2: building a reservoir or opening the floodgates to metastasis?" Breast Cancer Res **17**: 68.
- Hong, C. W. (2017). "Current Understanding in Neutrophil Differentiation and Heterogeneity." Immune Netw **17**(5): 298-306.
- Huang, T. H., T. Oka, T. Asai, T. Okada, B. W. Merrills, P. N. Gertson, R. H. Whitson and K. Itakura (1996). "Repression by a differentiation-specific factor of the human cytomegalovirus enhancer." Nucleic Acids Res **24**(9): 1695-1701.
- Hudson, J. D., M. A. Shoaibi, R. Maestro, A. Carnero, G. J. Hannon and D. H. Beach (1999). "A proinflammatory cytokine inhibits p53 tumor suppressor activity." J Exp Med **190**(10): 1375-1382.
- Imielinski, M., A. H. Berger, P. S. Hammerman, B. Hernandez, T. J. Pugh, E. Hodis, J. Cho, J. Suh, M. Capelletti, A. Sivachenko, C. Sougnez, D. Auclair, M. S. Lawrence, P. Stojanov, K. Cibulskis, K. Choi, L. de Waal, T. Sharifnia, A. Brooks, H. Greulich, S. Banerji, T. Zander, D. Seidel, F. Leenders, S. Ansen, C. Ludwig, W. Engel-Riedel, E. Stoelben, J. Wolf, C. Goparju, K. Thompson, W. Winckler, D. Kwiatkowski, B. E. Johnson, P. A. Janne, V. A. Miller, W. Pao, W. D. Travis, H. I. Pass, S. B. Gabriel, E. S. Lander, R. K. Thomas, L. A. Garraway, G. Getz and M. Meyerson (2012). "Mapping the hallmarks of lung adenocarcinoma with massively parallel sequencing." Cell **150**(6): 1107-1120.
- Inamura, K. (2017). "Lung Cancer: Understanding Its Molecular Pathology and the 2015 WHO Classification." Front Oncol **7**: 193.

- Jackute, J., M. Zemaitis, D. Pranys, B. Sitkauskiene, S. Miliauskas, S. Vaitkiene and R. Sakalauskas (2018). "Distribution of M1 and M2 macrophages in tumor islets and stroma in relation to prognosis of non-small cell lung cancer." BMC Immunol **19**(1): 3.
- Jiang, X., H. X. Hao, J. D. Gowney, S. Woolfenden, C. Bottiglio, N. Ng, B. Lu, M. H. Hsieh, L. Bagdasarian, R. Meyer, T. R. Smith, M. Avello, O. Charlat, Y. Xie, J. A. Porter, S. Pan, J. Liu, M. E. McLaughlin and F. Cong (2013). "Inactivating mutations of RNF43 confer Wnt dependency in pancreatic ductal adenocarcinoma." Proc Natl Acad Sci U S A **110**(31): 12649-12654.
- Jin, J., P. Zhan, M. Katoh, S. S. Kobayashi, K. Phan, H. Qian, H. Li, X. Wang, X. Wang, Y. Song and A. M. E. L. C. C. G. written on behalf of the (2017). "Prognostic significance of beta-catenin expression in patients with non-small cell lung cancer: a meta-analysis." Transl Lung Cancer Res **6**(1): 97-108.
- Johnson, T. S. and D. H. Munn (2012). "Host indoleamine 2,3-dioxygenase: contribution to systemic acquired tumor tolerance." Immunol Invest **41**(6-7): 765-797.
- Kaczanowska, S., A. M. Joseph and E. Davila (2013). "TLR agonists: our best frenemy in cancer immunotherapy." J Leukoc Biol **93**(6): 847-863.
- Kahn, M. (2014). "Can we safely target the WNT pathway?" Nat Rev Drug Discov **13**(7): 513-532.
- Kalari, S., M. Jung, K. H. Kernstine, T. Takahashi and G. P. Pfeifer (2013). "The DNA methylation landscape of small cell lung cancer suggests a differentiation defect of neuroendocrine cells." Oncogene **32**(30): 3559-3568.
- Kaler, P., L. Augenlicht and L. Klampfer (2009). "Macrophage-derived IL-1beta stimulates Wnt signaling and growth of colon cancer cells: a crosstalk interrupted by vitamin D3." Oncogene **28**(44): 3892-3902.
- Kaler, P., L. Augenlicht and L. Klampfer (2012). "Activating mutations in beta-catenin in colon cancer cells alter their interaction with macrophages; the role of snail." PLoS One **7**(9): e45462.
- Kaneda, M. M., K. S. Messer, N. Ralainirina, H. Li, C. J. Leem, S. Gorjestani, G. Woo, A. V. Nguyen, C. C. Figueiredo, P. Foubert, M. C. Schmid, M. Pink, D. G. Winkler, M. Rausch, V. J. Palombella, J. Kutok, K. McGovern, K. A. Frazer, X. Wu, M. Karin, R. Sasik, E. E. Cohen and J. A. Varner (2016). "PI3Kgamma is a molecular switch that controls immune suppression." Nature **539**(7629): 437-442.
- Khalil, M. and R. H. Vonderheide (2007). "Anti-CD40 agonist antibodies: preclinical and clinical experience." Update Cancer Ther **2**(2): 61-65.
- Kinoshita, T., G. Ishii, N. Hiraoka, S. Hirayama, C. Yamauchi, K. Aokage, T. Hishida, J. Yoshida, K. Nagai and A. Ochiai (2013). "Forkhead box P3 regulatory T cells coexisting with cancer associated fibroblasts are correlated with a poor outcome in lung adenocarcinoma." Cancer Sci **104**(4): 409-415.
- Kopf, M., C. Schneider and S. P. Nobs (2015). "The development and function of lung-resident macrophages and dendritic cells." Nat Immunol **16**(1): 36-44.
- Kren, L., M. Hermanova, V. N. Goncharuk, P. Kaur, J. S. Ross, Z. Pavlovsky and K. Dvorak (2003). "Downregulation of plasma membrane expression/cytoplasmic

accumulation of beta-catenin predicts shortened survival in non-small cell lung cancer. A clinicopathologic study of 100 cases." Cesk Patol **39**(1): 17-20.

Krewski, D., J. H. Lubin, J. M. Zielinski, M. Alavanja, V. S. Catalan, R. W. Field, J. B. Klotz, E. G. Letourneau, C. F. Lynch, J. I. Lyon, D. P. Sandler, J. B. Schoenberg, D. J. Steck, J. A. Stolwijk, C. Weinberg and H. B. Wilcox (2005). "Residential radon and risk of lung cancer: a combined analysis of 7 North American case-control studies." Epidemiology **16**(2): 137-145.

Krishnamurthy, N. and R. Kurzrock (2018). "Targeting the Wnt/beta-catenin pathway in cancer: Update on effectors and inhibitors." Cancer Treat Rev **62**: 50-60.

Kristeleit, H., D. Enting and R. Lai (2011). "Basic science of lung cancer." Eur J Cancer **47 Suppl 3**: S319-321.

Kuang, D. M., Q. Zhao, C. Peng, J. Xu, J. P. Zhang, C. Wu and L. Zheng (2009). "Activated monocytes in peritumoral stroma of hepatocellular carcinoma foster immune privilege and disease progression through PD-L1." J Exp Med **206**(6): 1327-1337.

Kwong, L. N. and W. F. Dove (2009). "APC and its modifiers in colon cancer." Adv Exp Med Biol **656**: 85-106.

Lackey, A. and J. S. Donington (2013). "Surgical management of lung cancer." Semin Intervent Radiol **30**(2): 133-140.

Landi, M. T., N. Chatterjee, K. Yu, L. R. Goldin, A. M. Goldstein, M. Rotunno, L. Mirabello, K. Jacobs, W. Wheeler, M. Yeager, A. W. Bergen, Q. Li, D. Consonni, A. C. Pesatori, S. Wacholder, M. Thun, R. Diver, M. Oken, J. Virtamo, D. Albanes, Z. Wang, L. Burdette, K. F. Doheny, E. W. Pugh, C. Laurie, P. Brennan, R. Hung, V. Gaborieau, J. D. McKay, M. Lathrop, J. McLaughlin, Y. Wang, M. S. Tsao, M. R. Spitz, Y. Wang, H. Krokan, L. Vatten, F. Skorpen, E. Arnesen, S. Benhamou, C. Bouchard, A. Metspalu, T. Vooder, M. Nelis, K. Valk, J. K. Field, C. Chen, G. Goodman, P. Sulem, G. Thorleifsson, T. Rafnar, T. Eisen, W. Sauter, A. Rosenberger, H. Bickeboller, A. Risch, J. Chang-Claude, H. E. Wichmann, K. Stefansson, R. Houlston, C. I. Amos, J. F. Fraumeni, Jr., S. A. Savage, P. A. Bertazzi, M. A. Tucker, S. Chanock and N. E. Caporaso (2009). "A genome-wide association study of lung cancer identifies a region of chromosome 5p15 associated with risk for adenocarcinoma." Am J Hum Genet **85**(5): 679-691.

Langer, S., C. F. Singer, G. Hudelist, B. Dampier, K. Kaserer, U. Vinatzer, H. Pehamberger, C. Zielinski, E. Kubista and M. Schreiber (2006). "Jun and Fos family protein expression in human breast cancer: correlation of protein expression and clinicopathological parameters." Eur J Gynaecol Oncol **27**(4): 345-352.

Le Mercier, I., D. Poujol, A. Sanlaville, V. Sisirak, M. Gobert, I. Durand, B. Dubois, I. Treilleux, J. Marvel, J. Vlach, J. Y. Blay, N. Bendriss-Vermare, C. Caux, I. Puisieux and N. Goutagny (2013). "Tumor promotion by intratumoral plasmacytoid dendritic cells is reversed by TLR7 ligand treatment." Cancer Res **73**(15): 4629-4640.

Levental, K. R., H. Yu, L. Kass, J. N. Lakins, M. Egeblad, J. T. Erler, S. F. Fong, K. Csiszar, A. Giaccia, W. Weninger, M. Yamauchi, D. L. Gasser and V. M. Weaver (2009). "Matrix crosslinking forces tumor progression by enhancing integrin signaling." Cell **139**(5): 891-906.

- Li, C., A. Menoret, C. Farragher, Z. Ouyang, C. Bonin, P. Holvoet, A. T. Vella and B. Zhou (2019). "Single cell transcriptomics based-MacSpectrum reveals novel macrophage activation signatures in diseases." JCI Insight **5**.
- Li, C., X. Zheng, Y. Han, Y. Lv, F. Lan and J. Zhao (2018). "XAV939 inhibits the proliferation and migration of lung adenocarcinoma A549 cells through the WNT pathway." Oncol Lett **15**(6): 8973-8982.
- Li, D., C. Beisswenger, C. Herr, J. Hellberg, G. Han, T. Zakharkina, M. Voss, R. Wiewrodt, R. M. Bohle, M. D. Menger, R. M. Schmid, D. Stöckel, H. P. Lenhof and R. Bals (2013). "Myeloid cell RelA/p65 promotes lung cancer proliferation through Wnt/ $\beta$ -catenin signaling in murine and human tumor cells." Oncogene **33**: 1239.
- Li, D., W. Liu, X. Wang, J. Wu, W. Quan, Y. Yao, R. Bals, S. Ji, K. Wu, J. Guo and H. Wan (2015). "Cathelicidin, an antimicrobial peptide produced by macrophages, promotes colon cancer by activating the Wnt/ $\beta$ -catenin pathway." Oncotarget **6**(5): 2939-2950.
- Li, F. and J. V. Ravetch (2011). "Inhibitory Fc $\gamma$  receptor engagement drives adjuvant and anti-tumor activities of agonistic CD40 antibodies." Science **333**(6045): 1030-1034.
- Li, S., X. D. Fang, X. Y. Wang and B. Y. Fei (2018). "Fos-like antigen 2 (FOSL2) promotes metastasis in colon cancer." Exp Cell Res **373**(1-2): 57-61.
- Liao, Y., G. K. Smyth and W. Shi (2014). "featureCounts: an efficient general purpose program for assigning sequence reads to genomic features." Bioinformatics **30**(7): 923-930.
- Lim, S. B., S. J. Tan, W. T. Lim and C. T. Lim (2017). "An extracellular matrix-related prognostic and predictive indicator for early-stage non-small cell lung cancer." Nat Commun **8**(1): 1734.
- Lin, C., W. Song, X. Bi, J. Zhao, Z. Huang, Z. Li, J. Zhou, J. Cai and H. Zhao (2014). "Recent advances in the ARID family: focusing on roles in human cancer." Onco Targets Ther **7**: 315-324.
- Lin, E. Y. and J. W. Pollard (2007). "Tumor-associated macrophages press the angiogenic switch in breast cancer." Cancer Res **67**(11): 5064-5066.
- Lin, Q., L. Xue, T. Tian, B. Zhang, L. Guo, G. Lin, Z. Chen, K. Fan and X. Gu (2015). "Prognostic value of serum IL-17 and VEGF levels in small cell lung cancer." Int J Biol Markers **30**(4): e359-363.
- Linabery, A. M., C. N. Blommer, L. G. Spector, S. M. Davies, L. L. Robison and J. A. Ross (2013). "ARID5B and IKZF1 variants, selected demographic factors, and childhood acute lymphoblastic leukemia: a report from the Children's Oncology Group." Leuk Res **37**(8): 936-942.
- Linde, N., M. Casanova-Acebes, M. S. Sosa, A. Mortha, A. Rahman, E. Farias, K. Harper, E. Tardio, I. Reyes Torres, J. Jones, J. Condeelis, M. Merad and J. A. Aguirre-Ghiso (2018). "Macrophages orchestrate breast cancer early dissemination and metastasis." Nature Communications **9**(1): 21.
- Lissowska, J., L. Foretova, J. Dabek, D. Zaridze, N. Szeszenia-Dabrowska, P. Rudnai, E. Fabianova, A. Cassidy, D. Mates, V. Bencko, V. Janout, R. J. Hung, P. Brennan and P. Boffetta (2010). "Family history and lung cancer risk: international multicentre case-

- control study in Eastern and Central Europe and meta-analyses." Cancer Causes Control **21**(7): 1091-1104.
- Liu, X. L., L. D. Liu, S. G. Zhang, S. D. Dai, W. Y. Li and L. Zhang (2015). "Correlation between expression and significance of delta-catenin, CD31, and VEGF of non-small cell lung cancer." Genet Mol Res **14**(4): 13496-13503.
- Loilome, W., P. Bungkanjana, A. Techasen, N. Namwat, P. Yongvanit, A. Puapairoj, N. Khuntikeo and G. J. Riggins (2014). "Activated macrophages promote Wnt/beta-catenin signaling in cholangiocarcinoma cells." Tumour Biol **35**(6): 5357-5367.
- Lou, G., X. Yu and Z. Song (2017). "Molecular Profiling and Survival of Completely Resected Primary Pulmonary Neuroendocrine Carcinoma." Clin Lung Cancer **18**(3): e197-e201.
- Love, M. I., W. Huber and S. Anders (2014). "Moderated estimation of fold change and dispersion for RNA-seq data with DESeq2." Genome Biol **15**(12): 550.
- Lugli, A., I. Zlobec, P. Minoo, K. Baker, L. Tornillo, L. Terracciano and J. R. Jass (2007). "Prognostic significance of the wnt signalling pathway molecules APC, beta-catenin and E-cadherin in colorectal cancer: a tissue microarray-based analysis." Histopathology **50**(4): 453-464.
- Luo, L., H. Chi and J. Ling (2018). "MiR-124-3p suppresses glioma aggressiveness via targeting of Fra-2." Pathol Res Pract **214**(11): 1825-1834.
- Luo, Y., H. Zhou, J. Krueger, C. Kaplan, S. H. Lee, C. Dolman, D. Markowitz, W. Wu, C. Liu, R. A. Reisfeld and R. Xiang (2006). "Targeting tumor-associated macrophages as a novel strategy against breast cancer." J Clin Invest **116**(8): 2132-2141.
- Ma, L., H. C. Bygd and K. M. Bratlie (2017). "Improving selective targeting to macrophage subpopulations through modifying liposomes with arginine based materials." Integr Biol (Camb) **9**(1): 58-67.
- MacDonald, B. T., K. Tamai and X. He (2009). "Wnt/beta-catenin signaling: components, mechanisms, and diseases." Dev Cell **17**(1): 9-26.
- Maciejczyk, A., I. Skrzypczynska and M. Janiszewska (2014). "Lung cancer. Radiotherapy in lung cancer: Actual methods and future trends." Rep Pract Oncol Radiother **19**(6): 353-360.
- Mangone, F. R., M. M. Brentani, S. Nonogaki, M. D. Begnami, A. H. Campos, F. Walder, M. B. Carvalho, F. A. Soares, H. Torloni, L. P. Kowalski and M. H. Federico (2005). "Overexpression of Fos-related antigen-1 in head and neck squamous cell carcinoma." Int J Exp Pathol **86**(4): 205-212.
- Mann, B., M. Gelos, A. Siedow, M. L. Hanski, A. Gratchev, M. Ilyas, W. F. Bodmer, M. P. Moyer, E. O. Riecken, H. J. Buhr and C. Hanski (1999). "Target genes of beta-catenin-T cell-factor/lymphoid-enhancer-factor signaling in human colorectal carcinomas." Proc Natl Acad Sci U S A **96**(4): 1603-1608.
- Mantovani, A., A. Sica, S. Sozzani, P. Allavena, A. Vecchi and M. Locati (2004). "The chemokine system in diverse forms of macrophage activation and polarization." Trends Immunol **25**(12): 677-686.

- Martinez, F. O. and S. Gordon (2014). "The M1 and M2 paradigm of macrophage activation: time for reassessment." F1000Prime Rep **6**: 13.
- Massarelli, E., V. Papadimitrakopoulou, J. Welsh, C. Tang and A. S. Tsao (2014). "Immunotherapy in lung cancer." Transl Lung Cancer Res **3**(1): 53-63.
- Masuda, K. and T. Kishimoto (2018). "A Potential Therapeutic Target RNA-binding Protein, Arid5a for the Treatment of Inflammatory Disease Associated with Aberrant Cytokine Expression." Curr Pharm Des **24**(16): 1766-1771.
- Masuda, K., B. Ripley, R. Nishimura, T. Mino, O. Takeuchi, G. Shioi, H. Kiyonari and T. Kishimoto (2013). "Arid5a controls IL-6 mRNA stability, which contributes to elevation of IL-6 level in vivo." Proc Natl Acad Sci U S A **110**(23): 9409-9414.
- Milde-Langosch, K., S. Janke, I. Wagner, C. Schroder, T. Streichert, A. M. Bamberger, F. Janicke and T. Loning (2008). "Role of Fra-2 in breast cancer: influence on tumor cell invasion and motility." Breast Cancer Res Treat **107**(3): 337-347.
- Moreau, M. F., C. Guillet, P. Massin, S. Chevalier, H. Gascan, M. F. Basle and D. Chappard (2007). "Comparative effects of five bisphosphonates on apoptosis of macrophage cells in vitro." Biochem Pharmacol **73**(5): 718-723.
- Munro, D. A. D. and J. Hughes (2017). "The Origins and Functions of Tissue-Resident Macrophages in Kidney Development." Front Physiol **8**: 837.
- Murray, P. J., J. E. Allen, S. K. Biswas, E. A. Fisher, D. W. Gilroy, S. Goerdts, S. Gordon, J. A. Hamilton, L. B. Ivashkiv, T. Lawrence, M. Locati, A. Mantovani, F. O. Martinez, J. L. Mege, D. M. Mosser, G. Natoli, J. P. Saeij, J. L. Schultze, K. A. Shirey, A. Sica, J. Suttles, I. Udalova, J. A. van Ginderachter, S. N. Vogel and T. A. Wynn (2014). "Macrophage activation and polarization: nomenclature and experimental guidelines." Immunity **41**(1): 14-20.
- Murray, P. J. and T. A. Wynn (2011). "Protective and pathogenic functions of macrophage subsets." Nat Rev Immunol **11**(11): 723-737.
- Nagai, T., M. Tanaka, Y. Tsuneyoshi, B. Xu, S. A. Michie, K. Hasui, H. Hirano, K. Arita and T. Matsuyama (2009). "Targeting tumor-associated macrophages in an experimental glioma model with a recombinant immunotoxin to folate receptor beta." Cancer Immunol Immunother **58**(10): 1577-1586.
- Nakamura, H., K. Tsuta, A. Yoshida, T. Shibata, S. Wakai, H. Asamura, K. Furuta and H. Tsuda (2013). "Aberrant anaplastic lymphoma kinase expression in high-grade pulmonary neuroendocrine carcinoma." J Clin Pathol **66**(8): 705-707.
- Nakata, A., R. Yoshida, R. Yamaguchi, M. Yamauchi, Y. Tamada, A. Fujita, T. Shimamura, S. Imoto, T. Higuchi, M. Nomura, T. Kimura, H. Nokihara, M. Higashiyama, K. Kondoh, H. Nishihara, A. Tojo, S. Yano, S. Miyano and N. Gotoh (2015). "Elevated beta-catenin pathway as a novel target for patients with resistance to EGF receptor targeting drugs." Sci Rep **5**: 13076.
- Nakayama, T., K. Hieshima, T. Arao, Z. Jin, D. Nagakubo, A. K. Shirakawa, Y. Yamada, M. Fujii, N. Oiso, A. Kawada, K. Nishio and O. Yoshie (2008). "Aberrant expression of Fra-2 promotes CCR4 expression and cell proliferation in adult T-cell leukemia." Oncogene **27**(23): 3221-3232.

- Naumnik, W., B. Naumnik, W. Niklinska, M. Ossolinska and E. Chyczewska (2016). "Clinical Implications of Hepatocyte Growth Factor, Interleukin-20, and Interleukin-22 in Serum and Bronchoalveolar Fluid of Patients with Non-Small Cell Lung Cancer." Adv Exp Med Biol **952**: 41-49.
- Ngambenjawong, C., H. H. Gustafson and S. H. Pun (2017). "Progress in tumor-associated macrophage (TAM)-targeted therapeutics." Adv Drug Deliv Rev **114**: 206-221.
- Nieder, C., T. Tollali, R. Yobuta, A. Reigstad, L. R. Flatoy and A. Pawinski (2017). "Palliative Thoracic Radiotherapy for Lung Cancer: What Is the Impact of Total Radiation Dose on Survival?" J Clin Med Res **9**(6): 482-487.
- Nishida, N., H. Yano, T. Nishida, T. Kamura and M. Kojiro (2006). "Angiogenesis in cancer." Vasc Health Risk Manag **2**(3): 213-219.
- Nissan, M. H., C. A. Pratilas, A. M. Jones, R. Ramirez, H. Won, C. Liu, S. Tiwari, L. Kong, A. J. Hanrahan, Z. Yao, T. Merghoub, A. Ribas, P. B. Chapman, R. Yaeger, B. S. Taylor, N. Schultz, M. F. Berger, N. Rosen and D. B. Solit (2014). "Loss of NF1 in cutaneous melanoma is associated with RAS activation and MEK dependence." Cancer Res **74**(8): 2340-2350.
- Nywening, T. M., A. Wang-Gillam, D. E. Sanford, B. A. Belt, R. Z. Panni, B. M. Cusworth, A. T. Toriola, R. K. Nieman, L. A. Worley, M. Yano, K. J. Fowler, A. C. Lockhart, R. Suresh, B. R. Tan, K. H. Lim, R. C. Fields, S. M. Strasberg, W. G. Hawkins, D. G. DeNardo, S. P. Goedegebuure and D. C. Linehan (2016). "Targeting tumour-associated macrophages with CCR2 inhibition in combination with FOLFIRINOX in patients with borderline resectable and locally advanced pancreatic cancer: a single-centre, open-label, dose-finding, non-randomised, phase 1b trial." Lancet Oncol **17**(5): 651-662.
- Ock, C. Y., J. E. Hwang, B. Keam, S. B. Kim, J. J. Shim, H. J. Jang, S. Park, B. H. Sohn, M. Cha, J. A. Ajani, S. Kopetz, K. W. Lee, T. M. Kim, D. S. Heo and J. S. Lee (2017). "Genomic landscape associated with potential response to anti-CTLA-4 treatment in cancers." Nat Commun **8**(1): 1050.
- Oguma, K., H. Oshima, M. Aoki, R. Uchio, K. Naka, S. Nakamura, A. Hirao, H. Saya, M. M. Taketo and M. Oshima (2008). "Activated macrophages promote Wnt signalling through tumour necrosis factor-alpha in gastric tumour cells." EMBO J **27**(12): 1671-1681.
- Ojalvo, L. S., C. A. Whittaker, J. S. Condeelis and J. W. Pollard (2010). "Gene expression analysis of macrophages that facilitate tumor invasion supports a role for Wnt-signaling in mediating their activity in primary mammary tumors." J Immunol **184**(2): 702-712.
- Orr, M. S. (2014). "Electronic cigarettes in the USA: a summary of available toxicology data and suggestions for the future." Tob Control **23 Suppl 2**: ii18-22.
- Pai, S. G., B. A. Carneiro, J. M. Mota, R. Costa, C. A. Leite, R. Barroso-Sousa, J. B. Kaplan, Y. K. Chae and F. J. Giles (2017). "Wnt/beta-catenin pathway: modulating anticancer immune response." J Hematol Oncol **10**(1): 101.
- Paulsson, J. and P. Micke (2014). "Prognostic relevance of cancer-associated fibroblasts in human cancer." Semin Cancer Biol **25**: 61-68.

- Pelosi, G., M. Barbareschi, A. Cavazza, P. Graziano, G. Rossi and M. Papotti (2015). "Large cell carcinoma of the lung: a tumor in search of an author. A clinically oriented critical reappraisal." Lung Cancer **87**(3): 226-231.
- Perrot, I., D. Blanchard, N. Freymond, S. Isaac, B. Guibert, Y. Pacheco and S. Lebecque (2007). "Dendritic cells infiltrating human non-small cell lung cancer are blocked at immature stage." J Immunol **178**(5): 2763-2769.
- Peyrouze, P., S. Guihard, N. Gardel, C. Berthon, N. Pottier, A. Pigneux, J. Y. Cahn, M. C. Bene, V. Lheritier, E. Delabesse, E. Macintyre, X. Thomas, H. Dombret, N. Ifrah and M. Cheok (2012). "Genetic polymorphisms in ARID5B, CEBPE, IKZF1 and CDKN2A in relation with risk of acute lymphoblastic leukaemia in adults: a Group for Research on Adult Acute Lymphoblastic Leukaemia (GRAALL) study." Br J Haematol **159**(5): 599-602.
- Platonova, S., J. Cherfils-Vicini, D. Damotte, L. Crozet, V. Vieillard, P. Validire, P. Andre, M. C. Dieu-Nosjean, M. Alifano, J. F. Regnard, W. H. Fridman, C. Sautes-Fridman and I. Cremer (2011). "Profound coordinated alterations of intratumoral NK cell phenotype and function in lung carcinoma." Cancer Res **71**(16): 5412-5422.
- Pukrop, T., F. Dehghani, H. N. Chuang, R. Lohaus, K. Bayanga, S. Heermann, T. Regen, D. Van Rossum, F. Klemm, M. Schulz, L. Siam, A. Hoffmann, L. Trumper, C. Stadelmann, I. Bechmann, U. K. Hanisch and C. Binder (2010). "Microglia promote colonization of brain tissue by breast cancer cells in a Wnt-dependent way." Glia **58**(12): 1477-1489.
- Pukrop, T., F. Klemm, T. Hagemann, D. Gradl, M. Schulz, S. Siemes, L. Trumper and C. Binder (2006). "Wnt 5a signaling is critical for macrophage-induced invasion of breast cancer cell lines." Proc Natl Acad Sci U S A **103**(14): 5454-5459.
- Pullamsetti, S. S., G. A. Banat, A. Schmall, M. Szibor, D. Pomagruk, J. Hanze, E. Kolosionek, J. Wilhelm, T. Braun, F. Grimminger, W. Seeger, R. T. Schermuly and R. Savai (2013). "Phosphodiesterase-4 promotes proliferation and angiogenesis of lung cancer by crosstalk with HIF." Oncogene **32**(9): 1121-1134.
- Pullamsetti, S. S., B. Kojonazarov, S. Storn, H. Gall, Y. Salazar, J. Wolf, A. Weigert, N. El-Nikhely, H. A. Ghofrani, G. A. Krombach, L. Fink, S. Gattenlohner, U. R. Rapp, R. T. Schermuly, F. Grimminger, W. Seeger and R. Savai (2017). "Lung cancer-associated pulmonary hypertension: Role of microenvironmental inflammation based on tumor cell-immune cell cross-talk." Sci Transl Med **9**(416).
- Pyfferoen, L., E. Brabants, C. Everaert, N. De Cabooter, K. Heyns, K. Deswarte, M. Vanheerswynghe, S. De Prijck, G. Waegemans, M. Dullaers, H. Hammad, O. De Wever, P. Mestdagh, J. Vandesompele, B. N. Lambrecht and K. Y. Vermaelen (2017). "The transcriptome of lung tumor-infiltrating dendritic cells reveals a tumor-supporting phenotype and a microRNA signature with negative impact on clinical outcome." Oncoimmunology **6**(1): e1253655.
- Qian, Y., S. Qiao, Y. Dai, G. Xu, B. Dai, L. Lu, X. Yu, Q. Luo and Z. Zhang (2017). "Molecular-Targeted Immunotherapeutic Strategy for Melanoma via Dual-Targeting Nanoparticles Delivering Small Interfering RNA to Tumor-Associated Macrophages." ACS Nano **11**(9): 9536-9549.
- Raghavan, S., P. Mehta, Y. Xie, Y. L. Lei and G. Mehta (2019). "Ovarian cancer stem cells and macrophages reciprocally interact through the WNT pathway to promote pro-

- tumoral and malignant phenotypes in 3D engineered microenvironments." Journal for ImmunoTherapy of Cancer **7**(1): 190.
- Rakaee, M., L. R. Busund, S. Jamaly, E. E. Paulsen, E. Richardsen, S. Andersen, S. Al-Saad, R. M. Bremnes, T. Donnem and T. K. Kilvaer (2019). "Prognostic Value of Macrophage Phenotypes in Resectable Non-Small Cell Lung Cancer Assessed by Multiplex Immunohistochemistry." Neoplasia **21**(3): 282-293.
- Rapp, J., L. Jaromi, K. Kvell, G. Miskei and J. E. Pongracz (2017). "WNT signaling - lung cancer is no exception." Respir Res **18**(1): 167.
- Rekhtman, N., M. C. Pietanza, M. D. Hellmann, J. Naidoo, A. Arora, H. Won, D. F. Halpenny, H. Wang, S. K. Tian, A. M. Litvak, P. K. Paik, A. E. Drilon, N. Socci, J. T. Poirier, R. Shen, M. F. Berger, A. L. Moreira, W. D. Travis, C. M. Rudin and M. Ladanyi (2016). "Next-Generation Sequencing of Pulmonary Large Cell Neuroendocrine Carcinoma Reveals Small Cell Carcinoma-like and Non-Small Cell Carcinoma-like Subsets." Clin Cancer Res **22**(14): 3618-3629.
- Rickman, O. B., P. K. Vohra, B. Sanyal, J. A. Vrana, M. C. Aubry, D. A. Wigle and C. F. Thomas, Jr. (2009). "Analysis of ErbB receptors in pulmonary carcinoid tumors." Clin Cancer Res **15**(10): 3315-3324.
- Ringleb, J., E. Strack, C. Angioni, G. Geisslinger, D. Steinhilber, A. Weigert and B. Brune (2018). "Apoptotic Cancer Cells Suppress 5-Lipoxygenase in Tumor-Associated Macrophages." J Immunol **200**(2): 857-868.
- Rivas-Fuentes, S., A. Salgado-Aguayo, S. Pertuz Belloso, P. Gorocica Rosete, N. Alvarado-Vasquez and G. Aquino-Jarquín (2015). "Role of Chemokines in Non-Small Cell Lung Cancer: Angiogenesis and Inflammation." J Cancer **6**(10): 938-952.
- Rodriguez, P. C., D. G. Quiceno, J. Zabaleta, B. Ortiz, A. H. Zea, M. B. Piazuelo, A. Delgado, P. Correa, J. Brayer, E. M. Sotomayor, S. Antonia, J. B. Ochoa and A. C. Ochoa (2004). "Arginase I production in the tumor microenvironment by mature myeloid cells inhibits T-cell receptor expression and antigen-specific T-cell responses." Cancer Res **64**(16): 5839-5849.
- Rogers, T. L. and I. Holen (2011). "Tumour macrophages as potential targets of bisphosphonates." J Transl Med **9**: 177.
- Roos, J., S. Grosch, O. Werz, P. Schroder, S. Ziegler, S. Fulda, P. Paulus, A. Urbschat, B. Kuhn, I. Maucher, J. Fettel, T. Vorup-Jensen, M. Piesche, C. Matrone, D. Steinhilber, M. J. Parnham and T. J. Maier (2016). "Regulation of tumorigenic Wnt signaling by cyclooxygenase-2, 5-lipoxygenase and their pharmacological inhibitors: A basis for novel drugs targeting cancer cells?" Pharmacol Ther **157**: 43-64.
- Roth, F., A. C. De La Fuente, J. L. Vella, A. Zoso, L. Inverardi and P. Serafini (2012). "Aptamer-mediated blockade of IL4Ralpha triggers apoptosis of MDSCs and limits tumor progression." Cancer Res **72**(6): 1373-1383.
- Roy, S., S. Schmeier, E. Arner, T. Alam, S. P. Parihar, M. Ozturk, O. Tamgue, H. Kawaji, M. J. de Hoon, M. Itoh, T. Lassmann, P. Carninci, Y. Hayashizaki, A. R. Forrest, V. B. Bajic, R. Guler, C. Fantom, F. Brombacher and H. Suzuki (2015). "Redefining the transcriptional regulatory dynamics of classically and alternatively activated macrophages by deepCAGE transcriptomics." Nucleic Acids Res **43**(14): 6969-6982.

Roy, S., S. Schmeier, B. Kaczowski, E. Arner, T. Alam, M. Ozturk, O. Tamgue, S. P. Parihar, H. Kawaji, M. Itoh, T. Lassmann, P. Carninci, Y. Hayashizaki, A. R. R. Forrest, R. Guler, V. B. Bajic, F. Brombacher and H. Suzuki (2018). "Transcriptional landscape of Mycobacterium tuberculosis infection in macrophages." Sci Rep **8**(1): 6758.

Rudant, J., L. Orsi, A. Bonaventure, S. Goujon-Bellec, E. Corda, A. Baruchel, Y. Bertrand, B. Nelken, A. Robert, G. Michel, N. Sirvent, P. Chastagner, S. Ducassou, X. Rialland, D. Hemon, G. Leverger and J. Clavel (2013). "Are ARID5B and IKZF1 polymorphisms also associated with childhood acute myeloblastic leukemia: the ESCALE study (SFCE)?" Leukemia **27**(3): 746-748.

Ryan, B. M., S. R. Pine, A. K. Chaturvedi, N. Caporaso and C. C. Harris (2014). "A combined prognostic serum interleukin-8 and interleukin-6 classifier for stage 1 lung cancer in the prostate, lung, colorectal, and ovarian cancer screening trial." J Thorac Oncol **9**(10): 1494-1503.

Samet, J. M. (1991). "Diseases of uranium miners and other underground miners exposed to radon." Occup Med **6**(4): 629-639.

Sanchez-Vega, F., M. Mina, J. Armenia, W. K. Chatila, A. Luna, K. C. La, S. Dimitriadoy, D. L. Liu, H. S. Kantheti, S. Saghafeinia, D. Chakravarty, F. Daian, Q. Gao, M. H. Bailey, W. W. Liang, S. M. Foltz, I. Shmulevich, L. Ding, Z. Heins, A. Ochoa, B. Gross, J. Gao, H. Zhang, R. Kundra, C. Kandoth, I. Bahceci, L. Dervishi, U. Dogrusoz, W. Zhou, H. Shen, P. W. Laird, G. P. Way, C. S. Greene, H. Liang, Y. Xiao, C. Wang, A. Iavarone, A. H. Berger, T. G. Bivona, A. J. Lazar, G. D. Hammer, T. Giordano, L. N. Kwong, G. McArthur, C. Huang, A. D. Tward, M. J. Frederick, F. McCormick, M. Meyerson, N. Cancer Genome Atlas Research, E. M. Van Allen, A. D. Cherniack, G. Ciriello, C. Sander and N. Schultz (2018). "Oncogenic Signaling Pathways in The Cancer Genome Atlas." Cell **173**(2): 321-337 e310.

Sandhu, S. K., K. Papadopoulos, P. C. Fong, A. Patnaik, C. Messiou, D. Olmos, G. Wang, B. J. Tromp, T. A. Puchalski, F. Balkwill, B. Berns, S. Seetharam, J. S. de Bono and A. W. Tolcher (2013). "A first-in-human, first-in-class, phase I study of carlumab (CNTO 888), a human monoclonal antibody against CC-chemokine ligand 2 in patients with solid tumors." Cancer Chemother Pharmacol **71**(4): 1041-1050.

Savai, R., H. M. Al-Tamari, D. Sedding, B. Kojonazarov, C. Muecke, R. Teske, M. R. Capecchi, N. Weissmann, F. Grimminger, W. Seeger, R. T. Schermuly and S. S. Pullamsetti (2014). "Pro-proliferative and inflammatory signaling converge on FoxO1 transcription factor in pulmonary hypertension." Nat Med **20**(11): 1289-1300.

Savai, R., R. T. Schermuly, S. S. Pullamsetti, M. Schneider, S. Greschus, H. A. Ghofrani, H. Traupe, F. Grimminger and G. A. Banat (2007). "A combination hybrid-based vaccination/adoptive cellular therapy to prevent tumor growth by involvement of T cells." Cancer Res **67**(11): 5443-5453.

Schalper, K. A., J. Brown, D. Carvajal-Hausdorf, J. McLaughlin, V. Velcheti, K. N. Syrigos, R. S. Herbst and D. L. Rimm (2015). "Objective measurement and clinical significance of TILs in non-small cell lung cancer." J Natl Cancer Inst **107**(3).

Schmall, A., H. M. Al-Tamari, S. Herold, M. Kampschulte, A. Weigert, A. Wietelmann, N. Vipotnik, F. Grimminger, W. Seeger, S. S. Pullamsetti and R. Savai (2015). "Macrophage and cancer cell cross-talk via CCR2 and CX3CR1 is a fundamental mechanism driving lung cancer." Am J Respir Crit Care Med **191**(4): 437-447.

Schrank, Z., G. Chhabra, L. Lin, T. Iderzorig, C. Osude, N. Khan, A. Kuckovic, S. Singh, R. J. Miller and N. Puri (2018). "Current Molecular-Targeted Therapies in NSCLC and Their Mechanism of Resistance." Cancers (Basel) **10**(7).

Schultze, J. L., A. Schmieder and S. Goerdts (2015). "Macrophage activation in human diseases." Semin Immunol **27**(4): 249-256.

Schwartz, A. G. and M. L. Cote (2016). "Epidemiology of Lung Cancer." Adv Exp Med Biol **893**: 21-41.

Schyns, J., F. Bureau and T. Marichal (2018). "Lung Interstitial Macrophages: Past, Present, and Future." J Immunol Res **2018**: 5160794.

Scodeller, P., L. Simon-Gracia, S. Kopanchuk, A. Tobi, K. Kilk, P. Saalik, K. Kurm, M. L. Squadrito, V. R. Kotamraju, A. Rinken, M. De Palma, E. Ruoslahti and T. Teesalu (2017). "Precision Targeting of Tumor Macrophages with a CD206 Binding Peptide." Sci Rep **7**(1): 14655.

Seidel, J. A., A. Otsuka and K. Kabashima (2018). "Anti-PD-1 and Anti-CTLA-4 Therapies in Cancer: Mechanisms of Action, Efficacy, and Limitations." Front Oncol **8**: 86.

Sequist, L. V., R. S. Heist, A. T. Shaw, P. Fidias, R. Rosovsky, J. S. Temel, I. T. Lennes, S. Digumarthy, B. A. Waltman, E. Bast, S. Tammireddy, L. Morrissey, A. Muzikansky, S. B. Goldberg, J. Gainor, C. L. Channick, J. C. Wain, H. Gaissert, D. M. Donahue, A. Muniappan, C. Wright, H. Willers, D. J. Mathisen, N. C. Choi, J. Baselga, T. J. Lynch, L. W. Ellisen, M. Mino-Kenudson, M. Lanuti, D. R. Borger, A. J. Iafrate, J. A. Engelman and D. Dias-Santagata (2011). "Implementing multiplexed genotyping of non-small-cell lung cancers into routine clinical practice." Ann Oncol **22**(12): 2616-2624.

Shea-Donohue, T., J. Stiltz, A. Zhao and L. Notari (2010). "Mast cells." Curr Gastroenterol Rep **12**(5): 349-357.

Shiga, K., M. Hara, T. Nagasaki, T. Sato, H. Takahashi and H. Takeyama (2015). "Cancer-Associated Fibroblasts: Their Characteristics and Their Roles in Tumor Growth." Cancers (Basel) **7**(4): 2443-2458.

Shtutman, M., J. Zhurinsky, I. Simcha, C. Albanese, M. D'Amico, R. Pestell and A. Ben-Ze'ev (1999). "The cyclin D1 gene is a target of the beta-catenin/LEF-1 pathway." Proc Natl Acad Sci U S A **96**(10): 5522-5527.

Sica, A., A. Sacconi, B. Bottazzi, N. Polentarutti, A. Vecchi, J. van Damme and A. Mantovani (2000). "Autocrine production of IL-10 mediates defective IL-12 production and NF-kappa B activation in tumor-associated macrophages." J Immunol **164**(2): 762-767.

Siegel, R. L., K. D. Miller and A. Jemal (2019). "Cancer statistics, 2019." CA Cancer J Clin **69**(1): 7-34.

Sikic, B. I., N. Lakhani, A. Patnaik, S. A. Shah, S. R. Chandana, D. Rasco, A. D. Colevas, T. O'Rourke, S. Narayanan, K. Papadopoulos, G. A. Fisher, V. Villalobos, S. S. Prohaska, M. Howard, M. Beeram, M. P. Chao, B. Agoram, J. Y. Chen, J. Huang, M. Axt, J. Liu, J. P. Volkmer, R. Majeti, I. L. Weissman, C. H. Takimoto, D. Supan, H. A. Wakelee, R. Aoki, M. D. Pegram and S. K. Padda (2019). "First-in-Human, First-in-Class

Phase I Trial of the Anti-CD47 Antibody Hu5F9-G4 in Patients With Advanced Cancers." J Clin Oncol **37**(12): 946-953.

Singh, M., H. Khong, Z. Dai, X. F. Huang, J. A. Wargo, Z. A. Cooper, J. P. Vasilakos, P. Hwu and W. W. Overwijk (2014). "Effective innate and adaptive antimelanoma immunity through localized TLR7/8 activation." J Immunol **193**(9): 4722-4731.

Smith, D. A., P. Conkling, D. A. Richards, J. J. Nemunaitis, T. E. Boyd, A. C. Mita, G. de La Bourdonnaye, D. Wages and A. S. Bexon (2014). "Antitumor activity and safety of combination therapy with the Toll-like receptor 9 agonist IMO-2055, erlotinib, and bevacizumab in advanced or metastatic non-small cell lung cancer patients who have progressed following chemotherapy." Cancer Immunol Immunother **63**(8): 787-796.

Smith, K., T. D. Bui, R. Poulsom, L. Kaklamanis, G. Williams and A. L. Harris (1999). "Up-regulation of macrophage wnt gene expression in adenoma-carcinoma progression of human colorectal cancer." Br J Cancer **81**(3): 496-502.

Soo, R. A., Z. Chen, R. S. Yan Teng, H. L. Tan, B. Iacopetta, B. C. Tai and R. Soong (2018). "Prognostic significance of immune cells in non-small cell lung cancer: meta-analysis." Oncotarget **9**(37): 24801-24820.

Spranger, S., R. Bao and T. F. Gajewski (2015). "Melanoma-intrinsic beta-catenin signalling prevents anti-tumour immunity." Nature **523**(7559): 231-235.

Squadrito, M. L., M. Etzrodt, M. De Palma and M. J. Pittet (2013). "MicroRNA-mediated control of macrophages and its implications for cancer." Trends Immunol **34**(7): 350-359.  
Stakheev, D., P. Taborska, Z. Strizova, M. Podrazil, J. Bartunkova and D. Smrz (2019). "The WNT/beta-catenin signaling inhibitor XAV939 enhances the elimination of LNCaP and PC-3 prostate cancer cells by prostate cancer patient lymphocytes in vitro." Sci Rep **9**(1): 4761.

Stathopoulos, G. T., T. P. Sherrill, D. S. Cheng, R. M. Scoggins, W. Han, V. V. Polosukhin, L. Connelly, F. E. Yull, B. Fingleton and T. S. Blackwell (2007). "Epithelial NF-kappaB activation promotes urethane-induced lung carcinogenesis." Proc Natl Acad Sci U S A **104**(47): 18514-18519.

Stewart, D. J. (2010). "Tumor and host factors that may limit efficacy of chemotherapy in non-small cell and small cell lung cancer." Crit Rev Oncol Hematol **75**(3): 173-234.

Stewart, D. J. (2014). "Wnt signaling pathway in non-small cell lung cancer." J Natl Cancer Inst **106**(1): djt356.

Sun, L., Z. Guo, J. Sun, J. Li, Z. Dong, Y. Zhang, J. Chen, Q. Kan and Z. Yu (2018). "MiR-133a acts as an anti-oncogene in Hepatocellular carcinoma by inhibiting FOSL2 through TGF-beta/Smad3 signaling pathway." Biomed Pharmacother **107**: 168-176.

Sun, X., G. Dai, L. Yu, Q. Hu, J. Chen and W. Guo (2018). "miR-143-3p inhibits the proliferation, migration and invasion in osteosarcoma by targeting FOSL2." Sci Rep **8**(1): 606.

Takada, T., Y. Yagi, T. Maekita, M. Imura, S. Nakagawa, S. W. Tsao, K. Miyamoto, O. Yoshino, T. Yasugi, Y. Taketani and T. Ushijima (2004). "Methylation-associated silencing of the Wnt antagonist SFRP1 gene in human ovarian cancers." Cancer Sci **95**(9): 741-744.

Takebe, N., L. Miele, P. J. Harris, W. Jeong, H. Bando, M. Kahn, S. X. Yang and S. P. Ivy (2015). "Targeting Notch, Hedgehog, and Wnt pathways in cancer stem cells: clinical update." *Nat Rev Clin Oncol* **12**(8): 445-464.

Teixido, C. and R. Rosell (2017). "Neutrophils dominate the immune landscape of non-small cell lung cancer." *J Thorac Dis* **9**(5): E468-E469.

Thorgeirsson, T. E., F. Geller, P. Sulem, T. Rafnar, A. Wiste, K. P. Magnusson, A. Manolescu, G. Thorleifsson, H. Stefansson, A. Ingason, S. N. Stacey, J. T. Bergthorsson, S. Thorlacius, J. Gudmundsson, T. Jonsson, M. Jakobsdottir, J. Saemundsdottir, O. Olafsdottir, L. J. Gudmundsson, G. Bjornsdottir, K. Kristjansson, H. Skuladottir, H. J. Isaksson, T. Gudbjartsson, G. T. Jones, T. Mueller, A. Gottsater, A. Flex, K. K. H. Aben, F. de Vegt, P. F. A. Mulders, D. Isla, M. J. Vidal, L. Asin, B. Saez, L. Murillo, T. Blondal, H. Kolbeinsson, J. G. Stefansson, I. Hansdottir, V. Runarsdottir, R. Pola, B. Lindblad, A. M. van Rij, B. Dieplinger, M. Haltmayer, J. I. Mayordomo, L. A. Kiemeny, S. E. Matthiasson, H. Oskarsson, T. Tyrfinngsson, D. F. Gudbjartsson, J. R. Gulcher, S. Jonsson, U. Thorsteinsdottir, A. Kong and K. Stefansson (2008). "A variant associated with nicotine dependence, lung cancer and peripheral arterial disease." *Nature* **452**(7187): 638-642.

Thorsson, V., D. L. Gibbs, S. D. Brown, D. Wolf, D. S. Bortone, T. H. Ou Yang, E. Porta-Pardo, G. F. Gao, C. L. Plaisier, J. A. Eddy, E. Ziv, A. C. Culhane, E. O. Paull, I. K. A. Sivakumar, A. J. Gentles, R. Malhotra, F. Farshidfar, A. Colaprico, J. S. Parker, L. E. Mose, N. S. Vo, J. Liu, Y. Liu, J. Rader, V. Dhankani, S. M. Reynolds, R. Bowlby, A. Califano, A. D. Cherniack, D. Anastassiou, D. Bedognetti, A. Rao, K. Chen, A. Krasnitz, H. Hu, T. M. Malta, H. Noushmehr, C. S. Pedomallu, S. Bullman, A. I. Ojesina, A. Lamb, W. Zhou, H. Shen, T. K. Choueiri, J. N. Weinstein, J. Guinney, J. Saltz, R. A. Holt, C. E. Rabkin, N. Cancer Genome Atlas Research, A. J. Lazar, J. S. Serody, E. G. Demicco, M. L. Disis, B. G. Vincent and L. Shmulevich (2018). "The Immune Landscape of Cancer." *Immunity* **48**(4): 812-830 e814.

Topalian, S. L., F. S. Hodi, J. R. Brahmer, S. N. Gettinger, D. C. Smith, D. F. McDermott, J. D. Powderly, R. D. Carvajal, J. A. Sosman, M. B. Atkins, P. D. Leming, D. R. Spigel, S. J. Antonia, L. Horn, C. G. Drake, D. M. Pardoll, L. Chen, W. H. Sharfman, R. A. Anders, J. M. Taube, T. L. McMiller, H. Xu, A. J. Korman, M. Jure-Kunkel, S. Agrawal, D. McDonald, G. D. Kollia, A. Gupta, J. M. Wigginton and M. Sznol (2012). "Safety, activity, and immune correlates of anti-PD-1 antibody in cancer." *N Engl J Med* **366**(26): 2443-2454.

Toyokawa, G., M. Takenoyama, K. Taguchi, R. Toyozawa, E. Inamasu, M. Kojo, Y. Shiraishi, Y. Morodomi, T. Takenaka, F. Hirai, M. Yamaguchi, T. Seto, M. Shimokawa and Y. Ichinose (2013). "An extremely rare case of small-cell lung cancer harboring variant 2 of the EML4-ALK fusion gene." *Lung Cancer* **81**(3): 487-490.

Tsuruoka, K., H. Horinouchi, Y. Goto, S. Kanda, Y. Fujiwara, H. Nokihara, N. Yamamoto, K. Asakura, K. Nakagawa, H. Sakurai, S. I. Watanabe, K. Tsuta and Y. Ohe (2017). "PD-L1 expression in neuroendocrine tumors of the lung." *Lung Cancer* **108**: 115-120.

Valenta, T., G. Hausmann and K. Basler (2012). "The many faces and functions of beta-catenin." *EMBO J* **31**(12): 2714-2736.

Van Acker, H. H., S. Anguille, Y. Willemen, E. L. Smits and V. F. Van Tendeloo (2016). "Bisphosphonates for cancer treatment: Mechanisms of action and lessons from clinical trials." *Pharmacol Ther* **158**: 24-40.

- van Kooten, C. and J. Banchereau (2000). "CD40-CD40 ligand." *J Leukoc Biol* **67**(1): 2-17.
- Varga, T., R. Mounier, A. Horvath, S. Cuvelier, F. Dumont, S. Poliska, H. Ardjoune, G. Juban, L. Nagy and B. Chazaud (2016). "Highly Dynamic Transcriptional Signature of Distinct Macrophage Subsets during Sterile Inflammation, Resolution, and Tissue Repair." *J Immunol* **196**(11): 4771-4782.
- Varricchi, G., M. R. Galdiero, S. Loffredo, G. Marone, R. Iannone, G. Marone and F. Granata (2017). "Are Mast Cells MASTers in Cancer?" *Front Immunol* **8**: 424.
- Vonderheide, R. H., K. T. Flaherty, M. Khalil, M. S. Stumacher, D. L. Bajor, N. A. Hutnick, P. Sullivan, J. J. Mahany, M. Gallagher, A. Kramer, S. J. Green, P. J. O'Dwyer, K. L. Running, R. D. Huhn and S. J. Antonia (2007). "Clinical activity and immune modulation in cancer patients treated with CP-870,893, a novel CD40 agonist monoclonal antibody." *J Clin Oncol* **25**(7): 876-883.
- Wakabayashi, O., K. Yamazaki, S. Oizumi, F. Hommura, I. Kinoshita, S. Ogura, H. Dosaka-Akita and M. Nishimura (2003). "CD4+ T cells in cancer stroma, not CD8+ T cells in cancer cell nests, are associated with favorable prognosis in human non-small cell lung cancers." *Cancer Sci* **94**(11): 1003-1009.
- Walter, R. F., C. Vollbrecht, D. Christoph, R. Werner, J. Schmeller, E. Flom, G. Trakada, A. Rapti, V. Adamidis, W. Hohenforst-Schmidt, J. Kollmeier, T. Mairinger, J. Wohlschlaeger, P. Zarogoulidis, K. Porpodis, K. W. Schmidt and F. D. Mairinger (2016). "Massive parallel sequencing and digital gene expression analysis reveals potential mechanisms to overcome therapy resistance in pulmonary neuroendocrine tumors." *J Cancer* **7**(15): 2165-2172.
- Wammers, M., A. K. Schupp, J. G. Bode, C. Ehling, S. Wolf, R. Deenen, K. Kohrer, D. Haussinger and D. Graf (2018). "Reprogramming of pro-inflammatory human macrophages to an anti-inflammatory phenotype by bile acids." *Sci Rep* **8**(1): 255.
- Wang, B., T. Tian, K. H. Kalland, X. Ke and Y. Qu (2018). "Targeting Wnt/beta-Catenin Signaling for Cancer Immunotherapy." *Trends Pharmacol Sci* **39**(7): 648-658.
- Wang, J., D. Sun, Y. Wang, F. Ren, S. Pang, D. Wang and S. Xu (2014). "FOSL2 positively regulates TGF-beta1 signalling in non-small cell lung cancer." *PLoS One* **9**(11): e112150.
- Wang, L., L. Cao, H. Wang, B. Liu, Q. Zhang, Z. Meng, X. Wu, Q. Zhou and K. Xu (2017). "Cancer-associated fibroblasts enhance metastatic potential of lung cancer cells through IL-6/STAT3 signaling pathway." *Oncotarget* **8**(44): 76116-76128.
- Wang, R., J. Zhang, S. Chen, M. Lu, X. Luo, S. Yao, S. Liu, Y. Qin and H. Chen (2011). "Tumor-associated macrophages provide a suitable microenvironment for non-small lung cancer invasion and progression." *Lung Cancer* **74**(2): 188-196.
- Weichand, B., R. Popp, S. Dziumbila, J. Mora, E. Strack, E. Elwakeel, A. C. Frank, K. Scholich, S. Pierre, S. N. Syed, C. Olesch, J. Ringleb, B. Oren, C. Doring, R. Savai, M. Jung, A. von Knethen, B. Levkau, I. Fleming, A. Weigert and B. Brune (2017). "S1PR1 on tumor-associated macrophages promotes lymphangiogenesis and metastasis via NLRP3/IL-1beta." *J Exp Med* **214**(9): 2695-2713.

- Weigert, A., N. Tzieply, A. von Knethen, A. M. Johann, H. Schmidt, G. Geisslinger and B. Brune (2007). "Tumor cell apoptosis polarizes macrophages role of sphingosine-1-phosphate." *Mol Biol Cell* **18**(10): 3810-3819.
- Weiss, J., M. L. Sos, D. Seidel, M. Peifer, T. Zander, J. M. Heuckmann, R. T. Ullrich, R. Menon, S. Maier, A. Soltermann, H. Moch, P. Wagener, F. Fischer, S. Heynck, M. Koker, J. Schottle, F. Leenders, F. Gabler, I. Dabow, S. Querings, L. C. Heukamp, H. Balke-Want, S. Ansen, D. Rauh, I. Baessmann, J. Altmuller, Z. Wainer, M. Conron, G. Wright, P. Russell, B. Solomon, E. Brambilla, C. Brambilla, P. Lorimier, S. Sollberg, O. T. Brustugun, W. Engel-Riedel, C. Ludwig, I. Petersen, J. Sanger, J. Clement, H. Groen, W. Timens, H. Sietsma, E. Thunnissen, E. Smit, D. Heideman, F. Cappuzzo, C. Ligorio, S. Damiani, M. Hallek, R. Beroukhim, W. Pao, B. Klebl, M. Baumann, R. Buettner, K. Ernestus, E. Stoelben, J. Wolf, P. Nurnberg, S. Perner and R. K. Thomas (2010). "Frequent and focal FGFR1 amplification associates with therapeutically tractable FGFR1 dependency in squamous cell lung cancer." *Sci Transl Med* **2**(62): 62ra93.
- Wenes, M., M. Shang, M. Di Matteo, J. Goveia, R. Martin-Perez, J. Serneels, H. Prenen, B. Ghesquiere, P. Carmeliet and M. Mazzone (2016). "Macrophage Metabolism Controls Tumor Blood Vessel Morphogenesis and Metastasis." *Cell Metab* **24**(5): 701-715.
- Wilkins, J. A. and O. J. Sansom (2008). "C-Myc is a critical mediator of the phenotypes of Apc loss in the intestine." *Cancer Res* **68**(13): 4963-4966.
- Winstone, T. A., S. F. P. Man, M. Hull, J. S. Montaner and D. D. Sin (2013). "Epidemic of lung cancer in patients with HIV infection." *Chest* **143**(2): 305-314.
- Wu, P., D. Wu, L. Zhao, L. Huang, G. Chen, G. Shen, J. Huang and Y. Chai (2016). "Inverse role of distinct subsets and distribution of macrophage in lung cancer prognosis: a meta-analysis." *Oncotarget* **7**(26): 40451-40460.
- Xu, H., C. Cheng, M. Devidas, D. Pei, Y. Fan, W. Yang, G. Neale, P. Scheet, E. G. Burchard, D. G. Torgerson, C. Eng, M. Dean, F. Antillon, N. J. Winick, P. L. Martin, C. L. Willman, B. M. Camitta, G. H. Reaman, W. L. Carroll, M. Loh, W. E. Evans, C. H. Pui, S. P. Hunger, M. V. Relling and J. J. Yang (2012). "ARID5B genetic polymorphisms contribute to racial disparities in the incidence and treatment outcome of childhood acute lymphoblastic leukemia." *J Clin Oncol* **30**(7): 751-757.
- Yahya, S., Q. Ghafoor, R. Stevenson, S. Watkins and B. Allos (2018). "Evolution of Stereotactic Ablative Radiotherapy in Lung Cancer and Birmingham's (UK) Experience." *Medicines (Basel)* **5**(3).
- Yan, D., J. Kowal, L. Akkari, A. J. Schuhmacher, J. T. Huse, B. L. West and J. A. Joyce (2017). "Inhibition of colony stimulating factor-1 receptor abrogates microenvironment-mediated therapeutic resistance in gliomas." *Oncogene* **36**(43): 6049-6058.
- Yang, J., J. Chen, J. He, J. Li, J. Shi, W. C. Cho and X. Liu (2016). "Wnt signaling as potential therapeutic target in lung cancer." *Expert Opin Ther Targets* **20**(8): 999-1015.
- Yang, M., D. McKay, J. W. Pollard and C. E. Lewis (2018). "Diverse Functions of Macrophages in Different Tumor Microenvironments." *Cancer Res* **78**(19): 5492-5503.
- Yang, Y., Y. C. Ye, Y. Chen, J. L. Zhao, C. C. Gao, H. Han, W. C. Liu and H. Y. Qin (2018). "Crosstalk between hepatic tumor cells and macrophages via Wnt/beta-catenin signaling promotes M2-like macrophage polarization and reinforces tumor malignant behaviors." *Cell Death Dis* **9**(8): 793.

- Ye, Y. C., J. L. Zhao, Y. T. Lu, C. C. Gao, Y. Yang, S. Q. Liang, Y. Y. Lu, L. Wang, S. Q. Yue, K. F. Dou, H. Y. Qin and H. Han (2019). "Notch signaling via Wnt regulates the proliferation of alternative, CCR2-independent tumor-associated macrophages in hepatocellular carcinoma." Cancer Res.
- Yeo, E. J., L. Cassetta, B. Z. Qian, I. Lewkowich, J. F. Li, J. A. Stefater, 3rd, A. N. Smith, L. S. Wiechmann, Y. Wang, J. W. Pollard and R. A. Lang (2014). "Myeloid WNT7b mediates the angiogenic switch and metastasis in breast cancer." Cancer Res **74**(11): 2962-2973.
- Yin, X., D. Yan, M. Qiu, L. Huang and S. X. Yan (2019). "Prophylactic cranial irradiation in small cell lung cancer: a systematic review and meta-analysis." BMC Cancer **19**(1): 95.
- Yokota, J., K. Shiraishi and T. Kohno (2010). "Genetic basis for susceptibility to lung cancer: Recent progress and future directions." Adv Cancer Res **109**: 51-72.
- Yuan, A., Y. J. Hsiao, H. Y. Chen, H. W. Chen, C. C. Ho, Y. Y. Chen, Y. C. Liu, T. H. Hong, S. L. Yu, J. J. Chen and P. C. Yang (2015). "Opposite Effects of M1 and M2 Macrophage Subtypes on Lung Cancer Progression." Sci Rep **5**: 14273.
- Zakiryanova, G. K., S. Wheeler and M. R. Shurin (2018). "Oncogenes in immune cells as potential therapeutic targets." Immunotargets Ther **7**: 21-28.
- Zappa, C. and S. A. Mousa (2016). "Non-small cell lung cancer: current treatment and future advances." Transl Lung Cancer Res **5**(3): 288-300.
- Zeilstra, J., S. P. Joosten, M. Dokter, E. Verwiel, M. Spaargaren and S. T. Pals (2008). "Deletion of the WNT target and cancer stem cell marker CD44 in Apc(Min/+) mice attenuates intestinal tumorigenesis." Cancer Res **68**(10): 3655-3661.
- Zhan, T., N. Rindtorff and M. Boutros (2017). "Wnt signaling in cancer." Oncogene **36**(11): 1461-1473.
- Zhang, H., H. Lu, L. Xiang, J. W. Bullen, C. Zhang, D. Samanta, D. M. Gilkes, J. He and G. L. Semenza (2015). "HIF-1 regulates CD47 expression in breast cancer cells to promote evasion of phagocytosis and maintenance of cancer stem cells." Proc Natl Acad Sci U S A **112**(45): E6215-6223.
- Zhao, H., J. Wang, X. Kong, E. Li, Y. Liu, X. Du, Z. Kang, Y. Tang, Y. Kuang, Z. Yang, Y. Zhou and Q. Wang (2016). "CD47 Promotes Tumor Invasion and Metastasis in Non-small Cell Lung Cancer." Sci Rep **6**: 29719.
- Zhao, J. L., F. Huang, F. He, C. C. Gao, S. Q. Liang, P. F. Ma, G. Y. Dong, H. Han and H. Y. Qin (2016). "Forced Activation of Notch in Macrophages Represses Tumor Growth by Upregulating miR-125a and Disabling Tumor-Associated Macrophages." Cancer Res **76**(6): 1403-1415.
- Zhao, S. J., Y. Q. Jiang, N. W. Xu, Q. Li, Q. Zhang, S. Y. Wang, J. Li, Y. H. Wang, Y. L. Zhang, S. H. Jiang, Y. J. Wang, Y. J. Huang, X. X. Zhang, G. A. Tian, C. C. Zhang, Y. Y. Lv, M. Dai, F. Liu, R. Zhang, D. Zhou and Z. G. Zhang (2017). "SPARCL1 suppresses osteosarcoma metastasis and recruits macrophages by activation of canonical WNT/ $\beta$ -catenin signaling through stabilization of the WNT-receptor complex." Oncogene **37**: 1049.

Zhu, S., M. Niu, H. O'Mary and Z. Cui (2013). "Targeting of tumor-associated macrophages made possible by PEG-sheddable, mannose-modified nanoparticles." Mol Pharm **10**(9): 3525-3530.

## 12. ERKLÄRUNG ZUR DISSERTATION

„Hiermit erkläre ich, dass ich die vorliegende Arbeit selbständig und ohne unzulässige Hilfe oder Benutzung anderer als der angegebenen Hilfsmittel angefertigt habe. Alle Textstellen, die wörtlich oder sinngemäß aus veröffentlichten oder nichtveröffentlichten Schriften entnommen sind, und alle Angaben, die auf mündlichen Auskünften beruhen, sind als solche kenntlich gemacht. Bei den von mir durchgeführten und in der Dissertation erwähnten Untersuchungen habe ich die Grundsätze guter wissenschaftlicher Praxis, wie sie in der „Satzung der Justus-Liebig-Universität Gießen zur Sicherung guter wissenschaftlicher Praxis“ niedergelegt sind, eingehalten sowie ethische, datenschutzrechtliche und tierschutzrechtliche Grundsätze befolgt. Ich versichere, dass Dritte von mir weder unmittelbar noch mittelbar geldwerte Leistungen für Arbeiten erhalten haben, die im Zusammenhang mit dem Inhalt der vorgelegten Dissertation stehen, oder habe diese nachstehend spezifiziert. Die vorgelegte Arbeit wurde weder im Inland noch im Ausland in gleicher oder ähnlicher Form einer anderen Prüfungsbehörde zum Zweck einer Promotion oder eines anderen Prüfungsverfahrens vorgelegt. Alles aus anderen Quellen und von anderen Personen übernommene Material, das in der Arbeit verwendet wurde oder auf das direkt Bezug genommen wird, wurde als solches kenntlich gemacht. Insbesondere wurden alle Personen genannt, die direkt und indirekt an der Entstehung der vorliegenden Arbeit beteiligt waren. Mit der Überprüfung meiner Arbeit durch eine Plagiatserkennungssoftware bzw. ein internetbasiertes Softwareprogramm erkläre ich mich einverstanden.“

---

Ort, Datum

---

Unterschrift

### 13. ACKNOWLEDGEMENT

Firstly, I would like to express my sincere gratitude to my advisor **PD Dr. Rajkumar Savai**, for the continuous support of my Ph.D. study and related research, for his patience, motivation, and immense knowledge. His guidance helped me in all the time of research and writing of this thesis. I could not have imagined having a better advisor and mentor for my Ph.D study.

Besides my advisor, I would like to thank **Prof. Dr. Werner Seeger, Dr. Soni Savai Pullamsetti, Dr. Andreas Weigert, Prof. Dr. Georgios Stathopoulos, and Prof. Dr. Thorsten Stiewe** for their insightful comments and encouragement, but also for the hard questions which incited me to widen my research from various perspectives.

I thank my fellow labmates and friends **Xiang Zheng, Ylia Salazar, Siavash Mansouri, Yanina Knepper, Vanessa Golchert, Annika Karger, David Brunn, Marianne Hoeck, Oeznur Cetin, Nefertiti El Nikhely, Swati Dabral, Alexandra Tretyn, Prakash Chelladurai, Dijana Iloska, Elisabeth Gamen, Natascha Wilker, and Georgia Giotopoulou** for the stimulating discussions, for working together, and for all the fun we have had in the last six years. I thank **Dr. Kati Turkowski** for help with the animal experiment proposal. I thank **Dr. Carsten Kuenne** and **Dr. Stefan Günther** for excellent technical assistance in bioinformatics analysis. I am also grateful to **Monika Haselbauer** for helping in all administration work.

In addition, I would like to thank **my husband Ashwin, parents, parents-in-law, sisters Sneha, Swati, Megha and brother Sripad** for their wise counsel and sympathetic ear. You are always there for me. Last but not least, I thank **my daughters Vihaa and Aarya** for providing a happy distraction to enjoy a few cherished moments outside of my research.

